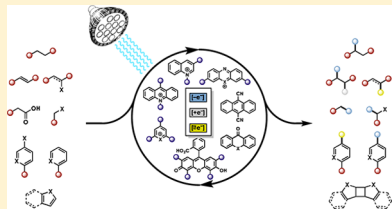


## Organic Photoredox Catalysis

Nathan A. Romero and David A. Nicewicz\*

Department of Chemistry, University of North Carolina at Chapel Hill, Chapel Hill, North Carolina 27599-3290, United States

**ABSTRACT:** In this review, we highlight the use of organic photoredox catalysts in a myriad of synthetic transformations with a range of applications. This overview is arranged by catalyst class where the photophysics and electrochemical characteristics of each is discussed to underscore the differences and advantages to each type of single electron redox agent. We highlight both net reductive and oxidative as well as redox neutral transformations that can be accomplished using purely organic photoredox-active catalysts. An overview of the basic photophysics and electron transfer theory is presented in order to provide a comprehensive guide for employing this class of catalysts in photoredox manifolds.



### CONTENTS

1. Introduction	10076	4.1. Photophysical and Electrochemical Characteristics	10084
1.1. Background and Importance	10076	4.2. Reactions	10084
1.2. Why Organic Photoredox Catalysts?	10076	4.2.1. Net Oxidative Transformations Involving Cyanoarene Photooxidants	10084
2. Photophysical and Electrochemical Considerations	10078	4.2.2. Net Redox Neutral Transformations with Cyanoarene Photooxidants	10086
2.1. Photophysical Processes	10078	4.2.3. Net Reductive Transformations Involving Cyanoarene Photoredox Catalysts	10094
2.2. Photophysical Properties of Organic Photoredox Catalysts	10078	4.3. Cyanoarene Catalyst Development	10094
2.2.1. $\lambda_{\text{max}}^{\text{abs}}$ : Local Absorbance Maximum for Lowest Energy Absorption	10078	5. Benzophenones and Quinones	10095
2.2.2. $\tau_f$ : Lifetime of Fluorescence (Equal to the Inverse of the Fluorescence Decay Rate Constant, or $1/k_f$ ) and $\phi_f$ : Quantum Yield of Fluorescence	10078	5.1. Benzophenones, Xanthones, Fluorenone: Photophysical and Electrochemical Characteristics	10095
2.2.3. $\phi_{\text{ISC}}$ : Quantum Yield of Intersystem Crossing (Frequently Used As Synonymous with Quantum Yield of Formation of $T_1$ , $\phi_{T_1}$ )	10080	5.2. Benzophenones, Xanthones, and Fluorenone: Reactions	10095
2.2.4. $E_{0,0}^S$ : Excited State Energy of the First Singlet Excited State $S_1$	10080	5.3. Quinones: Photophysical and Electrochemical Characteristics	10098
2.2.5. $E_{0,0}^T$ : Excited State Energy of the First Triplet Excited State $T_1$	10080	5.4. Quinones: Reactions	10098
2.3. Electrochemistry: Thermodynamics of Electron Transfer and Photoinduced Electron Transfer	10080	6. Pyryliums and Thiapyryliums	10099
2.3.1. Electron Transfer in the Ground State	10080	6.1. Triaryl Oxypyrylium Salts: Photophysical and Electrochemical Characteristics	10099
2.3.2. Photoinduced Electron Transfer	10081	6.2. Triaryl Oxypyryliums: Reactions	10100
3. General Mechanistic Schemes for Photoredox Catalysis	10081	6.2.1. Net Oxidative Transformations	10100
3.1. Definitions	10082	6.2.2. Net Redox Neutral Transformations	10100
3.2. Other Mechanistic Considerations	10082	6.3. Triaryl Thiapyrylium: Photophysical and Electrochemical Characteristics	10103
3.2.1. Chain Mechanisms	10082	6.4. Triaryl Thiapyrylium: Reactions	10103
3.2.2. EDA Complexes and Exciplexes	10083	6.4.1. Cycloreversion Reactions	10103
3.2.3. Energy Transfer vs Electron Transfer	10083	7. Quinoliniums	10104
3.2.4. Singlet or Triplet Excited States: Does It Matter?	10083	7.1. Photophysical and Electrochemical Characteristics	10104
4. Cyanoarenes: Polycyano-Benzene, Naphthalene, And Anthracenes	10084	7.2. Reactions	10104
		7.2.1. Oxygenation and Oxidation Reactions	10104
		8. Acridiniums	10107

Special Issue: Photochemistry in Organic Synthesis

Received: January 22, 2016

Published: June 10, 2016

8.1. Acr-Me <sup>+</sup> and 9-Substituted Acr-R <sup>+</sup> : Photophysical and Electrochemical Characteristics	10107	Biographies	10151
8.2. Acr-Me <sup>+</sup> and 9-Substituted Acr-R <sup>+</sup> : Reactions	10108	Acknowledgments	10152
8.2.1. Oxygenation and Oxidation Reactions	10108	Abbreviations	10152
8.2.2. Dehydrogenative Couplings	10111		
8.2.3. Alkene Hydrofunctionalization	10115	References	10152
8.2.4. Deborylative and Decarboxylative Transformations	10117		
8.2.5. Cycloadditions	10119		
8.3. Electron-Rich Acridines and Acridiniums: Acridine Orange (AO and AOH <sup>+</sup> ) and Proflavin (PF and PFH <sup>+</sup> )	10121		
8.3.1. AO/AOH <sup>+</sup> and PF/PFH <sup>+</sup> : Photophysical and Electrochemical Characteristics	10121		
8.3.2. AO/AOH <sup>+</sup> and PF/PFH <sup>+</sup> : Reactions	10121		
9. Xanthenes Dyes: Fluoresceins and Rhodamines	10122		
9.1. Fluorescein-Based Photoredox Catalysts (Eosin Y, Erythrosine, Rose Bengal, and Fluorescein): Photophysical and Electrochemical Characteristics	10122		
9.2. Fluorescein-Based Photoredox Catalysts: Reactions	10123		
9.2.1. Oxidation and Oxygenation Reactions	10123		
9.2.2. Dehydrogenative Couplings	10126		
9.2.3. Oxidative Transformations in the Synthesis of Heterocycles	10128		
9.2.4. Other Oxidative C–H Functionalization Reactions	10131		
9.2.5. Reductive Transformations	10134		
9.2.6. Reactions of Aryldiazonium Salts	10139		
9.2.7. Other Redox-Neutral Transformations	10142		
10. Rhodamines	10144		
10.1. Photophysical and Electrochemical Characteristics	10144		
10.2. Reactions	10144		
10.2.1. Oxidation and Oxygenation Reactions	10144		
10.2.2. Redox-Neutral Transformations	10144		
11. Phenothiazines	10145		
11.1. Methylene Blue: Photophysical and Electrochemical Characteristics	10145		
11.2. Methylene Blue: Reactions	10145		
11.2.1. Oxygenation and Oxidation Reactions	10145		
11.2.2. Trifluoromethylation Reactions	10146		
11.3. N-Phenyl Phenothiazine: Photophysical and Electrochemical Characteristics	10147		
11.4. N-Phenyl Phenothiazine: Reactions	10147		
11.4.1. Reductive Transformations	10147		
12. Other Organic Photoredox Catalysts	10147		
12.1. Perylene Diimides: Photophysical and Electrochemical Characteristics and Reactions	10148		
12.2. Diazapyrenium: Photophysical and Electrochemical Characteristics and Reactions	10148		
12.3. Phenazinium Salts: Photophysical and Electrochemical Characteristics/Reactions	10148		
12.4. Electron-Rich Anthracenes and Pyrenes: Photophysical and Electrochemical Characteristics/Reactions	10150		
12.5. Flavins	10150		
12.6. BODIPY Dyes	10150		
13. Conclusions	10151		
Author Information	10151		
Corresponding Author	10151		
Notes	10151		

## 1. INTRODUCTION

### 1.1. Background and Importance

The revival of radical chemistry in organic synthesis over the past decade has also initiated resurgence in the interest in photochemistry. Much of this renewed interest has come about due to the reactivity that can be accessed via the intermediacy of open shell reactive species that is otherwise difficult or impossible by other means of chemical catalysis. Radical reactivity often times offers a complementarity to polar or two-electron manifolds. Perhaps one of the most rapidly expanding areas of radical chemistry in synthesis is photoredox catalysis. Many researchers in chemistry ranging from biomedical to materials science are quickly adopting the use of photoredox catalysis as a mild means of achieving unique chemical reactivity.

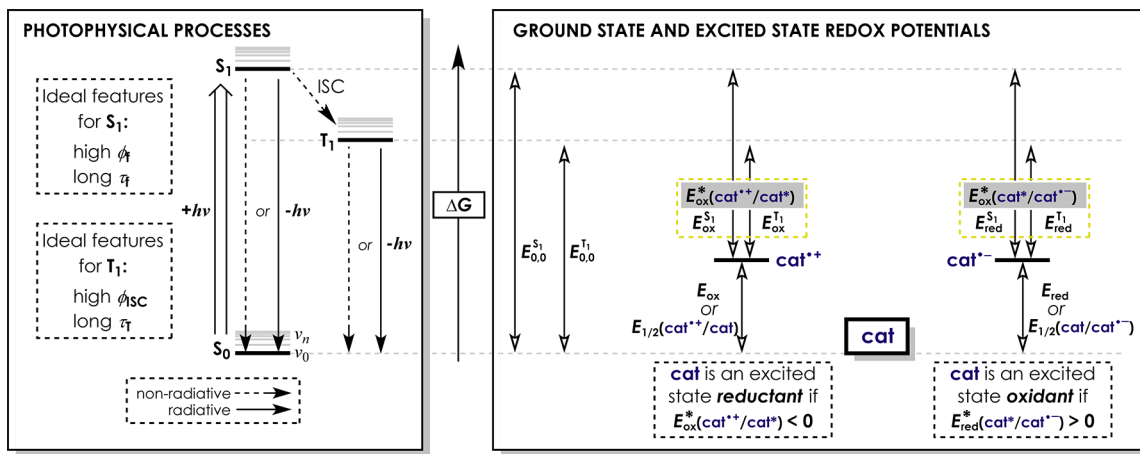
This review will highlight the advances from the past ~40 years that have laid the groundwork for current advances in photoredox catalysis as well as provide readers with the basic tools to approach the design and implementation of photoredox catalysis in organic synthesis. Importantly, this survey of the literature will be limited to purely organic photoredox catalyst systems and will describe the pros and cons for the use of organic photoredox catalysts over their organometallic and inorganic counterparts. We hope that this is just the start of what promises to be a fruitful area of research for many years to come.

### 1.2. Why Organic Photoredox Catalysts?

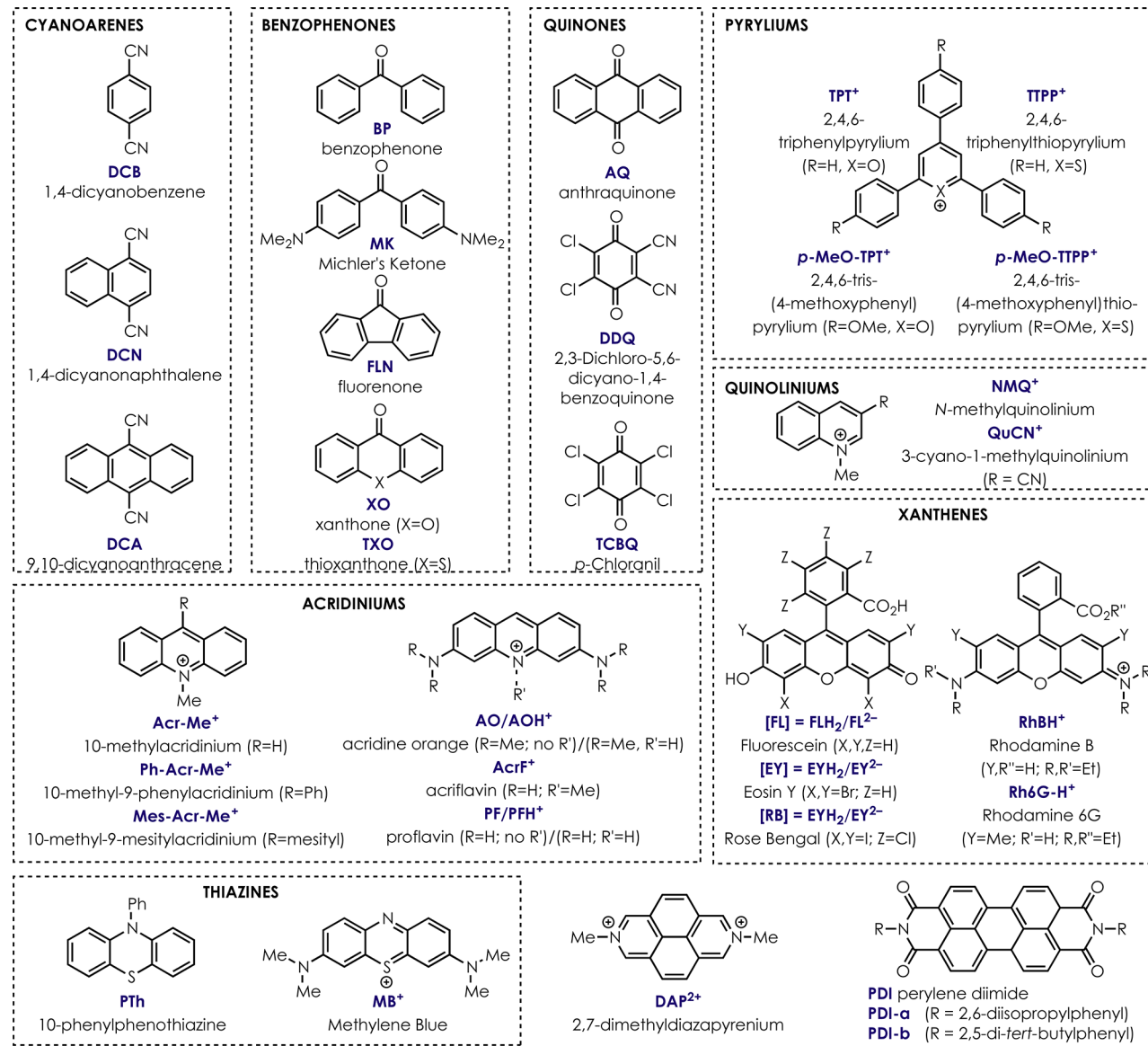
Recent literature reviews on photoredox catalysis have focused predominantly on the synthetic applications of transition metal chromophores.<sup>1–7</sup> Ruthenium and iridium polypyridyl complexes stand at the forefront of this class, and their well-demonstrated versatility in organic synthesis has garnered particular recognition of late. Despite the fact that organic chromophores have long been acknowledged for their ability to participate in photoinduced electron transfer (PET) processes, their catalytic use as applied to organic synthesis is somewhat less familiar. Topics in organic photoredox catalysis have been reviewed previously<sup>8–16</sup> but are relatively narrow in scope or predate recent important advances in catalyst development and the discovery of new reactivity. A comprehensive survey of the literature that encompasses the numerous organic photoredox classes and provides some historical context for new developments in the field is still lacking. It is our goal to provide this.

Still, one might inquire what organic photoredox catalysts have to offer compared to their transition metal counterparts. We hope the answer to this question will become clear as we explore the properties and reactivity of the organic molecules most commonly employed in synthesis as photoredox catalysts. Specifically, we wish to emphasize that organic photoredox catalysis offers far more than “metal-free” alternatives to transition metal catalyzed examples; namely, the potent reactivity afforded by many organic catalysts allows access to unique chemistries and a broad range of substrates that are unreactive in most synthetic contexts. Moreover, the diversity of these organic compounds presents a collection that promises to be useful in the discovery and optimization of new synthetic methodologies.

Scheme 1. Photophysical and Electrochemical Processes and Properties of Photoredox Catalysts



Scheme 2. Common Organic Photoredox Catalysts



## 2. PHOTOPHYSICAL AND ELECTROCHEMICAL CONSIDERATIONS

A recurring theme in this review is that the photophysical properties of an electronically excited molecule ultimately govern its photochemical reactivity. Accordingly, consideration of the properties of a photoredox catalyst in both the excited and ground states is crucial in effecting a desired reactivity. The recent surge of new synthetic applications for light-absorbing molecules was preceded by at least a century of photophysical and electrochemical studies of organic chromophores and ion radicals. Whether directly or indirectly, these efforts to characterize the behavior of excited state chromophores form the basis for their successful deployment as photoredox catalysts. Moreover, mechanistic studies on photoredox catalytic systems frequently rely on the same tools and techniques for analyzing the reaction mechanism and shaping the development of more effective catalysts. Given the indispensable role of photophysical studies in this recursive relationship between excited state properties and photochemical reactivity, we believe it is important to precede our survey of synthetic methodologies reported in the literature with a discussion of the photophysical and electrochemical foundations of organic photoredox catalysis.

### 2.1. Photophysical Processes

The rich photochemistry associated with organic molecules originates in a range of excited state energies and the rates which govern their photophysical processes. Simplified state energy diagrams such as the one pictured in Scheme 1 are used to frame the paradigm in which we understand the reactivity of a photoredox catalyst. This paradigm and the ensuing discussion of photophysical processes draw heavily from the treatise *Principles of Molecular Photochemistry* by Turro, Ramamurthy, and Scaiano.<sup>17</sup> We direct the reader toward this work for a more detailed description of the photophysical underpinnings of molecular excitation and photochemical reactions.

Absorption of light ( $+hv$ ) produces an electronically excited molecule. Typically, promotion of an electron to a higher energy level goes from a ground state singlet ( $S_0$ ) to a singlet excited state. With dependence on the energy of the electromagnetic radiation, a range of singlet excited states with different vibrational energies might be accessed, but within picoseconds, all higher lying excited states relax to the lowest energy, vibrationally equilibrated “first” singlet excited state,  $S_1$ . Considering only the photophysical pathways of an electronically excited molecule in isolation, the fate of  $S_1$  depends on both radiative and nonradiative pathways: radiative pathways are transitions to lower energy states by emitting light ( $-hv$ ), while the energy dissipated in a nonradiative transition is lost as heat.  $S_1$  can return to  $S_0$  either by fluorescence (a radiative transition) or by internal conversion, IC (a nonradiative transition), or it can proceed to  $T_1$  by a spin-forbidden, a nonradiative process known as intersystem crossing (ISC). Since the  $T_1 \rightarrow S_0$  transition is also spin forbidden,  $T_1$  states tend to be the longest-lived, decaying by radiative (phosphorescence) and nonradiative pathways as well, although the latter dominates under standard conditions.

With lifetimes stretching from the nanosecond to the millisecond regimes,  $S_1$  and  $T_1$  are the most likely excited states to participate in bimolecular reactions (i.e., reactions with a substrate), and each can undergo energy transfer (EnT) and electron transfer (ET). Photoinduced electron transfer, or PET, is a term used to refer to the overall process of excitation and electron transfer between the excited state molecule and a ground state molecule. The specific mechanisms by which each

bimolecular process occurs are beyond the scope of this review, but some general principles influencing both energy transfer and electron transfer emerge by considering the energies, lifetimes, and quantum yields of the excited states for a given molecule. Thus, we have compiled some relevant properties for the photoredox catalysts considered in this review (see Scheme 2) and provide this information in Table 1. Furthermore, we discuss how these values inform selection of an appropriate photoredox catalyst when probing new reactivity, along with how these properties impact analysis of photoredox reactions. The data illustrate the fact that the structural diversity of organic light-absorbing molecules gives rise to a diverse set of photophysical properties, which, in turn, influence their reactivity in PET processes.

### 2.2. Photophysical Properties of Organic Photoredox Catalysts

**2.2.1.  $\lambda_{\max}^{\text{abs}}$ : Local Absorbance Maximum for Lowest Energy Absorption.** One simple application of this value is in determining a source of irradiation for a given photoredox catalyst. The criterion that at least some overlap exists between an absorption of the molecule and emission of the lamp suffices for many purposes. Although excitation of any transition normally results in relaxation to the lowest energy singlet excited state, it is often desirable to irradiate the lowest energy (i.e., the most red-shifted) absorption from the standpoint of macroscopic energy efficiency and to reduce the likelihood of exciting other reactants with high-energy photons, which can lead to competing photochemical reactivity. In this regard, light emitting diodes (LEDs) have emerged as an important tool in photoredox catalysis, as they possess a relatively narrow emission band enabling selective excitation of chromophore and constitute an energy-efficient, high intensity light source.<sup>18–20</sup> Finally, the  $\lambda_{\max}^{\text{abs}}$  value gives some information about how much energy an excited state can contribute to a photoinduced electron transfer. Thus, although irradiation with visible light is attractive for a number of reasons, the longer the wavelength of absorption, the less energy the singlet and triplet excited states will possess.

**2.2.2.  $\tau_f$ : Lifetime of Fluorescence (Equal to the Inverse of the Fluorescence Decay Rate Constant, or  $1/k_f$ ) and  $\phi_f$ : Quantum Yield of Fluorescence.** These values are helpful in gauging whether the first singlet excited state  $S_1$  can effectively participate in a PET reaction by providing an approximate assessment of the lifetime of  $S_1$  and its propensity towards nonradiative deactivation pathways, namely, IC and ISC. The assumption that the nonradiative decay pathways are significantly slower than emission of a photon allows for the approximation that  $\tau_f \approx \tau_{S_1}$  (lifetime of  $S_1$ ). Fluorescence lifetimes of many organics range from 2 to 20 ns, and a general rule of thumb seems to be that fluorophores with  $\tau_f < 1$  ns will not readily participate in PET processes in the singlet state because the excited state decay approaches the rate constant of diffusion ( $k_{\text{diff}} \sim 1 \times 10^{10} - 2 \times 10^{10} \text{ s}^{-1}$ ). Generally speaking, the longer the lifetime of fluorescence, the greater the likelihood of encountering a quencher and undergoing PET. Moreover,  $\phi_f$  provides important information about nonradiative decay pathways: the higher the fluorescence quantum yield, the greater the likelihood of PET in the singlet excited state, because  $S_1$  is not highly susceptible to other deactivation pathways on the time scale that ET occurs. Fluorescence quantum yields near unity signify that essentially all molecules in  $S_1$  return to the ground state by emission of a photon and that nonradiative pathways are

**Table 1.** Photophysical and Electrochemical Properties of Organic Photoredox Catalysts

abbreviation	$\lambda_{\text{max}}^{\text{abs}}$ (nm)	$\tau_{\text{f}}$ (ns)	$\phi_{\text{f}}$	$\phi_{\text{ISC}}$	excited state energies (eV)		ground state redox potentials (V vs SCE)		excited state redox potentials (V vs SCE): S <sub>1</sub>		excited state redox potentials (V vs SCE): T <sub>1</sub>		
					$E_{0,0}^{\text{S}_1}$	$E_{0,0}^{\text{T}_1, \text{a}}$	$E_{1/2}^{\text{red}}$	$E_{1/2}^{\text{ox}}$	$E_{\text{red}}^{\text{S}_1}$	$E_{\text{ox}}^{\text{S}_1}$	$E_{\text{red}}^{\text{T}_1}$	$E_{\text{ox}}^{\text{T}_1}$	
DCB	290 <sup>21</sup>	9.7 <sup>22</sup>			4.01 <sup>22</sup>	3.04 <sup>23</sup>	-1.46 <sup>22</sup>		+2.55 <sup>22</sup>		+1.58 <sup>b,22,23</sup>		
DCN	325 <sup>24</sup>	10.3 <sup>25</sup>			3.57 <sup>25</sup>	2.41 <sup>23</sup>	-1.27 <sup>25</sup>		+2.3 <sup>b,25</sup>		+1.14 <sup>b,25,23</sup>		
DCA	422 <sup>26</sup>	14.9 <sup>25</sup>	0.76 <sup>c,27</sup>	0.0085 <sup>28</sup>	2.90 <sup>25</sup>	1.81 <sup>27</sup>	-0.91 <sup>25</sup>		+1.99 <sup>b,25</sup>		+0.9 <sup>b,25,27</sup>		
BP	335 <sup>d,29</sup>	0.008 <sup>30</sup>			1.0 <sup>31</sup>	3.22 <sup>30</sup>	3.0 <sup>30</sup>	-1.72 <sup>31</sup>	+2.39 <sup>31</sup>	+1.5 <sup>b,31,30</sup>	+1.28 <sup>b,31,30</sup>	-0.61 <sup>b,31,30</sup>	
MK	365 <sup>e,32</sup>				2.98 <sup>e,32</sup>	2.7 <sup>30</sup>	-2.20 <sup>f,34</sup>	+0.86 <sup>35</sup>	+0.76 <sup>b,34,32</sup>	-2.12 <sup>b,35,32</sup>	+0.48 <sup>b,34,30</sup>	-1.84 <sup>b,35,30</sup>	
FLN	377 <sup>36</sup>	16.2 <sup>31</sup>			0.97 <sup>31</sup>	2.31 <sup>31</sup>	-1.35 <sup>31</sup>	+1.7 <sup>31</sup>			+0.96 <sup>b,31</sup>	-0.61 <sup>b,31</sup>	
XO	340 <sup>37</sup>	<0.0 <sup>31</sup>			1.0 <sup>31</sup>	3.4 <sup>30</sup>	3.22 <sup>30</sup>	-1.65 <sup>31</sup>	+1.8 <sup>31</sup>	+1.76 <sup>b,31,30</sup>	-1.61 <sup>b,31,30</sup>	+1.57 <sup>b,31,30</sup>	-1.42 <sup>b,31,30</sup>
TXO	360 <sup>38</sup>	2 <sup>31</sup>			0.99 <sup>31</sup>	3.14 <sup>30</sup>	2.8 <sup>30</sup>	-1.62 <sup>31</sup>	+1.69 <sup>31</sup>	+1.52 <sup>b,31,30</sup>	-1.45 <sup>b,31,30</sup>	+1.18 <sup>b,31,30</sup>	-1.11 <sup>b,31,30</sup>
TCBQ	450 <sup>39</sup>				1.0 <sup>40</sup>	2.46 <sup>41</sup>	0.00 <sup>42</sup>				+2.46 <sup>b,42,41</sup>		
DDQ	~400 <sup>43</sup>				1.0 <sup>44</sup>	2.67 <sup>43</sup>	+0.49 <sup>42</sup>				+3.18 <sup>43</sup>		
AQ	326 <sup>e,45</sup>				1.04 <sup>46</sup>	2.73 <sup>46,47</sup>	-0.96 <sup>42</sup>				+1.77 <sup>b,42,46</sup>		
TPT <sup>+</sup>	415 <sup>g,48</sup>	4.38 <sup>25</sup>	0.58 <sup>g,48</sup>	0.42 <sup>48</sup>	2.83 <sup>25</sup>	2.3 <sup>h,49</sup>	-0.32 <sup>25</sup>		+2.55 <sup>b,48,25</sup>		+2.02 <sup>b,48,49</sup>		
p-OMeTPT <sup>+</sup>	422,470 <sup>h,50</sup>	4.0 <sup>9</sup>	0.95 <sup>9</sup>	0.03 <sup>52</sup>	2.34 <sup>i,50</sup>	2.21 <sup>h,49</sup>	-0.50 <sup>j,50</sup>		+1.84 <sup>b,50</sup>		+1.71 <sup>b,50,49</sup>		
			0.49 <sup>51</sup>										
TPPP <sup>+</sup>	414 <sup>50</sup>	3.6 <sup>g,54</sup>	0.03 <sup>54</sup>	0.94 <sup>52</sup>	2.64 <sup>i,50</sup>	2.28 <sup>55</sup>	-0.19 <sup>j,50</sup>		+2.45 <sup>b,50</sup>		+2.09 <sup>b,50,55</sup>		
p-OMeTPPP <sup>+</sup>	455 <sup>50</sup>				2.23 <sup>i,50</sup>		-0.33 <sup>j,50</sup>		+1.9 <sup>b,50</sup>				
NMQ <sub>+</sub>	315 <sup>56</sup>	20 <sup>57</sup>	0.79 <sup>k,58</sup>		3.50 <sup>22</sup>		-0.85 <sup>59</sup>		+2.70 <sup>59</sup>				
QuCN <sub>+</sub>	329 <sup>60</sup>	45 <sup>61</sup>			3.32 <sup>22</sup>		-0.60 <sup>62</sup>		+2.72 <sup>61</sup>				
			-0.79 <sup>63</sup>										
Acr-Me <sup>+</sup>		37, <sup>57</sup> 34 <sup>25</sup>	1.0 <sup>l,64</sup>		2.80 <sup>25</sup>		-0.46 <sup>25</sup>		+2.32 <sup>65</sup>				
Ph-Acr-Me <sup>+</sup>	424 <sup>66</sup>	1.5 <sup>66</sup>	0.063 <sup>66</sup>				-0.54 <sup>m,67</sup>						
Mes-Acr-Me <sup>+</sup>	425 <sup>68</sup>	6 <sup>69</sup>	0.035 <sup>69</sup>	0.38 <sup>69</sup>	LE: 2.67 <sup>69</sup>	LE: 1.94 <sup>69</sup>	-0.49 <sup>68</sup>		LE: +2.18 <sup>69</sup>		LE: +1.45 <sup>69</sup>		
			0.08 <sup>n,70</sup>		CT: 2.57 <sup>69</sup>		-0.57 <sup>71</sup>		CT: +2.08 <sup>69</sup>		CT: +1.88 <sup>72</sup>		
AO	425 <sup>73</sup>					2.58 <sup>73</sup>	-2.4 <sup>73</sup>				+0.60 <sup>o,73</sup>		
AOH <sup>+</sup>	495 <sup>73</sup>	1.8 <sup>75</sup>	0.18 <sup>l,76</sup>		2.58 <sup>d,77</sup>	2.07 <sup>77</sup>	-1.18 <sup>o,73</sup>				+0.95 <sup>o,73</sup>		
					2.43 <sup>p,78</sup>	2.13 <sup>p,78</sup>							
AcrF <sup>+</sup>	470 <sup>p,78</sup>		0.54 <sup>l,64</sup>		2.56 <sup>p,78</sup>	2.22 <sup>p,78</sup>							
PF	393 <sup>l,79</sup>												
PFH <sup>+</sup>	470 <sup>p,78</sup>	~5 <sup>l,80</sup>	0.39 <sup>l,76</sup>	0.10 <sup>l,81</sup>	2.56 <sup>p,78</sup>	2.22 <sup>p,78</sup>	-0.74 <sup>l,79</sup>		+1.82 <sup>b,79,78</sup>		+1.48 <sup>b,79,78</sup>		
PTh	<300 <sup>82</sup>	0.81-2.3 <sup>82</sup>			2.8 <sup>q,83</sup>	2.4 <sup>83</sup>	+0.68 <sup>83</sup>		-2.1 <sup>83</sup>		-1.7 <sup>b,83</sup>		
MB <sup>+</sup>	650 <sup>r,84</sup>	1.0 <sup>s,86</sup>	0.52 <sup>e,89</sup>	1.89 <sup>88</sup>	1.50 <sup>88</sup>	-0.30 <sup>d,f,77</sup>	+1.13 <sup>d,f,77</sup>	+1.56 <sup>d,f,77</sup>	-0.73 <sup>d,f,77</sup>	+1.60 <sup>d,f,77</sup>	-0.68 <sup>d,f,77</sup>		
		664 <sup>l,85</sup>	0.6 <sup>d,87,88</sup>		1.85 <sup>77</sup>						+1.14 <sup>b,77,88</sup>	-0.33 <sup>b,77,88</sup>	
[FL] <sup>t,u</sup>	FLH <sub>2</sub> :437 <sup>l,93</sup>	4.2 <sup>d,90</sup>	FLH <sub>2</sub> : 0.2 <sup>93</sup>	0.03 <sup>77</sup>	2.42 <sup>d,77</sup>	1.94 <sup>77</sup>	-1.17 <sup>d,f,77</sup>	+0.87 <sup>d,f,77</sup>	+1.25 <sup>d,f,77</sup>	-1.55 <sup>d,f,77</sup>	+0.77 <sup>d,f,77</sup>	-1.07 <sup>d,f,77</sup>	
		FL <sup>2-</sup> : 491 <sup>l,93</sup>	4.73 <sup>d,77</sup>	FL <sup>2-</sup> : 0.93 <sup>93</sup>			-1.22 <sup>d,f,90</sup>	+0.83 <sup>d,f,90</sup>					
[EY] <sup>u,t</sup>	S20 <sup>d,90</sup>	2.1 <sup>d,90</sup>	0.48 <sup>d,77</sup>	0.32 <sup>d,77</sup>	2.31 <sup>d,90</sup>	1.91 <sup>77</sup>	-1.08 <sup>d,f,77</sup>	+0.76 <sup>d,f,77</sup>	+1.23 <sup>d,f,77</sup>	-1.58 <sup>d,f,77</sup>	+0.83 <sup>d,f,77</sup>	-1.15 <sup>d,f,77</sup>	
		533 <sup>e,91</sup>	2.66 <sup>d,77</sup>	0.19 <sup>v,64</sup>			-1.13 <sup>d,f,90</sup>	+0.72 <sup>d,f,90</sup>					
[RB] <sup>u,t</sup>	549 <sup>92</sup>	0.50 <sup>77</sup>	0.09 <sup>d,77</sup>	0.77 <sup>d,77</sup>	2.17 <sup>d,77</sup>	1.8 <sup>77</sup>	-0.99 <sup>d,f,77</sup>	+0.84 <sup>d,f,77</sup>	+1.18 <sup>d,f,77</sup>	-1.33 <sup>d,f,77</sup>	+0.81 <sup>d,f,77</sup>	-0.96 <sup>d,f,77</sup>	
[RhB]	550 <sup>l,95</sup>	2.45 <sup>d,77</sup>	0.58 <sup>d,77</sup>	0.12 <sup>d,77</sup>	2.22 <sup>d,77</sup>	1.80 <sup>77</sup>	-0.96 <sup>d,f,77</sup>	+0.91 <sup>d,f,77</sup>	+1.26 <sup>d,f,77</sup>	-1.31 <sup>d,f,77</sup>	+0.84 <sup>d,f,77</sup>	-0.89 <sup>d,f,77</sup>	
[Rh6G]	530 <sup>e,96</sup>	4.13 <sup>d,97</sup>	0.90 <sup>l,98</sup>	0.002 <sup>99</sup>	2.32 <sup>100</sup>	2.09 <sup>99</sup>	-1.14 <sup>f,100</sup>	+1.23 <sup>102</sup>	+1.18 <sup>f,100</sup>	-1.09 <sup>b,100,102</sup>	+0.95 <sup>b,99,100</sup>	-0.86 <sup>b,99,102</sup>	

abbreviation	$\lambda_{\text{max}}^{\text{abs}}$ (nm)	$\tau_t$ (ns)	$\phi_r$	$\phi_{\text{ISC}}$	excited state energies (eV)		ground state redox potentials (V vs SCE)		excited state redox potentials (V vs SCE): $S_1$		excited state redox potentials (V vs SCE): $T_1$	
					$E_{0,0}^{S_1}$	$E_{0,0}^{T_1}$	$E_{1/2}^{\text{red}}$	$E_{1/2}^{\text{ox}}$	$E_{\text{red}}^{S_1}$	$E_{\text{ox}}^{S_1}$	$E_{\text{red}}^{T_1}$	$E_{\text{ox}}^{T_1}$
DAP <sup>a</sup>	418 <sup>103</sup>	10.5 <sup>1,104</sup>	0.5 <sup>1,104</sup>	~3.0 <sup>1,104</sup>	-0.46 <sup>m,103</sup>	-0.46 <sup>m,103</sup>	-0.46 <sup>m,105</sup>	-0.43 <sup>m,106</sup>	+1.63 <sup>m,f,107</sup>	+2.54	+0.77 <sup>b,106,105</sup>	+0.43 <sup>b,106,107</sup>
PDI-a/PDI-b	521 <sup>105</sup>	3.9 <sup>105</sup>	0.98 <sup>105</sup>	2.35 <sup>105</sup>	1.2 <sup>105</sup>	-0.92 <sup>g,101</sup>	-0.92 <sup>g,101</sup>	-0.92 <sup>g,101</sup>	+1.92 <sup>b</sup>	-0.72 <sup>b</sup>		

<sup>a</sup>Determined by the highest energy local maximum of phosphorescence spectrum, typically at 77 K in glassy medium; see reference for specific medium. <sup>b</sup>Calculated using the data from the indicated references. <sup>c</sup>In PhMe. <sup>d</sup>In MeOH. <sup>e</sup>Potential originally reported relative to the Ag/AgCl reference electrode; referenced to SCE by subtracting 0.039 V from the reported value.<sup>33</sup> <sup>g</sup>In DCM. <sup>h</sup>Medium not specified. <sup>j</sup>Determined from the highest energy fluorescence maximum. <sup>k</sup>Potential originally reported relative to NHE; referenced to SCE by subtracting 0.141 V from the value relative to NHE.<sup>53</sup> <sup>l</sup>Fluorescence quantum yield for N-ethylquinolinium in aqueous HClO<sub>4</sub>/NaClO<sub>4</sub> at pH 5.6.<sup>74</sup> <sup>m</sup>In H<sub>2</sub>O. <sup>n</sup>In DMF. <sup>o</sup>In DCE (1,2-dichloroethane). <sup>p</sup>Potential originally reported relative to the Fe<sup>2+</sup>/Fe couple; referenced to SCE by adding 0.42 V to the reported value.<sup>74</sup> <sup>r</sup>In 9:1 EtOH/MeOH. <sup>s</sup>In DMA. <sup>t</sup>4:1 MeCN/H<sub>2</sub>O. <sup>u</sup>In 0.1 M aq. NaOH. <sup>v</sup>In MeCN/CHCl<sub>3</sub>. <sup>w</sup>Disodium salt disodium used in refs 90–92.

Table 1. continued

much slower than  $k_f$ ; conversely, a low  $\phi_f$  indicates that the rate of nonradiative pathways are competitive with  $k_f$ .

**2.2.3.  $\phi_{\text{ISC}}$ : Quantum Yield of Intersystem Crossing (Frequently Used As Synonymous with Quantum Yield of Formation of  $T_1$ ,  $\phi_{T_1}$ ).** When  $k_{\text{ISC}}$  is fast enough to compete with  $k_f$  (and  $k_{\text{IC}}$ ), the  $T_1$  state can be populated and  $\phi_{\text{ISC}}$  can help to predict whether  $T_1$  will be an active excited state in a PET process. Lifetimes for triplet states ( $\tau_{T_1}$ ) are usually several orders of magnitude larger than  $S_1$  and on the order of microseconds to milliseconds. This is a consequence of the fact that the  $T_1 \rightarrow S_0$  is symmetry forbidden. We opt not to tabulate  $\tau_{T_1}$  lifetimes, in part because of the wide variability in these values is difficult to avoid, owing to the fact that strictly anaerobic conditions are required to preclude quenching by O<sub>2</sub>. Furthermore, decay of the  $T_1$  by phosphorescence or nonradiative pathways is usually orders of magnitude slower than electron transfer reactions. Thus,  $T_1$  are sufficiently long-lived that the efficacy of PET between a substrate and  $T_1$  is not significantly affected by  $\tau_{T_1}$ .

**2.2.4.  $E_{0,0}^{S_1}$ : Excited State Energy of the First Singlet Excited State  $S_1$ .** The excited state energy is often named with the subscript “<sub>0,0</sub>”, which refers to the transition between the lowest energy vibrational state ( $v = 0$ ) of  $S_1$  to  $v = 0$  of  $S_0$ , which can be estimated at the intersection between normalized symmetrical absorbance and emission spectra after converting the wavelength axis to an energy scale or by finding the midpoint between absorption and emission maxima (i.e., one-half the Stokes shift). Alternative methods for estimating excited state energy include selecting the energy at the earliest onset (highest energy) of fluorescence or at the fluorescence maximum. The “earliest onset” method is arbitrary and may overestimate the true excited state energy, while the “fluorescence maximum” method is likely to underestimate  $E_{0,0}^{S_1}$ .

**2.2.5.  $E_{0,0}^{T_1}$ : Excited State Energy of the First Triplet Excited State  $T_1$ .** Because  $S_0 \rightarrow T_1$  seldom occurs at room temperature and phosphorescence under the same conditions is also rare, this value is less readily obtained than for  $S_1$ . Moreover,  $E_{0,0}^{T_1}$  is most often read from the phosphorescence maximum, which almost always requires cryogenic conditions to maximize phosphorescence as the dominant decay pathway. Under these conditions, the emission spectrum usually exhibits enough structure to allow assignment of  $E_{0,0}^{T_1}$  as an  $E_{0,0}$ .

Note that we present  $E_{0,0}^{S_1}$  and  $E_{0,0}^{T_1}$  in units of eV to allow for easy combination with electrochemical potential (in units of V) in order to estimate excited state redox potentials. See the discussion below.

### 2.3. Electrochemistry: Thermodynamics of Electron Transfer and Photoinduced Electron Transfer

**2.3.1. Electron Transfer in the Ground State.** The general equation describing the free energy of a single electron transfer is

$$\Delta G_{\text{ET}} = -\mathcal{F}(\Delta E) = -\mathcal{F}(E_{\text{red}} - E_{\text{ox}}) \\ = -\mathcal{F}(E_{1/2}(\text{A}/\text{A}^{\bullet-}) - E_{1/2}(\text{D}^{\bullet+}/\text{D})) \quad (1)$$

where  $\mathcal{F}$  is the Faraday constant (23.061 kcal V<sup>-1</sup> mol<sup>-1</sup>) and  $E_{\text{red}}$  and  $E_{\text{ox}}$  are ground state redox potentials obtained experimentally for each species A and D undergoing reduction and oxidation, respectively.  $E_{\text{red}}$  refers to a reduction potential and is the common shorthand for  $E_{1/2}(\text{A}/\text{A}^{\bullet-})$ , or single electron reduction of an acceptor A according to the half reaction  $\text{A} \rightarrow \text{A}^{\bullet-}$ . As experimentally measured by electrochemical means,  $E_{\text{red}}$  values are negative (<0 V) for most ground state species, since

single electron reduction is thermodynamically unfavorable for most compounds under standard conditions.  $E_{\text{ox}}$  is, by convention, referred to as an oxidation potential but is more accurately written as  $E_{1/2}(\text{D}^+/\text{D})$ , describing the reduction half reaction  $\text{D}^+ \rightarrow \text{D}$ . This value is generally positive for most molecules of interest because single electron reduction of  $\text{D}^+$  is energetically favorable (by eq 1). Thus, despite their conventional handles, both  $E_{\text{red}}$  and  $E_{\text{ox}}$  actually describe reduction half reactions. This oddity in the convention of naming  $E_{1/2}(\text{D}^+/\text{D})$  as  $E_{\text{ox}}$  is a likely cause for confusion that probably originates in the voltammetric collection of the value, in which the oxidation event occurs at a positive potential.

Moreover, at the risk of perpetuating the confusion, use of the terms reduction potential and oxidation potential in reference to  $E_{\text{red}}$  and  $E_{\text{ox}}$  is unavoidable and may actually have value in describing which half reactions are under discussion for the components of a redox reaction. Whatever subscript is used, we advocate that the redox couple be parenthetically clarified wherever possible, always writing from right to left the (reactant/product) pair of a reduction half reaction. For example, we will use the following notation throughout this review:  $E_{\text{red}}$  or  $E_{\text{red}}(\text{A}/\text{A}^\bullet)$  is defined by the half reaction  $\text{A} \rightarrow \text{A}^\bullet$  and may be referred to as the “reduction potential of A.”  $E_{\text{ox}}$  or  $E_{\text{ox}}(\text{D}^\bullet/\text{D})$  is defined by the half reaction  $\text{D}^\bullet \rightarrow \text{D}$  and may be referred to as the “oxidation potential of D.” We also recommend always specifying the reference electrode and, where possible, the solvent used in the determination of a redox potential. All potentials reported in this review can be assumed to be collected in acetonitrile (MeCN) unless otherwise noted.

**2.3.2. Photoinduced Electron Transfer.** The common formulation for determining the free energy of a photoinduced electron transfer (PET) is

$$\Delta G_{\text{PET}} = -\mathcal{F}[E_{\text{ox}}(\text{D}^+/\text{D}) - E_{\text{red}}(\text{A}/\text{A}^\bullet)] - w - E_{0,0} \quad (2)$$

which is frequently and incorrectly referred to as the “Rehm-Weller Equation.” We emphasize that IUPAC defines this general equation form as the “Gibbs energy of photoinduced electron transfer” and expressly recommends that it should not be called the “Rehm-Weller equation”,<sup>108</sup> which is an empirical correlation that relates the bimolecular rate constant for PET ( $k_{\text{PET}}$ ) with  $\Delta G_{\text{PET}}$ .<sup>109–111</sup> An important feature of eq 2 is  $E_{0,0}$  (in the same units as  $\Delta G$  in this formulation), or the excited state energy for a given excited state  $\text{cat}^*$  (see above).

Eq 2 also includes an electrostatic work term  $w$ , which accounts for the solvent-dependent energy difference due to the Coulombic impact of charge separation. Rehm and Weller are recognized for including this term in their calculation of  $\Delta G_{\text{PET}}$ , which was estimated to be ~0.06 eV in acetonitrile.<sup>110,111</sup> Generally, this term is larger in magnitude in less polar solvents ( $w \propto 1/\epsilon$ , where  $\epsilon$  is the solvent dielectric constant), and it depends on the charge of the reactants and the products following ET. Except in detailed photophysical studies where solvent effects are analytically addressed, the  $w$  term is frequently omitted on the basis that the correction of  $w$  to  $\Delta G_{\text{PET}}$  is a relatively small one (generally <0.1 eV).<sup>112</sup> Additionally, in-depth studies in the past two decades have revealed that the sign and magnitude of  $w$  are highly system dependent,<sup>113–117</sup> precluding adoption of a general model for this correction as addressed in this review. We emphasize that there are certainly cases where the  $w$  term can have a significant impact on mechanistic analysis or reaction optimization; however, this is unlikely to be an important consideration when approaching the

development of a photoredox reaction, and we omit  $w$  in the ensuing discussion.

Moreover, omission of the  $w$  term allows for a simpler calculation of the excited state redox potential of a given photoredox catalyst  $\text{cat}$ . We find it instructive to consider the excited state redox potentials  $E_{\text{red}}^*(\text{cat}^*/\text{cat}^\bullet)$  or  $E_{\text{ox}}^*(\text{cat}^+/\text{cat}^*)$  as benchmarks when evaluating the plausibility of a substrate reacting with a photoredox catalyst in the excited state. When a PET involves reduction of the excited state  $\text{cat}^*$  and oxidation of the ground state substrate “sub”,

$$\Delta G_{\text{PET}} = -\mathcal{F}(E_{\text{red}}^*(\text{cat}^*/\text{cat}^\bullet) - E_{\text{ox}}(\text{sub}^\bullet/\text{sub})) \quad (3)$$

where  $E_{\text{red}}^*$  is the excited state reduction potential of  $\text{cat}$ .  $E_{\text{red}}^*$  is calculated by

$$E_{\text{red}}^*(\text{cat}^*/\text{cat}^\bullet) = E_{\text{red}}(\text{cat}/\text{cat}^\bullet) + E_{0,0} \quad (4)$$

Note that  $\text{cat}^*$  refers to either the  $S_1$  or  $T_1$  excited state, with the corresponding  $E_{0,0}$  value ( $E_{0,0}^{S_1}$  or  $E_{0,0}^{T_1}$ ).

When a PET involves oxidation of the excited state  $\text{cat}^*$  and reduction of the ground state  $\text{sub}$ ,

$$\Delta G_{\text{PET}} = -\mathcal{F}(E_{\text{red}}(\text{sub}/\text{sub}^\bullet) - E_{\text{ox}}^*(\text{cat}^\bullet/\text{cat}^*)) \quad (5)$$

where  $E_{\text{ox}}^*$  is the excited state oxidation potential of  $\text{cat}$  and is calculated by

$$E_{\text{ox}}^*(\text{cat}^\bullet/\text{cat}^*) = E_{\text{ox}}(\text{cat}^\bullet/\text{cat}) - E_{0,0} \quad (6)$$

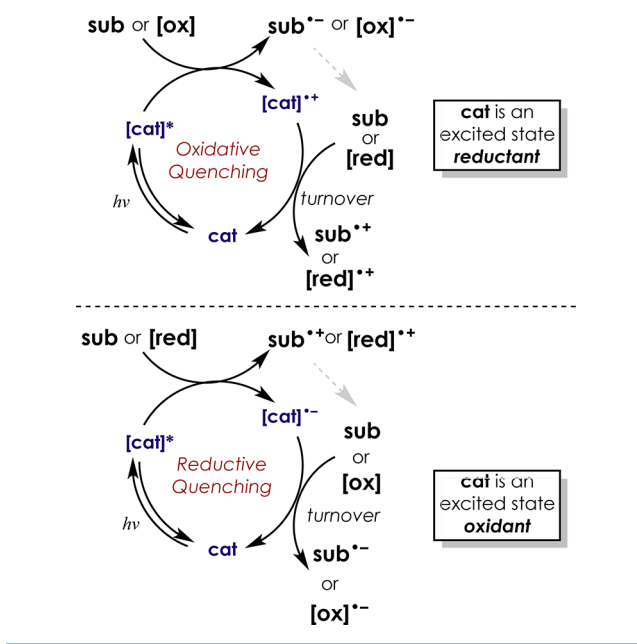
Note that we list  $E_{0,0}$  in units of electronvolts, while  $E_{\text{red}}$  and  $E_{\text{ox}}$  are in volts, but the two are combined in eqs 4 and 6 as if they possess the same units, assuming a conversion factor of 1 eV/V. This is commonplace when approaching a single electron transfer on a per molar basis.

Although eqs 3 and 5 are fundamentally equivalent to eq 2 (after the omission of  $w$ ), we believe they provide a more intuitive framework when approaching photoredox catalysis from the perspective that the structural and energetic characteristics of photoredox catalysts in the excited state define their unique patterns of PET reactivity. Thus, for a photoredox catalyst acting as an excited state oxidant,  $E_{\text{red}}^*$  is positive, and for a photoredox catalyst acting as an excited state reductant,  $E_{\text{ox}}^*$  is negative. Evaluation of a supposed PET process is essentially informed by qualitative estimation of  $\Delta G_{\text{PET}}$ . Accordingly, eqs 3 and 5 make for simple tools when selecting a photoredox catalyst for a desired transformation. If photoinduced oxidation of substrate  $\text{sub}$  is to be feasible,  $E_{\text{red}}^*$  of photoredox catalyst  $\text{cat}^*$  must be more positive than  $E_{\text{ox}}$  of substrate  $\text{sub}$ . Likewise, if reduction of substrate  $\text{sub}$  is intended,  $E_{\text{ox}}^*$  of photoredox catalyst  $\text{cat}^*$  must be more negative than  $E_{\text{red}}$  of substrate  $\text{sub}$  for PET to be thermodynamically favorable.

### 3. GENERAL MECHANISTIC SCHEMES FOR PHOTOREDOX CATALYSIS

Most photoredox catalytic reactions follow one of the two mechanistic schemes depicted in Scheme 3. Each of these PET cycles is categorized by the primary direction of the ET with respect to the excited state catalyst  $\text{cat}^*$ : in an oxidative quenching cycle, the excited state  $\text{cat}^*$  is quenched by donating an electron either to  $\text{sub}$  or an oxidant [ox] present in the reaction mixture; in a reductive quenching cycle,  $\text{cat}^*$  is quenched by accepting an electron from  $\text{sub}$  or a reductant [red]. The catalyst turnover step involves reduction of the oxidized  $[\text{cat}]^\bullet$  in the oxidative cycle and oxidation of the reduced  $[\text{cat}]^\bullet$  in the reductive cycle. In either case, the

**Scheme 3. Oxidative and Reductive Quenching Cycles of a Photoredox Catalyst**



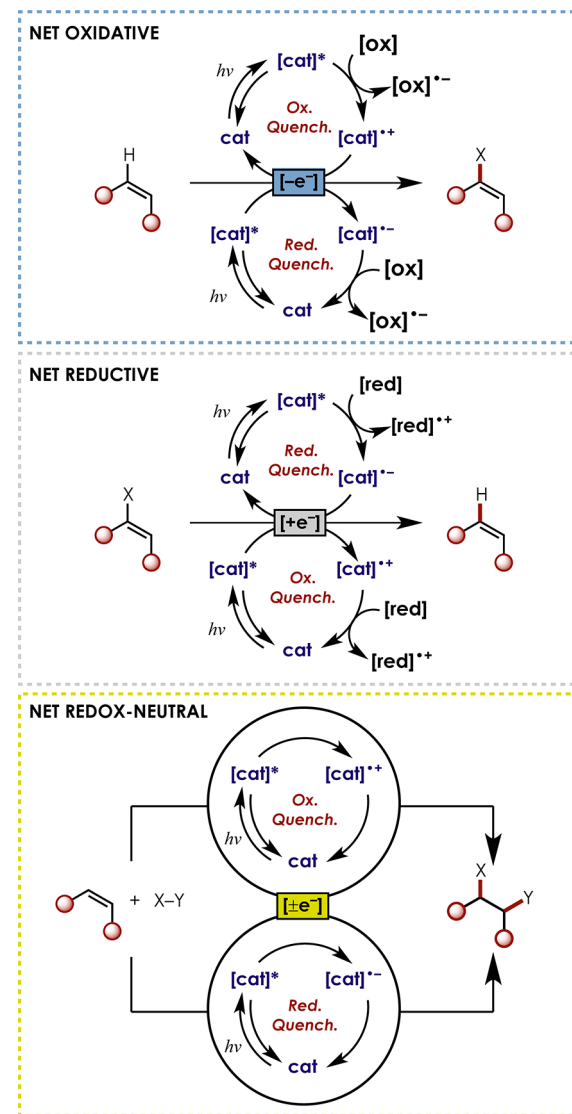
substrate, an external redox-active reagent, or an intermediate may be responsible for catalyst turnover.

Regardless of whether the substrate undergoes an ET reaction in the PET step or the turnover step, there are three general redox outcomes possible for the substrate in either quenching manifold: net oxidative, net reductive, and net redox-neutral. **Scheme 4** illustrates these groupings along with a general example for each overall reaction type. A net oxidative reaction requires an external oxidant, which can accept electrons in either the PET step or the turnover step. Likewise, net reductive reactions involve an external reductant donating electrons during the PET or turnover steps. Net redox-neutral processes are more complex and often involve return electron transfer with the oxidized or reduced catalyst, sometimes mediated by a redox-active co-catalyst. Additionally, **Scheme 4** introduces a symbolic representation for the net redox outcome that we will use throughout this review to denote reaction type. As indicated,  $[-e^-]$  refers to a net oxidative reaction,  $[+e^-]$  refers to a net reductive reaction, and  $[\pm e^-]$  refers to a net redox-neutral reaction. This symbolic representation is intended to be conceptual and does not specify the number of electrons transferred in a given process. Moreover, there are certainly exceptions to this general classification, including overall transformations that consist of multiple sequential photoredox steps, but these delineations are descriptive for a majority of photoredox catalytic reactions.

### 3.1. Definitions

We note that a number of different labels have been used to describe molecules which participate in light driven chemical processes without being consumed, including “photocatalyst”, “photosensitizer” (or simply “sensitizer”), and “PET sensitizer.” However, we believe the term “photoredox catalyst” provides a more precise term for several reasons: (a) “photocatalyst” implies the catalytic involvement of photons, which is relevant in transformations which proceed by chain mechanisms but is misleading for those that do not, and (b) we avoid the usage of any terms related to “sensitizer,” as this is traditionally used to

**Scheme 4. Net Redox Outcomes for Photoredox Transformations**



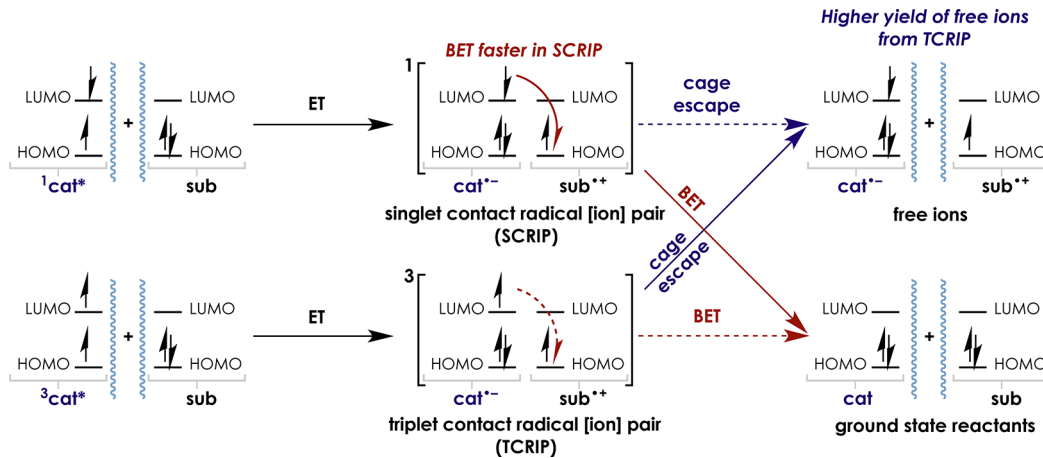
describe a molecule which participates in energy transfer processes, particularly the “sensitization” of dioxygen ( $O_2$ ).

Thus, the defining feature of a photoredox catalyst is the ability to undergo a redox reaction in the excited state, and a subsequent turnover step enables participation in light-driven catalytic redox cycles like those shown in **Scheme 3**. While the major focus of this review is on synthetic methodologies that employ catalytic quantities of an organic chromophore, we will highlight select cases where stoichiometric loadings are used, particularly in examples that eventually lead to catalytic conditions or in examples that demonstrate the limitations of a given photoredox system. In some of these cases, a photoredox catalytic cycle may be mechanistically tenable, but catalysis is precluded for other reasons.

### 3.2. Other Mechanistic Considerations

**3.2.1. Chain Mechanisms.** The mechanisms shown in **Scheme 3** are idealized representations of reactions proceeding exclusively through PET manifolds in a one photon/one product paradigm. Realistically, the efficiencies of many photoredox-catalyzed reactions are well below a quantum yield of reaction ( $\phi_R$ ) of 1, which is the maximum if only the PET cycles in

Scheme 5. Cage Escape and Back Electron Transfer (BET) in Singlet and Triplet Radical Ion Pairs



**Scheme 3** are operating. However, in some cases, an intermediate may be capable of donating or accepting an electron to initiate a new chain, rendering possible  $\phi_R$  values greater than unity. Recently, Yoon and Cismesia demonstrated that a number of transition metal photoredox reactions exhibit a significant component of chain transfer,<sup>118</sup> and these insights can be extended to analogous reactions using organic photoredox catalysts. Although not often considered as a mechanistic possibility, select cases discussed below confirm that chain transfer is operable in some reactions. Whether a proposed intermediate is capable of chain electron transfer can be estimated by considering the redox potential of the intermediate, which, although challenging to obtain, have been studied experimentally<sup>119,120</sup> and computationally.<sup>121</sup> Furthermore, the groups of Yoon<sup>118</sup> and König/Riedle<sup>122</sup> have each developed simplified methods for determining  $\phi_R$  and evaluating the extent of chain transfer.

**3.2.2. EDA Complexes and Exciplexes.** Occasionally, control experiments reveal that some degree of photolytic reactivity can occur in the absence of a photoredox catalyst, even when the individual reactants are transparent in the wavelength range of irradiation. A noticeable color change upon mixing the two reactants may signal the formation of an electron donor–acceptor (EDA) complex (alternatively referred to as a “charge-transfer complex”). The mechanistic underpinnings and reactivity of these species was established by Kochi<sup>123–126</sup> and has recently been harnessed by Melchiorre<sup>127–130</sup> and others<sup>131</sup> to achieve catalyst-free photolytic transformations using visible light, enabled by the fact that EDA complexes cooperatively absorb a photon at a lower energy (longer wavelength) than either reactant. As a mechanistic consideration in photoredox catalysis, EDA complexes may be responsible for background reactivity (i.e., uncatalyzed), although some examples will be addressed where direct irradiation of a reactant EDA complex leads to a divergent outcome. Moreover, EDA complexation can occur between a substrate and a photoredox catalyst, also resulting in a new, red-shifted absorbance feature. Although rarely characterized in photoredox catalytic methods because the ET outcome is presumably the same, this equilibrium can confer a favorable impact on reactivity through the effects of pre-association and a potentially broader cross section of irradiation.

Ground state EDA complexes are distinct from exciplexes, which are excited state complexes that cooperatively emit a photon. As it pertains to our discussion, exciplexes are often in play when an excited state electron-deficient photoredox catalyst,

such as a cyanoarene, encounters an electron-rich substrate. Evidence of exciplex formation is observed in the fluorescence spectra as a broad feature which is red-shifted relative to the maximum of the uncomplexed fluorescence. Exciplexes are not always characterized or considered as mechanistic intermediates, probably because these complexes usually lead to the same outcome (i.e., radical [ion] pairs) as if the exciplex did not form. On the other hand, photophysical study of PET processes involving exciplexes has been shown to require special treatment.<sup>113,114,132</sup>

**3.2.3. Energy Transfer vs Electron Transfer.** The first synthetic uses of a number of the light-absorbing molecules included in this review were as “photosensitizers,” initiating a reaction by transfer of their excited state energy to a substrate.<sup>133,134</sup> Examples such as methylene blue, rose bengal, and benzophenone possess relatively high triplet yields and long triplet lifetimes and are perhaps better known as triplet sensitizers than they are as PET catalysts. One of the most common applications of triplet energy transfer is in the generation of singlet dioxygen ( $^1\text{O}_2$ )<sup>135–138</sup> by photo-sensitization of the ground state triplet dioxygen ( $^3\text{O}_2$ ). Although  $^1\text{O}_2$  has useful applications in synthesis, it is often considered an unwelcome byproduct whose high reactivity is expected to interfere with intended chemistries.

By our definition, photoredox catalysis does not include mechanisms involving energy transfer. Although the outcome of energy transfer processes is distinct and recognizable in select cases (e.g., the Schenck-Ene reactivity of olefins and  $^1\text{O}_2$ <sup>139</sup>), ET and energy transfer might not be readily distinguishable in other systems. Thus, although we focus only on catalytic manifolds where a PET cycle is presumed, we recognize the possibility that some of the transformations we discuss may proceed partially or completely through energy transfer pathways. We discuss cases where the primary reports address the possible involvement of both pathways, but we also take note of a general observation that PET mechanisms seem to dominate even in examples where the photoredox catalyst is known to participate in either PET or energy transfer processes. For triplet sensitization, this may be rationalized by considering the relatively high triplet energies for typical organic molecules used as substrates in photoredox reactions, which usually exceed 60 kcal mol<sup>-1</sup> (2.6 eV).<sup>140</sup>

#### 3.2.4. Singlet or Triplet Excited States: Does It Matter?

It is clear from **Scheme 1** and the data in **Table 1** that the  $S_1$  states are more potent oxidants and reductants than the corresponding  $T_1$  states. For this reason,  $S_1$  states have a larger range of oxidizing

or reducing capabilities, and can engage substrates with redox potentials high in magnitude. Interestingly, even though ET with a  $\text{cat}^*$  in the  $T_1$  can occur with a fast bimolecular rate constant comparable to that of  $S_1$  when  $\Delta G_{\text{PET}}$  is largely negative for both states, the  $T_1$  state may actually be less susceptible to back electron transfer (BET) between radical [ion] pairs.

**Scheme 5** compares ET between sub and  ${}^1\text{cat}^*$  or  ${}^3\text{cat}^*$  for a reductive quenching event: the contact radical [ion] pairs following ET retain the overall spin multiplicity of the excited state catalyst. In either case, BET can lead to the free ions or the ground state reactants, but since BET in the triplet contact radical [ion] pair (TCRIP) would require an intersystem crossing, BET in the singlet contact radical [ion] pair (SCRIP) is faster. This is consistent with experimental studies in which the overall efficiency of free ion formation was higher when ET occurred from a triplet  ${}^3\text{cat}^*$ ,<sup>141</sup> with one study estimating that a  ${}^3\text{cat}^*$  produced twice as many free ions as the corresponding  ${}^1\text{cat}^*$ .<sup>142</sup> Thus, for reactions whose efficiencies suffer from BET, the triplet state of the photoredox catalyst may be the most important excited state.

#### 4. CYANOARENES: POLCYANO-BENZENES, NAPHTHALENE, AND ANTHRACENES

##### 4.1. Photophysical and Electrochemical Characteristics

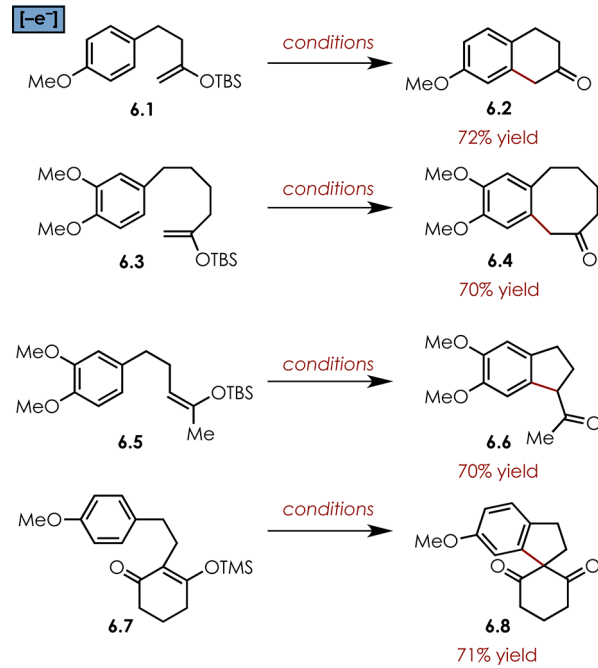
The photophysical and electron transfer properties of cyanoarenes have been investigated extensively and are classic exemplars of excited state electron transfer occurring primarily through the singlet excited state. Cyanoarenes, such as *p*-DCB, DCN, and DCA, have large singlet excited state energies, which, even when paired with moderately large ground state reduction potentials ranging from  $-0.7$  to  $-1.7$  V, render them capable of oxidizing compounds with oxidation potentials exceeding  $+2.0$  V. Furthermore, the radical anions resulting from photoinduced electron transfer are moderate to good reductants, and turnover with mild oxidants such as dioxygen ( $\text{O}_2$ ) is feasible under aerobic conditions [ $E_{1/2}(\text{O}_2/\text{O}_2\bullet^-) = -0.87$  V vs SCE in MeCN]<sup>143</sup>, producing the neutral, ground state cyanoarene and superoxide ( $\text{O}_2\bullet^-$ ). From a practical perspective, the cyanoarenes with increased benzannulation (i.e., DCN and DCA) are most useful, as they absorb in the near UV and visible and possess longer singlet lifetimes than simple cyanobenzenes. It is frequently the case with the neutral cyanoarenes that efficiency of PET suffers from BET, typically occurring before solvation of the contact radical [ion] pair. To combat BET, an appropriate mediator of ET is often included to improve cage escape; biphenyl ( $\text{Ph}-\text{Ph}$ ) is commonly employed for this purpose,<sup>144,145</sup> undergoing PET primarily and with high efficiency,<sup>146</sup> while the substrate is oxidized to the cation radical in a secondary ET with the biphenyl cation radical ( $\text{Ph}-\text{Ph}\bullet^+$ ).

##### 4.2. Reactions

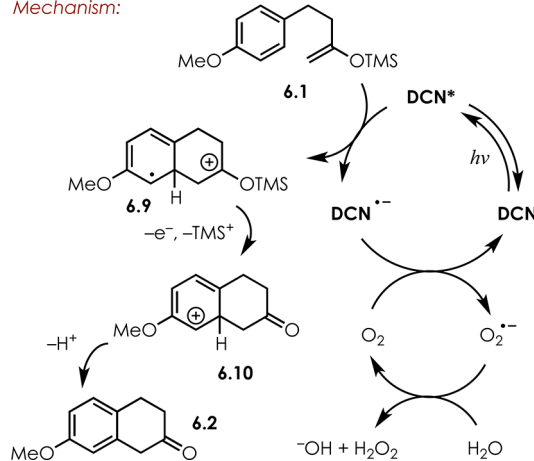
**4.2.1. Net Oxidative Transformations Involving Cyanoarene Photooxidants.** **4.2.1.1. Oxidative Arylation Reactions.** Dicyanoarenes are effective catalysts for net  $\alpha$ -arylation reactions of ketones. Pandey and coworkers demonstrated a series of oxidative annulation reactions of silyl enol ethers with pendant electron-rich aromatics.<sup>147</sup> Under aerobic conditions using DCN as the single electron photooxidation catalyst, a range of different cyclization modes were possible to form 5–8 membered ring systems via both *endo*- (**6.1**, **6.3**) and *exo*- (**6.5**, **6.7**)-type annulations (**Scheme 6**). All of the aromatics investigated in the transformations bore either one or two

methoxy substituents, seemingly a requirement for successful cyclization.

##### Scheme 6. Oxidative $\alpha$ -Arylation of Ketones



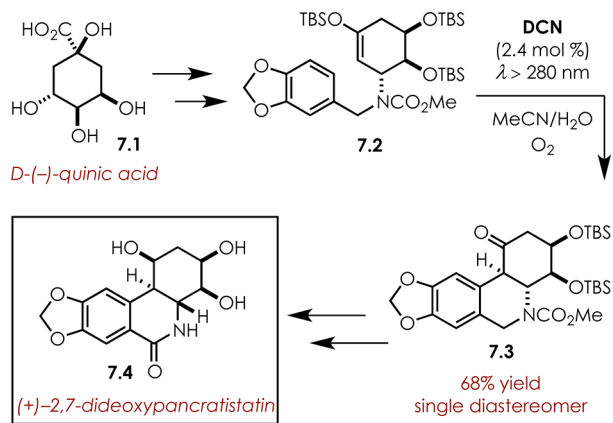
Mechanism:



The mechanism for these transformations is proposed to involve single electron oxidation of the silyl enol ether substrate (**6.1**), followed by cyclization to furnish distonic cation radical **6.9**. Loss of trimethylsilyl cation and a second single electron oxidation event leads to cyclohexadienyl cation **6.10**, which is poised to lose a proton to furnish the ketone adduct (**6.2**) observed. Regeneration of the DCN is proposed to occur via single electron oxidation of DCN anion radical by molecular oxygen, with the end result that hydrogen peroxide is produced as the side product as an overall two-electron oxidation process.<sup>148</sup>

This method was used in elegant fashion by the Pandey laboratory as the key step in the synthesis of (+)-2,7-dideoxypancratistatin (**7.4**) (**Scheme 7**).<sup>149</sup> Starting from (−)-quinic acid (**7.1**), elaboration to silyl enol ether **7.2**, provided the key intermediate for the oxidative annulation

**Scheme 7. Synthesis of (+)-2,7-Dideoxypancratistatin via Silyl Enol Ether Oxidative Cyclization**



reaction. Using similar conditions to those previously developed by the group,<sup>147</sup> irradiation of 7.2 with 2.4 mol % of DCN under aerobic conditions afforded tetrahydroisoquinoline 7.3 in a 68% yield and as a single diastereomer. Five additional synthetic steps completed the synthesis of (+)-2,7-dideoxypancratistatin (7.4).

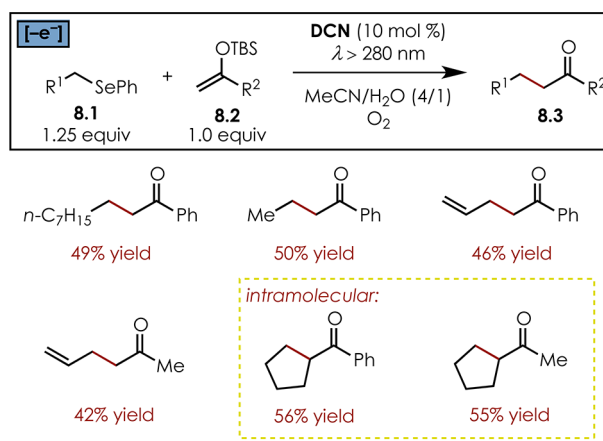
**4.2.1.2. Oxidative Alkylation Reactions.** In work by the same laboratory, a strategy for  $\alpha$ -alkylation of ketones was also accomplished using silyl enol ethers as nucleophiles.<sup>150</sup> Several primary alkyl and allyl phenyl selenides (8.1) were used as intermolecular alkylating agents for silyl enol ethers (8.2), affording the  $\alpha$ -alkylated ketones (8.3) in 42–50% isolated yields after an approximately 70% conversion (Scheme 8). Two additional intramolecular examples to form cyclopentane structures were also shown.

The reaction bears the mechanistic hallmarks of the ketone  $\alpha$ -arylation reaction reported by Pandey and coworkers (Scheme 8).<sup>147</sup> It is presumed that oxidation of the alkyl selenides 8.1 outcompetes the silyl enol ether (8.2) oxidation due to a more exergonic electron transfer event (cf.  $\Delta G_{ET} = -10.8 \text{ kcal mol}^{-1}$  for 8.2 and  $-13.0 \text{ kcal mol}^{-1}$  for 8.1).<sup>151</sup> On this basis, generation of cation radical 8.4 is anticipated to give the active electrophile which is intercepted by the silyl enol ether to furnish the alkylated adducts while expelling the phenyl selenyl radical and *tert*-butyldimethylsilyl cation. Regeneration of the photooxidant is proposed to occur as described in Scheme 8, and  $\text{PhSe}\bullet$  was observed to dimerize to  $\text{PhSeSePh}$ .

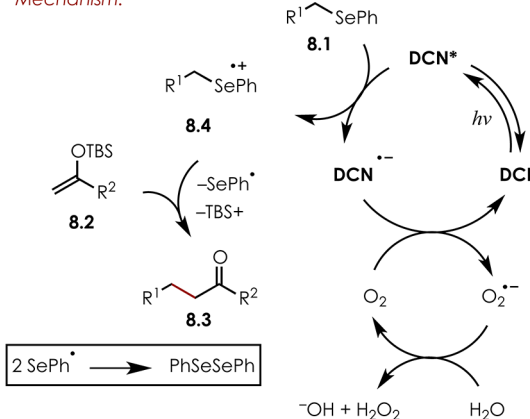
**4.2.1.3. Oxidative Aryl–Aryl Coupling Reactions.** An unusual intramolecular biaryl coupling of tri-1-naphthyl phosphates (9.1) was realized using DCA as a photoredox catalyst to give binaphthalenes (9.3) and mono-1-naphthyl phosphates (9.2).<sup>152,153</sup> Transient absorption spectroscopy measurements indicated that single electron oxidation of the trinaphthyl phosphate by excited state DCA occurs to furnish cation radical 9.4 (Scheme 9). A  $\pi$ -dimer of 9.4 was observed to form and after elimination gave rise to cation radical 9.6 as well as diradical 9.5. Reduction of 9.6 by  $\text{DCA}^\bullet-$  furnishes the final binaphthyl adduct (9.3), and it is presumed that 9.5 goes on to abstract hydrogen atoms from the solvent to furnish 9.2.

**4.2.1.4. Oxidative C–H Functionalization Reactions.** A dehydrogenative benzylic amination using organic photoredox catalysis was recently described by Pandey and coworkers.<sup>154</sup> Using *N*-methoxyamides (10.2) as the nitrogen source, a variety of substrates with benzylic protons (10.1) underwent amination under aerobic atmosphere with catalytic quantities of DCA when irradiated with a 450 W medium pressure mercury lamp with a

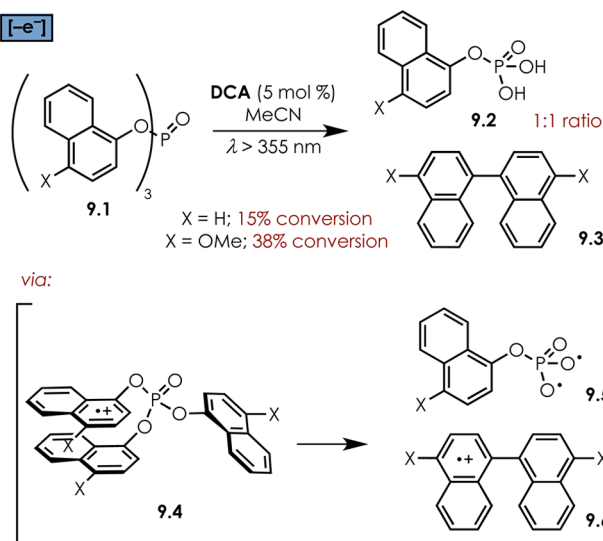
**Scheme 8. Oxidative Alkylation of Silyl Enol Ethers with Alkyl Phenyl Selenides**



#### Mechanism:

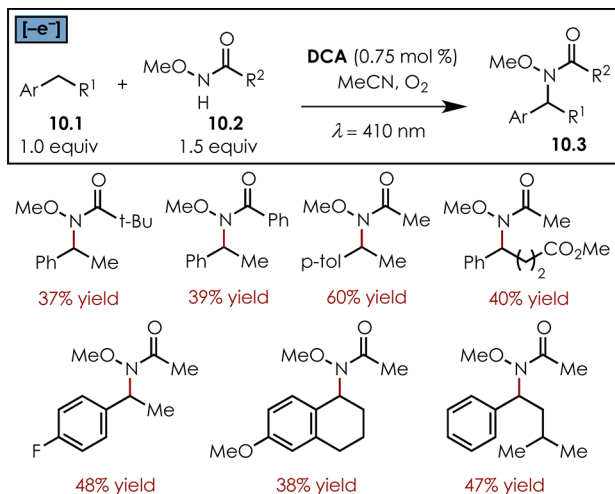


**Scheme 9. Oxidative Biaryl Coupling of Trinaphthyl Phosphates**



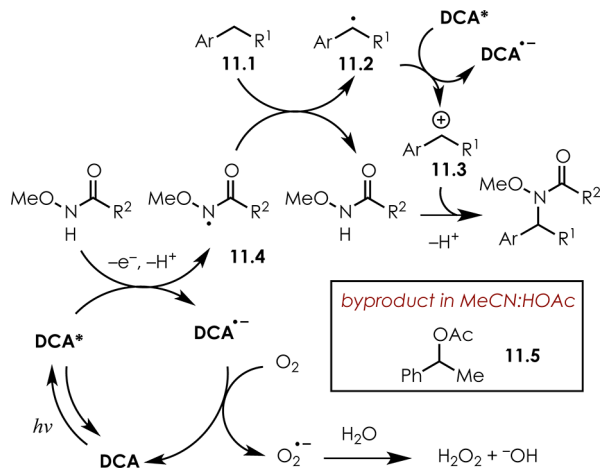
$\text{CuSO}_4:\text{NH}_3$  filter (Scheme 10). Functional group compatibility is good with respect to the aromatic substituents, and amination occurs at the most electron-rich benzylic C–H bond. Complete consumption of the benzylic substrates was never achieved, even after prolonged irradiation, potentially pointing to product inhibitory effects.

**Scheme 10. Benzylic Oxidative Aminations via Cyanoarene Photoredox Catalysis**



Control experiments lend support for the mechanism depicted in Scheme 11. Single electron oxidation of the methoxyamide,

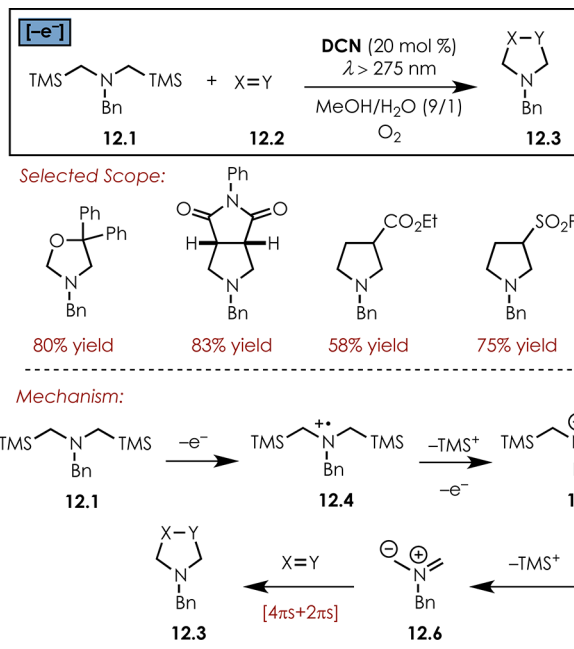
**Scheme 11. Proposed Mechanism for Benzylic Oxidative Aminations**



followed by deprotonation leads to *N*-centered radical 11.4. Benzylic hydrogen atom abstraction from 11.1 and subsequent single electron oxidation leads to benzyl cation 11.3. This cation is proposed to undergo reaction with the methoxyamide, furnishing the observed product after proton loss. Circumstantial evidence for intermediate benzyl cation 11.3 was obtained by running the reaction in MeCN:AcOH (9:1) and obtaining benzyl acetate 11.5 in 10% isolated yield along with 45% of the typical amination products. However, the authors do not note the formation of Ritter-type adducts despite the use of acetonitrile as solvent, which is surprising if the benzylic carbocation is the prevailing intermediate. This certainly raises the possibility of an alternative mechanism where radical–radical combination of 11.2 and 11.4 also leads to product formation and could be the dominant reaction pathway.

**4.2.1.5. Oxidative [3+2] Cycloaddition Reactions.** Azomethine ylides can be generated from  $\alpha,\alpha$ -disilylamines (12.1) and reacted with dipolarophiles (12.2) to give pyrrolidine adducts (12.3) (Scheme 12).<sup>155</sup> Single electron oxidation of 12.1 and loss of a silyl cation, followed by a second oxidation leads to 12.3.

**Scheme 12. Oxidative [3+2] Cycloaddition Reactions of  $\alpha,\alpha$ -Disilylamines**

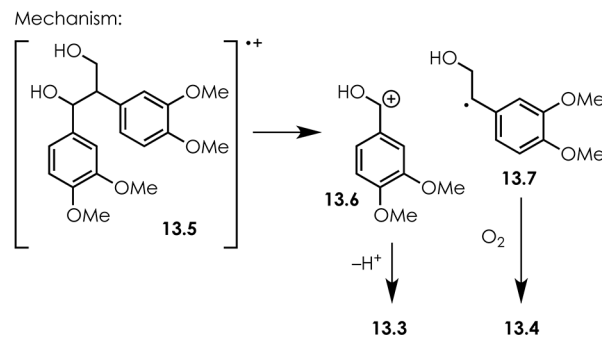
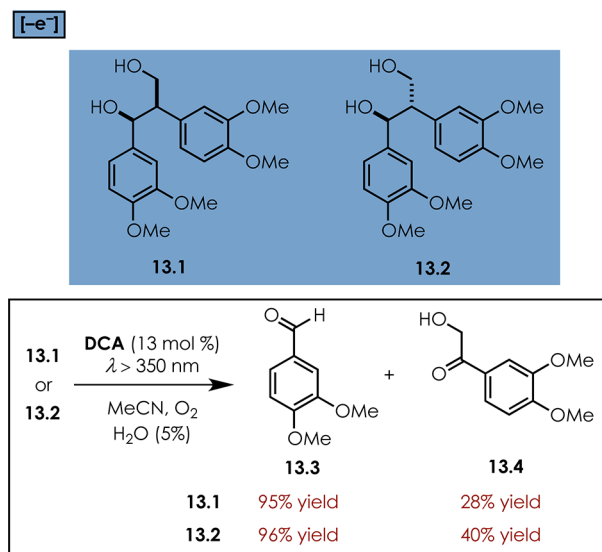


Following loss of a second TMS cation, a nonstabilized azomethine ylide (12.4) can be generated, which can intercept dipolarophiles (12.2) in solution to give the corresponding [3+2] adducts (12.3). A variety of dipolarophiles were investigated, and the yields of the formal cycloadducts was generally good (55–83%) with retention of the starting olefin geometry maintained in the final adducts. This method offers a unique alternative for azomethine ylide generation.

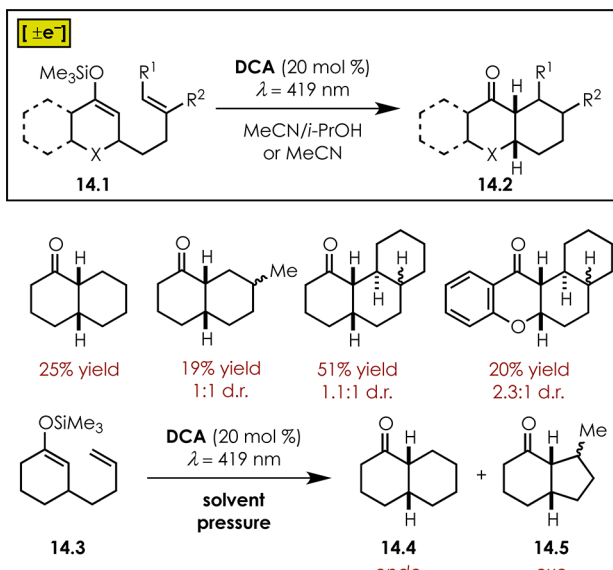
**4.2.1.6. Oxidative Cleavage Reactions.** Mariano and coworkers have studied the use of DCA as a single electron photooxidant to effect C–C bond cleavage of lignin model compounds (13.1 and 13.2, Scheme 13).<sup>156</sup> With irradiation of an O<sub>2</sub>-saturated solution of either *erythro* 13.1 or *threo* 13.2, nearly quantitative yields of veratrylaldehyde (13.3) were produced along with varying quantities of 13.4. Mechanistically, after single-electron oxidation of either 13.1 or 13.2 furnishes cation radical 13.5, C–C bond fissure gives rise to benzyl cation 13.6, which after proton loss, gives 13.3 and benzyl radical 13.7. Reaction of 13.7 with O<sub>2</sub> leads to formation of fragmentation product 13.4.

**4.2.2. Net Redox Neutral Transformations with Cyanoarene Photooxidants.** **4.2.2.1. Alkene Cyclization Reactions.** Mattay and coworkers have done extensive investigations on the cyclization of pendant alkenes and alkynes on silyl enol ethers (14.1) employing DCA as the single electron photooxidant (Scheme 14).<sup>157</sup> The main adducts of the reaction were *cis*-1-decalone systems (14.2) in all cases but one in which the alkene was disubstituted at the terminus. In that case, the product was the hexahydroindanone adduct. Intriguing solvent effects on the regioselectivity of the cyclization are noted in the case of monosubstituted alkene 14.3, wherein more of the *5-exo* adduct (14.4) is observed in the presence of an alcohol cosolvent. In addition, higher pressures (1500 bar) led to a complete reversal in regioselectivity from *6-endo* to *5-exo* adducts. This result is rationalized by invoking the argument that a smaller activation volume of the *5-exo* transition state is

**Scheme 13. Oxidative C–C Bond Cleavage of Lignin Model Compounds**



**Scheme 14. Oxidative Cyclization of Unsaturated Silyl Enol Ethers**

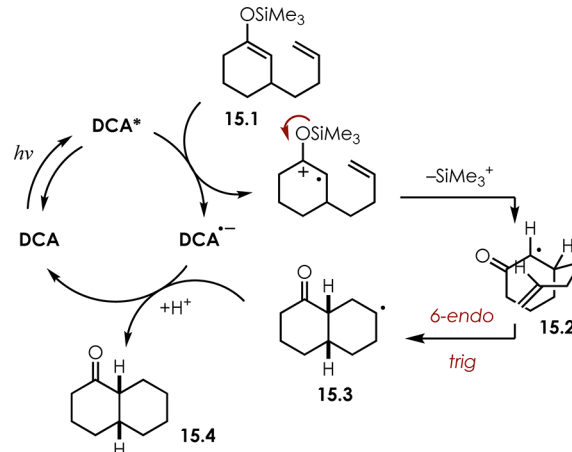


solvent	pressure	endo/exo
MeCN	1 bar	>20:1
MeCN/i-PrOH (17:3)	1 bar	3:2
MeCN	750 bar	2.2:1
MeCN	1500 bar	0.5:1

favored under higher pressures and leads to the hexahydroindanone isomer (**14.5**).

The mechanism of the transformation begins with single electron oxidation of the electron-rich enol silane (**15.1**) by DCA\*, followed by loss of the trimethylsilylum ion to generate  $\alpha$ -carbonyl radical **15.2** (**Scheme 15**). Subsequent 6-*endo*

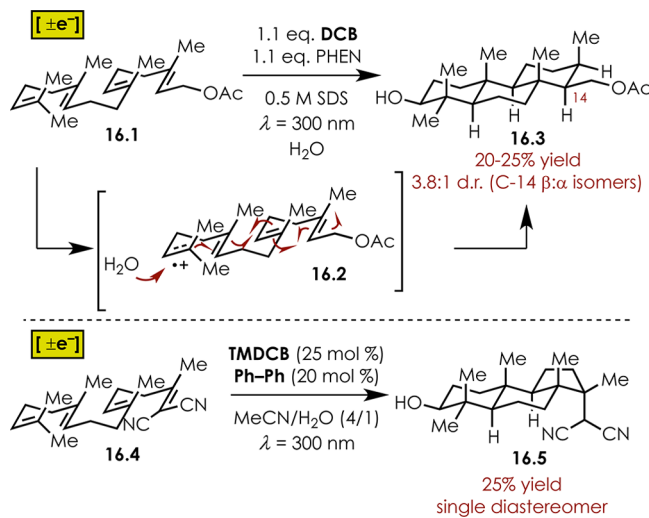
**Scheme 15. Mechanism of Oxidative Cyclization of Unsaturated Silyl Enol Ethers**



cyclization via a chairlike transition state proposed akin to the Beckwith stereoelectronic model<sup>158</sup> gives rise to radical **15.3**. Deuterium isotope experiments suggest that subsequent reduction of **15.3** by the radical anion of DCA and protonation yields the final adduct (**15.4**).

Oxidative cyclizations of polyenes such as acetylated farnesol (**16.1**) and geranylgeraniol are also possible using DCB as the single-electron photooxidant (**Scheme 16**).<sup>159</sup> Demuth and

**Scheme 16. Demuth's PET Polycyclization Reactions**

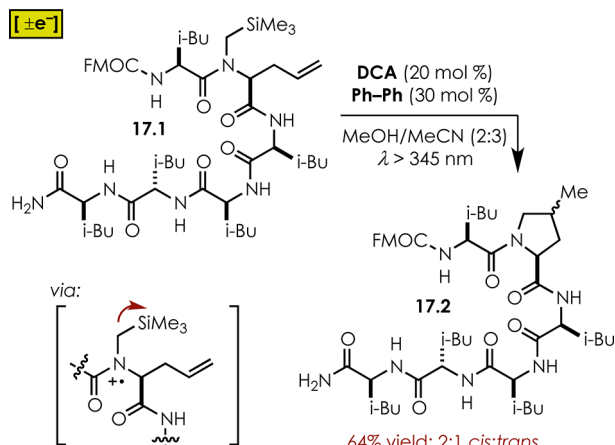


coworkers found that when the reaction is conducted in water with sodium dodecyl sulfate (SDS) as a surfactant, a polyannulation cascade is possible in a single synthetic transformation, albeit in trace yields (2–6%). The addition of phenanthrene (PHEN), in the case of acetylated geranylgeraniol (**16.1**), increases the yields of the steroidlike adduct **16.3** to 20–25% as a 3.8:1 mixture of C-14  $\beta:\alpha$  epimers. Interestingly, anti-

Markovnikov addition of water with complete diastereorecontrol is noted in the final alcohol adduct. It is presumed that polyene cation radical **16.2** is the key intermediate in the polycyclization, wherein the polyene adopts chairlike conformations, much like the proposed cationic polyene cyclizations.<sup>160</sup> A follow-up publication by Demuth found that a slight alteration of the polyene scaffold to include either unsaturated esters or nitriles (**16.4**) at the terminus afforded higher yields of the polycyclization adducts (**16.5**, 25–55% yields), though the final ring in the product is a cyclopentane, not a cyclohexane.<sup>24,161</sup> The divergence in isomer formation is likely due to the final cyclization proceeding via a radical rather than cationic manifold due to the electron-deficient nature of the alkene. The same group has also performed oxidative polycyclizations on polyenes bearing chiral auxiliaries, which effectively impart diastereorecontrol and afford steroid skeletons in enantiopure form after removal of the chiral controlling moiety.<sup>162</sup>

Radical cyclizations of  $\alpha$ -silylamines bearing pendant alkenes can be accomplished with catalytic quantities of DCA. Under photolysis with a 1000 W Xe arc lamp, Blechert and coworkers found that a variety of unsaturated  $\alpha$ -silyl amino acid derivatives could cyclize to give rise to pyrrolidine and piperidine adducts.<sup>163</sup> Perhaps most impressively, peptide **17.1** can be treated to the optimized reaction conditions to afford a proline-like residue in the resultant product **17.2** in good yield (Scheme 17). These

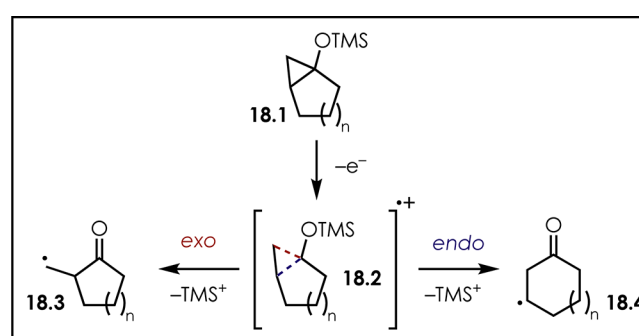
### Scheme 17. Radical Cyclization of $\alpha$ -Silyl Amines in Peptides



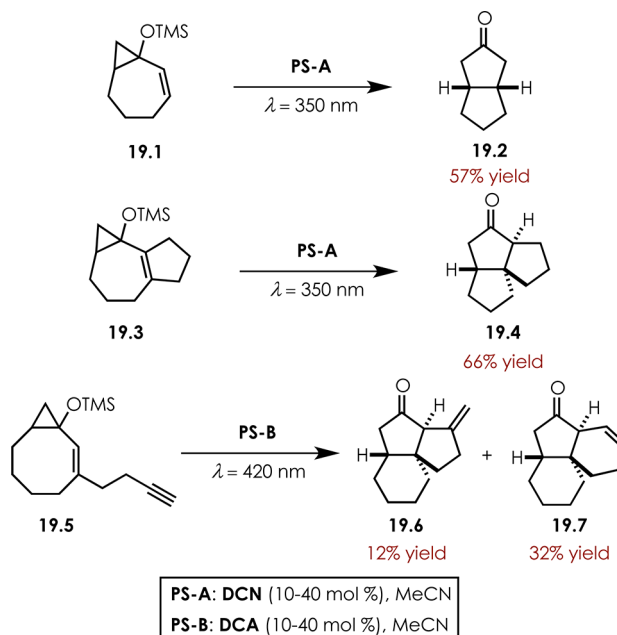
cyclization are believed to proceed via single-electron oxidation of the  $\alpha$ -silylamine moiety followed by loss of the silylum ion to generate the  $\alpha$ -amino radical. This then enables a rapid 5- or 6-*exo* radical cyclization, and the following reduction and protonation yields the final adducts.

Oxidative opening of silyloxycyclopropanes is also possible using organic photoredox catalysis and presents a practical method for accessing  $\beta$ -keto radicals (Scheme 18).<sup>164–166</sup> Mattay and coworkers have extensively studied the reactivity patterns of silyloxycyclopropanes of type **18.1**, which after oxidation to the cation radical (**18.2**) can undergo either an *exo*-type ring opening to afford primary radicals (**18.3**) or an *endo* cleavage with ring expansion to generate a more substituted radical (**18.4**) that can undergo a variety of secondary radical addition reactions or cyclization cascades (Scheme 19). The vast majority of the substrates investigated underwent the *endo*-ring opening to give the ring-expanded products when an alkene or alkyne trap was accessible following the cyclopropane cleavage. When no unsaturation was accessible, varying amounts of the *exo*-pathway

**Scheme 18. Oxidative Cleavage Pathways for Silyloxycyclopropanes**



**Scheme 19. Oxidative Cascade Reactions of Silyloxycyclopropanes**

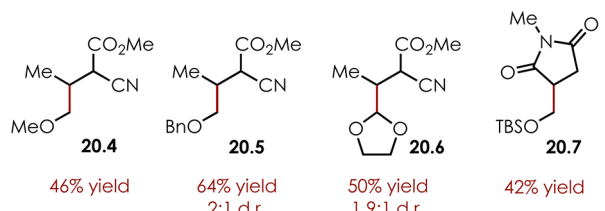
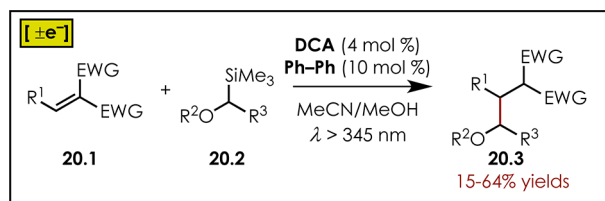


were observed, often with the end product the result of solvent hydrogen atom abstraction.

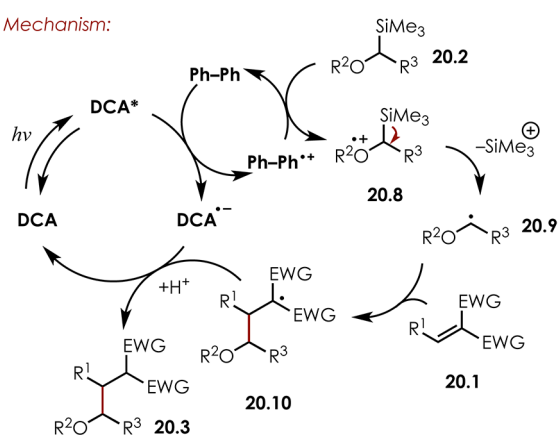
Representative examples of this oxidative cleavage cascade are shown in Scheme 19. Treatment of silyloxycyclopropane **19.1** to the PS-A conditions resulted in an *endo*-cleavage followed by a 5-*exo* radical cyclization onto the alkene and hydrogen atom abstraction to give rise to octahydropentalone **19.2** in 57% isolated yield. A similar reaction pathway is observed for **19.3** that yields a tricyclic fused ring system (**19.4**) bearing a quaternary spirocyclic stereocenter. Multiple cyclizations are possible utilizing this method, as demonstrated by alkyne-bearing substrate **19.5**, which affords a mixture of tricyclic adducts resulting from a final 5-*exo* (**19.6**) or 6-*endo*-dig cyclization (**19.7**).

**4.2.2.2. Oxidative Radical Generation/Conjugate Addition.** Radical conjugate addition reactions to Michael acceptors (**20.1**) were accomplished using a DCA/Ph-Ph photoredox catalyst system (Scheme 20).<sup>167</sup> The  $\alpha$ -oxy radicals were accessed from the corresponding  $\alpha$ -trimethylsilyl ethers (**20.2**) and gave the corresponding conjugate addition adducts (**20.3**). Methyl (**20.4**), benzyl (**20.5**), and silyl (**20.7**) protecting groups were utilized successfully in the  $\alpha$ -trimethylsilyl ether reaction partners. An aldehyde masked as a cyclic ketal underwent

**Scheme 20.** Radical Conjugate Addition Reactions of  $\alpha$ -Silyl Ethers



Mechanism:

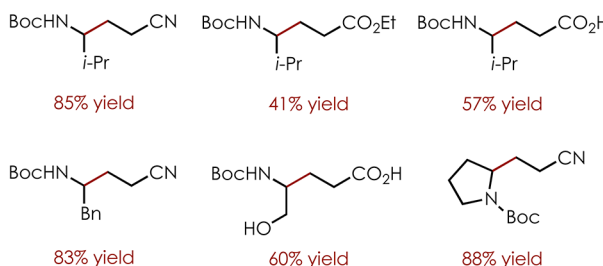
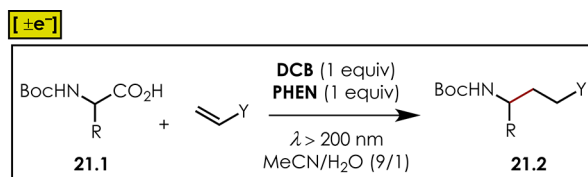


reaction with methyl 2-cyanocrotonate in 50% yield and 1.9:1 d.r. (20.6). In addition to methyl 2-cyanocrotonate, electron-deficient alkenes such as dimethyl maleate and substituted maleimides (20.7) also were competent Michael acceptors. In related work, it has also been shown that organostannanes can be utilized for nearly identical radical conjugate addition reactions.<sup>168</sup>

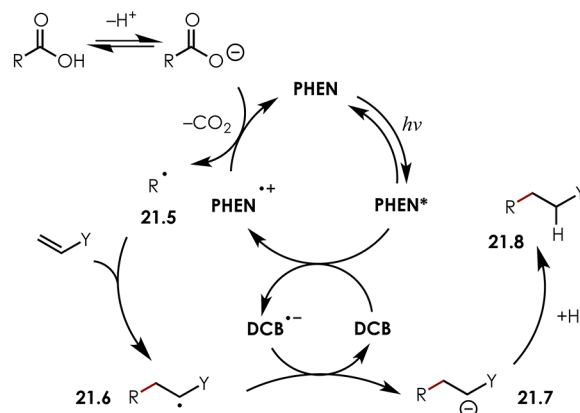
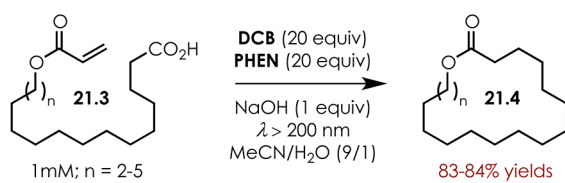
In a mechanism reminiscent of their  $\alpha$ -trimethylsilyl amide work (Scheme 20), Steckhan and Blechert propose that the  $\alpha$ -oxy radicals (20.9) are derived from single electron oxidation of 20.2 by biphenyl cation radical ( $\text{Ph-Ph}^{\bullet+}$ ), in turn, generated via oxidation of  $\text{Ph-Ph}$  by  $\text{DCA}^*$ . Addition of 20.9 to the electron deficient alkene, furnishes the electron-poor radical 20.10, which can be easily reduced by  $\text{DCA}^{\bullet-}$  and after protonation yields the final adduct (20.3). The use of MeOD as the solvent lended support for the final reduction–protonation sequence proposal, as 95% *d*-incorporation in the case of 20.4.

The use of carboxylic acids as radical precursors has also been utilized for conjugate addition reactions. In work from Yoshimi and Hatanaka, Boc-protected amino acids (21.1) undergo oxidative decarboxylation to generate nucleophilic radical species (Scheme 21).<sup>169,170</sup> In the presence of acrylates, acrylic acid, acrylonitrile, and phenyl vinylsulfone, net 1,4-addition products are obtained (21.2). In general, the yields are good to excellent when employing both 1 equiv of DCB and PHEN as the cooxidant system. In addition, both Boc-protected di- and tripeptides also underwent the aforementioned reaction in good yield. Perhaps most impressively, large lactones (21.4) (18-21 membered) could be forged from the corresponding carboxylic

**Scheme 21.** Radical Conjugate Addition Reactions via Oxidative Decarboxylation of Carboxylic Acids



18-21 Membered Lactone Formation:



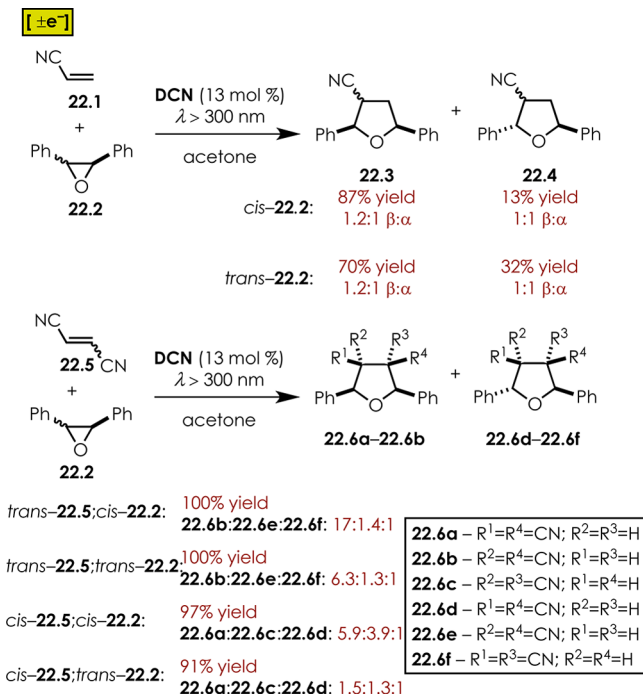
acids (21.3), albeit under dilute conditions and using 20 equiv of both of the organic cooxidants. Nevertheless, the yields were excellent (83–84%) considering the demands of the cyclization. Since this work, photooxidation catalyst systems based on Ir have also been reported.<sup>171</sup>

The active oxidant in this case for the carboxylate salt is believed to be  $\text{PHEN}^{\bullet+}$ , produced via single electron oxidation of  $\text{PHEN}^*$  by DCB. Following oxidative decarboxylation, the corresponding radical (21.5) reacts with the Michael acceptor, and then the subsequent radical (21.6) is reduced by  $\text{DCB}^{\bullet-}$  leading to anion 21.7, which is protonated to form the final adducts 21.8. While the DCB is not believed to be the actual photooxidant in this case, it is difficult to rule out the possibility of it playing that role, at least to a minor extent.

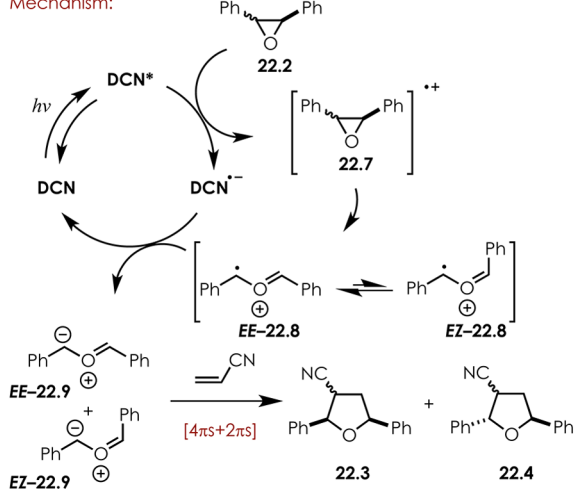
**4.2.2.3. Oxidative [3+2] Cycloaddition Reactions.** Transformations furnishing the equivalent of a 1,3-polar cycloaddition reactions between oxiranes (22.2) and acrylonitrile (22.1) have been reported by Arnold and Albini.<sup>172</sup> In the presence of catalytic quantities of DCN as the single electron photooxidant, both *cis* and *trans*-stilbene oxide (22.2) readily undergo

cycloaddition with acrylonitrile (**22.1**) to yield tetrahydrofuran adducts (**22.3–22.4**) (Scheme 22). Irradiation of a reaction

**Scheme 22. Oxidative [3+2] Cycloaddition Reactions of Epoxides**



Mechanism:



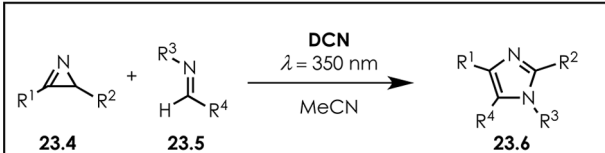
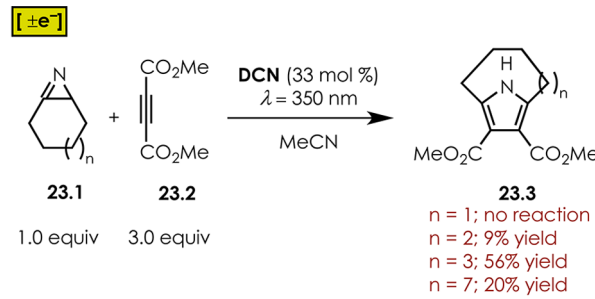
mixture containing either the *cis* or *trans*-stilbene oxide (**22.2**) leads to predominantly the tetrahydrofuran adducts (**22.3**) wherein the phenyl groups are in a *cis* relationship to one another. Using either fumaronitrile (*trans*-**22.5**) or maleonitrile (*cis*-**22.5**) as the dipolarophile with either diastereomer of stilbene oxide still leads predominately to the formation of the tetrahydrofuran diastereomers with the phenyl groups *cis* (**22.4a–22.4b**). It is important to note that in these latter cycloadditions, the stereochemistry of the starting dipolarophile is preserved in the final products, lending some insight into the mechanism for the transformation.

Given these observations, the authors propose that single electron oxidation of the stilbene oxides proceeds via the singlet excited state of DCN, as determined by fluorescence quenching

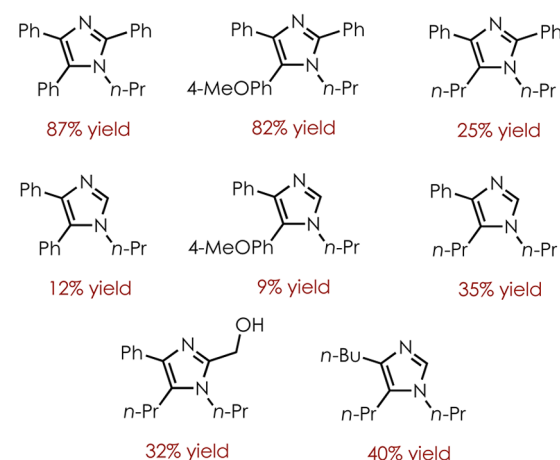
studies (Scheme 22). Upon generation of the stilbene oxide cation radical (**22.7**), rupture of the C–C bond occurs to afford a carbonyl ylide (**22.8**) deficient by one electron. It is at this point that isomerization of **22.8** is believed to occur with a slight preference for formation of *EE*–**22.8** over *EZ*–**22.8** due to unfavorable A<sup>1,3</sup> steric interactions. Back electron transfer to *EE*–**22.8** and *EZ*–**22.8** then gives rise to the corresponding carbonyl ylides (**22.9**), which undergo a [4πs+2πs] cycloaddition with the corresponding dipolarophile. Preservation of the starting dipolarophile stereochemistry in the final tetrahydrofuran adducts lends support for the concerted cycloaddition process.

Cycloaddition reactions of the [3+2] variety with azirines acting as the pseudo 1,3-dipolarophile have been investigated by Mattay and coworkers.<sup>173–176</sup> Treatment of azirines (**23.1**) with substoichiometric quantities of DCN in the presence of acetylene dicarboxylates (**23.2**) under irradiation gives rise to pyrrolidine adducts (**23.3**). Bicyclic azirines give rise to 2,4-imidazolophanes (**23.3**), where product formation is only observed in the larger ring series (Scheme 23, reactant **23.1**).

**Scheme 23. Oxidative [3+2] Cycloadditions of Azirines**



Reaction Scope:

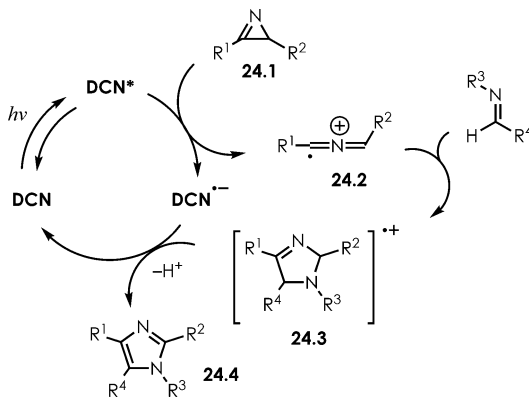


In a similar fashion, azirines (**23.4**) can be reacted with imines (**23.5**) to furnish the corresponding imidazoles (**23.6**) (Scheme 23, reactant **23.4**). Though the reaction conditions are not listed, it is presumed that substoichiometric quantities of DCN can also be employed in this case as the reaction is redox neutral. It is interesting to note that despite the notably lower yields, aliphatic imines can be utilized as substrates in the transformation.

Though the substrate scope was not extensively explored, the example where an azirine bears a free alcohol should be noted.

Detailed mechanistic investigations by Mattay (**Scheme 24**) reveal that the key intermediate is an azaallenyl cation radical

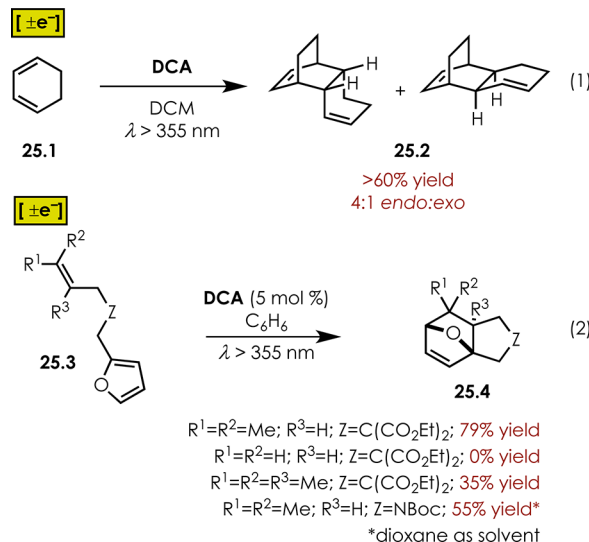
**Scheme 24.** Mechanism for Oxidative [3+2] Cycloadditions of Azirines



(**24.2**), formed via single electron oxidation of the azirine (**24.1**) by DCN\*. Evidence for the intermediacy of **24.2** was supported by trapping experiments with acrylonitrile and trifluoroethanol.<sup>176</sup> Subsequent reaction with the dipolarophile (**23.5**) followed by back electron transfer from DCN•<sup>-</sup> to **24.3** (and in the case of the imidazole formation, proton loss) regenerates the photoredox catalyst and furnishes the final cycloadducts (**24.4**). This is certainly a viable method for the synthesis of fully-substituted imidazoles.

**4.2.2.4. Oxidative [4+2] Cycloaddition Reactions.** Cycloaddition manifolds of the [4+2] variety are also catalyzed in the presence of DCA as the single electron photooxidant, though the loading is not indicated. In an early example, DCA promotes the cyclodimerization of cyclohexadiene (**25.1**) to **25.2** in 60% with a 4:1 ratio of endo/exo diastereoselectivity (**Scheme 25**, eq 1).<sup>177</sup> In this case, none of the [2+2] cycloadducts are formed, as is the case with direct UV photolysis ( $\lambda > 330$  nm) of the reaction mixture. The use of furans as dienes in [4+2] cycloadditions is also possible, as observed by Arai and Ohkuma.<sup>178</sup> Several

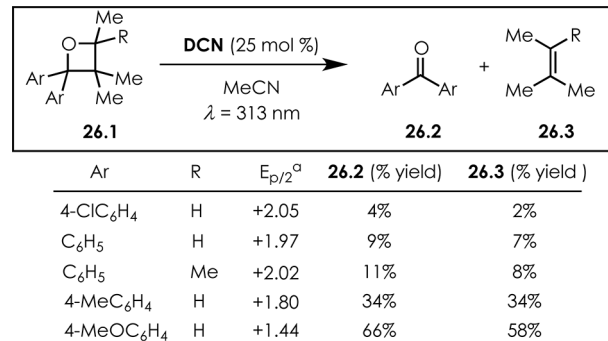
**Scheme 25.** Cation Radical [4+2] Cycloaddition Reactions



different furans (**25.3**) bearing a variety of olefin substitution patterns gave rise to the oxabicyclo[2.2.1]heptane adducts **25.4** shown in **Scheme 25** (eq 2). Unsubstituted terminal olefins were not suitable dienophiles, likely owing to their attenuated nucleophilicity. In both of these systems, the reaction likely proceeds through the intermediacy of an olefin cation radical, which accelerates the cycloaddition reaction by virtue of polarity reversal. Subsequent back electron transfer furnishes the cycloadducts and regenerates the photooxidant.

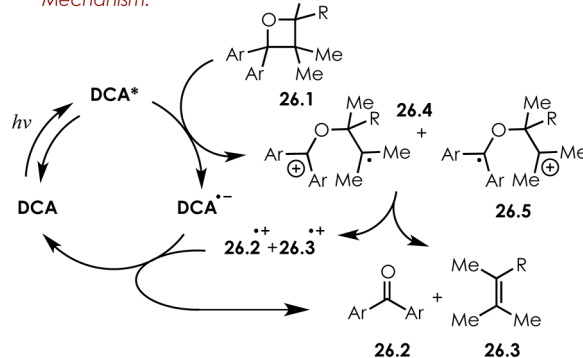
**4.2.2.5. Cycloreversion Reactions.** Oxetanes readily undergo cycloreversion under oxidative PET conditions. Shima and coworkers reported one of the first examples of photoinduced oxidative cycloreversion of oxetanes to their respective ketone and alkene fragments.<sup>179</sup> Using stoichiometric quantities of DCN (25 mol %) in MeCN under irradiation ( $\lambda = 313$  nm), **26.2** and **26.3** were observed in obtained varying quantities from the corresponding oxetanes (**26.1**) (**Scheme 26**). It is interesting to

**Scheme 26.** Oxidative Cleavage of Oxetanes



<sup>a</sup>V vs. Ag/AgNO<sub>3</sub> in MeCN

#### Mechanism:



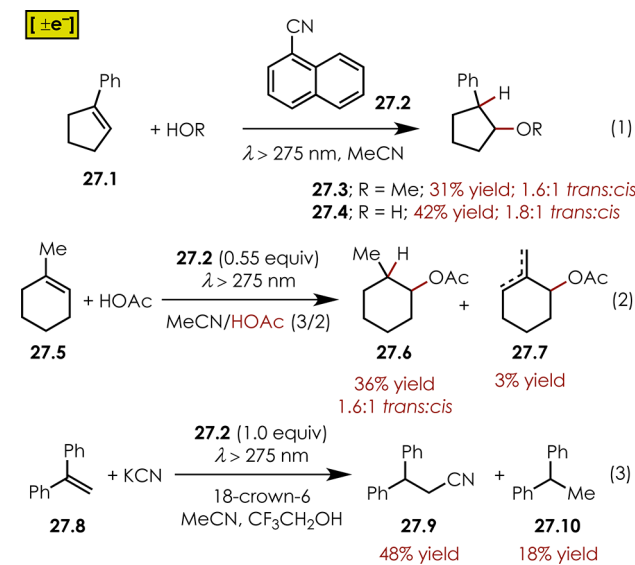
note that product yields seem to track inversely with the redox potential of the starting oxetanes. This could be due to the reversibility of the reaction under these conditions and that the more oxidizable the oxetane, the more the equilibrium lies toward the fragmented adducts.

Ultimately, the authors propose that single electron oxidation of the oxetanes leads to C–C bond cleavage to form distonic cation radicals **26.4** and **26.5**. A C–O bond fragmentation leads to the final adducts **26.2** and **26.3** while also giving rise to the cation radicals of **26.2** and **26.3**. Finally, single electron reduction by DCN•<sup>-</sup> also leads to the alkene and benzophenone adducts while regenerating the DCN catalyst.

**4.2.2.6. Alkene Hydrofunctionalization Reactions.** Several research labs have pioneered alkene hydrofunctionalization reactions of alkenes using cyanoarene single electron photo-oxidants.<sup>145,180–191</sup> The vast majority of these transformations

employ at least one equivalent of cyanoarene photooxidant. Some of the first work in this area was from the laboratory of Arnold, who demonstrated the addition of methanol and water to 1-phenylcyclopentene (**27.1**), although the amount of the 1-cyanonaphthalene (**27.2**) that was employed was not disclosed (eq 1, Scheme 27).<sup>180</sup> Despite the low yields of hydroalkoxylated

**Scheme 27. Anti-Markovnikov Alkene Hydrofunctionalization Reactions Promoted by Cyanoarene Photooxidants**

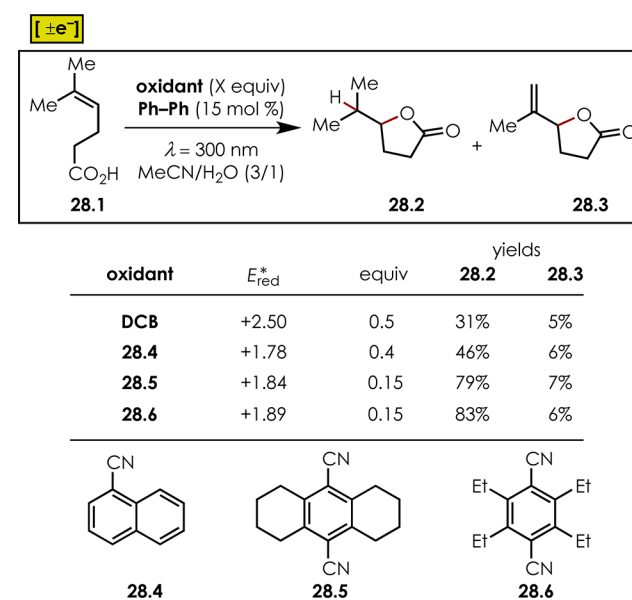


adducts (**27.3** and **27.4**; 31–42% yield), what is most compelling is the complete anti-Markovnikov regioselectivity for the transformations. Gassman also developed similar conditions for the addition of water, methanol, and acetic acid (eq 2, Scheme 27) to 1-methylcyclohexene (**27.5**).<sup>189</sup> The yields were similar and in the case of the acetic acid addition, small amounts of elimination adducts (**27.7**) were noted. Arnold also developed olefin anti-Markovnikov hydrocyanation reactions using 1-cyanonaphthalene and a combination of KCN/18-crown-6 to afford 48% of **27.9** from 1,1-diphenylethene (**27.8**), though reduction product **27.10** was also isolated (eq 3, Scheme 27).<sup>181</sup> Though these reactions are the first anti-Markovnikov alkene hydrofunctionalization reactions promoted by photoinduced electron transfer, none of the reactions use truly catalytic loadings of the cyanoarene photooxidant.

The first report of a catalytic PET olefin anti-Markovnikov hydrofunctionalization was in a follow-up report by Gassman in 1991.<sup>190</sup> The reaction studied involved an intramolecular hydrolactonization of unsaturated acid **28.1** to give lactone **28.2** and byproduct **28.3** (Scheme 28). The authors investigated a range of cyanoarene single-electron oxidants with  $E^{\text{red}}_{\text{red}}$  ranging from +1.84 to +2.50 V vs SCE. In general, the yields of the anti-Markovnikov adduct (**28.2**) increased as the excited state reduction potential of the cyanoarene decreased. Importantly, just 15 mol % of **28.6** could be used as a catalyst in conjunction with **Ph–Ph** as a cocatalyst (15 mol %) to give the lactone product.

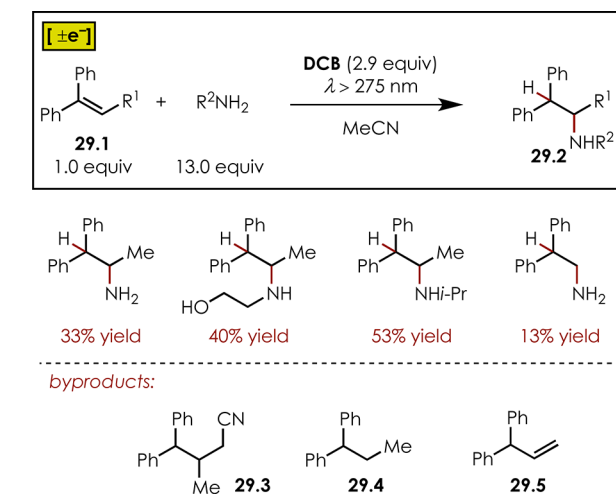
Amines can also be employed in PET reactions with alkenes to give anti-Markovnikov hydroamination reactions. Again, reports mainly involve the use of superstoichiometric quantities of cyanoarene oxidants. In a particular example, Yamashita and Yasuda investigated the addition of several different amines,

**Scheme 28. Gassman's Catalytic Intramolecular Anti-Markovnikov Hydrolactonization Reaction**



including ammonia to 1,1-diphenylethylene derivatives (**29.1**) using DCB as the photooxidant (Scheme 29).<sup>187</sup> A large excess

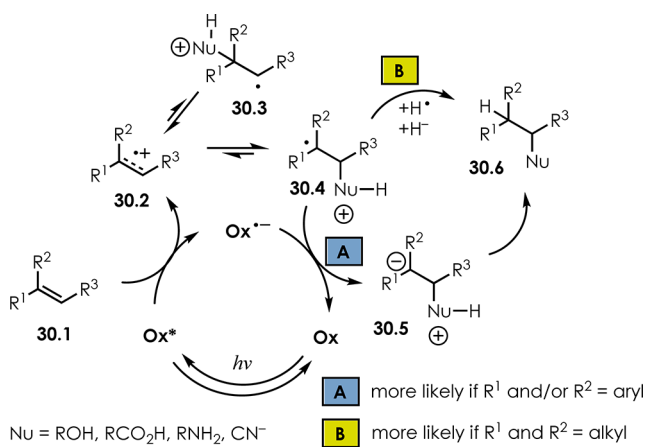
**Scheme 29. Anti-Markovnikov Alkene Hydroamination**



of the amine is required, and yields of the hydroaminated adduct **29.2** are modest to good. Several side products often accompany these reactions in varying quantities, including solvent addition (**29.3**), reduction (**29.4**), and olefin isomerization (**29.5**). In related work, incorporation of the cyanoarene photooxidant is observed to give the product of an amino arylation,<sup>188</sup> which is often a competing reaction using dicyanobenzene-type systems. Additional work by the same groups also demonstrates hydroamination of phenanthrenes.<sup>185</sup>

The anti-Markovnikov hydrofunctionalization reactions, by and large, all share a common mechanism. Single electron oxidation of the alkene (**30.1**) by the excited state of the cyanoarene photooxidant ( ${}^*\text{Ox}$ ) gives rise to an olefin cation radical (**30.2**) (Scheme 30). Addition of the nucleophile (water, alcohols, carboxylic acids, amines, and cyanide) leads to radical intermediates **30.3** and **30.4**. Important to understanding the regioselectivity in this process is that the addition step is likely

**Scheme 30. General Mechanism for Anti-Markovnikov Alkene Hydrofunctionalization Reactions**

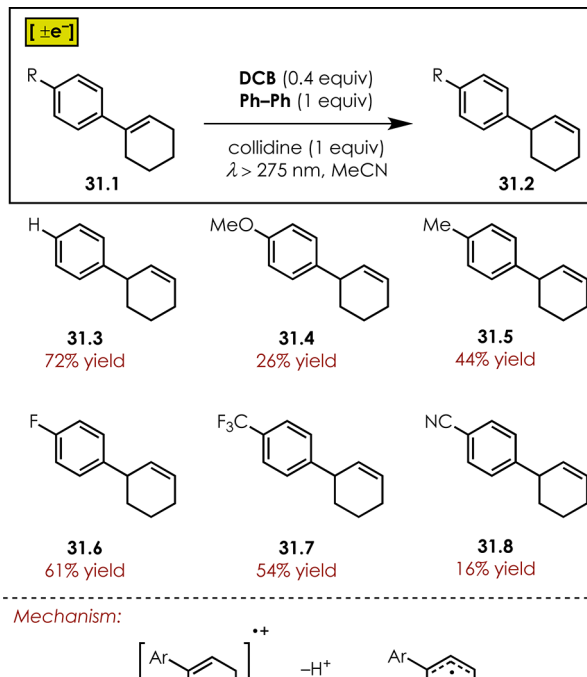


reversible in most cases. Ultimately what is presumed to dictate the regiospecificity is the stability of the incipient radical (**30.3** vs **30.4**), guiding the reaction toward the anti-Markovnikov pathway.<sup>192</sup> At this point, one of two pathways is plausible depending on the substitution pattern on the olefin. In pathway A, reduction of **30.4** by  $\text{Ox}\bullet^-$  followed by proton transfer leads to product formation (**30.6**) and resets the photooxidant. This is possible as a benzylic radical is generally reduced more easily by  $\text{Ox}\bullet^-$ . In the examples where the alkene has no aromatic groups, it is presumed that pathway B is operative, wherein hydrogen atom abstraction, likely from solvent, takes place to furnish the final adduct. It is also likely that a second oxidation of this radical, followed by elimination of a proton is responsible for the alkenes byproducts noted in several instances (Scheme 27 and Scheme 28). This collective body of research laid the groundwork for truly catalytic anti-Markovnikov olefin hydrofunctionalization reactions (Scheme 90).

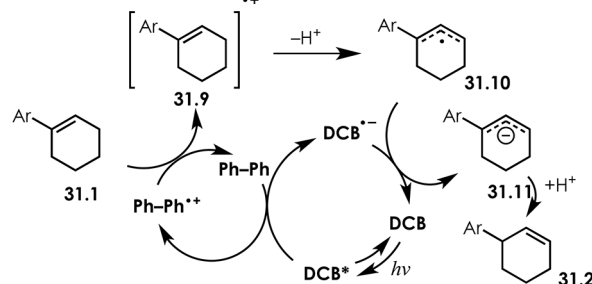
**4.2.2.7. Miscellaneous Reactions.** A deconjugation of para-substituted 1-arylcyclohexenes (**31.1**) has been disclosed that makes use of a DCB/Ph–Ph photoredox system (Scheme 31).<sup>21</sup> Aryl cyclohexenes bearing a variety of electronically different substituents on the aryl moiety were tested in the reaction and proceeded to give the alkene isomers (**31.2**) in modest to good yields (16–72%). One exception to this is the case of methoxy-substituted derivative **31.4**, which also produces 3-(4-cyano-phenyl)-1-(4-methoxyphenyl)cyclohexene as a byproduct in 40% isolated yield. In general, it was found that the presence of Ph–Ph in the reaction increased the yields of the deconjugated adducts. This is intriguing as the oxidation potential of Ph–Ph [ $E_{\text{ox}}(\text{Ph-Ph}\bullet^+/\text{Ph-Ph}) = +1.85 \text{ V vs SCE}$ <sup>193</sup>] is below that of nearly all of the substrates investigated. The authors speculate that Ph–Ph plays a crucial role in limiting back electron transfer processes that may hamper reactivity.

On the basis of these assertions, the proposed mechanism begins with single electron oxidation of Ph–Ph by DCB\* to give **31.9** as well as Ph–Ph•+ and DCB•-. In the case of the more electron-rich styrene derivatives (**31.3** – **31.5**), Ph–Ph•+ should be of sufficient potential to oxidize olefins with potentials  $< +1.85 \text{ V vs SCE}$ . With less electron-rich alkenes (**31.6**–**31.8**), it is highly likely that DCB\* ( $E_{\text{red}}^*(\text{DCB}^*/\text{DCB}\bullet^-) = +2.6 \text{ V vs SCE}$ ) is the oxidant. In either event, allylic deprotonation of cation radical **31.9** leads to allylic radical **31.10**, which is then reduced by DCB•- to regenerate the photoactive oxidant. Protonation of allyl anion **31.11** can occur at the 1 or 3

**Scheme 31. Oxidative Alkene Isomerizations**



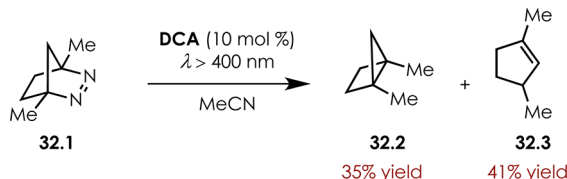
Mechanism:



positions leading to product (**31.2**) or back to starting materials (**31.1**), respectively. Ultimately, the reaction progresses to furnish the unconjugated alkene due to the higher redox potential of the product than the starting material, rendering the unconjugated alkene inert to oxidation.

Extrusion of dinitrogen from diazoalkanes has been shown to be catalyzed by DCA (Scheme 32).<sup>194,195</sup> With the use of 10 mol

**Scheme 32. Oxidative Denitrogenation of 1,4-Dimethyl-2,3-diazabicyclo[2.2.1]hept-2-ene**

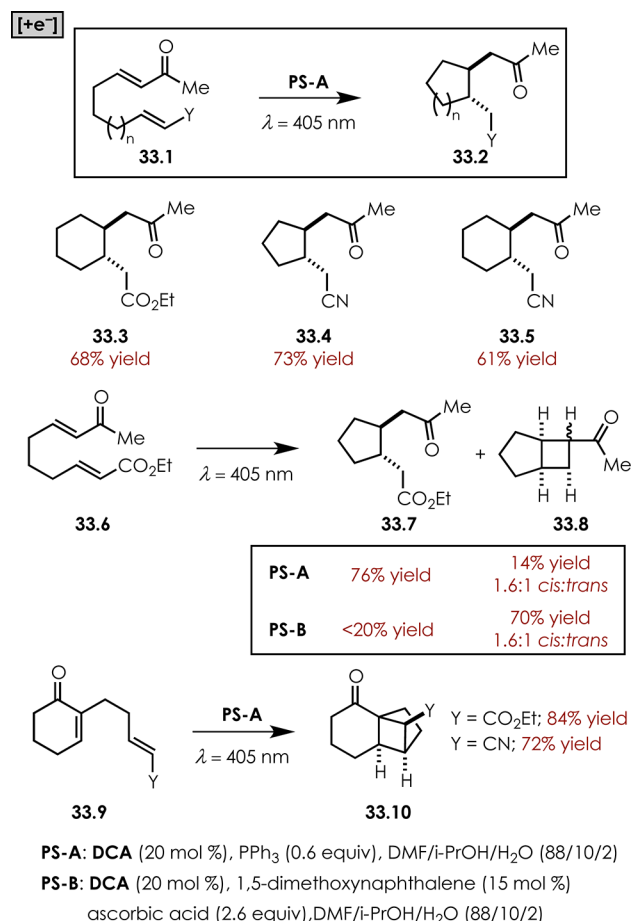


% of DCA, 1,4-dimethyl-2,3-diazabicyclo[2.2.1]hept-2-ene (**32.1**) was demonstrated to undergo loss of N<sub>2</sub> and afforded 1,4-dimethylbicyclo[2.1.0]pentane (**32.2**) and 1,3-dimethylcyclopent-1-ene (**32.3**). Through mechanistic studies, it was proposed that single-electron oxidation of **32.1** and denitrogenation furnishes a distonic 1,3-cation radical that can either accept an electron back from DCA•- and cyclize to form **32.2** or undergo a 1,2-hydrogen atom shift and back electron transfer from DCA•- to furnish cyclopentene **32.3**. Support for the back electron transfer pathway is found in the solvent selection. Use of CH<sub>2</sub>Cl<sub>2</sub> resulted in a higher ratio of bicyclopentane **32.2** formed

than cyclopentene 32.3 (62:38), presumably due to ion pairing between the cation radical and  $\text{DCA}^{\bullet-}$ . This allows for back electron transfer to occur more rapidly than the hydrogen atom shift.<sup>196,197</sup> This method, though underexplored, could offer a unique manner in which to regiospecifically generate distonic cation radicals.

**4.2.3. Net Reductive Transformations Involving Cyanoarene Photoredox Catalysts.** *4.2.3.1. Reductive Cyclization Reactions.* Net reductive cyclizations of substrates bearing two Michael acceptors (33.1) are possible using cyanoarene photooxidants. Two different photoredox systems were developed (**PS-A** and **PS-B**) using either triphenylphosphine (**PS-A**) or a combination of 1,4-dimethoxy naphthalene (**DMN**) as an electron relay and ascorbic acid (**PS-B**) as the terminal reductant (*Scheme 33*). Enones bearing pendant  $\alpha,\beta$ -unsaturated ester-

**Scheme 33. Reductive Cyclizations of Unsaturated Enones**

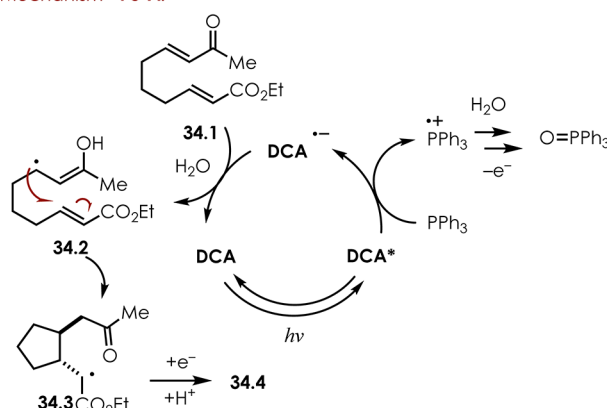


rated esters (33.3 and 33.7) as well as acrylonitriles (33.4–33.5) afforded mainly reductive cyclization adducts, while substrate 33.6 gave small amounts (14%) of cyclobutane 33.8. Interestingly, employing **PS-B** with 33.6 gave cyclobutane 33.8 as the major product, with only small amounts of 33.7 (<20%) observed. In the case of enone 33.9, exclusive formation of a cyclobutane adduct (33.10) is observed, despite the ring strain inherent to this system.

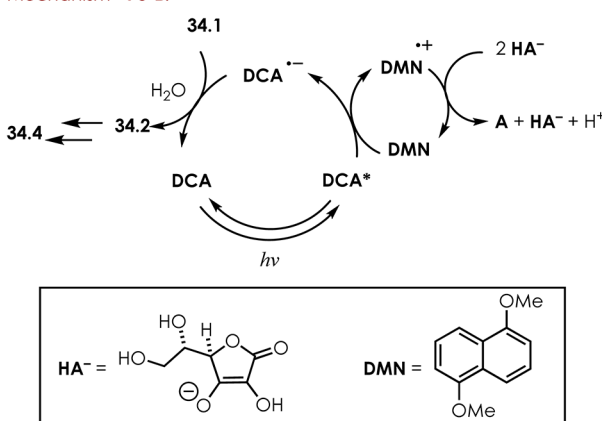
These reactions are predicated on a reductive quenching cycle of the photoexcited DCA (*Scheme 34*). In the case of **PS-A**, PPh<sub>3</sub> [ $E_{\text{ox}}(\text{PPh}_3^{\bullet+}/\text{PPh}_3) = +0.98 \text{ V vs SCE}$ ] is the putative reductant of  $\text{DCA}^*$ , while in **PS-B**, 1,5-dimethoxynaphthalene (**DMN**) [ $E_{\text{ox}}(\text{DMN}^{\bullet+}/\text{DMN}) = +1.28 \text{ V vs SCE}$ ] is the reductive quencher

**Scheme 34. Mechanism of Photoreductive Cyclizations**

*Mechanism - PS-A:*



*Mechanism - PS-B:*



of  $\text{DCA}^*$ . In **PS-A**, reduction of substrate 34.1 affords enol radical 34.2, which is poised to undergo a rapid intramolecular addition to the unsaturated ester. The electronics of the radical acceptor appear important; an unsubstituted terminal aliphatic alkene (34.1;  $n = 1$ ,  $Y = \text{H}$ ) only afforded a 19% yield of the cyclized adduct along with 8% of the reduced enone. Following a second reduction event, either by PPh<sub>3</sub> or by another molecule of  $\text{DCA}^{\bullet-}$  and protonation, the final reductive cyclization adduct (34.4) is obtained. Eventually, the triphenylphosphine cation radical is further oxidized to finally yield triphenylphosphine oxide, which is isolated as a byproduct in the reaction medium. The reaction pathway for the formation of the reductive cyclization products is similar in **PS-B**, with the main difference being that the ascorbate ion ( $\text{HA}^-$ ) goes on to reduce  $\text{DMN}^{\bullet+}$ , resultant from reductive quenching of  $\text{DCA}^*$ . This result represents one of the first examples of a photooxidant ultimately employed as a single electron reduction by virtue of a reductive quenching event and offers a mild method for reductive cyclizations.

### 4.3. Cyanoarene Catalyst Development

Few of the preceding examples employ the cyanoarene in less than 20 mol %, highlighting the fact that this class of photoredox catalysts is subject to a number of degradation pathways. Radicals or radical ions can react with the cyanoarene anion radical, resulting in dearomatization.<sup>198,199</sup> In fact, Arnold<sup>200</sup> and others<sup>201</sup> have found cyanoarenes to be competent coupling partners that can accomplish arylation reactions involving the displacement of the  $-\text{CN}$  nucleofuge. Accordingly, recent efforts have been directed at improving cyanoarene photoredox catalyst

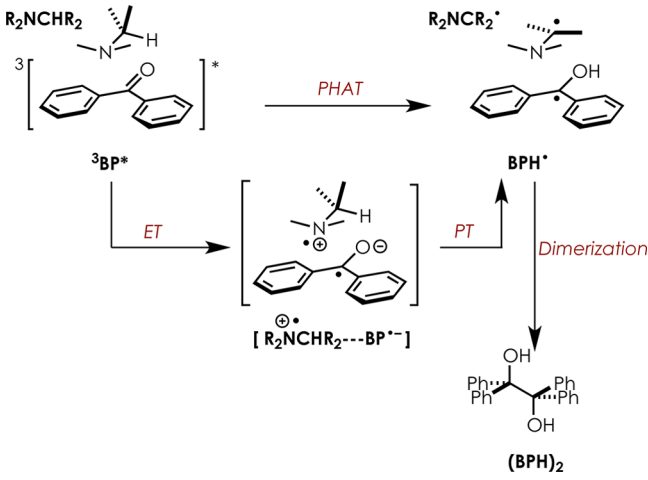
stability and efficiency, which has initiated the development of the next generation of cyanoarenes. To this end, donor–acceptor dicyanopyrazines offer the promise of dramatically lower catalyst loadings.<sup>202,203</sup> Additionally, cyanobenzenes with carbazole donors have demonstrated promise as highly active photoredox catalysts.<sup>204</sup>

## 5. BENZOPHENONES AND QUINONES

### 5.1. Benzophenones, Xanthones, Fluorenone: Photophysical and Electrochemical Characteristics

Benzophenone is often discussed as an archetypal example of organic molecules which undergo rapid intersystem crossing ( $k_{ISC} \sim 10^{11} \text{ s}^{-1}$ ) with effectively complete efficiency ( $\phi_{ISC} = 1.0$ ), which is characteristic of carbonyl compounds whose  $S_1(n,\pi^*)$  and  $T_1(\pi,\pi^*)$  are close in energy.<sup>17</sup> Indeed, other benzophenone derivatives (including xanthones such as **XO** and **TXO**, and fluorenone **FLN**) exhibit triplet quantum yields close to unity and share similar reactivity patterns. With high yielding and relatively high-lying  $T_1$  states, benzophenones are some of the most effective mediators of triplet energy transfer,<sup>205</sup> including sensitization of  ${}^3\text{O}_2$  to  ${}^1\text{O}_2$ . PET reactivity is possible with some substrates, although benzophenones are only moderate oxidants and poor reductants (with the exception of Michler's Ketone, **MK**) in the  $T_1$  state. The prototypical reactivity of benzophenone triplets is hydrogen atom transfer (HAT).<sup>206</sup> This process of photoinduced H atom transfer, or PHAT, results in ketyl radical of the type **BPH $\bullet$**  (Scheme 35), which can be

**Scheme 35.** Photoinduced HAT (PHAT) Reactivity of Excited State Benzophenones



viewed as having the same net outcome as sequential SET and proton transfer (PT) steps. In some cases, HAT and sequential ET/PT may not be dynamically distinguishable, especially in the well-studied H atom abstraction from alkyl amines (Scheme 35).<sup>207–210</sup> However, the direct H atom abstracting ability of benzophenones is underscored in the examples involving HAT from simple alkane hydrocarbons.<sup>211</sup> Ultimately, reverse hydrogen atom transfer (RHAT) or reverse ET/PT is required for turnover of the ketyl radical **BPH $\bullet$**  in order for **BP** to be employed catalytically; however, these processes are known to occur slowly,<sup>10</sup> and dimerization of **BPH $\bullet$**  to benzopinacol (**(BPH)<sub>2</sub>**) can be problematic.<sup>211</sup> HAT reactivity of the type discussed here can be accomplished by other triplet excited ketones (such as acetone or acetophenone), but benzophenones

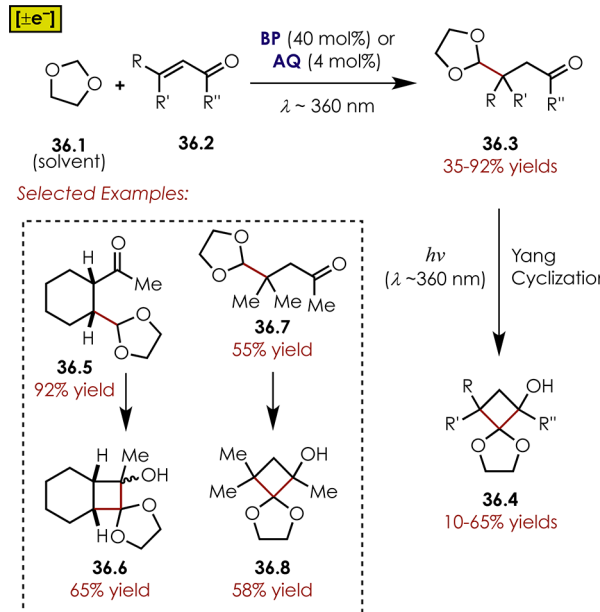
have absorptions closer to the visible (~300–380 nm), likely contributing to their preferred use as photoredox catalysts.

### 5.2. Benzophenones, Xanthones, and Fluorenone: Reactions

Strictly speaking, the PHAT mechanisms typical of benzophenones and quinones fall outside our definition of photoredox catalysis in this review. Thus, we refer the reader to previous reviews by Albini<sup>10,12,13</sup> for a comprehensive overview of other radical reactions initiated by the PHAT activity of benzophenones and anthraquinones. Nonetheless, we will highlight several recent examples where this reactivity is particularly useful in the synthetic context.

One common synthetic application of benzophenones found in earlier examples of photoredox catalysis is the generation and addition of carbon-centered radicals to enones. Examples of radical precursors include alcohols, acetals, and even alkanes. Albini and co-workers demonstrated that the conjugate addition products **36.3** (Scheme 36)<sup>212</sup> were particularly useful when the

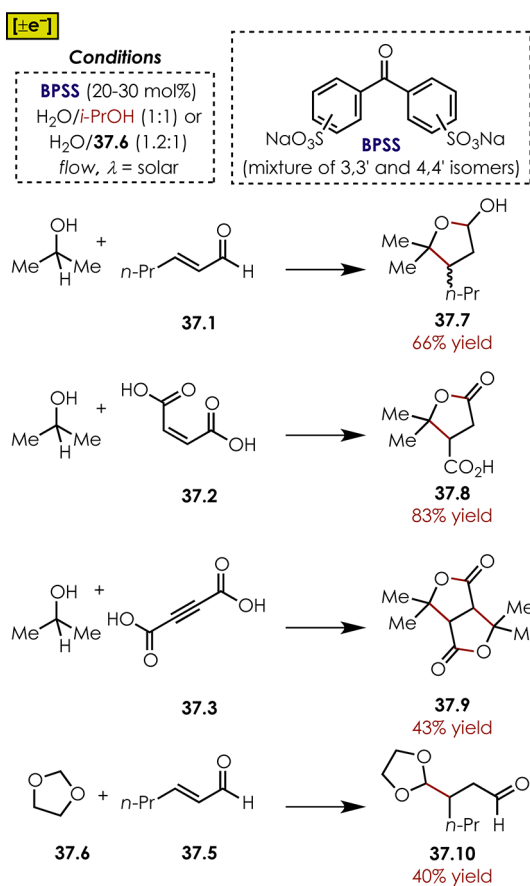
**Scheme 36.** Radical Conjugate Addition Initiated by BP or AQ Followed by Yang Cyclization



photoredox transformation was followed by direct photolysis, and cyclobutanes **36.4** were furnished by way of a Yang cyclization.<sup>213</sup> Benzophenone **BP** was initially used as the photoredox catalyst, but anthraquinone **AQ** was found to give higher yields of products **36.3** at much lower loadings.

A more recent example of a radical conjugate addition reaction was the fruit of an effort to harness sunlight to drive synthetic transformations by utilizing a flow reactor outfitted with a parabolic mirror to focus solar irradiation. To this end, *i*-propanol (*i*-PrOH) and acetal **37.6** were reacted with several unsaturated carbonyl compounds in the presence of the water-soluble benzophenone derivative **BPSS**, and the conjugate addition products **37.7–37.10** were returned in generally moderate yields (Scheme 37).<sup>214</sup> With *i*-PrOH as a radical precursor, the lactols **37.7** and lactones **37.8** and **37.9** were obtained upon reaction with enals, enoic acids, and ynoic acids, while cyclic acetals **37.6** gave the conjugate addition products without further reaction of the acetal **37.10** (cf. Scheme 36). Even with moderate yields, 10–20 g of product was generated

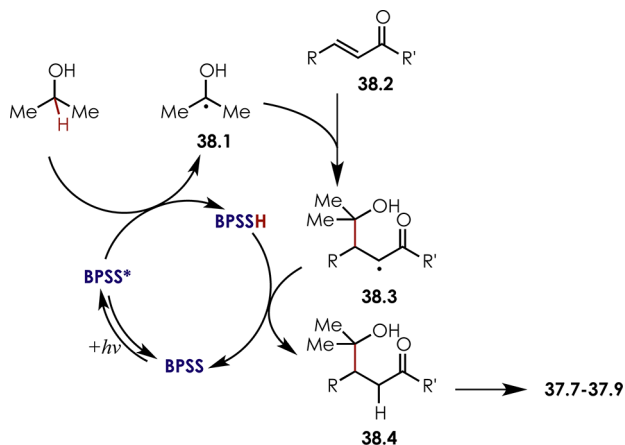
**Scheme 37.** Radical Conjugate Addition Reactions in Flow with Solar Irradiation



using this flow reactor apparatus after less than 20 h of total sunlight exposure.

The established mechanism for this transformation (Scheme 38) begins with H atom abstraction on *i*-PrOH (or acetal 37.6)

**Scheme 38.** Radical Conjugate Addition Mechanism

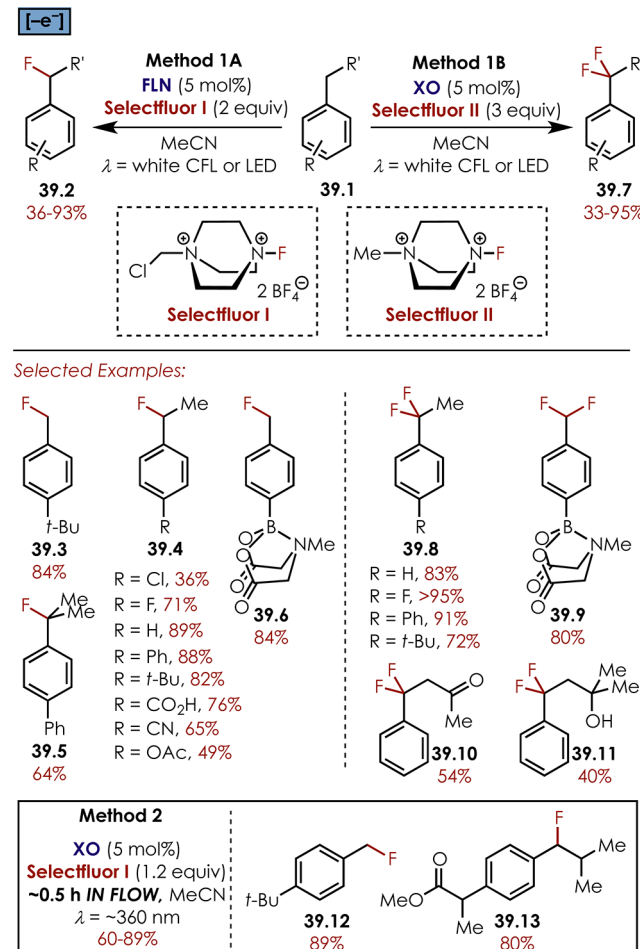


by excited state benzophenone BPSS\*. The ketyl radical 38.1 adds to alkene 38.2 (or alkyne), and the resulting radical adduct 38.3 undergoes RHAT with ketyl radical BPSSH•, thereby regenerating the photoredox catalyst BPSS and furnishing the saturated carbonyl compound 38.4. Ring closure subsequently

furnishes products 37.7–37.9 if *i*-PrOH is used as a coupling partner.

The ability of photo-excited benzophenones to abstract H atoms was put to use by Chen and co-workers, who accomplished selective benzylic C–H fluorination with fluorenone FLN (method 1A, Scheme 39).<sup>37</sup> Consistently high

**Scheme 39.** Benzylic Fluorination and Difluorination using FLN and XO

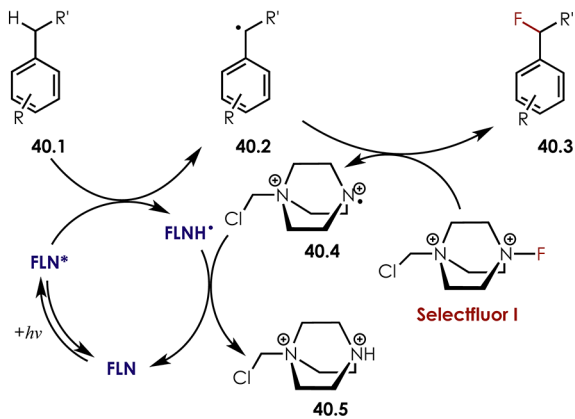


yields of the mono-fluorinated compounds 39.2 were obtained when Selectfluor® I as a fluorine transfer reagent, even when the starting materials 39.1 contained multiple benzylic C–H bonds. Interestingly, when the conditions were modified by employing xanthone XO as the photoredox catalyst and Selectfluor® II as the fluorine source, 83% yield of the *gem*-difluoro ethylbenzene 39.7 was obtained from ethylbenzene with 0% of the monofluorinated product 39.2 observed (method 1B, Scheme 39). Under the same conditions, FLN gave only 2% 39.7 and 62% monofluorinated 39.1, which was rationalized by the authors as indicating that the more electron-rich XO is more reactive towards HAT than FLN, enabling XO to overcome the deactivating effect incurred by installation of a fluorine geminal to the H atom undergoing abstraction. This methodology was adapted to be run in flow (method 2, Scheme 39),<sup>215</sup> resulting in comparable yields but much faster reaction times than the batch process. The authors were able to obtain multigram quantities of the products using this setup and demonstrated impressive selectivity in the fluorination of ibuprofen methyl ester (product 39.13).

The proposed reaction mechanism (Scheme 40) consists of benzylic H atom abstraction by the excited state ketone (e.g.

**Scheme 40. Mechanism of Radical Fluorination using FLN or XO and Selectfluor® I or II**

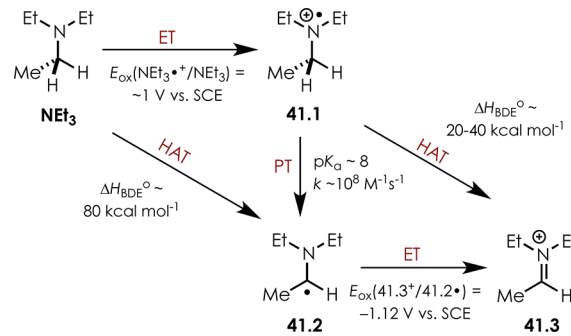
*Proposed Mechanism:*



FLN\*), followed by F atom transfer from Selectfluor® I to benzylic radical 40.2. The dication radical 40.4 generated by F atom transfer is thought to regenerate FLN by HAT.

Tertiary amines (Scheme 41), such as triethylamine ( $\text{NEt}_3$ ) diisopropylethylamine ( $i\text{-Pr}_2\text{NEt}$ , also known as Hunig's Base),

**Scheme 41. Mechanisms Involved in the PET-Induced Generation of  $\alpha$ -Amino Radicals and Iminiums from Alkylamines**

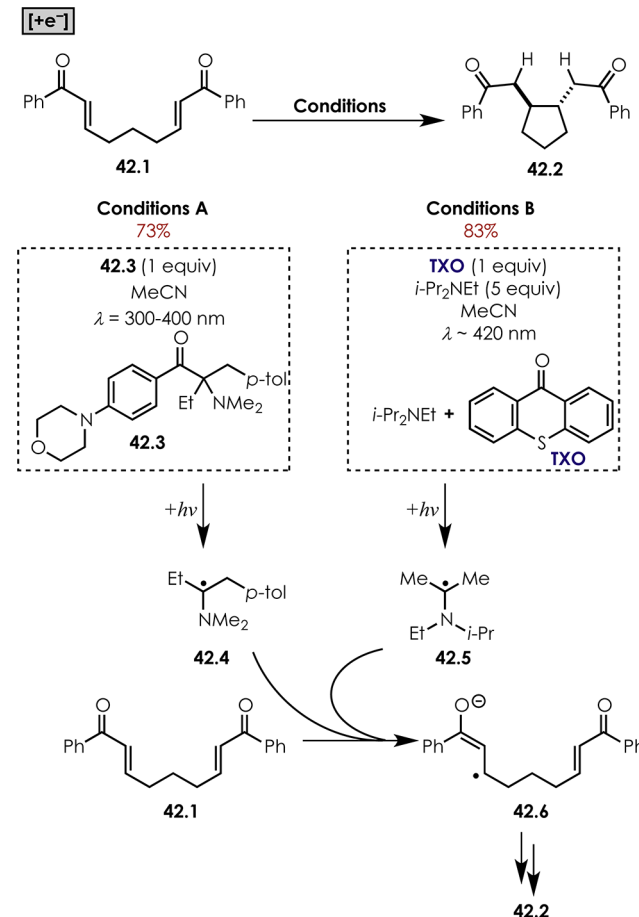


are the most common sacrificial reductants used in photoredox catalysis and exhibit low-lying oxidation potentials ( $E_{\text{ox}}(\text{NEt}_3\bullet^+/\text{NEt}_3) = +0.99 \text{ V vs SCE}$ , peak potential).<sup>216</sup> However, the particular mechanisms which allow them to be good reductants are relatively complex. The pathways shown in Scheme 41 summarize the insights from thorough mechanistic investigations on the photochemical oxidation of amines, and  $\text{NEt}_3$  is given as a representative example. In many systems, oxidation of a tertiary amine ultimately proceeds to an iminium, such as 41.3 in the case of  $\text{NEt}_3$ , constituting a net loss of two electrons and one proton. A key intermediate is the  $\alpha$ -amino radical 41.2, a good reductant that can be formed by deprotonation of cation radical 41.1. Although the  $pK_a$  values for  $\alpha\text{C}-\text{H}$  deprotonation<sup>217–220</sup> of simple tertiary alkylamine and aniline cation radicals have been estimated between  $\sim 3$  and  $20$ <sup>199,221,222</sup> [ $pK_a(\text{NMMe}_3\bullet^+) = 8$ <sup>223</sup>], the rate of deprotonation is known to be very fast, ranging from  $\sim 10^5 \text{ M}^{-1} \text{ s}^{-1}$ <sup>224,225</sup> to  $\sim 10^8 \text{ M}^{-1} \text{ s}^{-1}$ .<sup>223</sup> The  $\alpha$ -amino radical 41.2 formed in this fashion is a moderately strong reductant and readily donates an electron to form iminium 41.3 [ $E_{1/2}(41.3^\bullet/41.3) = -1.12 \text{ V vs SCE}$ ].<sup>216</sup>

**41.2•) =  $-1.12 \text{ V vs SCE}$ .**<sup>120</sup> An alternative pathway to the  $\alpha$ -amino radical 41.2 is by HAT from the amine. The BDE of the  $\alpha\text{C}-\text{H}$  bond in tertiary alkyl amines is approximately 80 kcal mol<sup>-1</sup>, and  $\alpha$ -amino radical 41.2 can be formed by direct HAT with another radical<sup>216,226,227</sup> or a photoredox catalyst such as benzophenone.<sup>207,225</sup> However, upon single electron oxidation of the amine, the BDE of the amine is drastically lowered ( $\Delta H_{\text{BDE}}^\circ$  estimated to be  $\sim 20$ – $40$  kcal mol<sup>-1</sup> for 41.1<sup>216,221</sup>), and HAT directly from cation radical 41.1 is also a proposed pathway to iminium 41.3.<sup>221,230,231</sup>

Sciaiano demonstrated the importance of  $\alpha$ -amino radicals as reductants in a bis-enone cyclization<sup>232</sup> reported previously by the Yoon group.<sup>233</sup> Sciaiano and co-workers discovered that a stoichiometric quantity of  $\alpha$ -amino radical 42.4 generated by UV photolysis of precursor 42.3 provided *trans*-cyclopentane 42.2 as the single product of reductive cyclization in 73% yield (Scheme 42). Reasoning that a buildup of  $\alpha$ -amino radical 42.5 may be

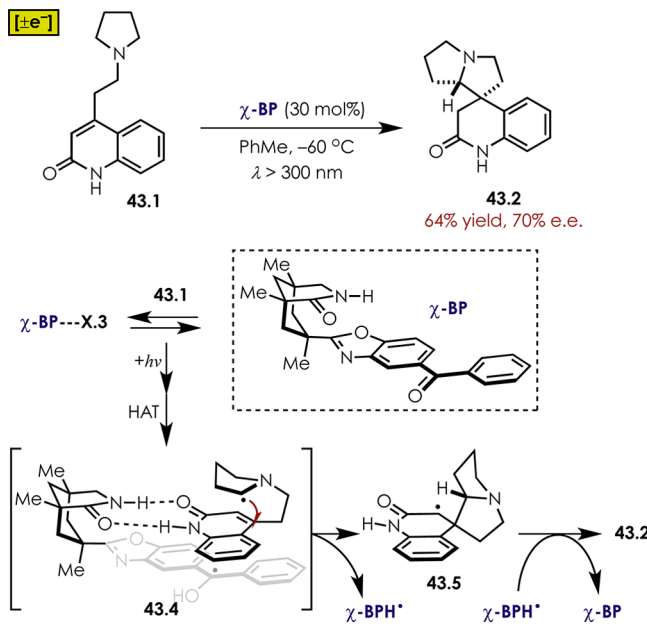
**Scheme 42. Reductive Cyclization Driven by  $\alpha$ -Amino Radicals**



sufficient to drive the cyclization, even in the absence of a photoredox catalyst that is not strongly reducing, the researchers employed thioxanthone TXO and  $i\text{-Pr}_2\text{NEt}$  in order to generate radical 42.5 through the photoredox HAT activity of the thioxanthone. This protocol, although not catalytic with respect to TXO, gave cyclopentane 42.2 in 83% yield under visible light irradiation demonstrates an important concept that even primarily oxidizing photoredox catalysts can accomplish reductive transformations by triggering a buildup of  $\alpha$ -amino radicals 42.5.

A relatively rare demonstration of enantioselective photoredox catalysis was provided by Bach and co-workers, who reported an intramolecular cyclization of quinolone **43.1** to give **43.2** in up to 72% e.e. (**Scheme 43**).<sup>234</sup> This strategy is based on the generation

**Scheme 43.** Enantioselective  $\alpha$ -Amino Radical Cyclization

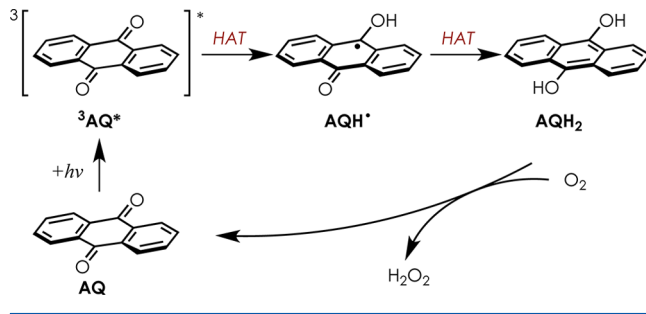


of an  $\alpha$ -amino radical by benzophenone  $\chi\text{-BP}$  possessing a rigid chiral recognition element which complexes with the amide portion of quinolone **43.1** by complementary H-bonding. The authors envisaged that the H-bonded complex **43.4** is the preferred configuration and provides facial selectivity in the radical cyclization step by blocking one face of the alkene with the ketyl radical portion of the benzophenone catalyst. HAT regenerates the benzophenone  $\chi\text{-BP}$  enabling it to act as a catalyst. It is unclear whether the substrate is complexed with benzophenone  $\chi\text{-BP}$  during excitation and/or the formation of  $\alpha$ -amino radical **43.4**, which occurs either by HAT or amine oxidation and  $\alpha$ -deprotonation. The highest combination of yield and e.e. was 64% yield in 70% e.e. and was achieved when employing 30 mol %  $\chi\text{-BP}$ . This report remains one of the furthest advancements in enantioselective organic photoredox catalysis.

### 5.3. Quinones: Photophysical and Electrochemical Characteristics

Most quinones are strongly absorbing around 300 nm with weaker absorptions in the near UV and visible region ( $\sim 400\text{ nm}$ ). In terms of photophysics and reactivity, benzannulated quinones such as naphthoquinone and anthraquinone bear many similarities with benzophenones. Namely, anthraquinone **AQ** and its water-soluble derivatives<sup>235–237</sup> undergo fast intersystem crossing to the triplet states, which efficiently accomplish H atom abstraction to form the semiquinone radicals of the type **AQH $\bullet$**  (**Scheme 44**). Unlike benzophenones, anthraquinones have the ability to perform a second H atom abstraction and proceed to the anthraquinol of the type **AQH<sub>2</sub>** almost quantitatively.<sup>235</sup> Mechanistic inquiries showed that introduction of oxygen to a solution of quinol **AQH<sub>2</sub>** allowed for complete recovery of the quinone (**Scheme 44**),<sup>133</sup> which had been put to use in the early 20th century as an important industrial process for the production of  $\text{H}_2\text{O}_2$ .<sup>238</sup> Quinones are reduced at significantly

**Scheme 44.** PHAT Ability of Anthraquinone (AQ)

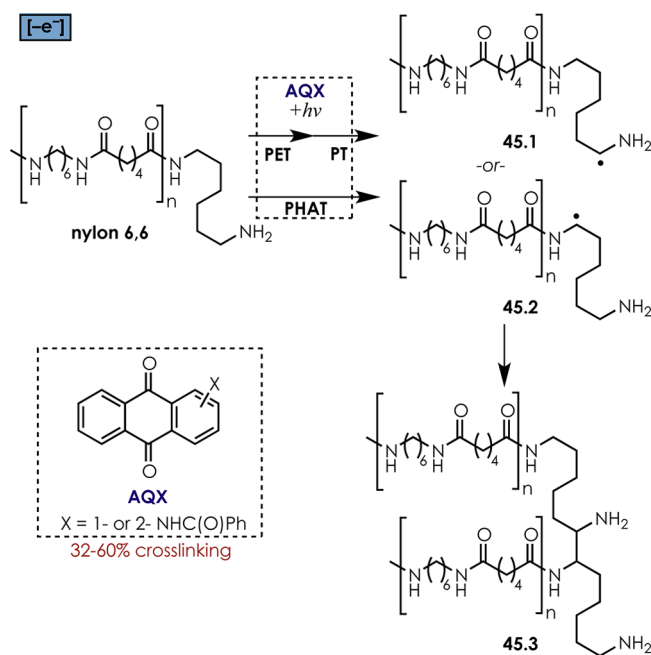


more positive potentials than benzophenones, a key difference which makes them excellent electron acceptors even in the triplet state.<sup>239</sup> Two extreme examples of this characteristic are 2,3,5,6-tetrachloro-1,4-benzoquinone (TCBQ) and 2,3-dichloro-5,6-dicyano-1,4-benzoquinone (DDQ), which are reduced at potentials near or above 0 V vs SCE. DDQ is known to mediate oxidation reactions in the ground state,<sup>240</sup> so it is not surprising that the efficiently formed triplet excited state species is a remarkable oxidant. Conversely, turnover of  $\text{DDQ}^{\bullet-}$  is expected to be problematic, as its positive reduction potential signifies that the reverse reaction ( $\text{DDQ}^{\bullet-} \rightarrow \text{DDQ}$ ) is an endergonic electron transfer. Perhaps for this reason, few catalytic photoredox systems employing DDQ have been reported; however, one existing methodology exploits the assistance of a chemical oxidant to turnover the quinol form  $\text{DDQH}_2$  using  $\text{O}_2$  (see below).<sup>43</sup>

### 5.4. Quinones: Reactions

One interesting application of anthraquinones has been in the photoinduced cross-linking of polymers such as nylon-6,6. Photo-excited anthraquinone dyes and textiles share a long history,<sup>237</sup> and the modification of polymers in this fashion has led to both degradation and stabilization of the materials in various cases.<sup>241</sup> For nylon-6,6, Allen and co-workers studied the particular mechanisms of crosslinking (**Scheme 45**) using 1- and

**Scheme 45.** Photo-Oxidative Crosslinking of Nylon 6,6

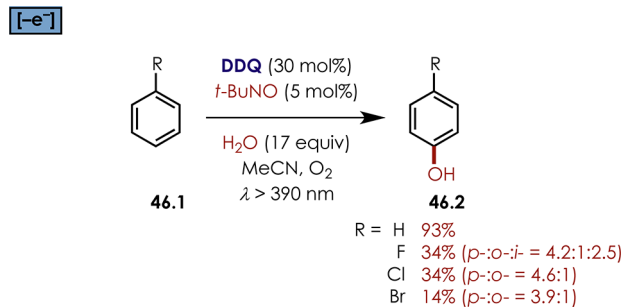


2-substituted anthraquinone derivatives (AQX), discovering that the triplet anthraquinones can both abstract an H atom or oxidize the terminal amine or amide in the polymer backbone.<sup>242,243</sup>

Both pathways lead to the generation of “macro-alkyl” radicals **45.1** or **45.2** which subsequently undergo cross-linking. Up to 60% cross-linking was observed for some anthraquinones, which were employed in 2 wt %.

**DDQ** is well known for its use as an organic oxidant,<sup>244,245</sup> and many non-photochemical reactions of this quinone are performed at elevated temperatures<sup>240</sup> as its ground state reduction potential, although anomalously high, is insufficient to oxidize unreactive substrates, such as benzene. However, Fukuzumi and co-workers took advantage of the fact that **DDQ** is a powerful oxidant when promoted to an excited state and were able to accomplish the catalytic coupling of benzenes **46.1** and  $\text{H}_2\text{O}$  to phenols **46.2** in 93% yield (Scheme 46).<sup>43</sup> The use of

Scheme 46. C–H Hydroxylation of Benzene and Halobenzenes



**DDQ** as a photoredox catalyst was enabled by including a catalytic amount of *tert*-butyl nitrite (*t*-BuNO) under aerobic conditions.<sup>246</sup> Fluoro-, chloro-, and bromo-benzenes underwent hydroxylation in lower yields, providing a mixture of para- and ortho-regioisomers, along with significant amounts of ipso-substitution of the fluorine substituent.

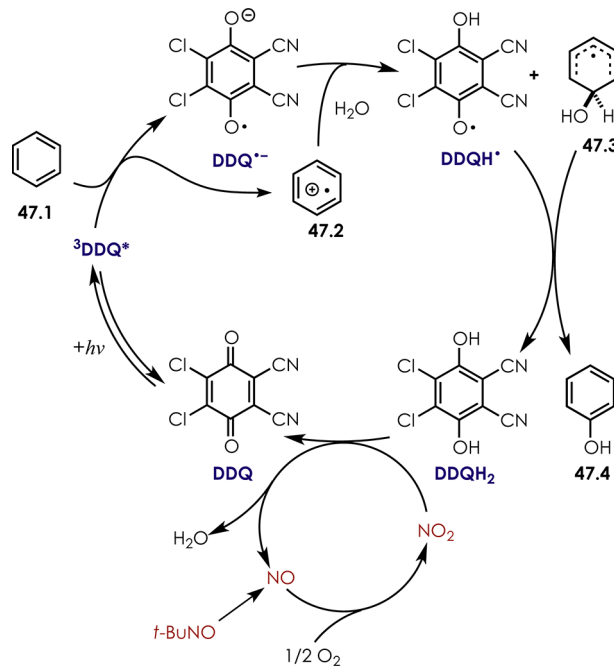
In accordance with the proposed mechanism (Scheme 47),  $\text{H}_2\text{O}$  adds to the benzene cation radical **47.2** generated by PET with  ${}^3\text{DDQ}^*$ . Protonation of  $\text{DDQ}\bullet^-$  produces quinolyl radical  $\text{DDQH}\bullet$ , which can accomplish HAT from the cyclohexadienyl radical **47.3** in the aromatization step that furnishes the phenol product. The fully reduced  $\text{DDQH}_2$  generated in this way is oxidized to **DDQ** by chemical oxidation with nitrogen dioxide ( $\text{NO}_2$ ), producing  $\text{H}_2\text{O}$  and nitric oxide (NO) in the process. NO is recycled to  $\text{NO}_2$  by aerobic oxidation after being initially formed in situ from *t*-BuNO. The authors reason that the C–H functionalization is possible for arenes **46.1** without significant over-oxidation of the phenolic products **46.2** because BET between cation radical **47.2** and  $\text{DDQ}\bullet^-$  may occur in the Marcus-inverted region,<sup>26,247</sup> whereas BET for the phenol cation radical is likely faster than diffusion. Evidence for this hypothesis is discussed in a later section (Scheme 63).

## 6. PYRYLIUMS AND THIAPYRYLIUMS

### 6.1. Triaryl Oxopyrylium Salts: Photophysical and Electrochemical Characteristics

Triarylpyryliums absorb in the visible range ( $\lambda_{\text{max}} \sim 415\text{--}440\text{ nm}$ ) and are strongly oxidizing in both the singlet and triplet excited states. Their singlet lifetimes tend to be short ( $\tau_{\text{F}} < 5\text{ ns}$ ), and consequently, high efficiency of PET is difficult to achieve from the singlet excited state. The parent compound of this class,

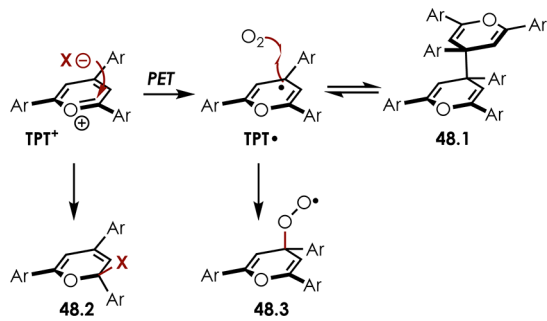
Scheme 47. Proposed Mechanism for Photoredox Catalytic Aryl C–H Hydroxylation



2,4,6-triphenylpyrylium (**TPT** $^+$ ), exhibits an ISC quantum yield ( $\phi_{\text{ISC}}$ ) of  $\sim 0.5$ , and the resultant triplet state is a strong oxidant ( $E_{\text{red}}^*({}^3\text{TPT}^{+*}/\text{TPT}^*) = \text{ca. } +1.9\text{ V}$ ) as well. For **TPT** $^+$ , substrates with sufficiently low oxidation potentials quench both the singlet and triplet excited states with rate constants near the diffusion limit, and PET in such cases is thought to arise from both states.<sup>48,142</sup> Triarylpypyliums with diverse substitution on the aryl groups can be prepared with relative ease,<sup>50,248</sup> providing access to chromophores with a range of electrochemical and photophysical properties. The redox potentials of these pyryliums trend with the electronic character of the arenes at the 2-, 4-, and 6-positions. Other triarylpypyliums do not undergo efficient ISC but are competent oxidants in the triplet state nonetheless. Since there is no charge separation between these cationic photoredox catalysts and a neutral substrate upon PET, a lack of coulombic attraction renders cage escape more favorable when compared to neutral photoredox catalysts,<sup>249</sup> which decreases the likelihood of BET within the contact pair. On these grounds, the efficacy of cationic photoredox catalysts is generally superior to neutral variants.

Whereas other excited state organics are responsible for  ${}^1\text{O}_2$  generation by energy transfer from the triplet excited species to ground state  ${}^3\text{O}_2$ , **TPT** $^+$  is thought to be free from this activity under normal conditions.<sup>250</sup> Although triplet  ${}^3\text{TPT}^{+*}$  can be quenched by  ${}^3\text{O}_2$ , electron donors quench  ${}^3\text{TPT}^{+*}$  several orders of magnitude faster than  ${}^3\text{O}_2$ .<sup>48</sup> Furthermore, the ground state reduction potential of **TPT** $^+$  is not sufficiently negative to cause the resulting pyranyl radical **TPT** $\bullet$  to undergo SET with  ${}^3\text{O}_2$  to generate superoxide ( $\text{O}_2\bullet^-$ ). Thus, **TPT** $^+$  avoids reactivity that is often considered undesirable under aerobic conditions. Interestingly, **TPT** $\bullet$  can react with  ${}^3\text{O}_2$  to give peroxy radical **48.3** (Scheme 48), which is implicated as an intermediate in some oxygenation reactions enabled by **TPT** $^+$ , although others have argued against such an intermediate.<sup>251</sup> Despite the moderate ground state reduction potential enabling **TPT** $\bullet$  to be returned to the ground state **TPT** $^+$  by a relatively weak oxidant, pyranyl radicals are prone to dimerization adducts **48.1**,<sup>252–256</sup> which,

**Scheme 48. Deactivation Pathways of Triarylpyryliums and Pyranyl Radicals**



although reversible for 2,4,6-triarylpyryliums,<sup>255</sup> can deactivate the catalyst in an off-cycle equilibrium. Likewise, nucleophiles can add to the pyrylium core and lead to catalyst degradation via the formation of addition adducts such as **48.2**.<sup>257</sup>

## 6.2. Triaryl Oxopyryliums: Reactions

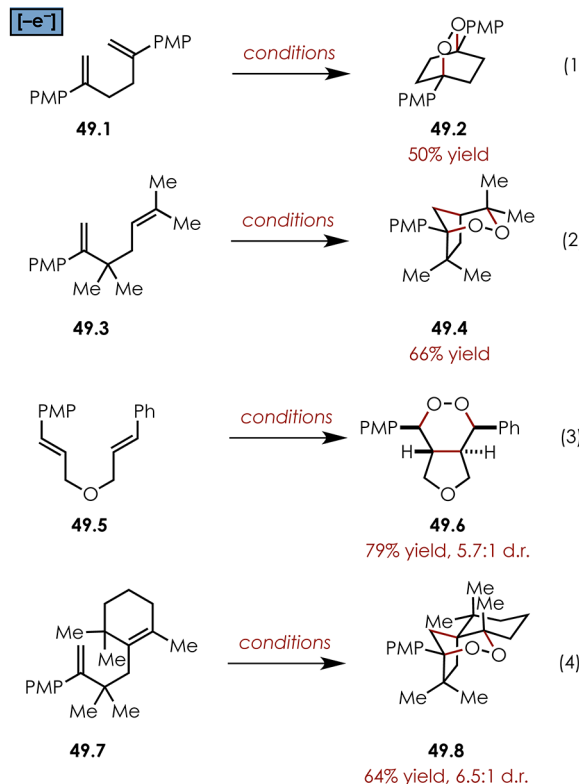
As Miranda reviewed pyrylium photoredox chemistry extensively in 1994,<sup>258</sup> we will only highlight examples that have been reported subsequently.

**6.2.1. Net Oxidative Transformations.** **6.2.1.1. Diene Cyclization-Endoperoxidation.** Early reports by Miyashi<sup>258</sup> of 1,5-diene cyclization-endoperoxidation catalyzed by DCA has inspired recent work in expanding the scope of this transformation and also investigating other classes of photoredox catalysts to facilitate this process.<sup>259,260</sup> A report using 2,4,6-tri(*p*-methoxyphenyl)pyrylium tetrafluoroborate (*p*-MeO-TPT) as the photoredox catalyst discloses unique cyclization-endoperoxidation cascade reactions of several different 1,5-dienes (Scheme 49).<sup>260</sup> Under 1 atm of O<sub>2</sub>, a series of 1,5-dienes (**49.1**, **49.3**, **49.5**, and **49.7**) were submitted to the photooxidation conditions and furnished endoperoxides **49.2**, **49.4**, **49.6**, and **49.8**, respectively.

A requirement for the endoperoxidation cascade reaction was the presence of an electron-rich styrene as well as a pendant olefin capable of reacting with the alkene cation radical. However, not all 1,5-dienes tested in the reaction gave the anticipated endoperoxide adducts, as several different classes of 1,5-dienes underwent a Cope-like rearrangement followed by oxidative cleavage to give the products of formal ketone  $\alpha$ -allylation. On the basis of the reactivity patterns observed, a similar mechanism to Miyashi's is invoked wherein single electron oxidation of the 1,5-diene, followed by cyclization, forms a distonic cation radical. Interception of the distonic cation radical by molecular O<sub>2</sub>, followed by reduction and a second cyclization, furnishes the 1,2-dioxane adducts.

**6.2.2. Net Redox Neutral Transformations.** **6.2.2.1. [2+2] Cycloaddition Reactions.** Cation radical-mediated [2+2] cycloaddition reactions of olefins have been the subject of many studies in the past 40 years<sup>261–263</sup> (see also Scheme 169). Recently, photoinduced electron transfer methods have been developed to realize alkene dimerization to cyclobutanes.<sup>264</sup> Nicewicz and Riener described the use of pyrylium salts as catalysts for cyclobutane formation via alkene dimerization.<sup>265</sup> The difficulty with developing oxidative cyclobutane dimerization reactions is the reversibility with respect to the reaction. The reversibility of the reaction hinges on the oxidation of the final adducts leading to retro [2+2] reactivity, as was discussed previously in Section 5. Since there is only a slight difference (ca. 200 mV) between the oxidation potentials of the cyclobutane

**Scheme 49. Cyclization-Endoperoxidation Cascade Reactions**



conditions: *p*-MeO-TPT (2 mol %),  $\lambda = 470$  nm, 1 atm O<sub>2</sub> MeCN, -41 °C

products and starting olefins, identifying a catalyst that is capable of being general for a range of substrates is difficult.

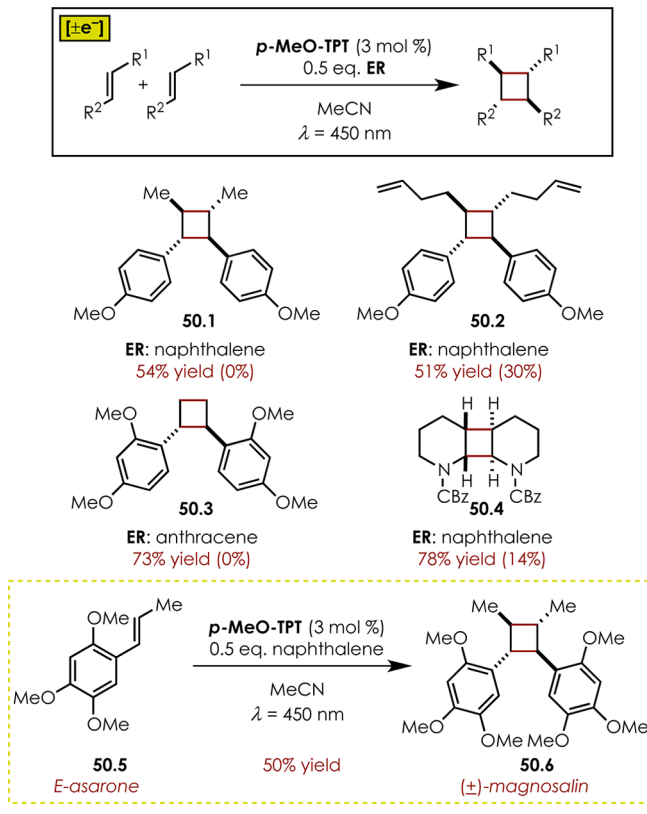
Nicewicz and Riener's approach was to employ simple aromatics as electron relays (ER) to closely match the redox potentials of the alkenes (Scheme 50). The hypothesis was that oxidation of the ER would occur first, and then go on to oxidize the alkene. Due to the fact that the electron relay, in general, had a lower redox potential than the final cyclobutane adducts, reoxidation and retro cycloaddition would be averted.

This strategy worked in principle to effect the homodimerization of a variety of alkenes (Scheme 50). A series of styrenes bearing various functional groups was investigated, but in general, the presence of at least one alkoxy group was required for reactivity (**50.1**–**50.3**). In addition, CBz-protected tetrahydropyridines readily dimerize in good yields (**50.4**). Lastly, this method was applied to the synthesis of ( $\pm$ )-magnosalin (**50.6**), from the naturally-occurring monomer *E*-asarone (**50.5**).

Shown in parentheses are the yields of the reactions in the absence of their respective ER. In nearly every case, the yields without the ER are markedly lower, supporting the assertion that minimizing cycloreversion is the key to achieving high cyclobutane yields. In further support of this mechanistic hypothesis, subjection of one of the cyclobutane adducts to photolytic conditions in the presence of *p*-MeO-TPT gave varying quantities of the alkene starting material. This cycloreversion was nearly completely suppressed with the addition of an ER.

**6.2.2.2. [4+2] Cycloaddition Reactions.** Blechert and Steckhan have done extensive studies on cation radical-mediated [4+2] cycloaddition reactions of indoles, where the 2,3-double bond acts as a dienophile.<sup>50,266–268</sup> Due to the electronics of the indole, only inverse demand Diels-Alder reactions are possible

Scheme 50. Styrene Cyclodimerization



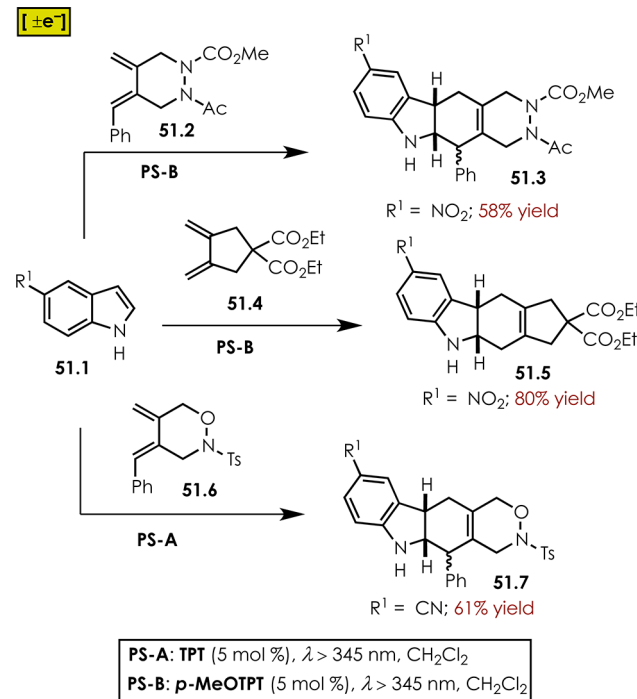
under thermal conditions. Single-electron oxidation of the indole effects a polarity reversal that enables reactivity with electron-neutral to electron-rich dienes and potentially unlocks the use of simple indole fragments in cycloaddition reactions for applications to complex alkaloid synthesis.

Blechert and Steckhan have studied a variety of dienes that react in this context and, in particular, have demonstrated the use of TPT and *p*-MeOTPT as single-electron redox catalysts for the cycloadditions depicted in Scheme 51.<sup>268</sup> Structurally unique dienes **51.2**, **51.4**, and **51.6** all reacted with 5-substituted indoles (**51.1**) to give indolines **51.3**, **51.5**, and **51.7** in good yields and, importantly, in the case of **51.2** and **51.6**, afford single regioisomers of products **51.3** and **51.7**. Cycloadducts **51.3** and **51.7** present excellent points for further elaboration by N–N and N–O bond cleavage.

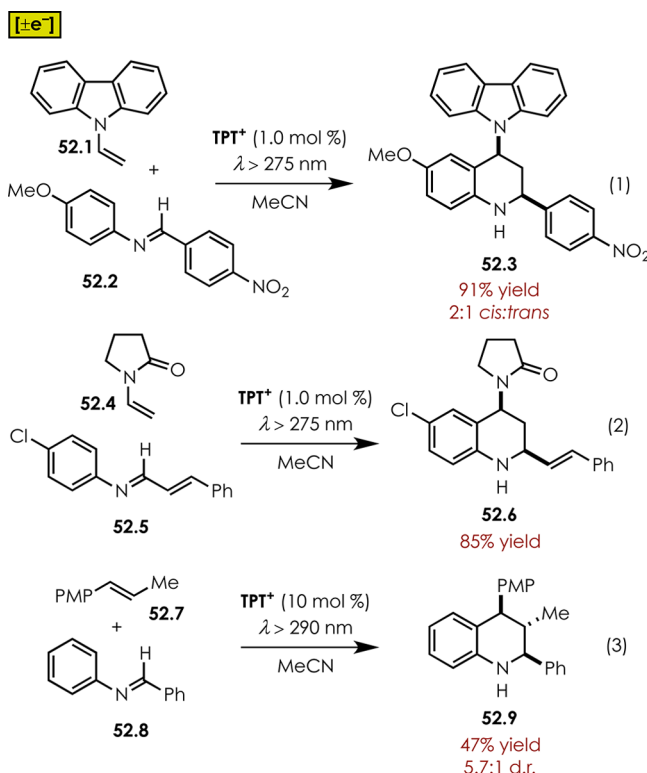
The use of PET to catalyze imino Diels-Alder reactions has been documented by several groups that report the use of pyrylium salts as photooxidants for the transformation.<sup>269–271</sup> In general, electron-rich alkenes are the apparent requirement for the transformation as *N*-vinyl carbazole (**52.1**), *N*-vinyl pyrrolidinone (**52.4**), and *p*-methoxy- $\beta$ -methylstyrene (**52.7**) all react with *N*-aryl benzaldehyde imines to forge tetrahydroquinoline products (Scheme 52). Thiobenzophenones have also been utilized in similar [4+2] transformations with pyrylium and thiapyrylium salts as catalysts.<sup>272,273</sup>

Miranda and coworkers have researched the mechanism of the imino Diels-Alder transformations using a combination of laser flash photolysis and DFT calculations. It was determined that the mechanism likely involves single-electron oxidation of the alkene component first, as **53.2** was detected by transient absorption spectroscopy (Scheme 53). DFT calculations indicate that reaction with the imine in a highly asynchronous manner likely gives rise to **53.3**. A 1,3-hydride shift ensues to give intermediate

Scheme 51. Indole [4+2] Cycloaddition Reactions

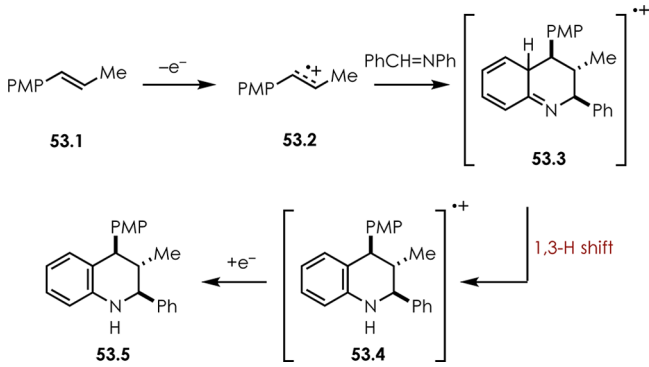
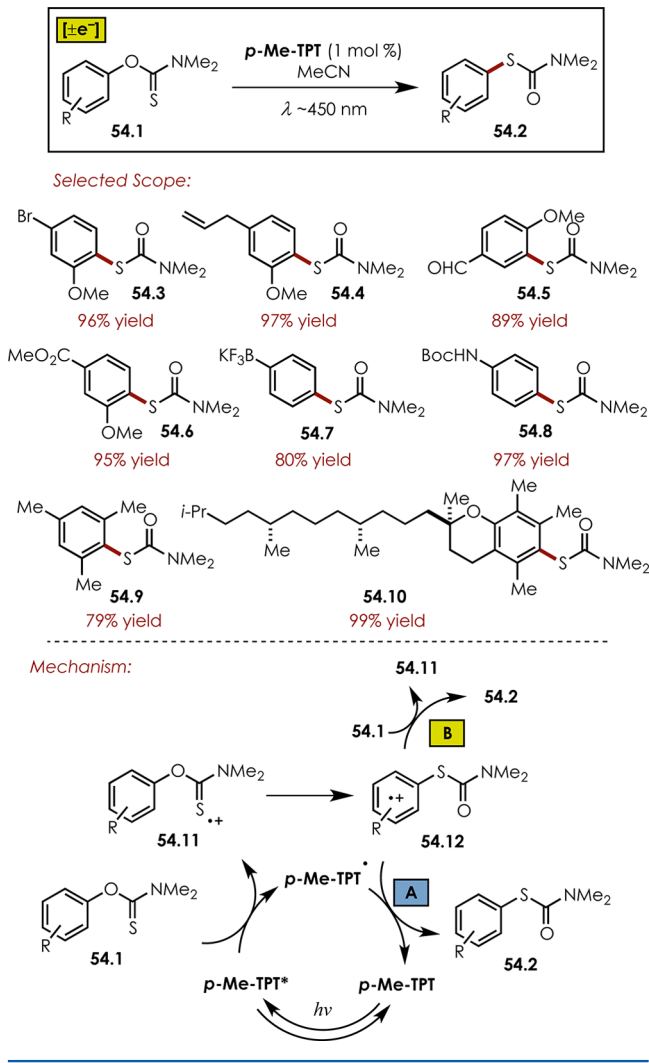


Scheme 52. Pyrylium-Catalyzed Diels-Alder Reactions



**53.4**, and following back electron transfer, the final adducts (**53.5**) are obtained.

**6.2.2.3. Rearrangements.** Recent work from the Nicewicz laboratory demonstrates acceleration for the Newman-Kwart rearrangement of *O*-aryl carbamothioates (**54.1**) to *S*-aryl carbamothioates (**54.2**) at room temperature (Scheme 54).<sup>274</sup> Using 1 mol % of *p*-Me-TPT as the single-electron photo-

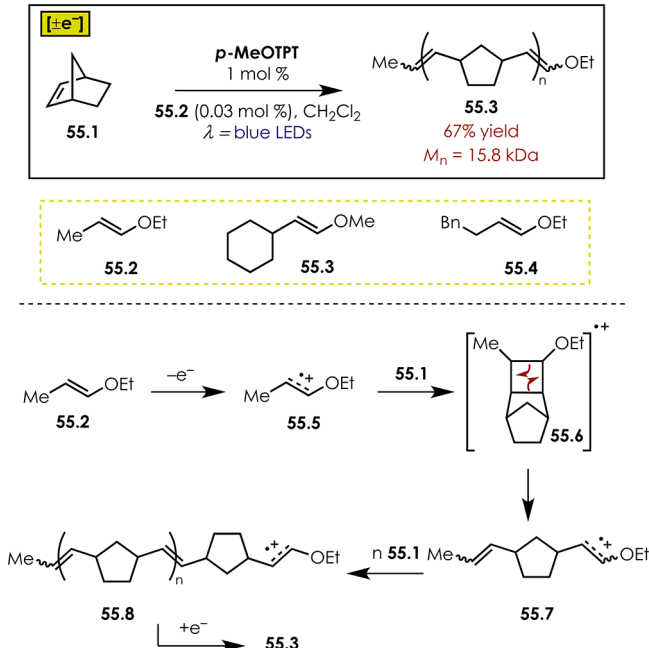
**Scheme 53. Mechanism of PET Imino Diels-Alder Reaction****Scheme 54. Photoredox Catalysis of the Newman-Kwart Rearrangement**

oxidation catalyst, the Newman-Kwart rearrangement could be facilitated for a variety of aromatic compounds bearing a range of functional groups including alkyl (**54.9**), alkoxy (**54.3–54.5**), halides (**54.3**), carbamates (**54.8**), esters (**54.6**), aldehydes (**54.5**), and potassium trifluoroborates (**54.7**). As a more complex example, ( $\pm$ )- $\alpha$ -tocopherol (**54.10**) underwent clean O- to S-migration in nearly quantitative yield. Simple treatment of the rearranged products to basic conditions furnishes the corresponding thiophenol derivatives. The current limitations of

the reaction are the necessary presence of at least a mildly electron-donating group as well as this substituent being in either the ortho- or para-positions. Interestingly, *meta*-substituted O-aryl carbamothioates failed to undergo the rearrangement unless an ortho- or para-electron releasing substituent was present.

The authors propose that the mechanism proceeds via single-electron oxidation of the sulfur atom by *p*-Me-TPT\*, supported by cyclic voltammetry data. Following generation of cation radical **54.11** and based on the substitution patterns that are productive in the reaction, it was proposed that the aromatic ring attacks the sulfur cation radical and after C–O bond cleavage gives rise to **54.12**. The termination step is less clear and two scenarios are possible: reduction of **54.12** by *p*-Me-TPT• (path A) or in a chain process, another molecule of **54.1** could donate an electron to complete the reaction and generate **54.11** (path B). It is conceivable that both pathways are operative, though further mechanistic investigation is necessary. The observation that lower reaction concentrations led to an increase in reaction kinetics is somewhat perplexing but may point to the intermediciy of a **54.1–54.11** dimer that decreases reaction rates. Regardless, this work amounts to a substantial reduction in the typically high temperatures ( $>250$  °C) required for the thermal Newman-Kwart rearrangement.

**6.2.2.4. Polymerization Reactions.** Boydston and coworkers have recently disclosed a metal-free approach to ring-opening metathesis polymerization (ROMP) that makes use of *p*-methoxy triphenylpyrylium tetrafluoroborate (*p*-MeOTPT) as the catalyst (Scheme 55). On the basis of electrolytically-

**Scheme 55. Ring-Opening Metathesis Polymerization of Norbornene**

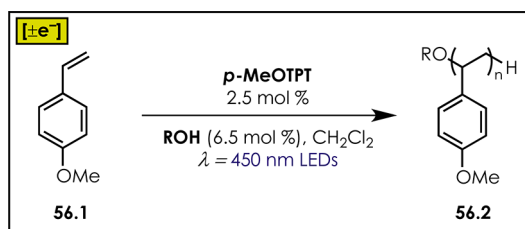
promoted cross metatheses disclosed by Chiba<sup>278–279</sup> as well as work in [2+2] cycloaddition reactions catalyzed by pyrylium salts, the authors hypothesized that a single-electron oxidation strategy could also facilitate ROMP of norbornene (**55.1**). With the use of 1 mol % of the pyrylium salt, a number of enol ether cocatalysts (**55.2–55.4**) were evaluated and gave the ROMP product **55.3** in good levels of reaction efficiency. In follow-up work from the same laboratory, dicyclopentadiene was also

employed as the monomer; however, significant crosslinking was observed via a secondary cross metathesis with the additional alkene present in the substrate.

Mechanistically, the reaction requires the use of the enol ether cocatalyst to provide a constant redox handle for further oxidation. To this end, single-electron oxidation of **55.2** by the pyrylium salt gives rise to olefin cation radical **55.5**. In much the same manner as the cycloaddition manifolds previously described, the monomer (**55.1**) can engage **55.5** in a [2+2] cycloaddition manifold to lead to cyclobutane cation radical **55.6**. Due to the ring strain inherent to the bicyclic structure, rapid cyclobutane ring opening occurs in the opposite direction before a return electron transfer can occur to give **55.7**, the propagating chain end. This cation radical can continue to engage additional monomer units until **55.8** is reduced to the final polymer product **55.3**. Since the chain end is still an oxidizable enol ether, even if reduction occurs, it is possible to reactivate the chain end via oxidation. This process should be controlled by light and is exactly what the authors found via control light/dark experiments.

In recent work, You and Nicewicz were able to catalyze the polymerization of *p*-methoxystyrene **56.1** with *p*-MeOTPT as the single-electron oxidation catalyst (Scheme 56).<sup>280</sup> The most

**Scheme 56. Polymerization of *p*-Methoxystyrene**



Entry	ROH	M <sub>n</sub> (kg/mol)	D	Yield %
1	—	72.5	3.04	92
2	MeOH	5.41	1.18	92
3	EtOH	6.12	1.22	96
4	i-PrOH	10.5	1.31	96
5	t-BuOH	26.0	1.86	97
6	CF <sub>3</sub> CH <sub>2</sub> OH	33.7	2.05	97

important finding was that alcohol cocatalysts (ROH) were able to provide exquisite control over both the molecular weight and polydispersity (D) of the resultant polystyrenes. The authors found that in the absence of the alcohol cocatalyst, the resultant polymer was formed with a broad polydispersity (D = 3.04 kg/mol, entry 1). However, upon addition of an alcohol in 6.5 mol %, much more narrow molecular weight distributions were achieved to the point where sterically small alcohols afforded nearly monodisperse polymers, especially in the case of MeOH (entry 2). The polydispersity generally tracked with both sterics (entries 2–5) as well as electronics, where more electron-deficient alcohols provided little in the way of control for polydispersity (entry 6). Polymer number-average (M<sub>n</sub>) also followed this general trend. The authors ascribe the control of M<sub>n</sub> and D to a mechanism similar to a reversible addition–fragmentation chain transfer (RAFT)-type mechanism wherein the *p*-MeO-TPT mainly serves as an initiator.

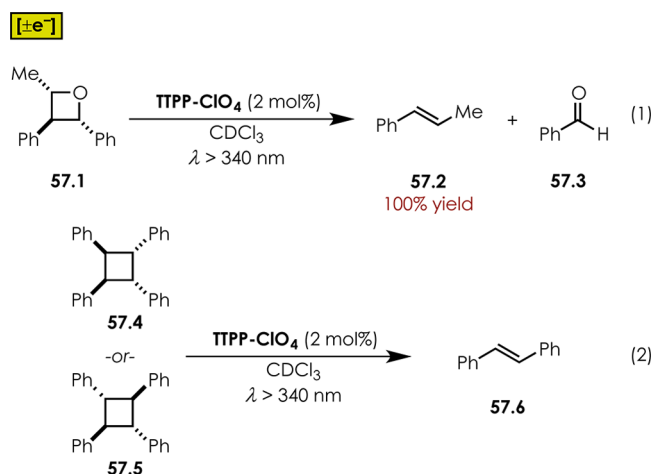
### 6.3. Triaryl Thiapyrylium: Photophysical and Electrochemical Characteristics

The most significant difference between triarylpyryliums and their sulfur-containing analogues, the triarylthiopyryliums, is their comparative singlet and triplet excited state populations. Although the singlet state lifetime of triphenyl thiapyrylium (TTPP<sup>+</sup>; τ<sub>F</sub> = 3.6 ns) is similar to that of oxopyrylium TPP<sup>+</sup>, the quantum yield of fluorescence is extremely low (ϕ<sub>F</sub> = 0.03), accompanied by a high triplet yield (ϕ<sub>ISC</sub> = 0.94). Given the high efficiency of ISC, <sup>3</sup>TTPP<sup>\*\*</sup> is typically considered the most relevant excited state, although both are shown to oxidize substrates with rate constants approaching the diffusion limit. TTPP<sup>+</sup> is reduced at a more positive potential than TPP<sup>+</sup> and resides at similar energies in the singlet (2.64 eV) and triplet (2.28 eV) excited states, rendering both good electron acceptors and comparable to <sup>1</sup>TPP<sup>\*\*</sup> and <sup>3</sup>TPP<sup>\*\*</sup>. Like TPP<sup>•</sup>, the thiopyranyl radical TTPP<sup>•</sup> cannot be oxidized by molecular oxygen and is thought to react in a similar fashion to the formation of peroxy radical **48.3**. The efficacy of TTPP<sup>+</sup> as a photoredox catalyst when compared to TPP<sup>+</sup> seems to be dependent on the transformation in question. Some examples have shown only marginal differences in overall catalytic performance,<sup>54</sup> while other studies have found that TTPP<sup>+</sup> is superior, which appears to be particularly relevant under conditions where PET between substrate and a triplet excited state molecule is most fruitful.

### 6.4. Triaryl Thiapyrylium: Reactions

**6.4.1. Cycloreversion Reactions.** Miranda and coworkers have done extensive investigations on cycloreversion reactions of 4-membered rings catalyzed by thiapyrylium salts.<sup>281–286</sup> For example, oxetane **57.1** readily undergoes cycloreversion to the corresponding alkene (**57.2**) in quantitative yield along with the expected aldehyde (**57.3**) (Scheme 57, eq 1). This is in stark

**Scheme 57. Oxetane and Cyclobutane Cycloreversion**

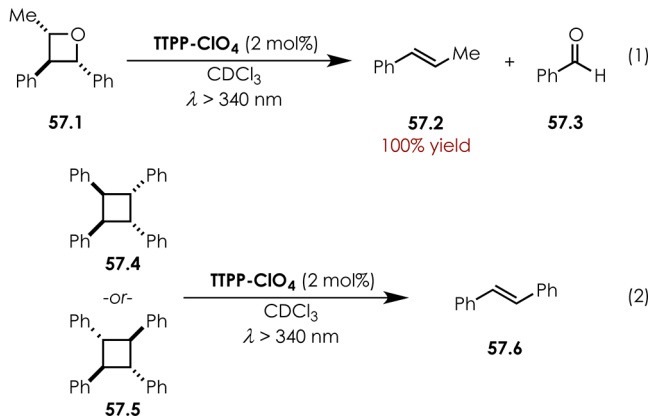


contrast to the reaction using TPT<sup>+</sup> as catalyst where only 8% of the cycloreversion is observed. Since the triplet state <sup>3</sup>TTPP<sup>\*\*</sup> is accessed more efficiently than <sup>3</sup>TPT<sup>\*\*</sup>, this difference points to the importance of the triplet as the active excited state in the PET process, as explained in Scheme 5.<sup>283</sup> In laser flash photolysis experiments, either cyclobutane isomer **57.4** or **57.5** afforded only *trans*-stilbene (**57.6**) upon irradiation in the presence of TTPP-ClO<sub>4</sub> as the catalyst (eq 2). Thietanes can also undergo cycloreversion under similar reaction conditions.

Evidence for a stepwise fragmentation mechanism was observed in the case of oxetane **58.1** (Scheme 58). Treatment

**Scheme 58. Oxetane Fragmentation and Intramolecular Reaction**

[ $-e^-$ ]



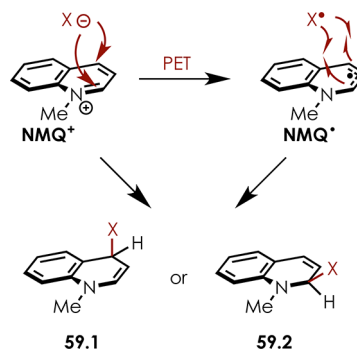
of **58.1** with 2 mol % TPP-ClO<sub>4</sub> under irradiation resulted in the formation of *trans*-stilbene (73% yield) along with tetrahydrofuran **58.3** (27% yield). The latter product can be explained via oxidation to **58.4** and C–O bond cleavage to access **58.5**. After a C–C bond rotation, rotamer **58.6** is poised to undergo addition to the carbocation and after a back electron transfer and proton shift, tetrahydrofuran **58.3** is formed. It should be noted that neither benzaldehyde nor cinnamyl alcohol was detected in the reaction and the use of TPT<sup>+</sup> gave a 48% yield of **58.2** along with a 17% yield of **58.3**.

## 7. QUINOLINIUMS

### 7.1. Photophysical and Electrochemical Characteristics

N-alkyl quinolinium ions absorb in the near UV ( $\sim 315$ – $350$  nm) and are some of the most potent photo-oxidants to be used as photoredox catalysts. With high-lying singlet energies ( $>3.3$  eV) and reduction potentials above  $-1.0$  V, quinoliniums are extremely oxidizing in the singlet excited state ( $>2.5$  V). Long singlet lifetimes and relatively high fluorescence quantum yields contribute to the efficacy of these salts in oxidative PET reactions. Moreover, their corresponding neutral quinolinyl radicals (such as **NMQ**) generated upon single electron reduction are sufficiently reducing so as to be turned over by relatively weak oxidants, including O<sub>2</sub>. Unfortunately, quinoliniums display a propensity towards addition of nucleophiles at the 2- and 4-positions in the ground state cations,<sup>287–290</sup> as well as radical reactions of quinolinyl radicals at the same positions (Scheme 59).<sup>57,59,291</sup> Both pathways lead to partial dearomatization of the chromophore, which can severely limit their application as photoredox catalysts. Although quinoliniums substituted at the 2- and 4-positions possess similar properties, their resistance to these deactivation pathways has not been thoroughly investigated. Interestingly, the most useful quinolinium in the synthetic setting seems to be 3-cyano-1-methylquinolinium QuCN<sup>+</sup>, containing substituents at neither of the most electrophilic positions. However, the singlet excited state reduction potential for this compound is reported to be  $+2.72$  V, rendering ET with unreactive hydrocarbons such as benzene [ $E_{\text{ox}}(\text{PhH}\bullet^+/\text{PhH}) = 2.35$  V vs SCE<sup>65</sup>] exergonic, while a fluorescence lifetime of 45 ns significantly exceeds the singlet

**Scheme 59. Deactivation of Quinolinium Salts by Nucleophilic or Radical Addition**



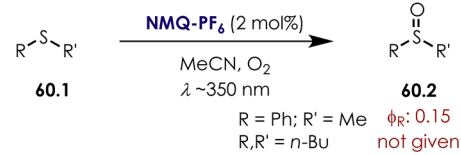
lifetime of most organic photoredox catalysts. That quinoliniums generally have long fluorescence lifetimes and high quantum yields indicates minimal involvement of nonradiative decay pathways of the singlet state, including ISC, and little mention is made of the triplet states of quinoliniums (with the exception of systems which can access a triplet ET state<sup>292</sup>).

## 7.2. Reactions

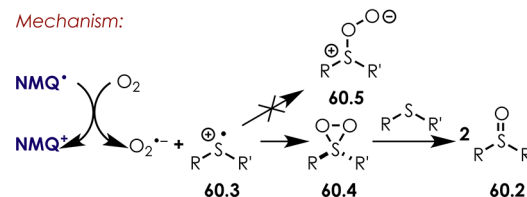
**7.2.1. Oxygenation and Oxidation Reactions.** Oxidation reactions of sulfur-containing compounds are possible using quinolinium photoredox catalysts. **NMQ<sup>+</sup>** is an efficient mediator of the PET-induced aerobic oxygenation of sulfides, including mono-aryl and dialkyl sulfides, with sulfoxides **60.2** as the main products (Scheme 60).<sup>56</sup> In contrast to the many examples where

**Scheme 60. NMQ-Mediated Oxygenation of Sulfides**

[ $-e^-$ ]



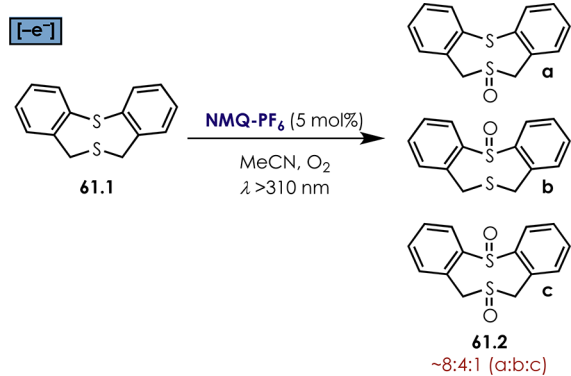
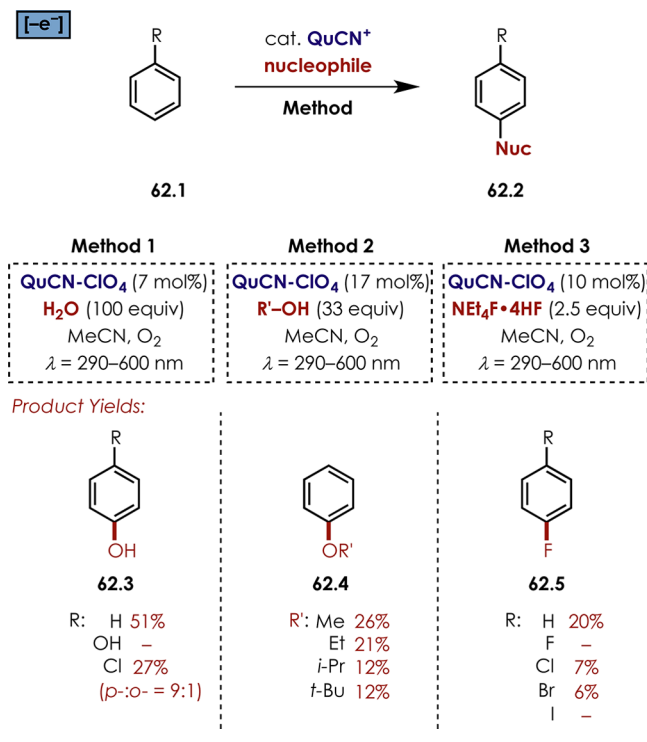
Mechanism:



photolytic oxygenation of sulfides **60.1** occurs by the generation of  ${}^1\text{O}_2$ .<sup>14</sup> **NMQ<sup>+</sup>** operates by a PET mechanism for all substrates. Product distribution and computational studies support a thiadioxirane **60.4** intermediate in favor of peroxy sulfonium ylides **60.5**. Oxygenation of more complex bis-sulfides **61.1** was also investigated, in which some degree of chemoselectivity was possible (Scheme 61).<sup>293</sup> However, the synthetic utility offered by these methods is expected to be limited, as sulfoxides **60.2** are known to undergo further reaction by PET processes, ultimately resulting in C–S bond cleavage.<sup>60,294</sup> Nonetheless, the importance of sulfide oxygenation in removing sulfides as pollutants has been noted.<sup>56</sup>

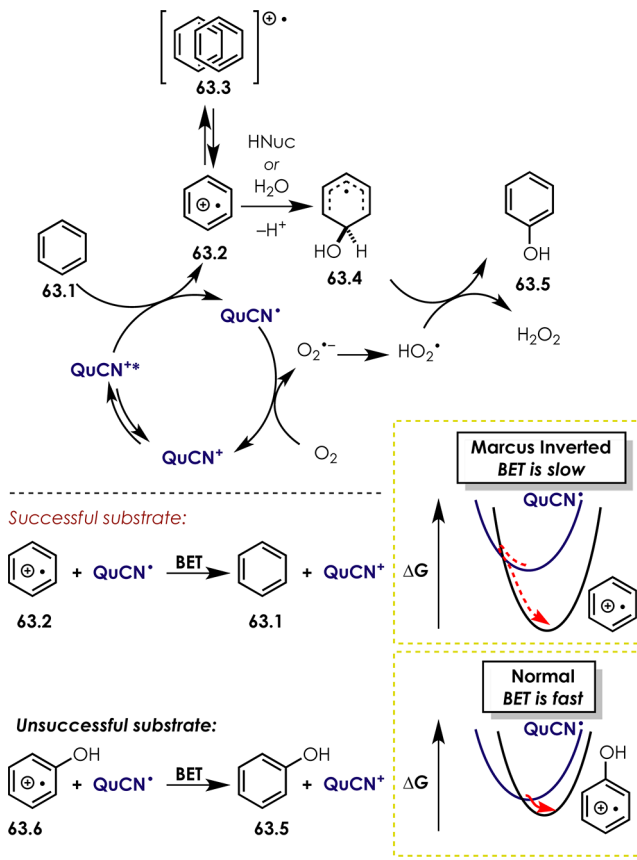
The potency of the highly oxidizing QuCN<sup>+</sup> was showcased by Fukuzumi, who demonstrated the aryl C–H functionalization of benzene and electron-deficient arenes (**62.1**, Scheme 62) accomplished through the addition of oxygen<sup>295,296</sup> and

Scheme 61. NMQ-Mediated Oxygenation of Bis-Sulfides

Scheme 62. Aryl C–H Hydroxylation, Alkoxylation, and Fluorination Using QuCN<sup>+</sup>

fluoride<sup>297</sup> nucleophiles to arene cation radicals with O<sub>2</sub> as a stoichiometric oxidant. Despite its high redox potential, benzene proved the highest-yielding substrate in the hydroxylation, alkoxylation, and fluorination reactions. Particularly interesting was the fact that phenol gave no product under method 1, while chlorobenzene gave a comparable yield of the chlorophenols, suggesting that the redox potential of the substrate was not the primary factor enabling reactivity [ $E_{\text{ox}}(\text{PhCl}\bullet^+/\text{PhCl}) = +2.61 \text{ V vs SCE}$ <sup>74</sup>].

Mechanistic studies on this photoredox system support the mechanism shown in Scheme 63,<sup>295</sup> wherein generation of the arene cation radical is followed by addition of H<sub>2</sub>O and deprotonation to give the cyclohexadienyl radical 63.4. Furthermore, the benzene cation radical 63.2 was observed to reversibly form a π-complex 63.3 with a neutral benzene molecule before nucleophile addition could occur. Aromatization to phenol 63.5 was thought to be accomplished by hydroperoxy radical HO<sub>2</sub>• produced by O<sub>2</sub>-mediated turnover of quinolinyl radical QuCN• and protonation of superoxide. The

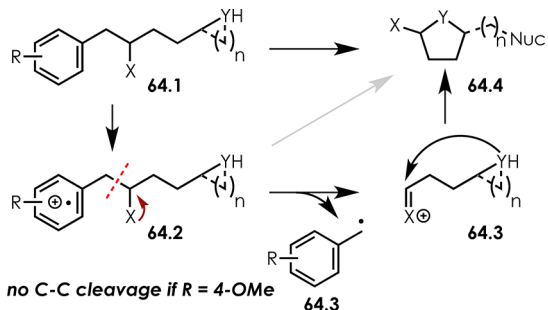
Scheme 63. Proposed Mechanism for QuCN<sup>+</sup>-Mediated Aryl C–H Functionalization Reactions

high selectivity for mono-hydroxylation corresponded to an absence of QuCN• in transient absorption spectra with phenol 63.5 as a quencher, even though phenol 63.5 strongly quenched QuCN<sup>+</sup> fluorescence. This observation, and the lack of reactivity for phenol 63.5, was rationalized by considering that BET between benzene cation radical 63.2 and QuCN<sup>+</sup> is likely to be slow as it lies in the Marcus-inverted region, whereas the lower potential of the (PhOH<sup>•+</sup>/PhOH) couple positions the exergonic BET event to be extremely fast.

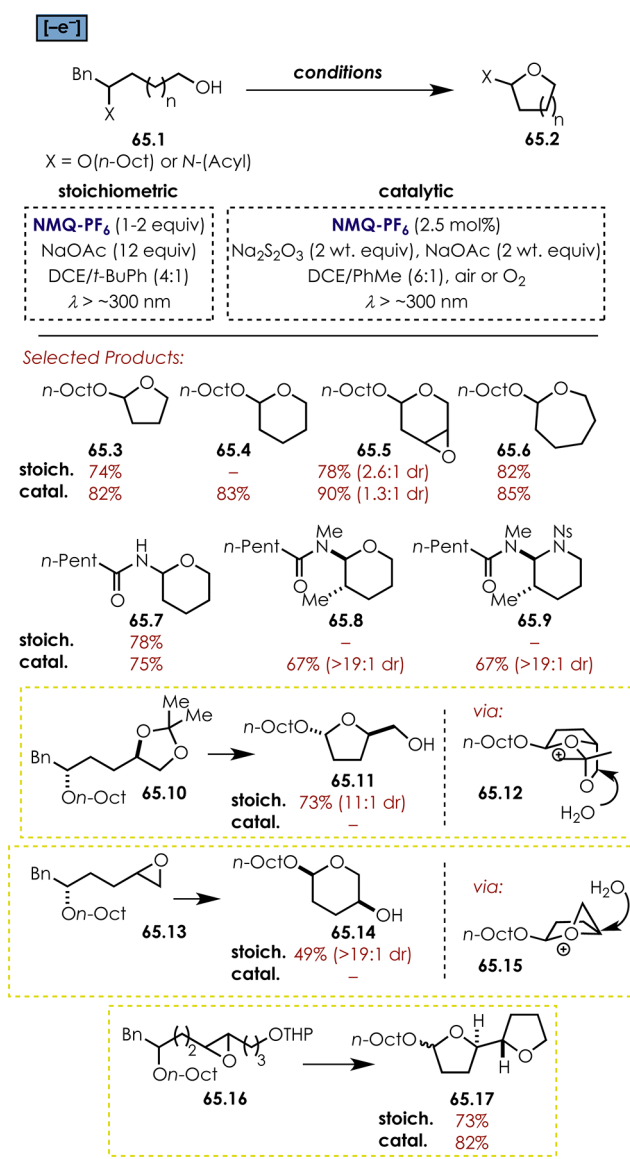
With alcohols as nucleophiles, low yields of the phenyl ethers 62.4 could be obtained.<sup>296</sup> Likewise, the fluorination of benzene using tetraethylammonium fluoride tetrahydrofluoride (NEt<sub>4</sub>F·4HF) proceeded in 20% yield (62.5, R=H), and lower yields of the chloro- and bromo- fluorobenzenes 62.5 (R=Cl and R=Br) were also noted.<sup>297</sup> All three transformations were thought to proceed by similar mechanisms (Scheme 63).

Floreancig and co-workers have developed a series of cyclizations initiated by oxidative cleavage/cyclization of a benzyl group in substrates 64.1 bearing a heteroatom β to the aryl ring (Scheme 64). In an initial report,<sup>298</sup> stoichiometric NMQ·PF<sub>6</sub> was employed in the cyclization of alcohols 65.1 to acetals 65.2 (Scheme 65). Substrates with a p-methoxybenzyl group did not provide the desired products, which is counter to the expectation that a more electron-rich benzyl group would improve reaction efficiency by increasing the facility of cation radical (64.2) formation. This observation was explained by reasoning that the 4-methoxy group strengthens the α-C–β-C bond of the cation radical 64.2,<sup>299</sup> which is corroborated by studies in a related benzylsilane cation radical system.<sup>300</sup>

## Scheme 64. Oxidative Benzylic Cleavage/Cyclization



## Scheme 65. Synthesis of Acetals and Aminals by Oxidative Benzylic Cleavage/Cyclization

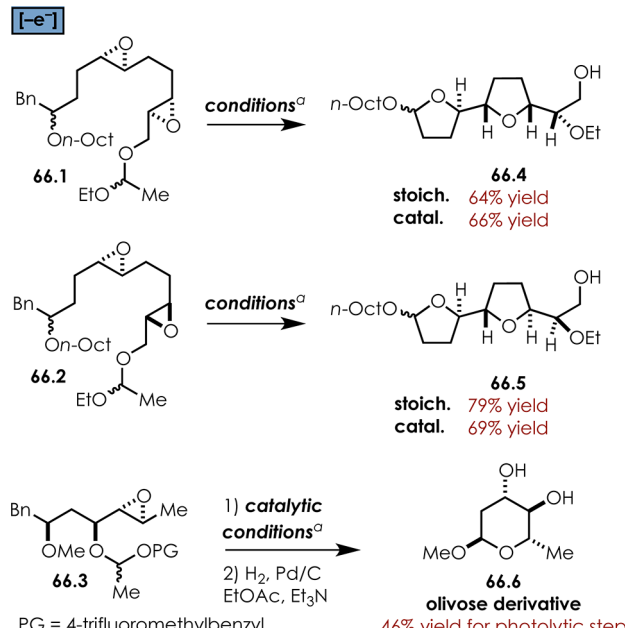


It was later determined that this reaction could be catalytic when run under O<sub>2</sub> (Scheme 65), although Na<sub>2</sub>S<sub>2</sub>O<sub>3</sub> was included as a mild reductant to suppress decomposition reactions presumably arising from oxygen-centered radicals.<sup>301</sup> When the β-heteroatom was nitrogen, production of aminals (65.7–65.9) was achieved in reasonable yields.<sup>301,302</sup> Interestingly, tethered heterocycles such as 65.10 and 65.13 could also function as

nucleophiles, and the proposed bicyclic oxonium intermediates (65.12 and 65.15) furnished products 65.11 and 65.14 upon hydrolysis in moderate yields but high diastereoselectivity.<sup>298</sup>

By a similar approach, substrates such as 65.16 that contained both a cyclic ether and an additional distal nucleophile could undergo a cascade cyclization (65.17, Scheme 65).<sup>298,301</sup> This strategy was successfully extended to the synthesis of more elaborate polyethers (e.g. 66.4–66.6) from epoxides 66.1–66.3 (Scheme 66).<sup>303</sup>

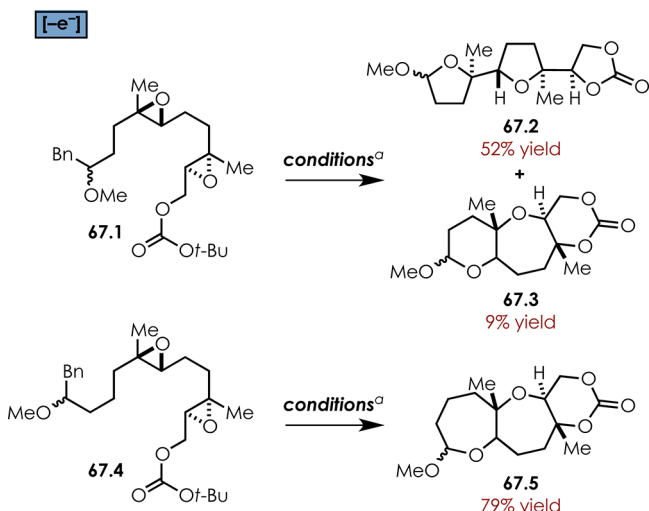
## Scheme 66. Polyether Synthesis by Oxidative Cleavage/Cyclization Cascade



<sup>a</sup>Stoichiometric or catalytic conditions given in Scheme 65

Even greater structural diversity could be accessed by including a carbonate group in substrates, which produced polyethers containing up to three rings (e.g., 67.2, 67.3, and 67.5) formed in a single transformation (Scheme 67).<sup>299</sup> The

## Scheme 67. Tricyclic Polyethers from Bis-epoxy Carbonates

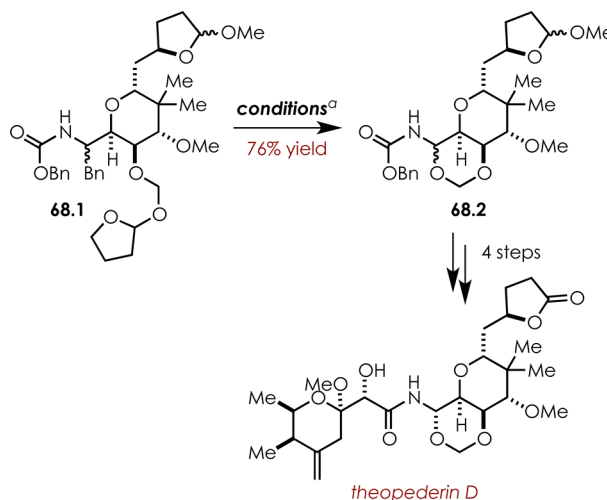


<sup>a</sup>Catalytic conditions given in Scheme 65

regiochemical outcome of the cyclization for bisepoxides **67.1** and **67.4** was strongly influenced by the relative configurations of each epoxide unit and the size of the ring formed in the first cyclization. Remarkably, only the fused tricycle **67.5** was obtained in the reaction of **67.4** under the conditions, while the homologous **67.1** gave predominantly the bis-tetrahydrofuran **67.2**.

Finally, this photoredox-catalyzed cyclization methodology was applied in the total synthesis of Theopederin D (Scheme 68).<sup>304</sup> The substrate **68.1** underwent cyclization in 76% yield, and target was obtained after 4 additional steps.

**Scheme 68. Synthesis of Theopederin D Enabled by Photoredox Oxidative Cleavage/Cyclization**



<sup>a</sup>Catalytic conditions given in Scheme 65

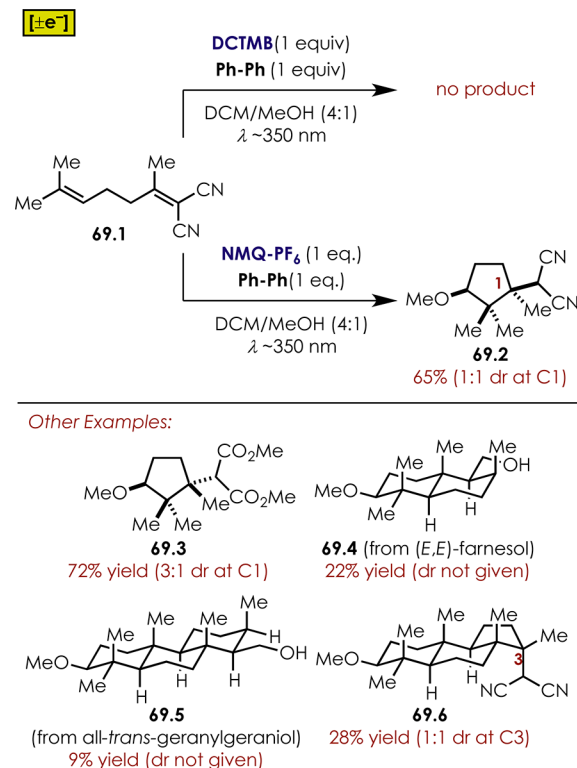
In an effort to improve the efficiency of the polyene cyclization reactions presented in Scheme 16, Demuth and co-workers<sup>305</sup> turned to  $\text{NMQ}^+$  as an alternative to the cyanoarenes previously employed, reasoning that a cationic photoredox catalyst would allow for greater cage escape of the contact radical pair even in nonpolar solvents.<sup>249,300</sup> In support of this strategy, the authors demonstrated that cyclopentane **69.2** (Scheme 69) could be produced under the conditions employing  $\text{NMQ-PF}_6/\text{Ph-Ph}$ , in which MeOH acts as a nucleophile and adds to the initially formed alkene cation radical. In contrast,  $\text{DCTMB}$  gave no product when used as a PET reagent. Other cyclizations were explored, including both electron-withdrawing groups and free alcohols at the termini. Although, yields for tricyclic products did not exceed those obtained in the cyanoarene system, the most notable advance in this report was the direct use of (*E,E*)-farnesol and all-*trans*-geranylgeraniol to give products **69.4** and **69.5**.

## 8. ACRIDINIUMS

### 8.1. Acr-Me<sup>+</sup> and 9-Substituted Acr-R<sup>+</sup>: Photophysical and Electrochemical Characteristics

The acridinium class can be viewed as benzannulated analogues of quinoliniums and offer improvements to the drawbacks that limit the efficacy of quinoliniums. Namely, an additional aromatic ring obstructs nucleophile addition at what would be the 2-position of a quinolinium, and the more extensive conjugated  $\pi$ -system leads to absorption in the visible range. Acridiniums generally constitute powerful oxidants in the singlet excited state. Ground state reduction of acridinium ions occurs at moderate

**Scheme 69. NMQ-Induced Polyene Cyclizations**

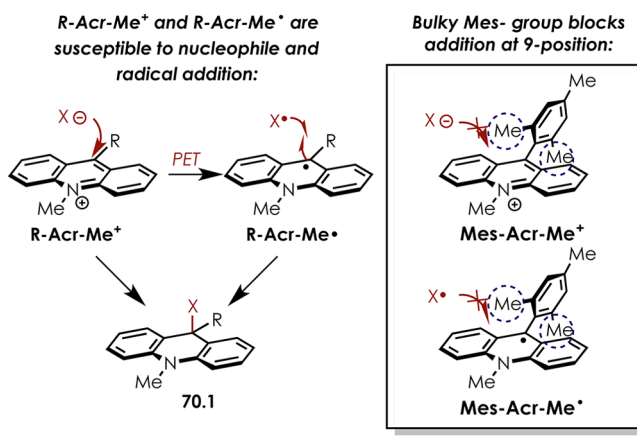


potentials (approximately  $-0.5 \text{ V}$  vs SCE), with the consequence that the excited state reduction potentials are large and positive (above  $2.0 \text{ V}$  for the singlet state acridiniums), while the corresponding acridinyl radicals formed upon single electron transfer are fairly weak reductants, incapable of reducing  $\text{O}_2$  to superoxide  $\text{O}_2\bullet^-$  by an ET mechanism. However, production of  $\text{O}_2\bullet^-$  in acridinium systems is nonetheless proposed in some of the following examples.

*N*-Methyl Acridinium (Acr-Me<sup>+</sup>) is an exemplar for the photophysical and electrochemical properties of this group. With a singlet excited state reduction potential [ $E_{\text{red}}^*(\text{Acr-Me}^+/\text{Acr-Me}\bullet)$ ] of  $+2.32 \text{ V}$ ,<sup>65</sup> Acr-Me<sup>+</sup> is a powerful oxidant in the singlet excited state. Additionally, Acr-Me<sup>+</sup> possesses a quantum yield of fluorescence equal to  $1.0$ ,<sup>64</sup> and an extremely long lifetime of fluorescence at  $31 \text{ ns}$ .<sup>69</sup> Despite these promising properties, Acr-Me<sup>+</sup> has found limited use as a photoredox catalyst because of its susceptibility to nucleophile addition at the 9-position in the ground state cation (Scheme 70),<sup>289</sup> as well as radical reactions of the acridinyl radical Acr-Me<sup>•</sup>,<sup>306</sup> both reactivity modes generating dihydroacridines **70.1**. The 9-phenyl substituted Ph-Acr-Me<sup>+</sup> showed no evidence of radical–radical reactivity at the 9-position in one study.<sup>306</sup> Unfortunately, Ph-Acr-Me<sup>+</sup> is subject to nucleophilic deactivation,<sup>307</sup> and, furthermore, possesses a drastically shorter singlet lifetime ( $\sim 2.0 \text{ ns}$ ) and low quantum yield of fluorescence ( $\phi_f < 0.09$ ),<sup>66</sup> due to nonradiative decay pathways related to the rotational flexibility of the phenyl substituent.<sup>308</sup>

In other 9-aryl-substituted acridiniums where the aryl substituent is sufficiently electron rich, intramolecular electron transfer can occur in the first singlet excited state localized on the acridinium (termed “locally excited” or LE) to form a charge transfer (CT) state (also called a charge shift state).<sup>66,308,309</sup> One such molecule, Mes-Acr-Me<sup>+</sup>, has become the most widely used acridinium photoredox catalyst in recent years, but its photo-

**Scheme 70.** Deactivation Pathways of Acridiniums and Acridinyl Radicals



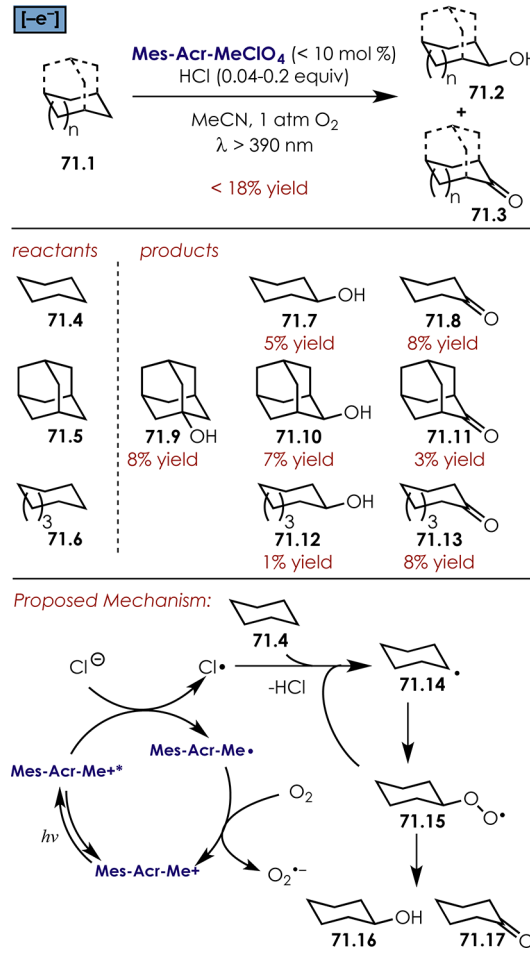
physical properties were initially the subject of controversy after the initial report of its synthesis by Fukuzumi in 2004.<sup>310</sup> The photo-oxidative activity of **Mes-Acr-Me<sup>+</sup>**, which shows evidence of <sup>1</sup>LE and <sup>1</sup>CT states in equilibrium (in the singlet state),<sup>69,70</sup> was initially attributed to a CT state (possibly <sup>1</sup>CT or <sup>3</sup>CT),<sup>311</sup> although subsequent studies have clarified that the singlet CT state is not a necessary excited state in PET reactions of this acridinium class.<sup>69,70,312</sup> The identity of the long-lived species now presumed to be the triplet state <sup>3</sup>Mes-Acr-Me<sup>•\*</sup> was at the center of the debate,<sup>68,313–316</sup> and the triplet was considered to possess either CT (<sup>3</sup>CT) or LE (<sup>3</sup>LE) character. The <sup>3</sup>CT was estimated to have a reduction potential of +1.88 V,<sup>317</sup> while the <sup>3</sup>LE would possess a much lower reduction potential of +1.45 V.<sup>69</sup> By comparison, <sup>1</sup>Mes-Acr-Me<sup>•\*</sup> (i.e., the singlet excited state: either <sup>1</sup>LE or <sup>1</sup>CT) is a significantly better oxidant and has an excited state reduction potential of ~2.1–2.2 V, with a fluorescence lifetime of 6–7 ns and a fluorescence quantum yield of <0.10, which demonstrates the consequence of intramolecular CT in nonradiative deactivation of the singlet state when compared to Acr-Me<sup>+</sup>.

Ultimately, we believe the unique success of **Mes-Acr-Me<sup>+</sup>** as a photoredox catalyst is largely attributable to the protective effect of the methyl substituents on the mesityl group in blocking nucleophile<sup>318</sup> and radical addition to the acridinium/acridinyl radical (Scheme 70), rather than the fact that photo-excitation of **Mes-Acr-Me<sup>+</sup>** can access CT states. In an effort to improve the robustness of this class, other 9-mesityl acridiniums have been synthesized, bearing alkyl substituents on the acridinium ring system<sup>319–321</sup> as well as N-phenyl substitution to prevent dealkylation.<sup>319</sup>

## 8.2. Acr-Me<sup>+</sup> and 9-Substituted Acr-R<sup>+</sup>: Reactions

**8.2.1. Oxygenation and Oxidation Reactions.** **8.2.1.1. Alkane Oxygenation.** Fukuzumi and co-workers report C–H oxidation of cycloalkanes **71.1** (Scheme 71) using **Mes-Acr-Me<sup>+</sup>** in the presence of O<sub>2</sub> and 2.0 mM HCl, which yielded a mixture of alcohols **71.2** and ketones **71.3** with unremarkable selectivity.<sup>322</sup> Although combined yields of **71.2** and **71.3** are low (9–18%), the authors report a turnover number (TON) of 7 based on the consumption of cyclohexane **71.4**, demonstrating the catalytic activity of **Mes-Acr-Me<sup>+</sup>**. As the cycloalkanes possess prohibitively high oxidation potentials, the proposed mechanism involves oxidation of Cl<sup>-</sup> to Cl<sup>•</sup> by **Mes-Acr-Me<sup>+</sup>** [E<sub>1/2</sub>(Cl<sup>•</sup>/Cl<sup>-</sup>) = +1.15 V vs SCE].<sup>323</sup> The alkyl C–H bond is thought to be cleaved by H atom abstraction with Cl<sup>•</sup>. The alkyl

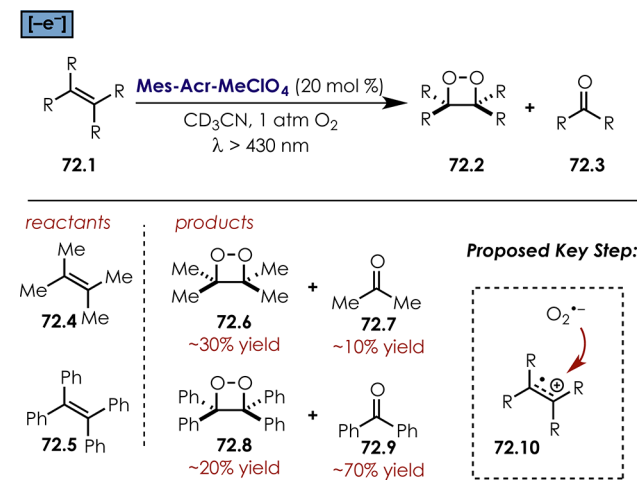
**Scheme 71.** Aerobic C–H Oxidation of Cyclic Hydrocarbons



radical **71.14•** is captured by O<sub>2</sub> to generate alkyl peroxy radical **71.15•**, which is detected in the steady EPR spectrum, and the alcohol and ketone products are ultimately formed by disproportionation. A radical chain propagation mechanism was suggested to operate at higher alkane concentrations, in which case, peroxy radical **71.15•** accomplishes the HAT step on **71.4**. The authors maintain that acridine radical **Mes-Acr-Me<sup>•</sup>** is turned over by reduction of O<sub>2</sub> to O<sub>2</sub><sup>•-</sup>, citing a previous investigation where O<sub>2</sub><sup>•-</sup> generated from the photolytic activity of **Mes-Acr-Me<sup>+</sup>** was observed spectroscopically.<sup>311</sup>

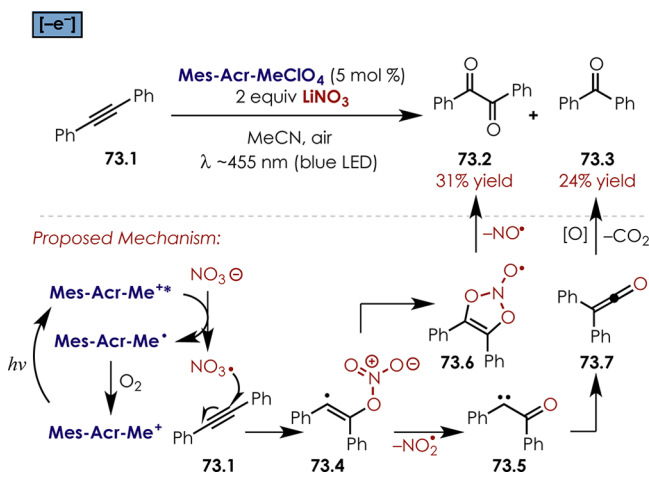
**8.2.1.2. Alkene Oxygenation.** A previous study by Fukuzumi disclosed the formation of dioxetanes **72.2** from alkenes **72.1** (Scheme 72).<sup>311</sup> Ketones **72.3**, the product of dioxetane cleavage, were also observed. The dioxetane product is favored in the case of alkene **72.4**, whereas alkene **72.5** goes to higher conversion of **72.8** and **72.9**, with the product distribution shifted in favor of ketone **72.9** (BP). This type of alkene oxygenation is known to result from the addition of O<sub>2</sub><sup>•-</sup> to an alkene cation radical (**72.10**), both generated by the redox activity of a photo-oxidant.<sup>48,324–326</sup> Although the cycloreversion of **72.2** to **72.3** was not interrogated, the authors suggested the possibility of an oxidative PET-mediated cleavage.<sup>282</sup> Oxidative cleavage of  $\alpha$ -methylstyrene under similar conditions was also studied.<sup>327</sup> Interestingly, Griesbeck and Cho<sup>328</sup> show that alkenes bearing allylic C–H bonds react to give the Schenck-Ene products under similar conditions, suggesting that **Mes-Acr-Me<sup>+</sup>** is also capable of generating singlet oxygen.

**Scheme 72.** Tetrasubstituted Alkene Oxygenation and Oxidative Cleavage



**8.2.1.3. Alkyne Oxygenation.** The highly oxidizing nature of Mes-Acr-Me<sup>+</sup>\* was highlighted in work by König et al. where  $\text{NO}_3^-$  is oxidized to the reactive nitrate radical  $\text{NO}_3^{\bullet}$ , which participates in a number of oxidation chemistries.<sup>312</sup> This method of generating  $\text{NO}_3^{\bullet}$  was first applied to the oxidation of alkynes (Scheme 73). In the presence of Mes-Acr-Me<sup>+</sup> and

**Scheme 73.** Alkyne Oxygenation via Generation of  $\text{NO}_3^{\bullet}$



$\text{LiNO}_3$ , diphenylacetylene 73.1 reacts to give a mixture of benzil 73.2 and benzophenone 73.3 in a moderate overall yield, which is proposed to follow a mechanistic scheme which diverges from intermediate 73.4 after radical addition of  $\text{NO}_3^{\bullet}$  to the alkyne (Scheme 73). Cyclization, then extrusion of  $\text{NO}_2^{\bullet}$  from 73.6 leads to 73.2, while benzophenone 73.3 is thought to result from elimination of  $\text{NO}_2^{\bullet}$  from 73.4, followed by Wolff rearrangement and oxidative decarboxylation. Given the high oxidation potential of  $\text{NO}_3^-$  [ $E_{1/2}(\text{NO}_3^{\bullet}/\text{NO}_3^-) = +2.0$  V vs SCE in MeCN],<sup>329</sup> it seemed unlikely that  $\text{NO}_3^-$  could be oxidized by Mes-Acr-Me<sup>+</sup>\* in a triplet state, as both postulated triplet states would possess insufficient excited state reduction potentials [ $E_{\text{red}}^*(\text{CT-Mes-Acr-Me}^{+*}/\text{Mes-Acr-Me}^{\bullet}) = +1.88$  V;  
 $E_{\text{red}}^*(\text{LE-Mes-Acr-Me}^{+*}/\text{Mes-Acr-Me}^{\bullet}) = +1.45$  V<sup>69</sup>]. It was confirmed that photoinduced oxidation of  $\text{NO}_3^-$  proceeds by a singlet excited state  ${}^1\text{Mes-Acr-Me}^{+*}$  through fluorescence quenching studies. Additionally, laser flash photolysis experi-

ments show no evidence of quenching of the long-lived triplet state by  $\text{NO}_3^-$ . Under aerobic conditions,  $\text{O}_2$  was presumed to be the terminal oxidant (55% yield of 73.2 + 73.3), but ammonium persulfate could be used under inert atmosphere with only a minor penalty in yield (46% yield of 73.2 + 73.3).

The authors provide an additional example of alkyne reactivity in this system in the cyclization of alkyne 74.1a,b to give tetrahydrofuran 74.2a,b (Scheme 74).<sup>312</sup> This radical cascade

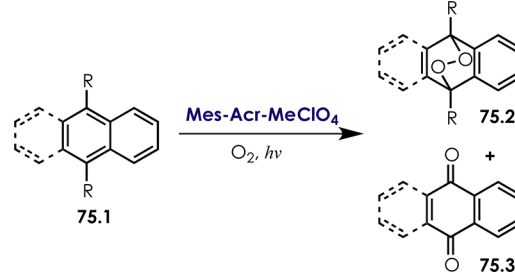
**Scheme 74.**  $\text{NO}_3^{\bullet}$  Mediated Alkyne Oxidation/Cyclization



was studied previously<sup>330,331</sup> and is thought to be initiated by addition of  $\text{NO}_3^{\bullet}$  to alkyne 74.1 to give a vinyl radical, which undergoes 1,5 HAT then a 5-exo cyclization. On the basis of significant bleaching of the Mes-Acr-Me<sup>+</sup> absorption, low yields were attributed to catalyst degradation, possibly by way of oxidation at the mesitylene portion of Mes-Acr-Me<sup>+</sup>.<sup>332</sup>

**8.2.1.4. Arene Oxygenation.** Oxygenation of anthracenes 75.1 using Mes-Acr-Me<sup>+</sup> has been reported (Scheme 75).<sup>311</sup>

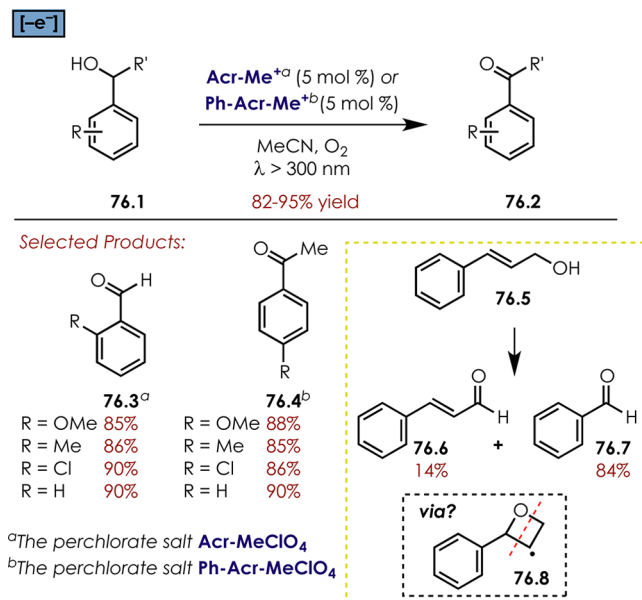
**Scheme 75.** Oxygenation of Anthracenes



Mixtures of the endoperoxide 75.2 and quinone 75.3 were observed, with quinone formation dominating if the 9 and 10 positions were unsubstituted. A mechanism involving coupling between anthracene cation radicals and superoxide was proposed, but [4+2] cycloaddition with  ${}^1\text{O}_2$  is difficult to rule out. Oxygenation of naphthalenes as reported by Griesbeck and Cho<sup>328</sup> demonstrates contrasting reactivity when benzylic C–H bonds are adjacent to the naphthyl ring: benzylic oxidation to the aldehyde (as in Scheme 76) dominates with only minor products resulting from endoperoxides as shown in Scheme 75.

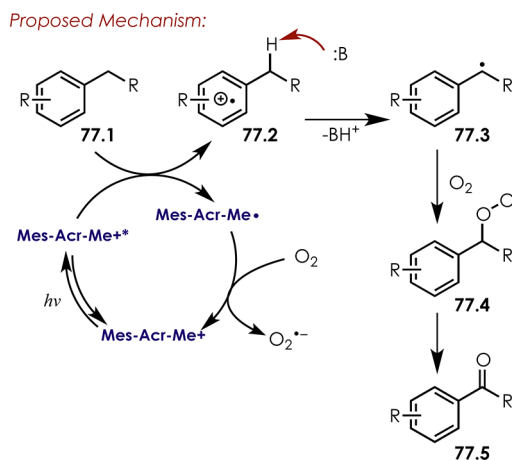
**8.2.1.5. Benzylic Oxygenation and Oxidation.** Acr-Me<sup>+</sup> and Ph-Acr-Me<sup>+</sup> were found to efficiently oxidize primary and secondary benzylic alcohols (76.1) to the corresponding aldehydes (76.3) and ketones (76.4) under an atmosphere of oxygen (Scheme 76).<sup>333</sup> High yields were obtained for the oxidation of benzylic alcohols bearing arenes with both electron-donating and -withdrawing substituents. While comparable results were achieved using either of the two catalysts, Ph-Acr-Me<sup>+</sup> generally allowed for shorter reaction times (20 h compared to 50 h for Acr-Me<sup>+</sup>). A likely mechanism involves oxidation of the arene to the cation radical 77.2 followed by deprotonation of

Scheme 76. Aerobic Oxidation of Benzylic Alcohols



77.2, a reactivity that is well-accepted<sup>334–337</sup> and probably general for most of the benzylic oxidations discussed in this review (Scheme 77). Interestingly, cinnamaldehyde (76.6) was

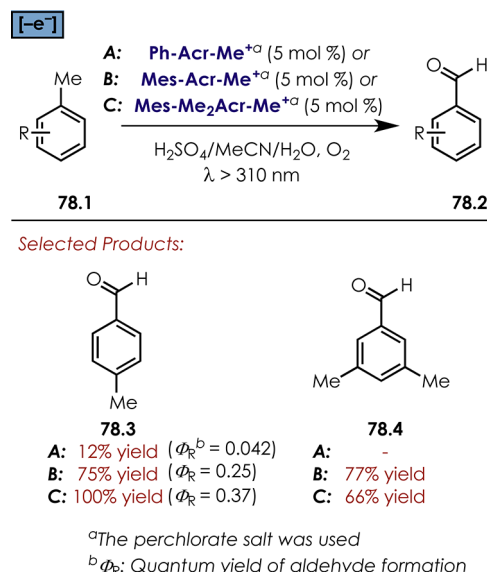
Scheme 77. Proposed Mechanism for Aerobic Benzylic Oxidation Reactions



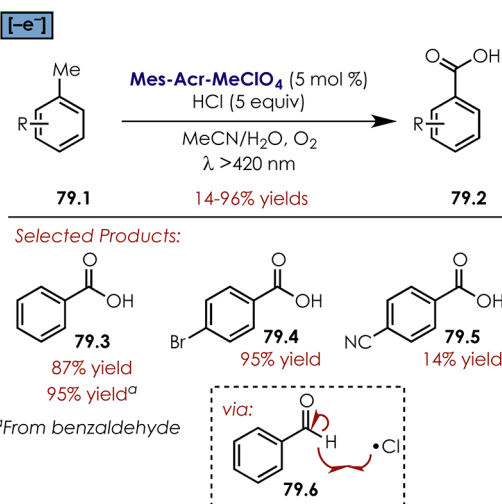
obtained in a low yield from cinnamyl alcohol, while the major product was benzaldehyde (76.7). This product was not thought to result from oxidative cleavage of the alkene, since benzaldehyde was the exclusive product under argon atmosphere. Instead, the authors proposed cyclization to give an oxetane radical (76.8), which could undergo  $\beta$ -scission to give the aldehyde.

Benzylic oxidation of methylbenzenes using acridinium photoredox catalysts has been thoroughly explored. Fukuzumi has reported a number of studies on the oxidation of methyl arenes 78.1 to the corresponding aldehydes 78.2 under an atmosphere of O<sub>2</sub> (Scheme 78).<sup>321,338,339</sup> Notably, these reactions are selective for oxidation at a single methyl group when multiple are present, as in the case of *p*-xylene (78.3) and mesitylene (78.4). When HCl is included in the reaction mixture, complete oxidation to the carboxylic acids 79.2 can be achieved (Scheme 79).<sup>339</sup> These transformations likely share a number of

Scheme 78. Aerobic Benzylic Oxidation of Methylbenzenes to Benzaldehydes



Scheme 79. Aerobic Benzylic Oxidation of Methylbenzenes to Benzoic Acids

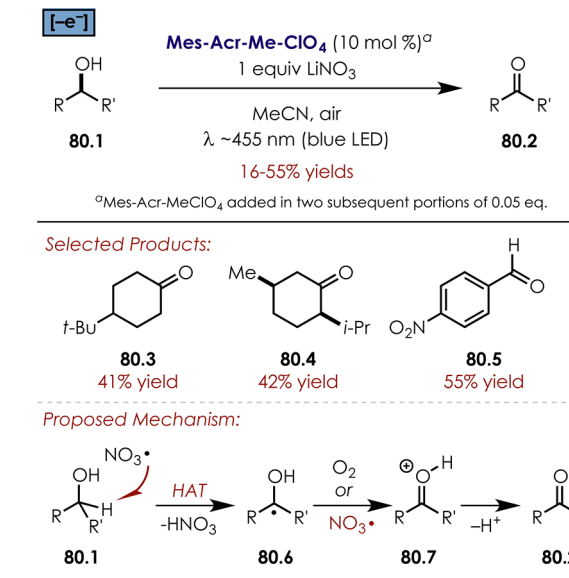


common mechanistic steps, including deprotonation of the arene cation radical 77.2 at the benzylic position and trapping of the resulting benzylic radical 77.3 by O<sub>2</sub> (Scheme 77). Subsequent steps may involve disproportionation of peroxy radicals 77.4 or additional photoinduced oxidations at the arene.<sup>337</sup> Dioxygen is presumed to regenerate the ground state acridinium by SET, which is the rationale for the higher catalytic performance of Mes-Me<sub>2</sub>Acr-Me<sup>+</sup> compared to Mes-Acr-Me<sup>•</sup>:  $E_{red}(\text{Mes-Me}_2\text{Acr-Me}^+/\text{Mes-Me}_2\text{Acr-Me}\bullet) = -0.67 \text{ V vs SCE}$ ,<sup>321</sup> signifying that Mes-Me<sub>2</sub>Acr-Me<sup>+</sup> is 0.1 V more reducing than Mes-Acr-Me<sup>•</sup>, which may explain why higher chemical yields and photochemical quantum yields are observed with Mes-Me<sub>2</sub>Acr-Me<sup>+</sup>. Since complete oxidation to benzoic acids is only observed in the presence of Cl<sup>−</sup>, the authors suggest that Cl<sup>•</sup> abstracts the formyl hydrogen atom of benzaldehyde 79.6, presumably followed by trapping with O<sub>2</sub>.

**8.2.1.6. Other Oxygenation and Oxidation Reactions.** Whereas the examples of oxidation in Scheme 76 above appear to be limited to benzylic positions by the requirement that the

substrate possess a sufficiently low redox potential, a more general range of alcohols **80.1** can be oxidized by  $\text{NO}_3\bullet$ , generated by PET (Scheme 80).<sup>312</sup> Moderate yields (16–55%)

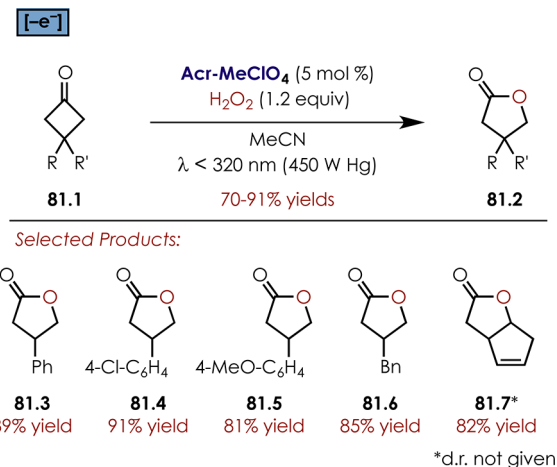
**Scheme 80.** Alcohol Oxidation Enabled by  $\text{NO}_3\bullet$



of the corresponding carbonyl compounds (e.g., **80.3**, **80.4**, and **80.5**) are obtained for secondary aliphatic alcohols and electron-deficient benzyllic alcohols, and over oxidation to the benzoic acid was not observed for **80.5**. This procedure benefited from two sequential additions of **Mes-Acr-Me<sup>+</sup>** to mitigate catalyst decomposition.  $\text{NO}_3\bullet$  is thought to abstract a hydrogen atom from alcohol **80.1**,<sup>340</sup> followed by single-electron oxidation of the ketyl radical **80.6** either by a second equivalent of  $\text{NO}_3\bullet$  or  $\text{O}_2$ .

**Acr-Me<sup>+</sup>** was reported to catalyze the Baeyer-Villiger oxidation of cyclobutanones **81.1** to  $\gamma$ -lactones **81.2** in high yields using 1.2 eq.  $\text{H}_2\text{O}_2$  (Scheme 81).<sup>341</sup> The best yields were obtained with

**Scheme 81.** Baeyer-Villiger Oxygenation of Cyclobutanones

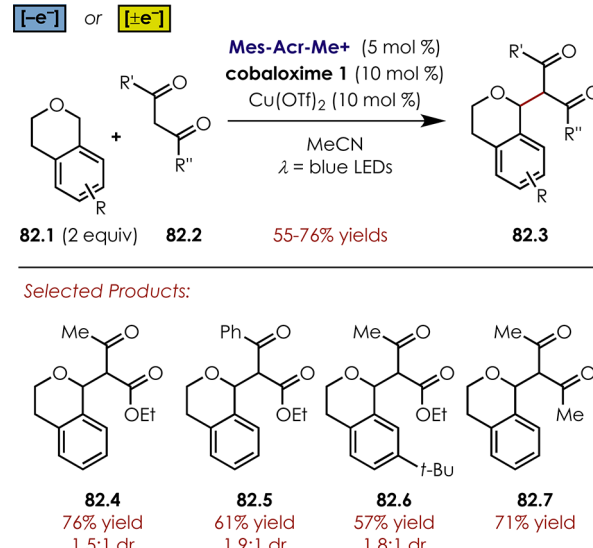


irradiation at room temperature; however, control reactions revealed significant background reactivity: the dark reaction (still including the acridinium in the reaction mixture) gave 42% yield of **81.3** at room temperature, while at 80 °C, 82% yield was observed. Heteroarenum salts are known to activate hydrogen peroxide by formation of a hydroperoxide adduct,<sup>290,342</sup> which

likely explains the catalytic activity of the acridinium in the dark. In fact, flavinium salts are known to catalyze this reaction at low temperature without photolysis.<sup>343</sup> A satisfactory account of the photoredox activity of **Acr-Me<sup>+</sup>** was not supplied by the authors.

**8.2.2. Dehydrogenative Couplings.** **8.2.2.1. Benzyllic Coupling.** Dehydrogenative cross-couplings of the type shown in Scheme 82 (see also Scheme 122) are thought to proceed

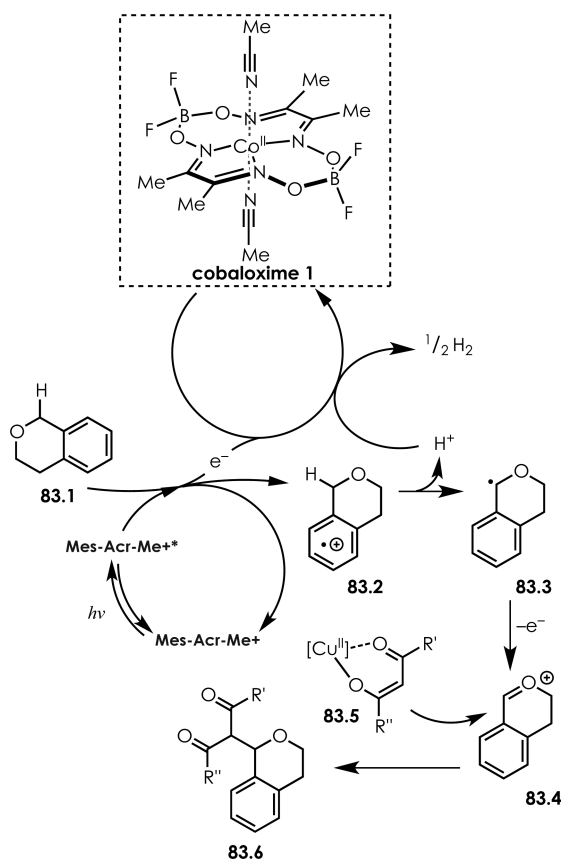
**Scheme 82.** Dehydrogenative Benzylic Coupling of Isochromans with 1,3-Dicarbonyl Compounds



through an oxocarbenium (**83.4**) and normally require a stoichiometric oxidant to functionalize the  $\text{sp}^3$  C–H bond.<sup>344</sup> Recently, **Mes-Acr-Me<sup>+</sup>** was used in cooperation with **cobaloxime 1** (Scheme 83) and copper(II)-triflate ( $\text{Cu}(\text{OTf})_2$ ) co-catalysts to accomplish the dehydrogenative benzylic coupling of isochromans and 1,3-dicarbonyls (Scheme 82) in the absence of an oxidative equivalent by coupling C–H functionalization to the evolution of  $\text{H}_2$ .<sup>345</sup> Indeed, the **cobaloxime 1** realized the goal of  $\text{H}_2$  evolution,<sup>346</sup> which was detected during the coupling of various isochromans **82.1** and 1,3-dicarbonyls **82.2**. The proposed mechanism (Scheme 83) involves formation of oxocarbenium **83.4** after PET oxidation of the aryl ring, deprotonation to give benzylic radical **83.3**, then an additional single electron oxidation. The Cu(II) co-catalyst is presumed to activate the dicarbonyl towards nucleophilic addition to the oxocarbenium (**83.5**). On the basis that both isochroman **83.1** and **cobaloxime 1** individually quenched the triplet state  ${}^3\text{Mes-Acr-Me}^{+*}$  with comparable bimolecular rate constants, the authors suggested that a CT- ${}^3\text{Mes-Acr-Me}^{+*}$  excited state simultaneously reduces  $[\text{Co}(\text{II})]$  and oxidizes **83.1**, although additional experiments to address the possibility of a termolecular PET process were not disclosed. Given that the reduction potential of the **cobaloxime 1**  $[E_{\text{red}}([\text{Co}(\text{II})]/[\text{Co}(\text{I})]) = -0.55 \text{ V vs SCE}]^{347}$  signifies a feasible electron transfer from **Mes-Acr-Me<sup>+</sup>** to  $[\text{Co}(\text{II})]$ , a mechanism involving a ternary electron transfer arrangement appears unnecessary.

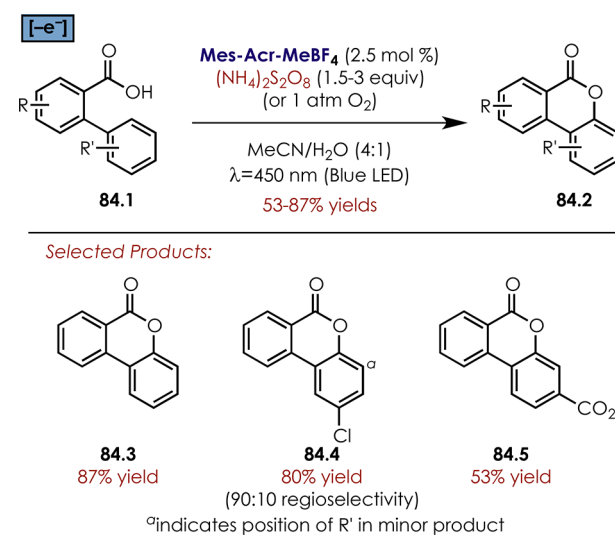
**8.2.2.2. Arene C–H Functionalization.** The decarboxylative transformations discussed below in section 8.2.4 all rely on the proclivity of aliphatic acyloxy radicals towards fragmentation to  $\text{CO}_2$  and alkyl radicals; in contrast, aroyloxy radicals undergo decarboxylation several orders of magnitude slower than their alkyl analogues ( $k_{-\text{CO}_2} = 2 \times 10^6 \text{ s}^{-1}$  for benzoyloxy radical).<sup>348</sup>

**Scheme 83. Proposed Mechanism for Dehydrogenative Coupling of Ketones and Isochromans**

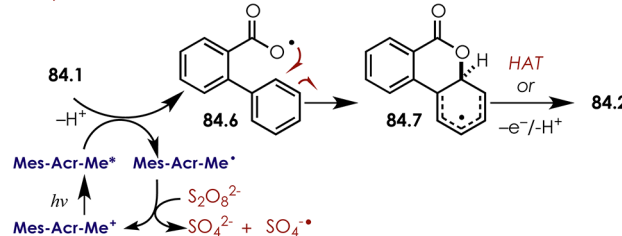


Gonzalez-Gomez and co-workers take advantage of this fact and are able to achieve intramolecular dehydrogenative lactonization in 2-arylbenzoic acids 84.1 by generating aryoxy radicals through the oxidative photoredox activity of Mes-Acr-Me<sup>+</sup> (Scheme 84).<sup>349</sup> A considerable number of benzo-3,4-coumarins 84.2 were synthesized by this protocol which employs ammonium persulfate ( $(\text{NH}_4)_2\text{S}_2\text{O}_8$ ) as a terminal oxidant, many in excellent yields (e.g., 84.3–84.5). Varying degrees of regioselectivity were observed when the 2-aryl group possessed a substituent at the 3' position (e.g., lactone 84.4). The proposed mechanism features the relatively long-lived aryoxy radical 84.6 engaging in a radical cyclization onto the adjacent arene to form a cyclohexadienyl radical 84.7. An alternative mechanism which involves intramolecular COOH addition to arene cation radicals may be tenable for electron-rich biphenyls,<sup>350</sup> although a homolytic aromatic substitution mechanism similar to the one shown has been presented previously.<sup>351</sup> The aromatization step was said to occur by sequential single-electron oxidation and deprotonation or by direct HAT from 84.7, possibly by sulfate radical anion  $\text{SO}_4^{\bullet-}$  generated through reductive cleavage of  $\text{S}_2\text{O}_8^{2-}$  during the catalyst turnover step. Lack of a significant kinetic isotope effect when the 2-aryl ring is fully-deuterated led the authors to conclude that a C–H cleavage step accomplishing aromatization is not operable as a rate-limiting step. Instead, the rate-limiting step was suggested to be the radical cyclization. With regard to this hypothesis, it is interesting to note that even the intermolecular addition of aryoxy radicals to benzene was measured to be very fast (faster than the unimolecular decarboxylation process).<sup>348</sup>

**Scheme 84. Intramolecular C–H Carboxylation of 2-Arylbenzoic Acids**



*Proposed Mechanism:*



In their account of the oxidation of methylbenzenes to benzoic acids (Scheme 79), Fukuzumi and co-workers noted that 1,2,4-trimethoxybenzene and 1,3,5-trimethoxybenzene gave minor amounts of the aryl chloride 85.2 when irradiated in the presence of Mes-Acr-Me<sup>+</sup> and HCl (Scheme 85).<sup>339</sup> On the observation

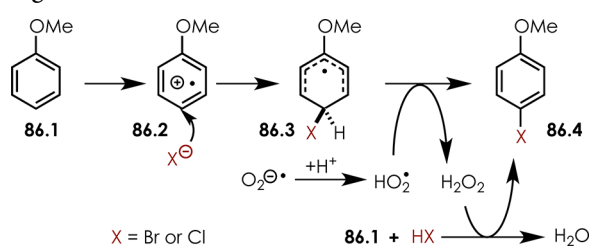
**Scheme 85. Aryl C–H Chlorination**



that the chloride radical  $\text{Cl}\bullet$  exhibited a much shorter lifetime than the arene cation radical 86.2, the latter was proposed to be the active intermediate to which  $\text{Cl}^-$  adds, producing a cyclohexadienyl radical 86.3 (Scheme 86). Presumably, oxygen turns over the photoredox catalytic cycle and is involved in the aromatization of 86.3 to give the C–H-functionalized product 86.4.

Anisole and 1,3-dimethoxybenzene do not exhibit product formation in the aforementioned C–H chlorination reaction; however, Fukuzumi has also reported that HBr can be used in an analogous aerobic aryl C–H bromination, which proceeds with very high yields of the mono-brominated arene for a variety of methoxybenzenes 87.1 (Scheme 87).<sup>352</sup> The regioselectivity of this addition is not specified where nonequivalent sites of  $\text{Br}^-$  addition exist. Yields of methoxyarenes with methyl substituents give significantly lower yields (e.g., 87.4), owing to competitive

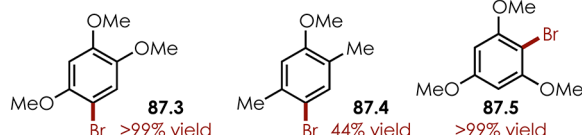
**Scheme 86. Proposed Mechanism for Aryl C–H Halogenation**



**Scheme 87. Aryl C–H Bromination**



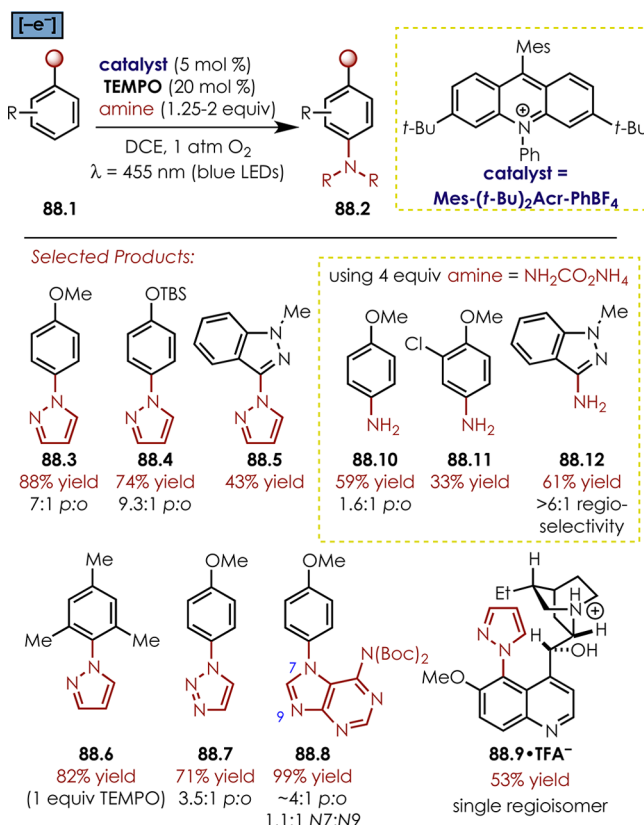
Selected Products:



benzylic oxidation, while mesitylene and durene give only the corresponding aldehydes (as in Scheme 78). The C–H bromination process is thought to follow an analogous mechanism to the C–H chlorination (Scheme 86), with addition of  $\text{Br}^-$  to cation radical 86.2 occurring with a rate constant on the order of  $10^8 \text{ M}^{-1}\text{s}^{-1}$  as indicated by transient absorption measurements. The authors also suggest that if  $\text{H}_2\text{O}_2$  is produced, it will likely react with arene 86.1 and HBr to produce an additional equivalent of brominated product 86.4 (Scheme 86).<sup>353</sup>

Nicewicz and co-workers have recently developed a method based on the intermediacy of Mes-Acr-R<sup>+</sup>-generated arene cation radicals in a para-selective aryl C–H amination reaction (Scheme 88).<sup>320</sup> It was discovered that inclusion of TEMPO (2,2,6,6-tetramethylpiperidine-1-oxyl) as a co-catalyst led to greatly improved yields of 88.3 and diminished byproduct formation. Ultimately, optimal yields were realized with the use of 3,6-di-*tert*-butyl-substituted acridinium Mes-(*t*-Bu)<sub>2</sub>Acr-Ph<sup>+</sup>, which was designed to combat putative degradation processes of the acridinium catalyst, which are expected to occur at the 3- and 6-positions.<sup>354</sup> With  $\text{O}_2$  as the terminal oxidant, an atmosphere of oxygen provided excellent yields after less than 1 day of irradiation, although nearly quantitative yields could be achieved after 3 days of irradiation under air. The substrate scope featured the coupling of arenes with various heterocyclic amines, including pyrazoles (e.g., 88.3–88.6), triazoles (e.g., 88.7), and other biologically relevant derivatives (e.g., 88.8). Heterocycles gave modest yields (e.g., 88.5 and 88.9) as the arene coupling partner, albeit as single regioisomers. Methylbenzenes such as mesitylene and xylene gave the aryl C–H amination products (e.g. 88.6) when  $\text{O}_2$  was excluded and 1 equiv of TEMPO was used as a terminal oxidant to avoid benzylic oxidation as reported by Fukuzumi.<sup>352</sup> That aryl amination occurs over benzylic amination in these substrates is surprising considering the divergent outcome in an electrochemically-mediated method, which results exclusively in benzylic amination.<sup>355</sup> When using

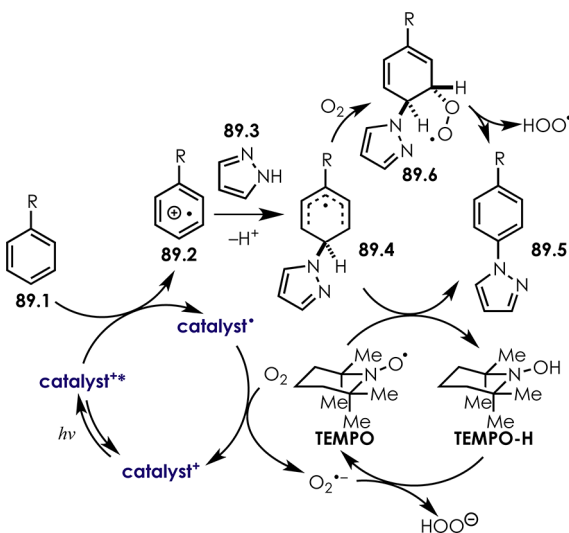
**Scheme 88. Aryl C–H Amination**



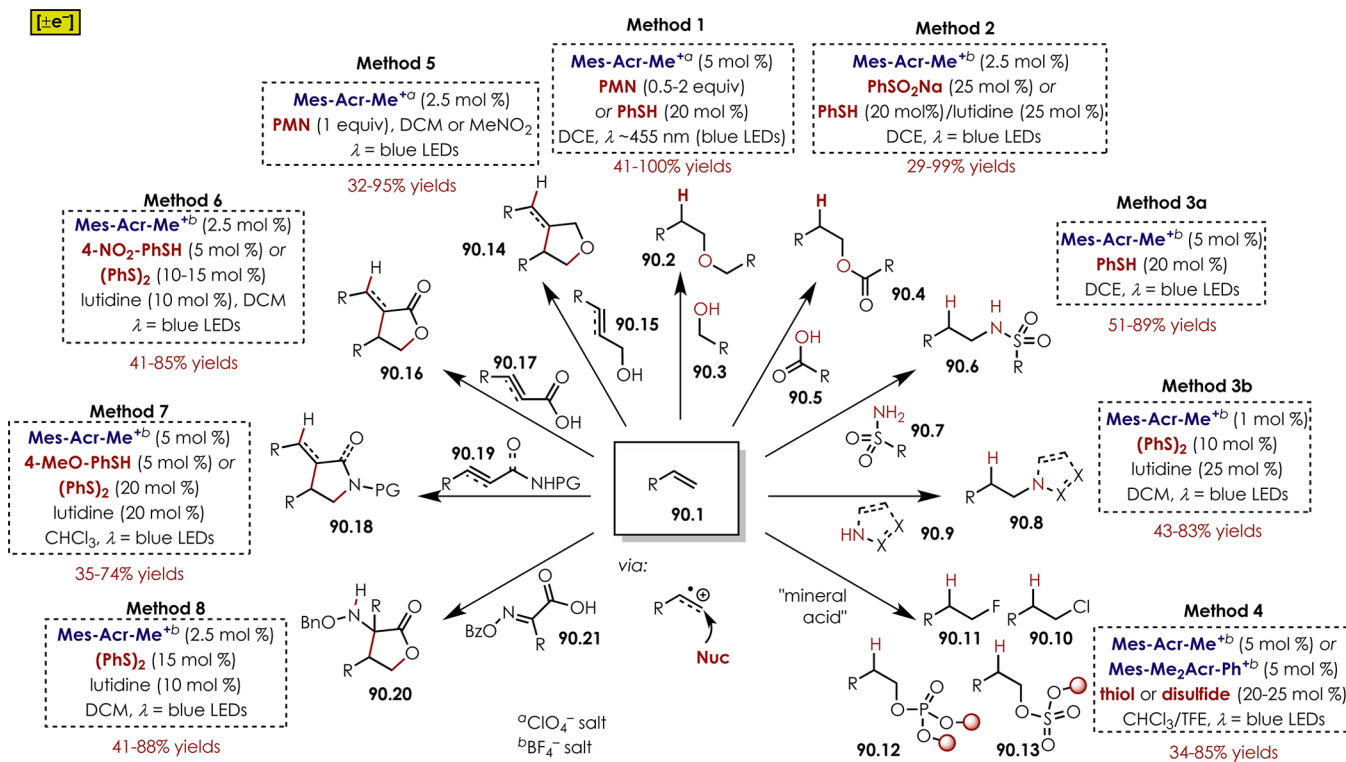
ammonium carbamate as a source of “NH<sub>3</sub>,” it was demonstrated that anilines (e.g., 88.10–88.12) could be accessed directly from an arene. Somewhat lower yields and regioselectivities were seen in this modification to the protocol, but this advance is, nonetheless, an attractive alternative to the nitration-hydrogenation sequence traditionally used to synthesize anilines.

The mechanism (Scheme 89) is presumably similar to that presented by Fukuzumi for the addition of halide nucleophiles to arene cation radicals. It was considered that TEMPO may be capable of assisting in H atom abstraction on the cyclohexadienyl

**Scheme 89. Proposed Mechanism for Aerobic Aryl C–H Amination**

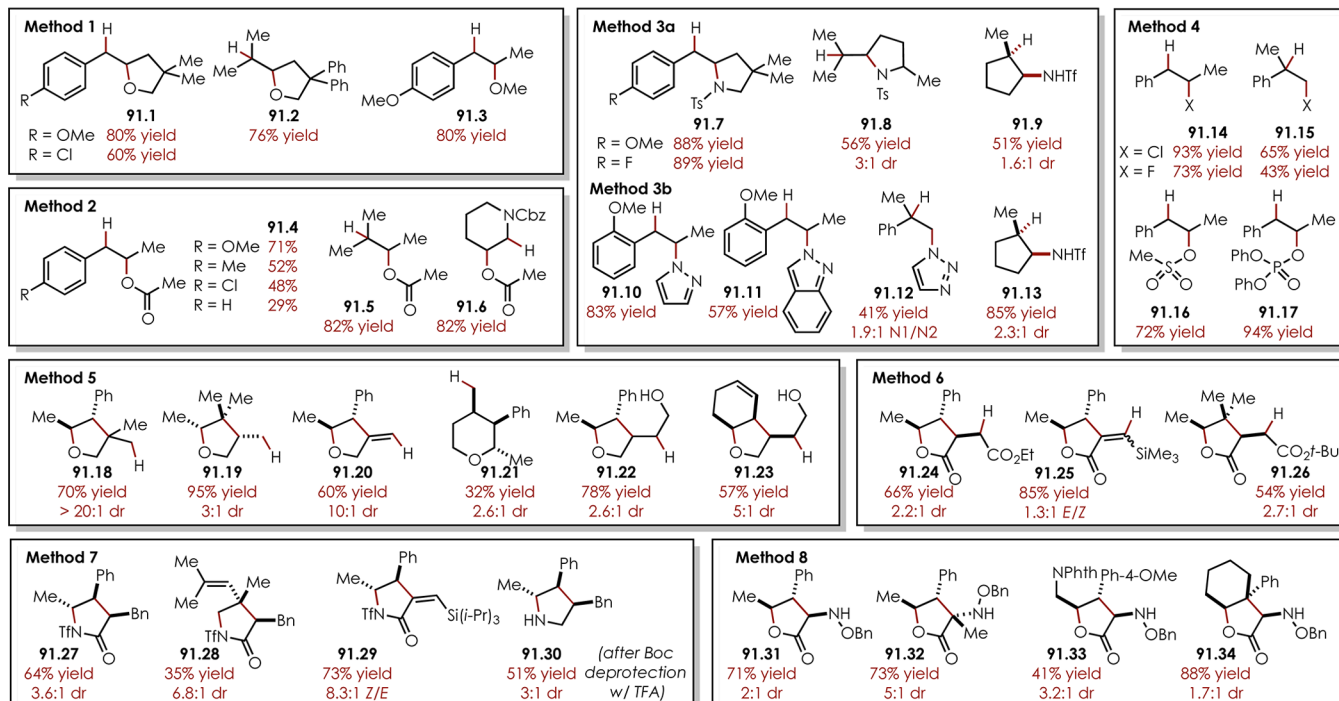


Scheme 90. Anti-Markovnikov Alkene Hydrofunctionalization and PRCC Reactions (2 Column)



Scheme 91. Substrate Scope for Anti-Markovnikov Alkene Hydrofunctionalization and PRCC Reactions

Selected Examples:

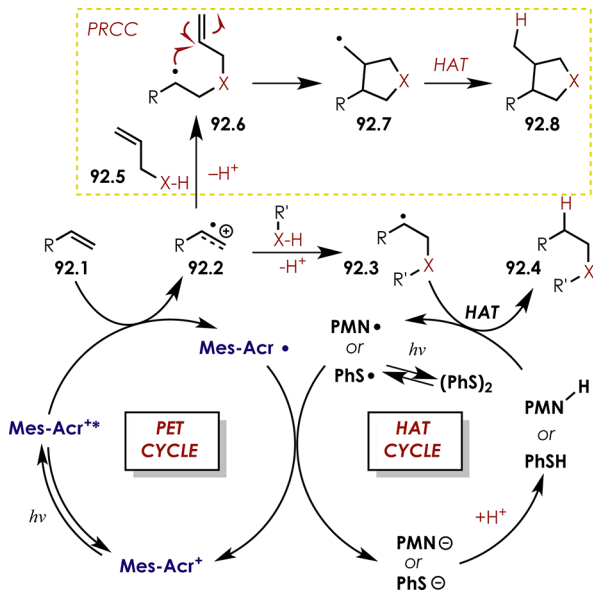


radical **89.4** to furnish the aromatic product, while the hydroxylamine TEMPO-H is likely to be oxidized by superoxide or another oxygen-centered radical species, consistent with the fact that TEMPO appears to mitigate unproductive oxidation pathways. Whereas others have conjectured that  $O_2\bullet^-$  or  $HO_2\bullet$  is responsible for HAT/aromatization in similar systems (see Scheme 63 and Scheme 86), we prefer the pathway shown in

Scheme 89 where trapping of  $O_2$  by cyclohexadienyl radical **89.4** is followed by internal HAT/elimination from peroxy radical **89.6**, supported by the extensive work of von Sonntag.<sup>356–358</sup> The high regioselectivity of the process is difficult to rationalize but provides a useful complement to the wealth of transition metal catalyzed aryl amination reactions which give  $\alpha$ -addition.<sup>359,360</sup>

**8.2.3. Alkene Hydrofunctionalization.** A significant body of work has been devoted to the anti-Markovnikov hydrofunctionalization of alkenes using **Mes-Acr-Me<sup>+</sup>** (and related derivatives) as photoredox catalysts (**Scheme 90** and **Scheme 91**). These methods harness the regioselective addition of nucleophiles to alkene cation radicals, occurring at the less-substituted position or the position which gives a more stabilized radical  $\beta$  to the nucleophile.<sup>361</sup> A key advance enabling the development of methodologies for anti-Markovnikov addition of a range of nucleophiles was the discovery of catalytic amounts of a redox-active hydrogen atom transfer agent drastically improved yields. Phenyl malononitrile (PMN) was initially employed to fill this role, but superior performance was eventually realized when using aryl thiols (such as thiophenol, PhSH) and disulfides as HAT catalysts. The beneficial activity of the HAT catalyst can be understood by considering the mechanism in **Scheme 92**, which

**Scheme 92. Proposed Mechanism for Anti-Markovnikov Alkene Hydrofunctionalization and PRCC Reactions**



features dual catalytic cycles: the PET cycle involves the activity of **Mes-Acr-R<sup>+</sup>** in oxidizing alkenes **92.1** to cation radicals **92.2**, while the HAT catalyst operates in a separate cycle in which HAT to **92.3** furnishes the hydrofunctionalization product **92.4**, simultaneously producing a redox-active radical **PMN•** or **PhS•** which regenerates **Mes-Acr-R<sup>+</sup>** by oxidizing **Mes-Acr-R<sup>•</sup>**. The activity of **PhS•** in this key step was confirmed by laser flash photolysis studies<sup>70</sup> and is supported by the literature report that reduction of **PhS•** occurs at a positive potential [ $E_{1/2}(\text{PhS}^{\bullet}/\text{PhS}^-) = +0.16 \text{ V vs SCE}$ ].<sup>362</sup> Protonation of **PhS<sup>-</sup>** or **PMN<sup>-</sup>**, likely coupled to deprotonation of the nucleophile-cation radical adduct, recycles the HAT catalyst.

The initial report of alkene hydrofunctionalization using **Mes-Acr-Me<sup>+</sup>** as a photoredox catalyst was the anti-Markovnikov hydroalkoxylation of styrenes and trisubstituted aliphatic alkenes (**Scheme 90** and **Scheme 91**, method 1).<sup>363</sup> A majority of the substrates contained a tethered alcohol, which accomplishes an intramolecular etherification (**91.1** and **91.2**), although a single example of methanol addition to the alkene (**91.3**) demonstrated that this reaction could be applied to intermolecular couplings. PMN was used as a hydrogen atom donor and could generally be employed in substoichiometric quantities, although some

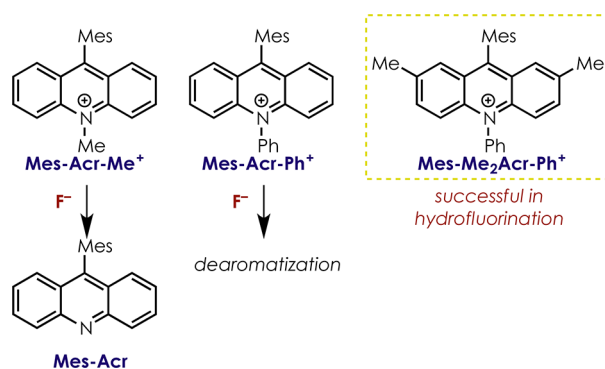
substrates required more than one equivalent for synthetically useful yields. The oxidation potentials for the reported substrates ( $E_{\text{ox}} = +1.22$  to  $+2.06 \text{ V vs SCE}$ ) highlight the highly oxidizing nature of **Mes-Acr-Me<sup>+</sup>** in the excited state. Control reactions with an acid catalyst confirmed that the regioselectivity of nucleophile addition was unique to the reactivity pattern of alkene cation radicals and not the result of acid activation.

A subsequent report detailed the addition of carboxylic acids to alkenes in an anti-Markovnikov fashion (**Scheme 90** and **Scheme 91**, method 2).<sup>364</sup> A number of alkyl carboxylic acids and benzoic acid could be added to styrenes and electron-rich aliphatic alkenes using either **PhSH** (20 mol %) or sodium benzenesulfinate **PhSO<sub>2</sub>Na** (25 mol %) as HAT catalysts (a catalytic amount of 2,6-lutidine was included when **PhSH** was the HAT catalyst). Good yields of products such as **91.4–91.6** were obtained using only 2.5 mol % **Mes-Acr-Me<sup>+</sup>**.

This transformation was extended to include nitrogen nucleophiles in a series of anti-Markovnikov hydroamination reactions (**Scheme 90** and **Scheme 91**, methods 3a and 3b).<sup>365,366</sup> An initial report detailed the intramolecular anti-Markovnikov addition of sulfonamides to alkenes (method 3a).<sup>365</sup> A similar substrate scope to the hydroetherification (method 1) was realized (**91.7–91.8**), and it was found that **PhSH** or diphenyl disulfide (**(PhS)<sub>2</sub>**) function comparably as HAT catalysts. This discovery of **(PhS)<sub>2</sub>** as a co-catalyst was prompted by the observation of minor amounts of **(PhS)<sub>2</sub>** in crude reaction mixtures, suggesting that **(PhS)<sub>2</sub>** could interconvert with **PhSH**. It was later demonstrated that direct photolysis of the disulfide bond by blue light was sufficient to generate **PhS•** as a common intermediate.<sup>70</sup> From a practical standpoint, **(PhS)<sub>2</sub>**, an odorless solid, offers an appealing alternative to the malodorous liquid **PhSH**. This report also demonstrated that the intermolecular coupling between alkenes and triflame (**90.9**, R = CF<sub>3</sub>) was feasible if 2,6-lutidine was included as a catalytic base (25 mol %), and the scope and yield of this reaction was expanded in a subsequent study wherein the loading of **(PhS)<sub>2</sub>** and **Mes-Acr-Me<sup>+</sup>** were 10 mol % and 1 mol %, respectively. Isolated yields ranging from 35% to 84% were achieved for styrenes and 72–85% for aliphatic alkenes. The same methodology could be applied to the anti-Markovnikov addition of nitrogen-containing heteroaromatics **90.9** to alkenes (**91.12–91.12**, **Scheme 90** and **Scheme 91**, method 3b),<sup>366</sup> providing access to a valuable class of compounds prevalent in pharmaceuticals and agrochemicals.

The regioselective addition of hydrogen halides to unsymmetrical alkenes was the subject of what has come to be known as the “Markovnikov Rule” for addition of nucleophiles to alkenes.<sup>367</sup> Accordingly, it is not surprising that the anti-Markovnikov addition of H-X (i.e., a mineral acid) constitutes a significant challenge to which peroxide-initiated radical bromination is among the few solutions but still requiring harsh conditions and precluding addition of the other hydrogen halides.<sup>368</sup> Remarkably, a photoredox catalyzed addition of “H-Cl” and “H-F” was achieved using acridinium catalysts and thiol/disulfide co-catalysts (**Scheme 90** and **Scheme 91**, method 4).<sup>319</sup> When using 2,6-lutidine-HCl or slow in situ generation of HCl from pivaloyl chloride and trifluoroethanol (TFE), Markovnikov addition was largely suppressed and good yields of the anti-Markovnikov chlorination products (e.g. **91.14**) were obtained from a series of substituted styrenes. **Mes-Acr-Me<sup>+</sup>** (5 mol %) and 4-methoxythiophenol (**4-MeOPhSH**, 20 mol %) were appropriate for the hydrochlorination reaction, but **Mes-Acr-Me<sup>+</sup>** was found to be incompatible with nucleophilic fluoride reagents (**Scheme 93**). When treated with CsF, **Mes-Acr-Me<sup>+</sup>**

**Scheme 93. Development of Robust Acridinium Photoredox Catalysts**

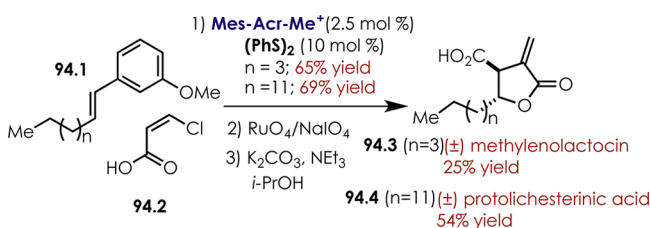


experienced demethylation to the corresponding acridine **Mes-Acr**, while the analogous **Mes-Acr-Ph<sup>+</sup>** showed evidence of nucleophilic dearomatization at the acridinium.<sup>318</sup> Although the most electrophilic sites of acridiniums **Mes-Acr-R<sup>+</sup>** are expected to be the 3- and 6-positions, the 2,7-dimethyl-substituted *N*-phenylacridinium **Mes-Me<sub>2</sub>Acr-Ph<sup>+</sup>** was sufficiently robust as to provide good to excellent yields of the anti-Markovnikov hydrofluorinated styrenes (e.g., **91.15**). Triethylamine trihydrofluoride ( $\text{Et}_3\text{N}\cdot 3\text{HF}$ ) was the optimal source of HF and 25 mol % 4-nitrophenyl disulfide ( $4\text{-NO}_2\text{PhS}_2$ ) the key HAT catalyst. Moreover, sulfonates and phosphates participated in the anti-Markovnikov addition to  $\beta$ -methylstyrene in good yields (e.g., **91.16** and **91.17**), using either catalytic 2,6-lutidine/ $(\text{PhS})_2$  (10 mol % each) with the free acid nucleophile or 20 mol % 4-MeOPhSH and the lutidinium salt of the nucleophile.

A related transformation is shown in Scheme 90, methods 5–8, called polar radical crossover cycloaddition (PRCC), and can be viewed as an anti-Markovnikov hydrofunctionalization interrupted by a radical cyclization onto pendant unsaturation tethered to the nucleophile (Scheme 92). Allylic and propargylic alcohols **90.15** participated in the cyclization (Scheme 90 and Scheme 91, method 5),<sup>369</sup> yielding cyclic ethers **90.14** (e.g., **91.18**–**91.23**) with moderate diastereoselectivity. A full equivalent of PMN was required in this system, but extension of the methodology to acrylic and propiolic acids **90.17** (Scheme 90 and Scheme 91, method 6)<sup>370</sup> was enabled by catalytic 2,6-lutidine and  $(\text{PhS})_2$  or 4-NO<sub>2</sub>PhSH. The  $\gamma$ -butyrolactones **90.16** map onto the natural products methylenolactocin **94.3** and protolichesterinic acid **94.4** (Scheme 94), which were synthesized using the photoredox PRCC procedure as the first step, cyclizing acid **94.2** with alkenes **94.1**. Arene oxidation and chloride elimination provided **94.3** and **94.4** in reasonable yields over 3 steps (25% and 54% yield, respectively).

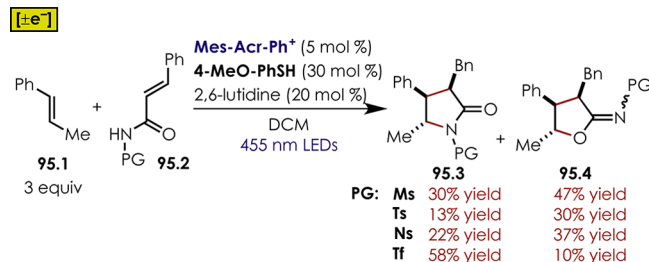
The photoredox PRCC reaction was also applied to the synthesis of  $\gamma$ -butyrolactams and pyrrolidines **90.18** with amide

**Scheme 94. Natural Product Synthesis Using Photoredox PRCC Reaction**



and amine nucleophiles **90.19** (Scheme 90 and Scheme 91, method 7).<sup>371</sup> While other sulfonyl protecting groups gave a higher proportion of the cyclic imide **95.4** (occurring via nucleophilic addition through oxygen), triflyl protected amides **95.2** (PG = Tf) favored lactam **95.3** formation (Scheme 95).

**Scheme 95. Development of a Sulfonyl Amide–Alkene Photoredox PRCC Reaction**

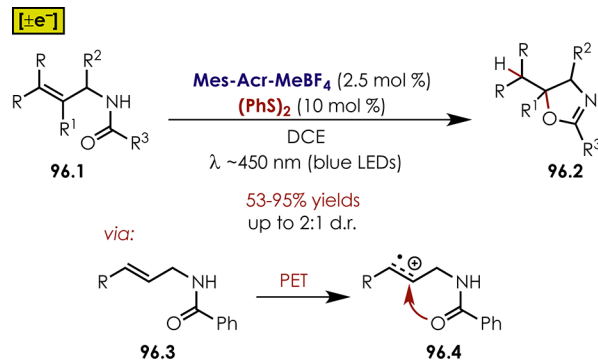


Moderate to good yields (35–74%) of lactams (e.g. **91.27**–**91.29**) were obtained over a broad substrate scope covering a range of alkenes and sulfonylamides when using **Mes-Acr-Ph<sup>+</sup>** with catalytic 2,6-lutidine and  $(\text{PhS})_2$  or 4-MeOPhSH. An *N*-Boc allylic amine also underwent the cyclization with several alkenes in moderate yields, with the pyrrolidines **91.30** furnished after Boc deprotection by TFA.

Finally, *O*-benzyloxime acids **90.21** could be engaged in a photoredox catalytic PRCC with alkenes to give  $\alpha$ -(benzyloxy)-amino- $\gamma$ -butyrolactones **90.20** (Scheme 90, method 8).<sup>372</sup> The **Mes-Acr-Me<sup>+</sup>** catalyst was sufficient for high-catalytic performance, and  $(\text{PhS})_2$  was found to be the optimal HAT catalyst, giving moderate to excellent yields and varying diastereoselectivities (Scheme 91, method 8).

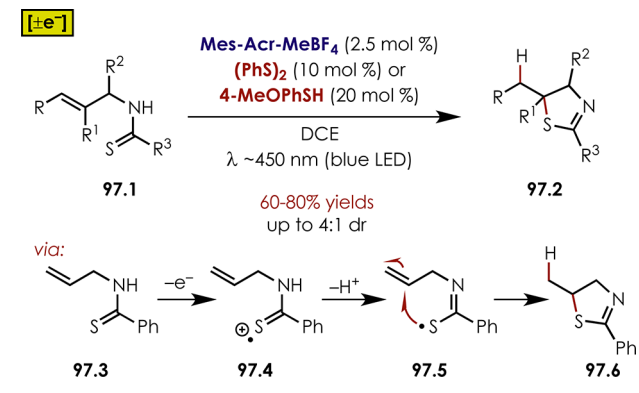
The cooperative activity of an HAT catalyst and **Mes-Acr-Me<sup>+</sup>** also enabled the intramolecular cyclization of allylic amides **96.1** to oxazolines **96.2** (Scheme 96). Notably, this method

**Scheme 96. Cation Radical Amide Cyclization**



provides direct access to oxazolines substituted at the 5 position, whereas preparations involving the condensation of an amino alcohol typically result in 4-substituted oxazolines owing to the comparative availability of  $\beta$ -amino alcohols.<sup>374</sup> The photoredox catalytic protocol employs  $(\text{PhS})_2$  and gives moderate to excellent yields. This transformation is believed to be mechanistically related to the alkene hydrofunctionalizations discussed above: nucleophilic addition of the amide oxygen (**96.4**) and eventual conversion to the oxazoline product by HAT. Thioamides **97.1** likewise participate in the intramolecular cyclization (Scheme 97), but this modulation appears to be

Scheme 97. Cation Radical Thioamide Cyclization

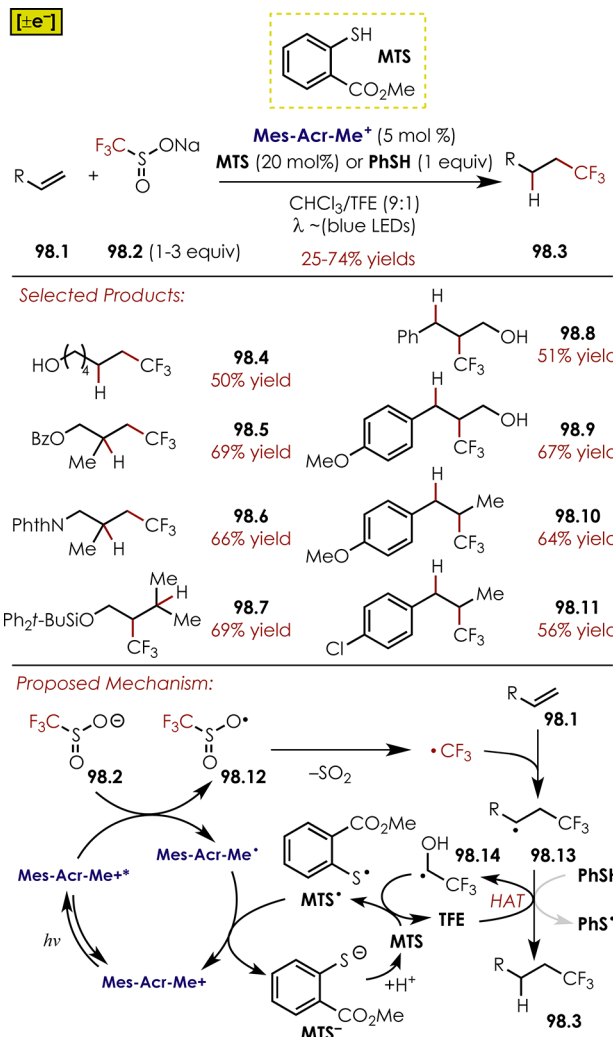


accompanied by a change in mechanism. Whereas amide **96.3** ( $R = H$ ), containing a terminal aliphatic alkene, possesses an oxidation potential [ $E_{ox}$  (**96.3**•<sup>+</sup>/**96.4**) = +2.5 V vs SCE] well beyond the  $E_{red}^*$  of **Mes-Acr-Me<sup>+</sup>** and does not cyclize to the oxazoline, thioamide **97.3** exhibits an  $E_{ox}$  (**97.3**•<sup>+</sup>/**97.4**) = +1.53 V vs SCE and gives a good yield of thioxazoline **97.6**. This is consistent with the hypothesis that cation radical **97.4** is best described as a thioamide-centered cation radical, which, upon deprotonation, gives sulfur-centered radical **97.5** primed for cyclization.

**Mes-Acr-Me<sup>+</sup>** was also utilized in the hydro-trifluoromethylation of alkenes (Scheme 98)<sup>375</sup> through the photoredox generation of the trifluoromethyl radical •CF<sub>3</sub> via single electron oxidation of sodium trifluoromethanesulfinate **98.2**, known as the Langlois Reagent.<sup>376–378</sup> The products of the reaction (**98.3**) are provided in high regioselectivity, owing to preferential addition of •CF<sub>3</sub> at the less-substituted position of an alkene to give the more stabilized carbon-centered radical **98.13**. Because the alkene substrates are not limited by the oxidation potential of the olefin in this manifold, a range of alkenes were found to be compatible. For aliphatic alkenes, such as 5-hexen-1-ol, optimized conditions utilized 5 mol % **Mes-Acr-Me<sup>+</sup>** and 20 mol % methylthiosalicylate (MTS) in 9:1 CHCl<sub>3</sub>/TFE. Control reactions revealed that TFE was crucial in attaining catalytic production of **98.3**, suggestive of a redox-active role or a role in proton/hydrogen transfer. The conditions were modified slightly to accommodate styrenyl substrates, which also provided synthetically valuable yields when using a stoichiometric equivalent of PhSH (products **98.9**–**98.11**). A number of possible explanations for the beneficial combination of TFE and thiol were considered, including TFE acting as an intermediary H atom donor<sup>379</sup> between β-trifluoromethyl radical **98.13** and MTS, with MTS• accomplishing catalyst turnover. Moreover, ketol radical **98.14** may be involved in regeneration of the thiol, as the pK<sub>a</sub> of **98.14** is expected to be several decades lower than that of TFE<sup>119</sup> (pK<sub>a</sub>(TFE) = 12.4 in H<sub>2</sub>O).<sup>380</sup>

**8.2.4. Deborylative and Decarboxylative Transformations.** Organoborates are known to fragment to form C-centered radicals upon single-electron oxidation, and a number of chemistries which harness this reactivity have been reported, which utilize either chemical oxidants<sup>381,382</sup> or transition metal photoredox catalysts.<sup>383–386</sup> Akita and co-workers explored the use of **Mes-Acr-Me<sup>+</sup>** in the addition of alkyl radicals generated from alkyl-trifluoroborates **99.1** to activated alkenes (Scheme 99).<sup>387</sup> Excellent yields of the conjugate addition products **99.3** could be achieved for a number of alkyltrifluoroborate coupling partners, with the cycloalkyl-trifluoroborates giving superior

Scheme 98. Hydrotrifluoromethylation of Alkenes Using the Langlois Reagent

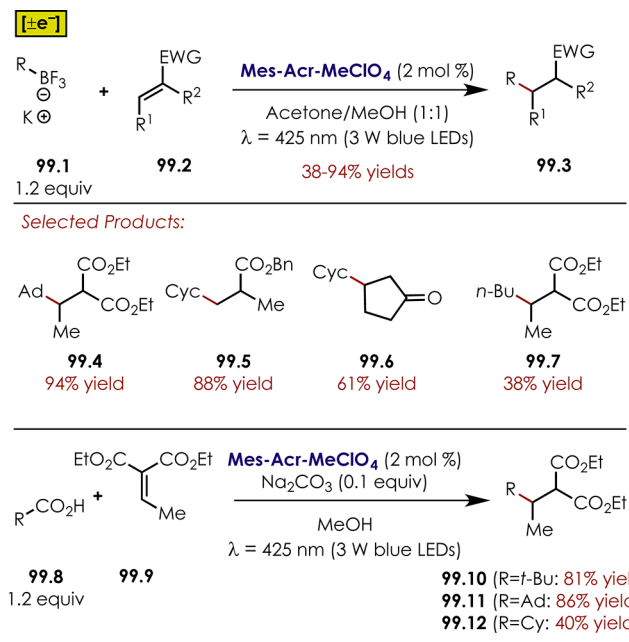


yields to linear alkyl substrates. In demonstrating activation of alkyltrifluoroborates, this report provides a considerable expansion in scope compared to previous methodologies relying on transition metal photoredox catalysts, which is attributed to the more positive reduction potential of **Mes-Acr-Me<sup>+</sup>\*** than [Ir]- or [Ru]-based catalysts [ $E_{ox}$  (**99.1**•<sup>+</sup>/**99.1**<sup>-</sup>) = +1.41 V vs Fc<sup>+/Fc</sup>]. **Mes-Acr-Me<sup>+</sup>** was the only photoredox catalyst to give significant product formation when tested alongside Ru(bpy)<sub>3</sub><sup>2+</sup> and two Ir(ppy)<sub>3</sub> catalysts.

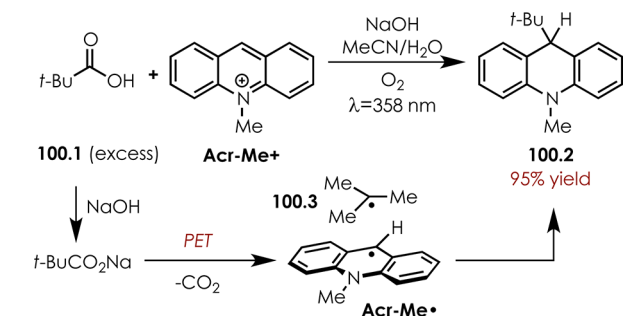
In the same report, the authors demonstrated the use of **Mes-Acr-Me<sup>+</sup>** in generating C-centered radicals by decarboxylation of carboxylic acids **99.8**. The conjugate addition reaction in Scheme 99 operated for several carboxylic acids in varying yields (**99.10**–**99.12**).

Moreover, decarboxylative reactions enabled by acridinium photoredox catalysts are preceded. Fukuzumi studied the decarboxylation of pivalic acid **100.1** and other aliphatic acids using **Acr-Me<sup>+</sup>**.<sup>338</sup> However, when irradiated with pivalic acid and NaOH, the sensitivity of **Acr-Me<sup>+</sup>** to side-reactions was evidenced by bleaching of the **Acr-Me<sup>+</sup>** absorption and in the isolation of dihydroacridine **100.2** in 95% yield (Scheme 100). Evidently, the radical–radical coupling between the *t*-Bu radical **100.3** and **Acr-Me<sup>+</sup>** is sufficiently fast that **100.3** avoids trapping by O<sub>2</sub>. In contrast, pivalic acid underwent decarboxylation-

**Scheme 99. Deborylative and Decarboxylative Radical Conjugate Addition Reactions**

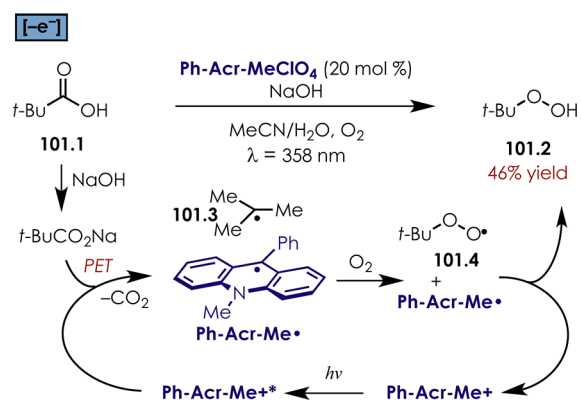


**Scheme 100. Decarboxylative Addition of Alkyl Radicals to Acridinyl Radical**



oxygenation to form hydroperoxide **101.2** (*t*-BuOOH) along with *t*-BuOH with catalytic quantities of Ph-Acr-Me<sup>+</sup> (Scheme 101). The steric bulk of the 9-phenyl substituent is thought to slow radical coupling, and *t*-BuOO• is formed upon trapping with O<sub>2</sub>. After reduction of *t*-BuOO• by Ph-Acr-Me•, protonation furnishes hydroperoxide *t*-BuOOH. Accompanying

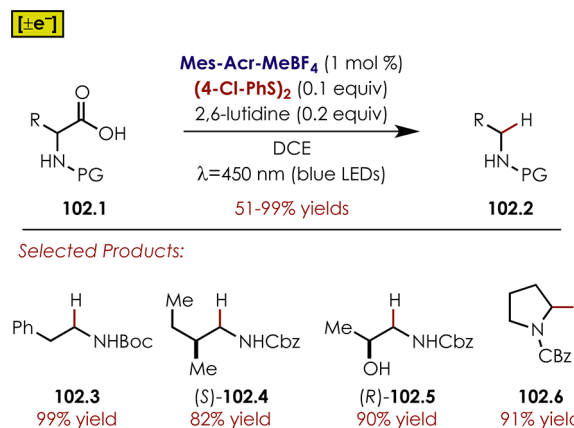
**Scheme 101. Photoredox Catalytic Decarboxylation-Oxygenation of Pivalic Acid**



laser flash photolysis studies confirmed that PET occurs between the carboxylate to the singlet excited state <sup>1</sup>Ph-Acr-Me<sup>+</sup>, while EPR measurements support the presence of *t*-BuOO• together with Ph-Acr-Me•.

Two separate reports detail similar photoredox systems employing mesityl acridinium catalysts and disulfide co-catalysts in the reductive decarboxylation (or hydrodecarboxylation) of carboxylic acids: the method reported by Wallentin and co-workers utilizes Mes-Acr-Me<sup>+</sup> (1 mol %) and (4-Cl-PhS)<sub>2</sub> (10 mol %) in the hydrodecarboxylation of  $\alpha$ -amino acids **102.1**, along with a few examples of phenylacetic acids as substrates (Scheme 102).<sup>388</sup> Excellent yields could be obtained, and

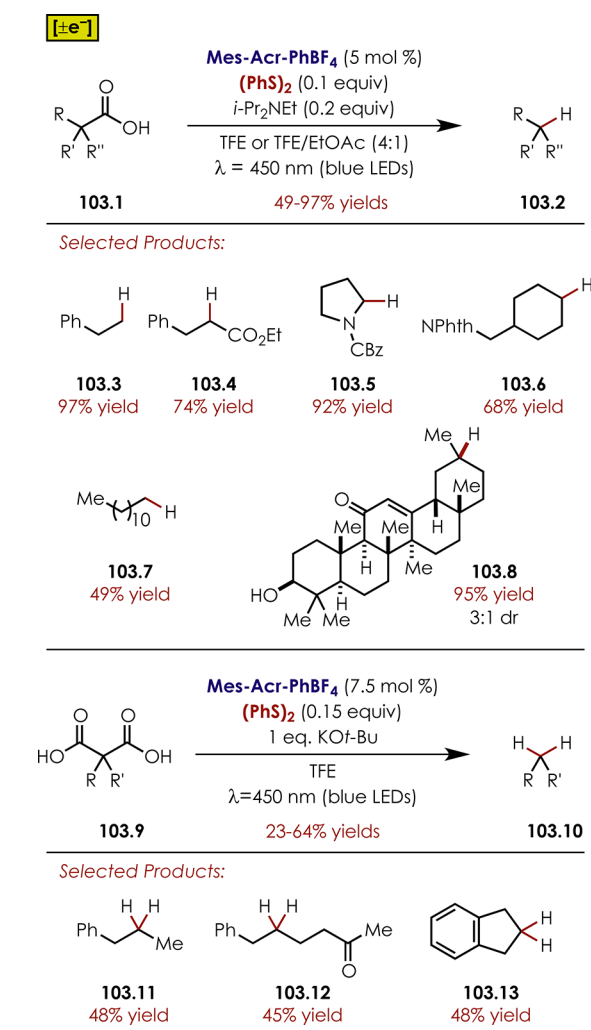
**Scheme 102. Reductive Decarboxylation of Amino Acids**



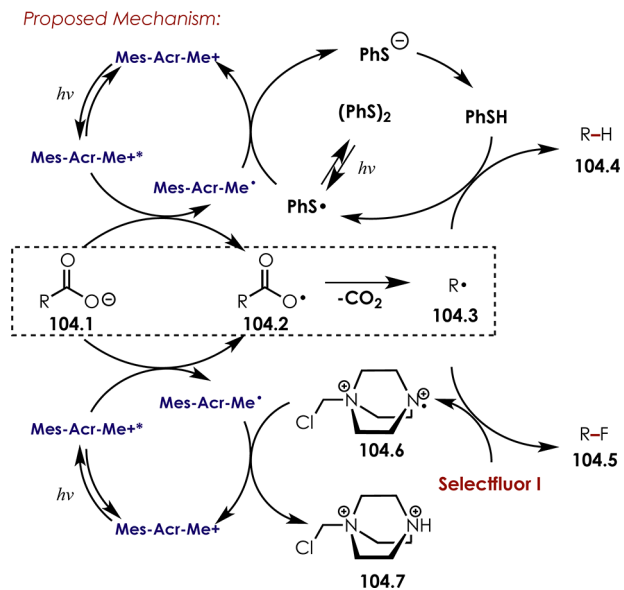
minimal erosion of enantiopurity was generally observed when the starting materials were optically active (e.g. **102.4** and **102.4**). Whereas this protocol appeared limited to substrates which would produce a C-centered radical stabilized by an adjacent heteroatom or aryl ring, Nicewicz and co-workers demonstrated hydrodecarboxylation in substrates **103.1**, ranging from primary alkyl- to tertiary benzylic-substituted carboxylic acids (Scheme 103).<sup>389</sup> (PhS)<sub>2</sub> was used as the HAT catalyst with Mes-Acr-Ph<sup>+</sup> as the optimal photoredox catalyst. TFE was found to be crucial to the success of the protocol, with highly hydrophobic substrates requiring EtOAc for dissolution in the reaction medium (e.g., product **103.8**, from enoxolone). When using one equivalent of KOt-Bu as a base, malonic acids **103.9** could be doubly decarboxylated to the corresponding alkanes **103.10**, although these conditions required somewhat higher loadings of Mes-Acr-Ph<sup>+</sup> and (PhS)<sub>2</sub>.

Both hydrodecarboxylation methods are believed to proceed by the same mechanism (Scheme 104). Single electron oxidation of the carboxylate **104.1** generates acyloxyradical **104.2**, a well-studied intermediate which is known to rapidly fragment to CO<sub>2</sub> and carbon-centered radical **104.3**.<sup>390,391</sup> HAT from aryl thiol furnishes the product **104.4**, while the thiyl radical is responsible for catalyst turnover. Mechanistic studies by Nicewicz and co-workers elucidated key insights into the catalytic process. Deuterium KIE studies indicated that the HAT step is not rate-limiting, while apparent zero-order kinetic dependence on [Mes-Acr-Ph<sup>+</sup>] and variable intensity irradiation qualitatively suggested that the reaction rate was photon flux dependent. Additionally, even though fluorescence quenching studies on Mes-Acr-Ph<sup>+</sup> revealed that the carboxylates exhibit large quenching constants (*k*<sub>q</sub>) of  $\sim 3 \times 10^8 \text{ M}^{-1}\text{s}^{-1}$ , indicating a fast PET reaction, the efficiency of quenching was found to be very low (5 mM potassium hydrocinnamate quenches  $\sim 2\%$  of

**Scheme 103. Reductive Decarboxylation Including Primary Carboxylic Acids and Malonates**



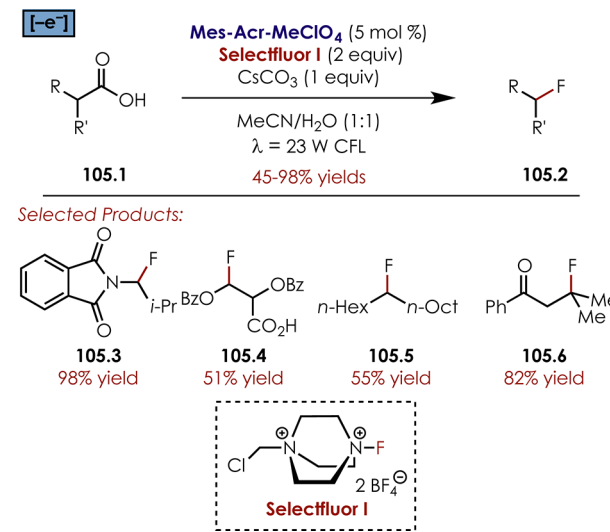
**Scheme 104. Mechanisms for Decarboxylative Fluorination and Reductive Decarboxylation**



fluorescence). In combination with NMR evidence of ion exchange between the  $\text{BF}_4^-$  and carboxylate salts of the acridinium, the authors concluded that inefficient PET may be significantly rate limiting, especially when considered in concert with a pre-complexation equilibrium.

Drawing upon previous photoredox methodologies for decarboxylative fluorination,<sup>392,393</sup> Ye and co-workers demonstrated that Mes-Acr-Me<sup>+</sup> was a competent organic photoredox catalyst in the synthesis of fluorinated alkanes (Scheme 105).<sup>394</sup>

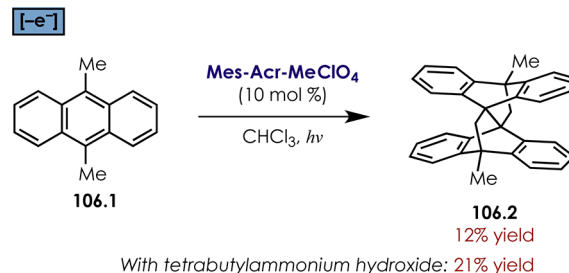
**Scheme 105. Decarboxylative Fluorination**



Moderate to excellent yields of fluoroalkanes 105.2 were observed for primary, secondary, and tertiary carboxylic acid substrates 105.1 when 2 eq. Selectfluor® I was used as a “F-atom source, although the highest yields were obtained from  $\alpha$ -imido carboxylic acids (e.g., 105.3). The proposed mechanism involves the same pathway to C-centered radical as discussed above (Scheme 104),<sup>388,389</sup> followed by fluorine atom transfer to furnish the fluoroalkane 104.5 and dication radical 104.6, which is presumed to be sufficiently oxidizing as to turnover Mes-Acr-Me<sup>+</sup> to Mes-Acr-Me<sup>+</sup>.

**8.2.5. Cycloadditions.** *8.2.5.1. Arene cycloaddition.* The complex multi-fused-ring structure dimethyllepidopterene 106.2 was discovered to form under the photoredox activity of Mes-Acr-Me<sup>+</sup> from the simple starting material 9,10-dimethylanthracene 106.1 (Scheme 106).<sup>395</sup> The stepwise mechanism likely first involves removal of a benzylic hydrogen, seeing as addition of tetrabutylammonium hydroxide led to increased yield,

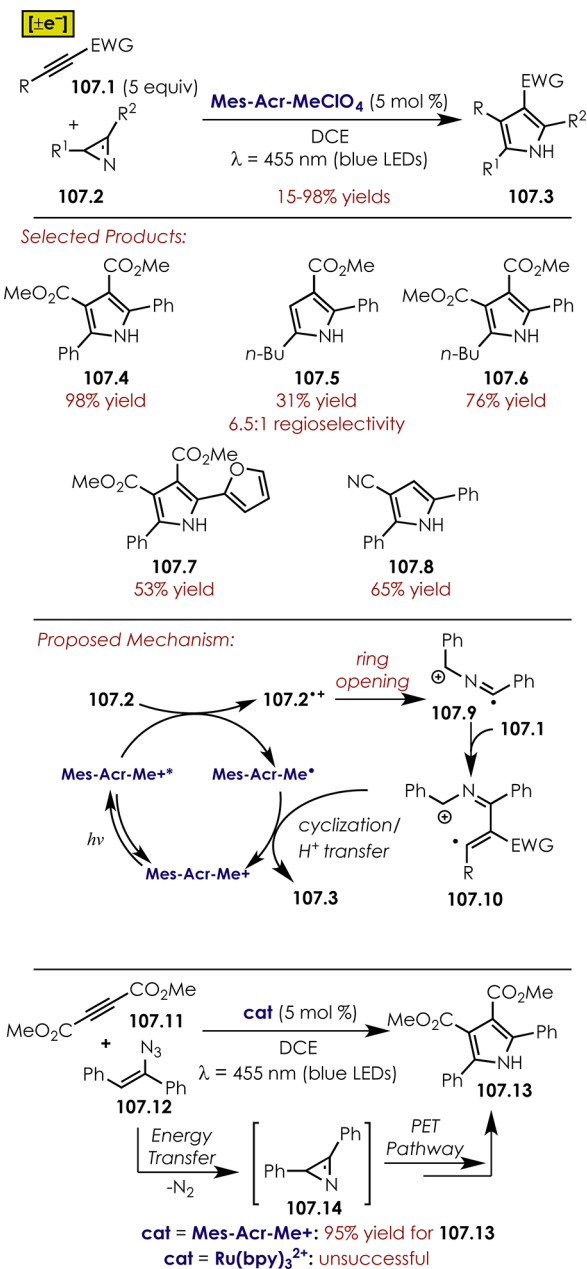
**Scheme 106. Dimerization of 9,10-Dimethylanthracene to Dimethyllepidopterene**



probably by accelerating deprotonation of the arene cation radical.

**8.2.5.2. Formal [3+2] Cycloadditions.** The use of **Mes-Acr-Me<sup>+</sup>** has enabled access to aromatic heterocycles through oxidative ring opening of 2H-azirines and subsequent (formal) cycloaddition reactions. Azaallenyl radical cations, which result from ring opening after PET oxidation of 2H-azirines, and their [3+2]-type cycloaddition chemistry to give imidazoles and pyrroles were studied by Müller and Mattay as shown in **Scheme 23** and **Scheme 24**.<sup>173–176</sup> More recently, **Mes-Acr-Me<sup>+</sup>** was reported to catalyze the synthesis of pyrroles **107.3** from 2H-azirines **107.2** and activated alkynes **107.1** (**Scheme 107**).<sup>396</sup> While a 98% yield of **107.4** could be achieved with **Mes-Acr-Me<sup>+</sup>**, neither  $\text{Ru}(\text{bpy})_3^{2+}$  nor  $\text{Ir}(\text{ppy})_2(\text{dtbbpy})$  gave any of the cycloaddition product, which highlights the ability of **Mes-Acr-Me<sup>+</sup>** to oxidize substrates with high oxidation potentials [ $E_{\text{ox}}(107.2\bullet^+/107.2) = +1.65 \text{ V vs Ag/AgNO}_3$ ].<sup>176</sup> Substituents on both the activated alkynyl coupling partner **107.1** and the azirine **107.2** were varied, providing diverse, unsymmetrically substituted pyrroles in wide-ranging yields. Consistent with the earlier proposal by Müller and Mattay, azaallenyl cation radical **107.9** participates in a stepwise cyclization with alkyne **107.1**, first forming distonic cation radical **107.10** by radical addition. Subsequent reduction by **Mes-Acr-Me<sup>•</sup>** precedes ring closure, while the particular mechanism of the final aromatization step is not specified. Following a report from the Yoon group that 2H-azirines could be generated from vinyl azides by way of triplet energy transfer from  ${}^3[\text{Ru}]^*$  and  ${}^3[\text{Ir}]^*$  complexes,<sup>397</sup> the researchers established that a cascade reaction of vinyl azide **107.12** and alkyne **107.11** was operable using **Mes-Acr-Me<sup>+</sup>**. While the azirine intermediate **107.14** is thought to be the result of a triplet energy transfer process, the subsequent steps proceed through the same redox neutral pathway shown in **Scheme 107**.

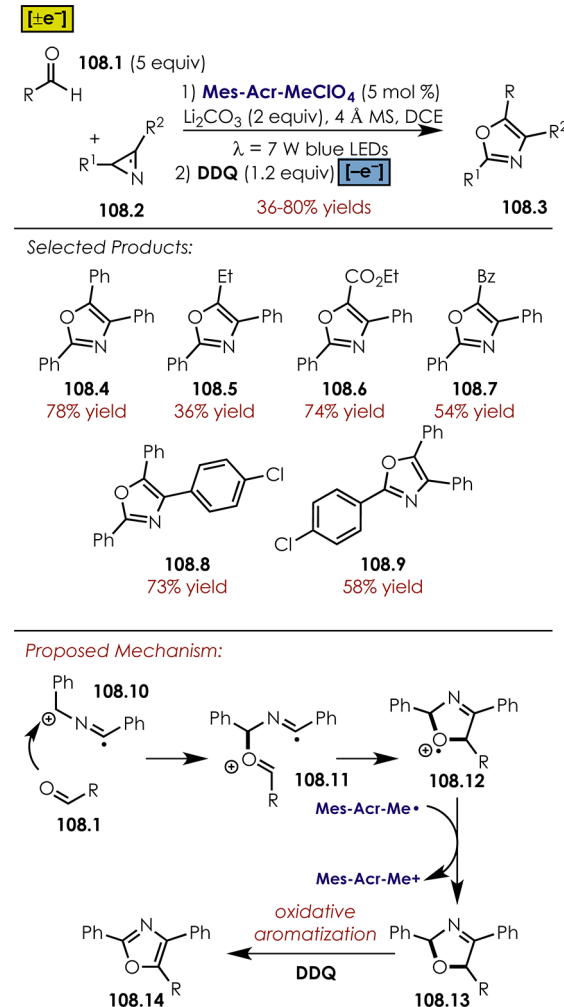
**Scheme 107. Pyrrole Synthesis through Formal [3+2] Cycloaddition of 2H-Azirines and Alkynes**



**Me<sup>•\*</sup>** to oxidize substrates with high oxidation potentials [ $E_{\text{ox}}(107.2\bullet^+/107.2) = +1.65 \text{ V vs Ag/AgNO}_3$ ].<sup>176</sup> Substituents on both the activated alkynyl coupling partner **107.1** and the azirine **107.2** were varied, providing diverse, unsymmetrically substituted pyrroles in wide-ranging yields. Consistent with the earlier proposal by Müller and Mattay, azaallenyl cation radical **107.9** participates in a stepwise cyclization with alkyne **107.1**, first forming distonic cation radical **107.10** by radical addition. Subsequent reduction by **Mes-Acr-Me<sup>•</sup>** precedes ring closure, while the particular mechanism of the final aromatization step is not specified. Following a report from the Yoon group that 2H-azirines could be generated from vinyl azides by way of triplet energy transfer from  ${}^3[\text{Ru}]^*$  and  ${}^3[\text{Ir}]^*$  complexes,<sup>397</sup> the researchers established that a cascade reaction of vinyl azide **107.12** and alkyne **107.11** was operable using **Mes-Acr-Me<sup>+</sup>**. While the azirine intermediate **107.14** is thought to be the result of a triplet energy transfer process, the subsequent steps proceed through the same redox neutral pathway shown in **Scheme 107**.

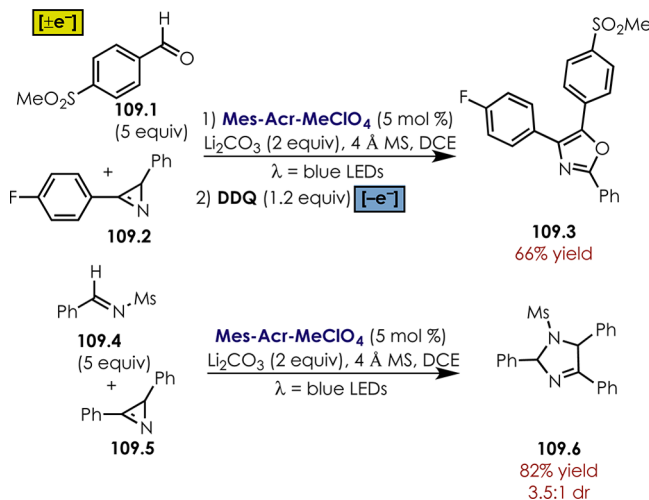
A two-step synthesis of highly substituted oxazoles **108.3** was recently disclosed, where the first step was a similar photoredox-mediated [3+2] cycloaddition between 2H-azirines **108.2** and aldehydes **108.1** (**Scheme 108**).<sup>398</sup> The proposed mechanism involved addition of the aldehyde to azaallenyl radical cation **108.10** through oxygen; cyclization and reduction of cation

**Scheme 108. Oxazole Synthesis through Formal [3+2] Cycloaddition of 2H-Azirines and Aldehydes**



radical **108.12** by Mes-Acr-Me $\bullet$  furnished 2,5-dihydrooxazole **108.13**, although the researchers did not explicitly rule out the possibility that reduction of the cation radical may proceed by a chain propagating electron transfer from **108.12** to 2*H*-azirine **108.2**. The second step in the sequence was addition of **DDQ** to the reaction mixture, which accomplishes oxidative aromatization to oxazole **108.14**. The photoredox conditions were optimized based on the formation of dihydrooxazole **108.13**, and the conditions included 2 eq. Li<sub>2</sub>CO<sub>3</sub> and 4 Å mol sieves with Mes-Acr-Me $^+$ . The acridinium catalyst resulted in 77% yield, whereas Ir[*d*F(CF<sub>3</sub>)ppy]<sub>2</sub>(dtbbpy) $^+$  gave 22% and Ru(bpy)<sub>3</sub> $^{2+}$  gave 0%. The method was applied to synthesis of a cyclo-oxygenase-2 inhibitor (**109.3**, Scheme 109), and imidazoline **109.6** was obtained by reaction of **109.5** with imine **109.4** under the photoredox conditions.

**Scheme 109. Other Formal [3+2] Cycloadditions of 2*H*-Azirines**



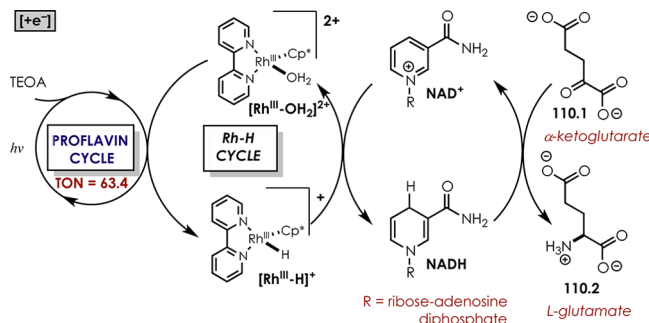
### 8.3. Electron-Rich Acridines and Acridiniums: Acridine Orange (AO and AOH $^+$ ) and Proflavin (PF and PFH $^+$ )

**8.3.1. AO/AOH $^+$  and PF/PFH $^+$ : Photophysical and Electrochemical Characteristics.** The series of 3,6-diamino acridiniums have seen limited use in synthetic contexts but are worth briefly considering as their utility as biological stains and dyes in solar energy conversion highlights their potentially useful photoredox properties. The closely related acridine orange (AO) and proflavin (PF) can be used in neutral and protonated forms (AOH $^+$  and PFH $^+$  respectively), which can be in equilibrium in buffered aqueous solutions. Singlet lifetimes of AO/AOH $^+$  are short, and the triplet state  $^3$ AO is typically regarded as the most important excited state. These compounds exhibit complex photophysical features involving proton and electron transfers, and in the case of AO, it has been recently shown that coupled proton/electron transfer is operative in the reaction of triplet excited state  $^3$ AO with phenols and hydroxylamines. The triplet  $^3$ AO is formed in high efficiency but presents difficult photophysics due to triplet-triplet annihilation, likely involving disproportionation to the semi-reduced and semi-oxidized forms of the dye (AO $\bullet^-$  and AO $\bullet^+$ , respectively).<sup>75,399,400</sup> Accordingly, AO might be expected to act as both a reductant and an oxidant in the excited state. The activity of excited state AOH $^{**}$  is primarily as an oxidant<sup>75,399,401</sup> as are the related acriflavine AcrF $^+$  and protonated proflavin PFH $^+$ .<sup>402</sup> When reduced, the resulting acridinyl radicals are moderate reductants owing to the

diamino substituents. Although the photoinduced formation of acridinyl radical AO $\bullet^-$  by reduction of AO $^*$  ( $^1$ AO or  $^3$ AO) requires a donor with a relatively low oxidation potential, AO $\bullet^-$  is expected to be an extremely strong reductant as indicated by its ground state reduction potential [ $E_{\text{red}}(\text{AO}/\text{AO}\bullet^-)$ ] = -2.0 V vs SCE]. However, this activity may be rarely encountered due to the strong basicity of AO $\bullet^-$  [ $pK_a(\text{AOH}\bullet^-)$  = 33.4 in MeCN],<sup>73</sup> which may lead to solvent or substrate deprotonation over reduction. On the other hand, the analogous, strongly reducing PF $\bullet^-$  is proposed as an intermediate formed by deprotonation of PFH $\bullet$ .<sup>79</sup>

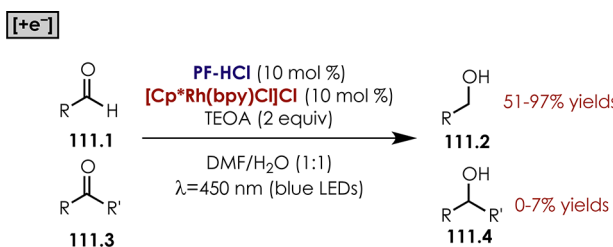
**8.3.2. AO/AOH $^+$  and PF/PFH $^+$ : Reactions.** **8.3.2.1. Reduction Reactions/Regeneration of [Rh]-H.** In the synthetic setting, proflavin has found valuable application as a photoredox catalyst in the light-driven regeneration of the rhodium(III) hydride [Cp $^*$ Rh $^{III}$ (bpy)H] $^+$  ([Rh $^{III}$ -H] $^+$ ),<sup>403</sup> which has shown excellent selectivity in the reduction of NAD $^{+}$ <sup>404,405</sup> and in the transfer hydrogenation of aldehydes and ketones.<sup>406,407</sup> Nam and Park demonstrated that PF (in phosphate-buffered H<sub>2</sub>O, pH = 7.0) could be used as a light-absorbing electron transfer catalyst capable of generating [Rh $^{III}$ -H] $^+$  from [Cp $^*$ Rh $^{III}$ (bpy)H<sub>2</sub>O] $^{2+}$  ([Rh $^{III}$ -OH<sub>2</sub>] $^{2+}$ ) when irradiated in the presence of triethanolamine (TEOA) as a reducing equivalent.<sup>408</sup> NAD $^+$  was reduced to NADH with a catalytic turnover number of 63.4, and the NADH was coupled to the enzymatic reduction of L-glutamate using L-glutamate dehydrogenase (Scheme 110). The rhodium catalyst was confirmed to be an essential component in this process.

**Scheme 110. Proflavin Regeneration of [Rh]-H in the Enzymatic Reduction of  $\alpha$ -Ketoglutarate**



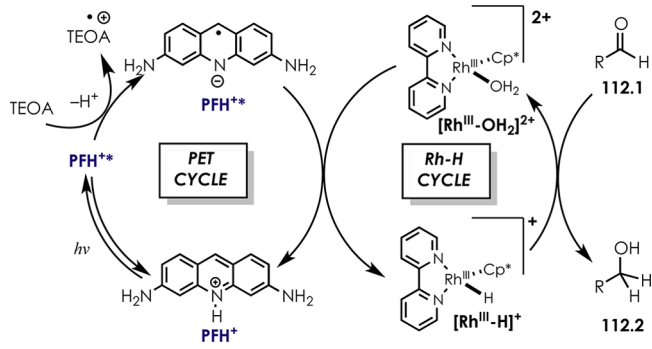
König and co-workers extended this strategy to the catalytic hydrogenation of aldehydes **111.1** using 10 mol % of PFH $^+$  and [Cp $^*$ Rh $^{III}$ (bpy)Cl]Cl with 2 eq. TEOA (Scheme 111),<sup>79</sup> obtaining excellent yields of alcohols **111.2** under both batch and flow conditions. When a mixture of aldehydes **111.1** and ketones **111.3** was submitted to the conditions, less than 5% of

**Scheme 111. Selective Aldehyde Reduction by [Cp $^*$ Rh $^{II}$ (bpy)] Regenerated by PFH $^+$**



the ketone **111.3** was reduced in all cases, demonstrating the high selectivity for reduction of aldehyde substrates by  $[\text{Rh}^{\text{III}}\text{-H}]^+$ . A thorough mechanistic investigation illuminated the complexity of the catalytic system (**Scheme 112**), including the discovery that

**Scheme 112.** Mechanistic Study of  $[\text{Rh}]$ -H Regeneration by Proflavin



two distinct photophysical mechanisms were involved in the reduction of  $[\text{Rh}^{\text{III}}\text{-OH}_2]^{2+}$ . One pathway features ionization of the singlet state  $^1\text{PFH}^{+*}$ <sup>80</sup> concomitant with reduction of the  $[\text{Rh}^{\text{III}}\text{-OH}_2]^{2+}$  species in an outer sphere process (not shown). Additionally, the authors provide evidence for another mechanism, outlined in **Scheme 112**, which begins with ET from TEOA to the triplet  $^3\text{PFH}^{+*}$ . The subsequent step, deprotonation of  $\text{PFH}\bullet$  to give  $\text{PF}\bullet^-$ , is substantiated by spectroelectrochemical analysis. The strongly reducing  $\text{PF}\bullet^-$  effects single-electron reduction of  $[\text{Rh}^{\text{III}}\text{-OH}_2]^{2+}$  at rates near the diffusion limit ( $>5 \times 10^9 \text{ M}^{-1}\text{s}^{-1}$ ) and the resulting  $[\text{Cp}^*\text{Rh}^{\text{II}}(\text{bpy})\text{H}_2\text{O}]^+$  is unstable, undergoing disproportiona-

tion then protonation from the solvent to give the  $[\text{Rh}^{\text{III}}\text{-H}]^+$  species. Ultimately, the formation of the catalytically active  $[\text{Rh}^{\text{III}}\text{-H}]^+$  is relatively slow, which is in contrast to non-photolytic transfer hydrogenation protocols using this rhodium catalyst,<sup>406</sup> and this factor is offered to account for the kinetic discrimination between aldehydes and ketones.

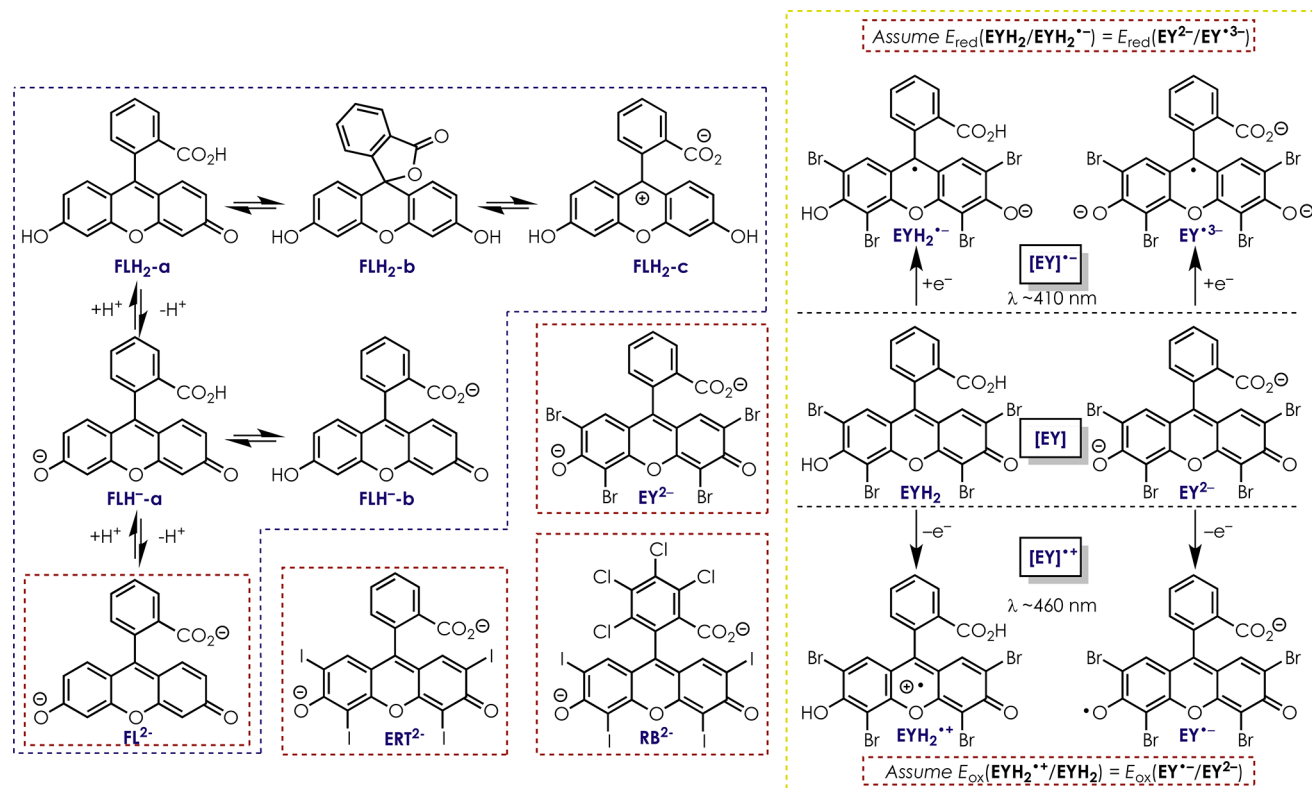
## 9. XANTHENES DYES: FLUORESCINS AND RHODAMINES

### 9.1. Fluorescein-Based Photoredox Catalysts (Eosin Y, Erythrosine, Rose Bengal, and Fluorescein): Photophysical and Electrochemical Characteristics

The properties of fluorescein ([FL]) and its derivatives have been the subject of investigation for more than a century,<sup>409,410</sup> yet the excited state behavior of these molecules remains somewhat enigmatic owing to complex protolytic equilibria within and between neutral and ionized forms. As depicted for fluorescein in **Scheme 113**, neutral fluorescein exists in three forms: quinonoid **FLH<sub>2</sub>-a**, lactone **FLH<sub>2</sub>-b**, and zwitterion **FLH<sub>2</sub>-c**. Mono-anion **FLH<sub>2</sub>** is thought to be convertible between phenolate **FLH<sub>2</sub>-a** and carboxylate **FLH<sub>2</sub>-b**, while di-anion **FL<sup>2-</sup>** is fully deprotonated. Not surprisingly, the absorption wavelength and intensity are pH-dependent, with di-anion **FL<sup>2-</sup>** exhibiting the longest wavelength absorption. The neutral form **FLH<sub>2</sub>** displays drastically diminished absorbance due to significant proportion of lactone **FLH<sub>2</sub>-b**, which does not absorb in the visible. **FL<sup>2-</sup>** exhibits a high quantum yield of fluorescence ( $\phi_{\text{ISC}} = 0.93$ ) with minimal intersystem crossing to the triplet ( $\tau_f \sim 4 \text{ ns}$ ).

The halogenated analogues of fluorescein are subject to tautomeric/protolytic equilibria similar to [FL], which can lead to drastic differences in photoredox reactivity dependent on

**Scheme 113.** Equilibria and Forms of Fluorescein-Based Dyes



solvent and the form of the dye employed. While rose bengal ( $[RB]$ ) is most often supplied as the disodium salt  $RB\text{-Na}_2$  ( $RB^{2-}$ ), eosin Y ( $[EY]$ ) is found as the neutral ( $EYH_2$ ), mono- ( $EYH\text{-Na}$  or  $EYH^-$ ), or disodium salt ( $EY\text{-Na}_2$  or  $EY^{2-}$ ). As in  $[FL]$ , the neutral lactones do not absorb in the visible. Although significant spectral differences exist for the fluorescein family dependent on ionization, the redox potentials do not appear to differ significantly. As indicated in Table 1, when  $E_{\text{red}}$  and  $E_{\text{ox}}$  are measured in MeOH for  $FLH_2$  or  $FL^{2-}$  and  $EYH_2$  or  $EY^{2-}$ , very similar potentials are recorded. Accordingly, we will assume that  $E_{\text{red}}(EYH_2/EYH_2\bullet^-) = E_{\text{red}}(EY^{2-}/EY\bullet^3-)$  and  $E_{\text{ox}}(EYH_2\bullet^+/EYH_2) = E_{\text{ox}}(EY\bullet^-/EY^{2-})$  and that the same assumption holds for the other fluoresceins.

Yet, considering the differences between the ionic forms of the fluoresceins, it is unfortunate that a large number of reports do not specify whether the ionic or neutral dye was employed. Addressing this point, one study demonstrated that  $EYH_2$  was an effective photoredox catalyst only if base was added or if DMSO was used in place of MeCN, an effect attributed to the stronger basicity of DMSO.<sup>411</sup> When indicated in the original publications, we will specify which ionic form was used (i.e.,  $EYH_2$  or  $EY^{2-}$ ). However, when it has not been indicated, or when referring generally to either  $EYH_2$  or  $EY^{2-}$ , we will denote the photoredox catalyst generically using brackets (i.e.,  $[EY]$  refers to either  $EYH_2$  or  $EY^{2-}$ ).

Concerning the electron transfer properties of fluoresceins, the singlet  $^1FL^{2-*}$  is both a moderate oxidant and a strong reductant and the triplet excited state  $^3FL^{2-*}$ , while formed with low efficiency, maintains oxidizing and reducing character. Yet fluorescein finds relatively limited use in photoredox catalysis. In contrast, eosin Y, erythrosine ( $[ERT]$ ), and rose bengal undergo fast ISC<sup>412,413</sup> and  $\phi_{\text{ISC}}$  increases across this series<sup>77</sup> with the degree of halogenation, a trend attributed to the heavy atom effect.<sup>112</sup> These higher  $\phi_{\text{ISC}}$  values correspond to very brief ( $\sim 0.5$ – $2.7$  ns) singlet lifetimes, and accordingly, the triplet state is typically considered to be the most relevant excited state in photoredox reactions, which can likewise act both as a moderate oxidant and reductant in the  $^3[EY]*$ ,  $^3[ERT]*$ , or  $^3[RB]*$  state. Halogen substitution also shifts the absorption and emission wavelengths to lower energies and has subtle effects on redox potentials.<sup>90</sup> The excited (triplet) state reduction potentials of these three are approximately equal ( $\sim 0.85$  V), while the excited state oxidation potentials show that  $^3[RB]*$  is roughly 0.2 V less reducing than  $^3[EY]*$  or  $^3[ERT]*$ . Interestingly, eosin Y<sup>414</sup> and rose bengal<sup>94,415</sup> are known to undergo ionization by self-quenching ET between ground state and excited state. In this way, oxidized ( $[EY]\bullet^+$  or  $[RB]\bullet^+$ ) and reduced portions ( $[EY]\bullet^-$  or  $[RB]\bullet^-$ ) can build up in the absence of external redox equivalents. It is surprising that this behavior is seldom considered in mechanistic hypotheses on photoredox transformations employing these catalysts.

An additional consequence of relatively high triplet state yields and energies is that the halogenated fluoresceins are prone to triplet energy transfer pathways, including the generation of singlet oxygen,<sup>416,417</sup> which has been a primary application of these molecules prior to their recent application in reactions relying on PET.<sup>418,419</sup> Interestingly, electron transfer appears compete with  $^1O_2$  sensitization in the presence of electron donors,<sup>420</sup> and oxygenation reactions are often proposed to result from  $O_2\bullet^-$  as an intermediate, which can be generated by either PET to  $O_2\bullet^-$  or ground state ET to  $O_2$  from the reduced  $[EY]\bullet^-$  or  $[RB]\bullet^-$ .

## 9.2. Fluorescein-Based Photoredox Catalysts: Reactions

Although Hari and König reviewed the topic of eosin Y in synthesis recently,<sup>16</sup> many new methods using this and other fluorescein-based catalysts have been subsequently reported. Moreover, in our survey of eosin Y, rose bengal, and fluorescein, we include these more recent examples along with much earlier photoredox catalytic reactions of xanthenes.

Of the organic photoredox catalysts covered in this review, this class is most analogous to the photoredox activity of transition metal complexes. The ground state excited state redox potentials of  $[EY]$ ,  $[RB]$ , and  $[FL]$  are similar to their transition metal counterparts, which gives rise to many similarities in the reactions these species are able to catalyze. This is to say that many of the methods reviewed in this section have a transition metal photoredox catalyzed equivalent; however, we highlight examples where the organic photoredox catalyst and transition metal catalysts are not interchangeable.

### 9.2.1. Oxidation and Oxygenation Reactions.

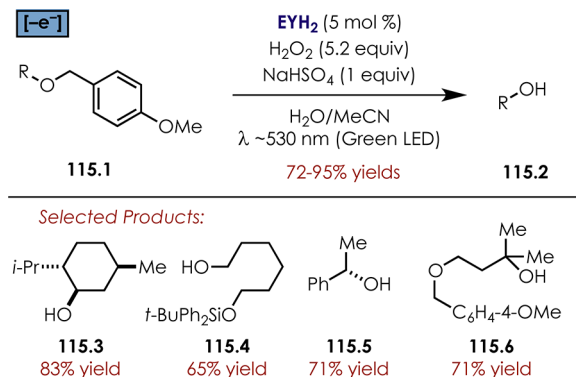
**9.2.1.1. Benzylic Oxidation.** Eosin Y was also used in the conversion of benzylic bromides **114.1** to benzaldehydes **114.3** in a formal Kornblum Oxidation<sup>422,423</sup> (Scheme 114).<sup>424</sup> In an

Scheme 114. Oxidation of Benzylic Bromides to Alcohols and Aldehydes

$[e^-]$	reagents	$\text{Ar}-\text{CH}_2\text{Br}$	r.t.	$\text{Ar}-\text{CH}_2\text{OH}$	reagents	$80^\circ\text{C}$	$\text{Ar}-\text{CHO}$	<b>114.3</b>	Ar	% yield <b>114.3</b>								
<b>114.1</b>		<b>114.2</b>		<b>114.3</b>														
reagents: $[EY]$ (5 mol %) <sup>a</sup> DMSO, Air $\lambda = 24\text{W CFL}$																		
<sup>a</sup> $[EY]$ form not specified																		
Ph 51 4-Cl-Ph 37 4-MeO-Ph 31 4-i-Pr-Ph 40 2-NO <sub>2</sub> -Ph 67																		

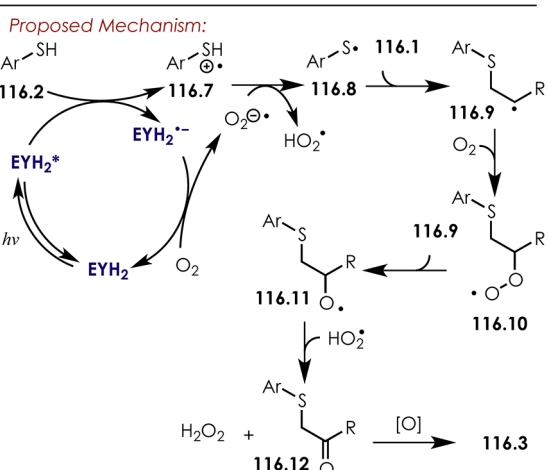
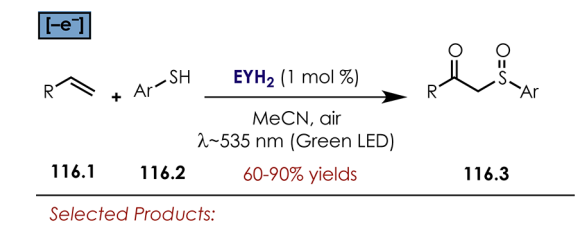
initial survey of reaction conditions, the alcohol (**114.2**) was returned in high yield with a small amount of the corresponding aldehyde at ambient conditions. The alcohols could be isolated, but simply heating the reaction mixture to  $80^\circ\text{C}$  after conversion of bromide **114.1** was complete afforded moderate to good yields of various benzaldehydes (**114.3**) and heteroarene-aldehydes. In contrast to a prior report<sup>425</sup> in which  $\text{Ru}(\text{bpy})_3^{2+}$  was used as a photoredox catalyst for a similar transformation of benzylic chlorides and bromides, benzyl chloride was not a successful substrate in this system. DMSO and  $\text{O}_2$  were found to be crucial to the success of the transformation, but a reaction mechanism was not proposed.

Eosin Y was found to be useful in a catalytic removal of the *p*-methoxybenzyl (PMB) ether protecting group (Scheme 115).<sup>426</sup> This oxidative benzylic cleavage employs  $\text{H}_2\text{O}_2$  as a stoichiometric oxidant, and the method was found to be orthogonal to a number of other protecting groups, including silyl ethers (e.g., **115.4**), pivalate, and Fmoc. Additionally, a substrate with both PMB ether and benzyl ether groups showed exclusive selectivity for the removal of the PMB ether (**115.5**). Furthermore, enantiomerically pure substrates containing sensitive chiral centers gave no evidence of stereochemical erosion in the products (**115.3**). The mechanism for this transformation likely involves oxidation of the PMB group to the cation radical (Scheme 77), followed by deprotonation and subsequent oxidation processes resulting in the cleavage of the C–O bond.

**Scheme 115.** Removal of PMB Ether Protecting Group

It is unclear from the report whether  $\text{H}_2\text{O}_2$  can turn over the reduced photoredox catalyst directly.

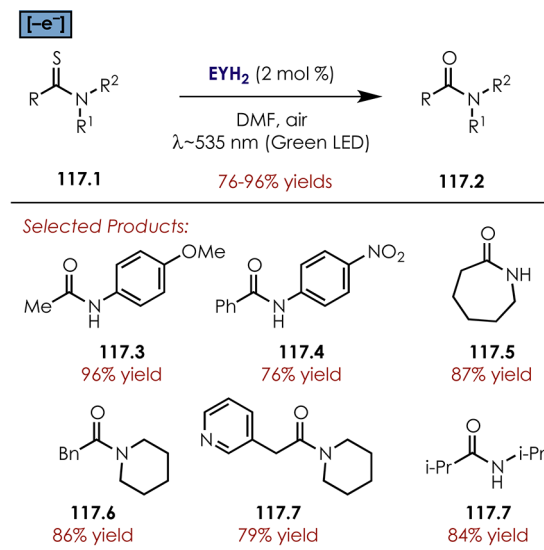
**9.2.1.2. Oxidation Reactions at Sulfur.** A photoredox catalytic method employing  $\text{EYH}_2$  accomplished the synthesis of  $\beta$ -keto sulfoxides **116.3** from alkenes **116.1** and thiols **116.2** under aerobic conditions (Scheme 116).<sup>427</sup> The protocol worked

**Scheme 116.** Synthesis of  $\beta$ -keto Sulfoxides

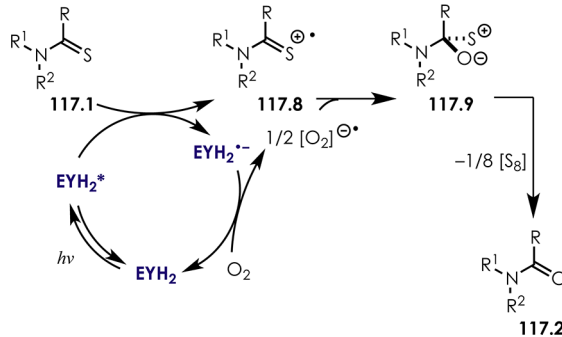
well with both styrenyl and aliphatic alkene substrates and seemed largely independent of alkene electronics, while the thiol scope was limited to aryl thiols. This requirement is consistent with the proposed mechanism, which involves a thiol–ene type reactivity initiated by oxidation of the aryl thiol **116.2** and deprotonation to give thiyl radical **116.8**. Addition to the alkene gives radical **116.9**, which is trapped by  $\text{O}_2$  and forms peroxy radical **116.10**. Ultimately,  $\beta$ -keto sulfide **116.12** is generated,

along with  $\text{H}_2\text{O}_2$ , which is expected to oxidize the sulfide to the observed  $\beta$ -keto sulfoxide product **116.3**. The authors did not remark on the possibility that any of these radical intermediates might initiate a new thiol–ene chain by H atom abstraction from thiol **116.2**. Moreover, the limitation of relatively electron-rich aryl thiols may be related to the fact that alkyl thiols are less easily oxidized.

In an earlier contribution which likewise employs  $\text{EYH}_2$  under aerobic contributions, Yadav and co-workers detailed the conversion of thioamides **117.1** to amides **117.2** by photoredox catalysis (Scheme 117).<sup>428</sup> This simple transformation proceeds

**Scheme 117.** Photoredox Catalytic Conversion of Thioamides to Amides

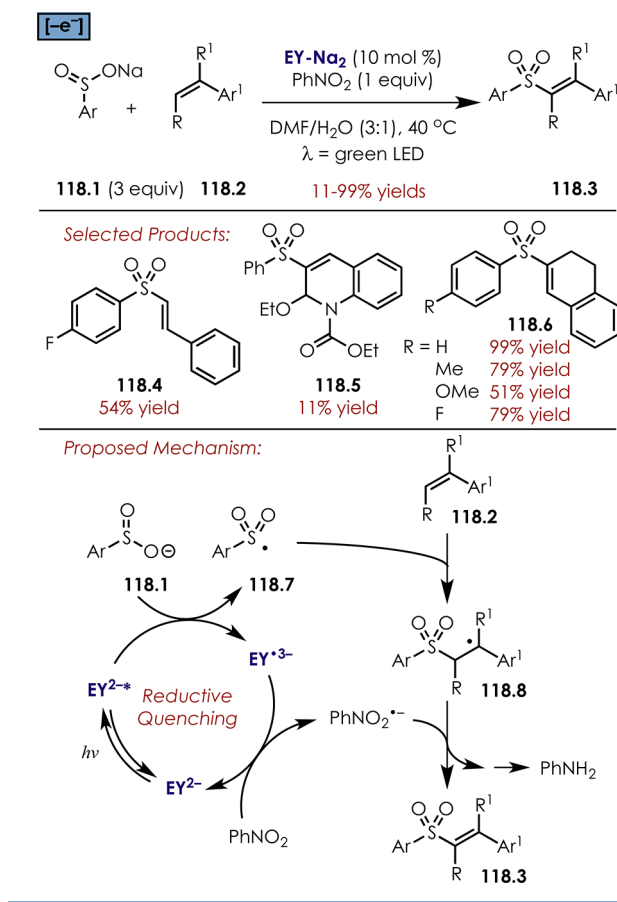
Proposed Mechanism:



in good to excellent yields for substrates containing alkyl or aryl substituents at R, R', or R''. Interestingly, the authors note that elemental sulfur ( $\text{S}_8$ ) is the only measurable by-product of the reaction (although  $\text{H}_2\text{O}_2$  was evidently detected during the course of reaction), prompting the proposed mechanism shown in Scheme 117, which proceeds by superoxide addition to thione cation radical **117.8**. Zwitterion **117.9** is suggested as an eventual intermediate, from which elimination of  $\text{S}_8$  produces the amide product **117.2**.

Like thiyl radicals, sulfinyl radicals can also add to alkenes, and König took advantage of this reactivity in the coupling of aryl sulfinate **118.1** with alkenes **118.2** to give vinyl sulfones **118.3** (Scheme 118).<sup>429</sup> This photoredox catalyzed process is possible with  $\text{Ru}(\text{bpy})_3^{+}$  or  $\text{Ir}(\text{ppy})_2(\text{dtb-bpy})^{+}$ , but eosin Y ( $\text{EY-Na}_2$ , 10 mol %) gave a slightly better yield. This net oxidative

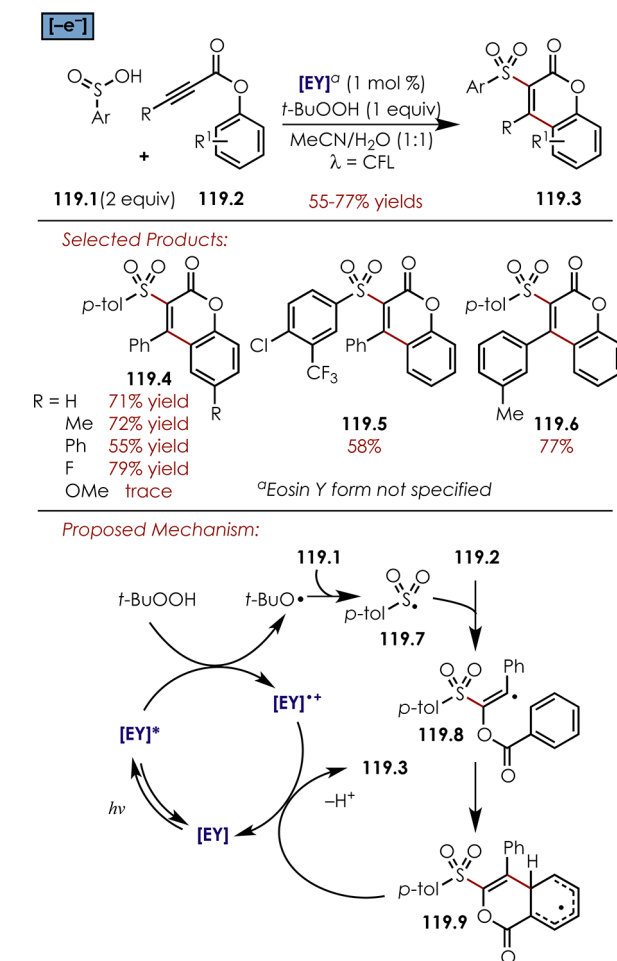
**Scheme 118.** Vinyl C–H Sulfenylation via PET-Generated Sulfinyl Radicals



transformation employed nitrobenzene ( $\text{PhNO}_2$ ) as a terminal oxidant. While the use of  $\text{PhNO}_2$  as an oxidizing equivalent is uncommon, its ability to accept electrons in a photoredox catalytic cycle is nonetheless preceded (see Scheme 146 below).<sup>430,431</sup> A wide range of yields (see 118.4–118.6) were reported for the coupling of various sodium arylsulfonates 118.1 and styrenyl substrates 118.2, but excellent yields could be obtained in some cases (up to 99%). The mechanism shown in Scheme 118 is one of two possible PET modes considered and proceeds by reductive quenching of the excited state  $EY^{2+}\bullet$  by the anionic sulfinate, which is oxidized to sulfinyl radical 118.7. This mechanism is tenable based on the oxidation potential for sulfinate 118.1 [ $E_{\text{ox}}$  (118.1<sup>-</sup>/118.1<sup>•</sup>) = +0.37 V vs SCE]. However, an alternative oxidative quenching cycle involving  $EY^{2+}\bullet$  oxidation by  $\text{PhNO}_2$  and subsequent sulfinate 118.1 oxidation by  $EY\bullet^-$  was also deemed possible. In the reductive quenching cycle,  $EY^{2+}\bullet$  is regenerated by  $EY\bullet^-$  reduction of  $\text{PhNO}_2$ . By either PET mechanism, the vinyl sulfone products 118.3 were thought to result from HAT by the reduced nitroarene  $\text{PhNO}_2\bullet^-$  and benzylic radical 118.8 formed by radical addition of the sulfinyl radical 118.7 to the alkene.

Another report showed that arylsulfinyl radicals generated from sulfinic acids 119.1 could be added to alkynes 119.2 (Scheme 119),<sup>432</sup> with the presumed vinyl radical intermediates 119.8 proceeding in a cyclization onto a pendant arene. Oxidative aromatization ultimately leads to the coumarin products 119.3, which were provided in generally good yields. The authors proposed initiation of this sequence by formation of  $t\text{-BuO}\bullet$  through oxidative quenching of  $[EY]^*$ , followed by HAT

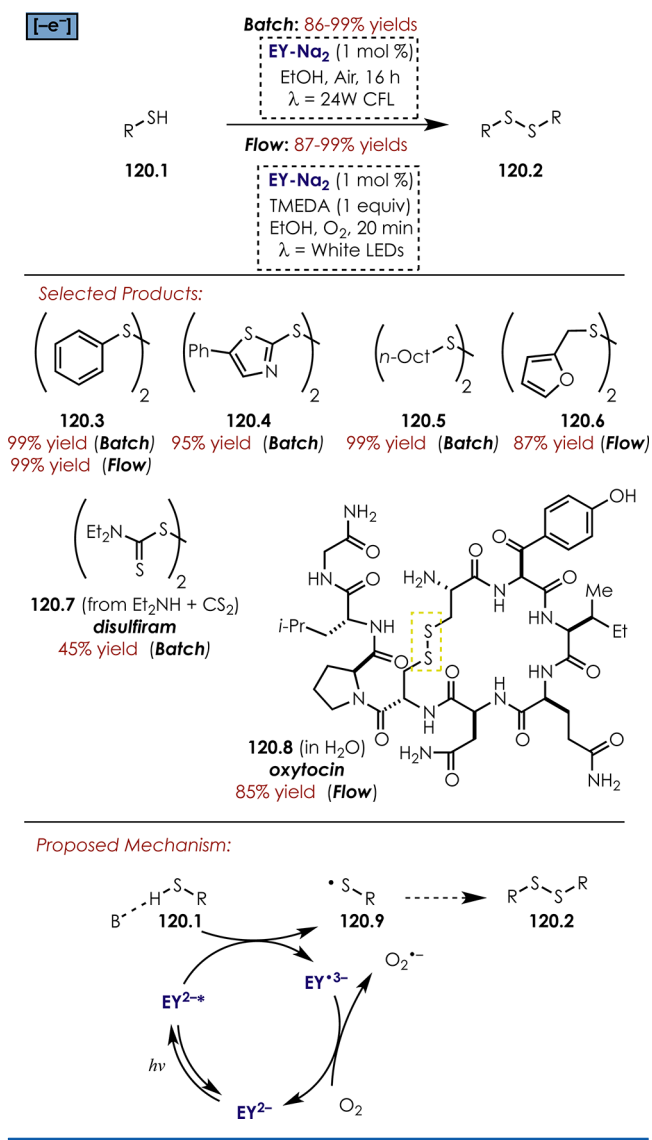
**Scheme 119.** Coumarin Synthesis by Sulfinyl Radical Addition/Cyclization



with sulfinic acid 119.1. Turnover of the catalyst might be accomplished by oxidation of a cyclohexadienyl radical intermediate 119.9.

Aerobic oxidation of thiols is among the most common strategies for the preparation of symmetrical disulfides and is often accomplished with the assistance of metal catalysts,<sup>433</sup> which can present difficulties in purification of disulfides intended for use as pharmaceuticals. Offering a metal-free alternative, the Noël group recently developed a photoredox catalyzed aerobic coupling of thiols to disulfides using eosin Y as a catalyst (Scheme 120).<sup>91</sup> Batch irradiation gave high yields under an atmosphere of air of disulfides 120.2 from electronically diverse thiols 120.1, including alkyl and heteroaryl thiols. The batch conditions were also amenable to the synthesis of the drug Disulfiram 120.7, which could be prepared in a one pot procedure from diethylamine and carbon disulfide which form the dithiocarbamic acid in solution en route to the coupled product. The implementation of a flow reactor setup was enabled through the use of a mass flow controller (MFC) to introduce oxygen into solution. With 1 eq tetramethyl ethylenediamine (TMEDA), the flow conditions gave near quantitative yields of disulfides with only 20 min residence time. Remarkably, the disulfide bridged peptide hormone oxytocin (120.8) could be produced from its precursor peptide after only 200 seconds in the flow reactor. While  $\text{Ru}(\text{bpy})_3^{2+}$  was a poor catalyst for the transformation in the absence of base, its activity was comparable to  $EY^{2+}$  when base was added. This prompted the investigators

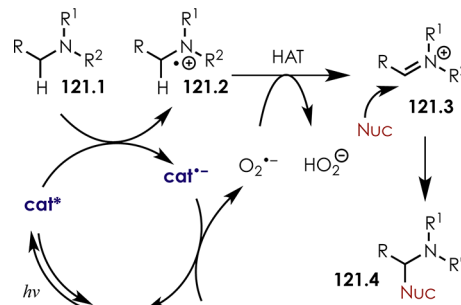
**Scheme 120. Aerobic Oxidative Coupling of Thiols to Disulfides in Flow**



to postulate that a proton-coupled electron transfer (PCET) was operable in the oxidation of the thiol **120.1** to thiyl radical **120.9**. The dianionic  $\text{EY}^{2-}$  was thought to be capable of catalysis in the absence of external base by virtue of its intrinsic basicity. Moreover, that alkyl disulfides could be generated in this way may be enabled by the PCET mechanism, as alkyl thiols are otherwise difficult to oxidize. The photoredox catalytic cycle could be turned over by oxidation of  $\text{EY}^{\bullet 3-}$  by  $\text{O}_2$ . Superoxide generated in this way might be expected to generate another equivalent of thiyl radical **120.9**.

**9.2.2. Dehydrogenative Couplings.** Among the most extensively explored reaction types in organic photoredox catalysis are the dehydrogenative couplings of nucleophiles and tertiary alkyl amines. These reactions are mechanistically related through iminium **121.3** (Scheme 121), which is generated by oxidation of tertiary amine **121.1** to the amine cation radical **121.2** and subsequent oxidation processes in a net loss of two electrons and one proton (see discussion above: Scheme 41). Under aerobic conditions,  $\text{O}_2^{\bullet -}$  is often assumed to be involved in the “HAT” step.

**Scheme 121. Common Mechanism Proposed for Aerobic Dehydrogenative Couplings between Alkylamines and Nucleophiles**



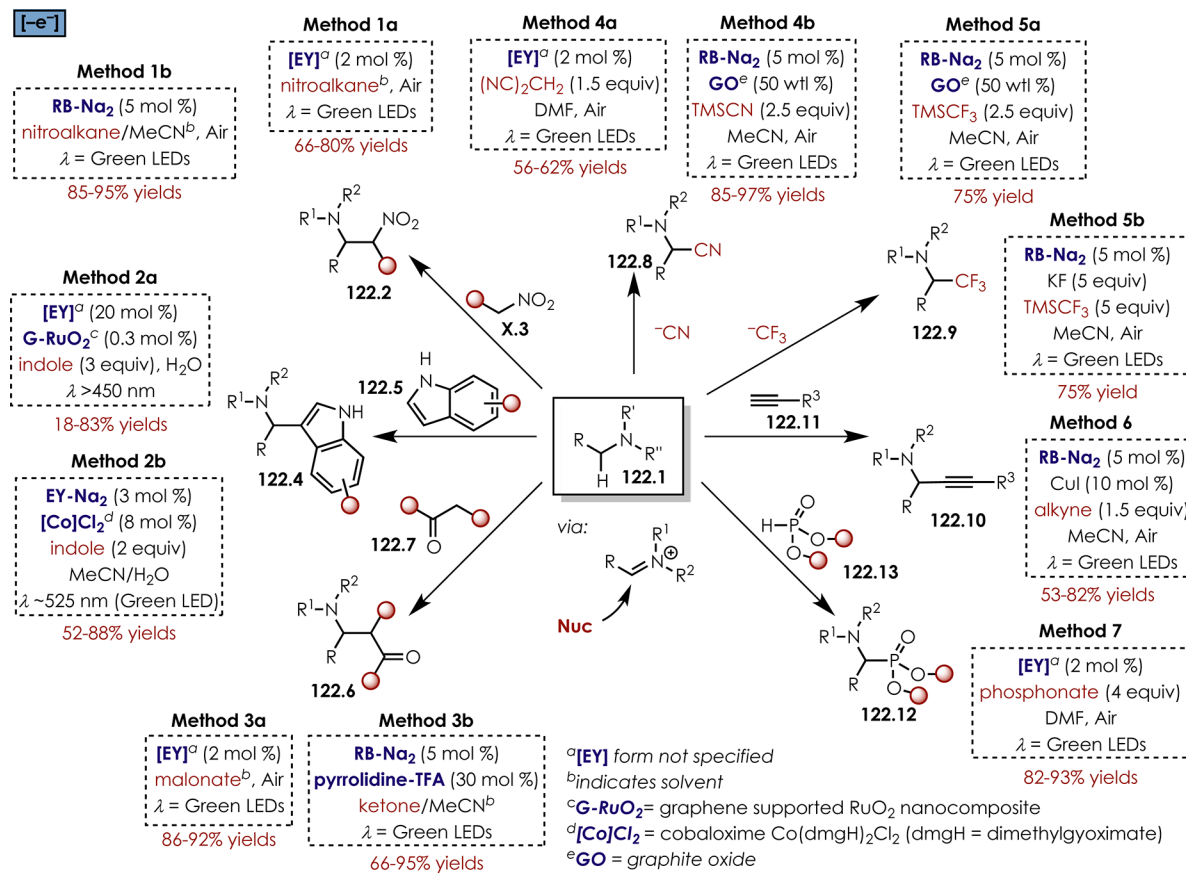
A number of reactions between nucleophiles and iminiums **121.3** are enabled by photoredox catalysis. To this end, eosin Y and rose bengal were shown to be competent visible-light-absorbing photoredox catalysts for an array of dehydrogenative couplings (Scheme 122), with a majority of these reactions featuring tetrahydroisoquinolines as model substrates. The analogy between the xanthene dyes and ruthenium(II) and iridium(III) photoredox catalysts is especially apparent when considering these examples (cf. ref.<sup>1</sup>).

Carbon–carbon bond formation in this manifold is exemplified by the aza-Henry<sup>434</sup> reaction catalyzed by either eosin Y<sup>420,435</sup> or rose bengal<sup>436</sup> (Scheme 122 and Scheme 123, methods 1a and 1b). The reaction catalyzed by eosin Y (method 1a) was first reported by König and co-workers, who developed conditions for the coupling of *N*-aryltetrahydroisoquinolines with nitroalkanes **122.3**, and good yields could be obtained under aerobic conditions.<sup>435</sup> A cursory evaluation of substrates showed that substitution of the *N*-aryl group did not impact yields, while nitro-*n*-propane gave a slightly lower yield and dialkyl-anilines proved poor substrates (products **123.4** and **123.5**). The use of rose bengal under a similar set of conditions (method 1b) was reported shortly after by Tan and co-workers.<sup>436</sup> A direct comparison between methods 1a and 1b shows some improved performance with  $\text{RB}^{2-}$ , particularly in the capacity of this system to engage dialkylanilines in the coupling, albeit in a fair yield (e.g., product **123.4**).

Indoles **122.5** were also found to be competent nucleophiles in the dehydrogenative couplings reported by Wu and co-workers (Scheme 122 and Scheme 123, methods 2a and 2b).<sup>437,438</sup> Unlike the other “dehydrogenative” couplings discussed in this section, these systems are truly dehydrogenative in the sense that they employ a co-catalyst which couples the oxidative activation of the amine  $\alpha$ -C–H bond to evolution of  $\text{H}_2$  (as in Scheme 82), obviating the need for an external oxidant. A first generation system utilized  $\text{EY-Na}_2$  along with a graphene-supported  $\text{RuO}_2$  nanocomposite (G- $\text{RuO}_2$ , Scheme 124) as a hydrogen evolution catalyst (method 2a),<sup>437</sup> producing the coupled indoles **123.6**–**123.6** in generally good yields, the most noticeable trend being that electron deficient indoles were poor substrates. A subsequent report showed that a cobaloxime (cobaloxime 2, Scheme 124) could be employed as a co-catalyst (method 2b), providing an improvement in the yield of many substrates and a noble-metal free system.

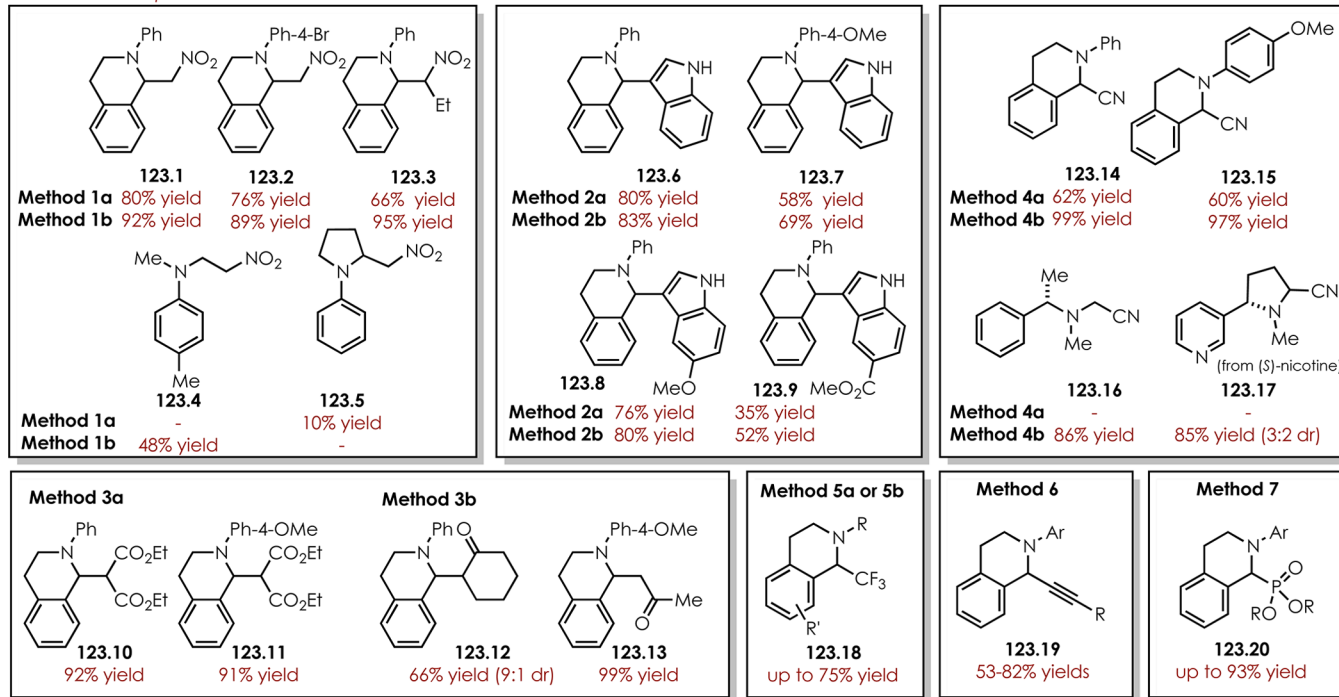
Under very similar conditions employed in the aza-Henry reaction, König demonstrated that Mannich reactions were also practicable (Scheme 122 and Scheme 123, method 3a),<sup>435</sup> although malonates were the only nucleophiles explored and

Scheme 122. Deydrogenative Couplings of Tetrahydroisoquinolines



Scheme 123. Deydrogenative Couplings of Tetrahydroisoquinolines

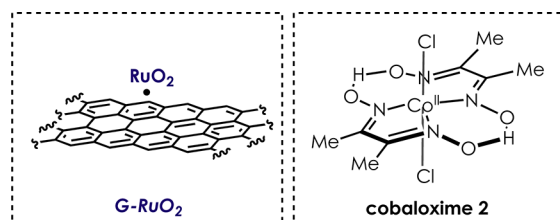
Selected Examples:



were used as the reaction solvent. The method reported by Tan (method 3b) featured the cooperative use of rose bengal and pyrrolidine as an organocatalyst to catalytically generate an

enamine nucleophile (Scheme 122 and Scheme 123).<sup>436</sup> This advance enabled ketones to be employed as coupling partners and portends the possibility of an enantioselective coupling,

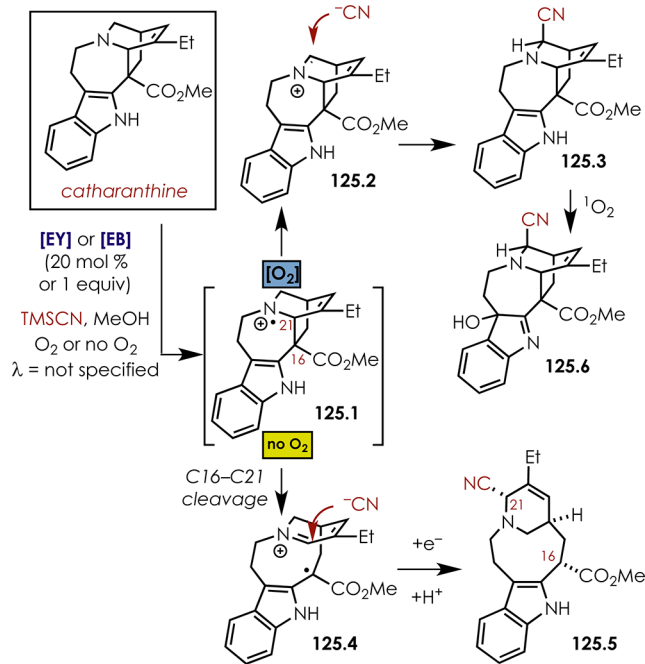
**Scheme 124. Hydrogen Evolution Catalysts Used in Dehydrogenative Couplings of Indoles**



although initial attempts with a proline-derived organocatalyst showed a maximum e.e. of 15%.

Addition of cyanide ( $\text{^-\text{CN}}$ ) to photoredox-generated iminiums was demonstrated by Sundberg in 1991 in the cyanation of the vinca alkaloid catharanthine (Scheme 125).<sup>439</sup>

**Scheme 125. Cyanation of Catharanthine**

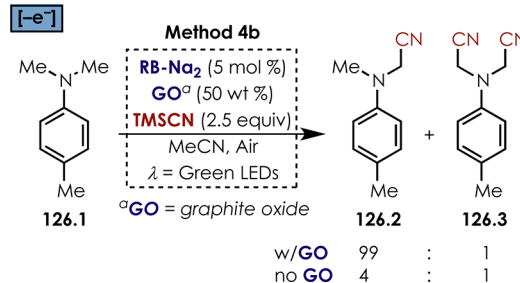


Using either eosin Y or eosin B [**EB**] (see Scheme 131) under aerobic conditions, a mixture of nitrile products was obtained, including **125.3** and **125.6**, the latter resulting from  ${}^1\text{O}_2$  oxygenation of **125.3**. Exclusive selectivity for **125.6** was observed when using a full equivalent of [**EY**] under  $\text{O}_2$ . When  $\text{O}_2$  was excluded, iminium **125.4** was generated by fragmentation of the C16–C21 bond, leading to **125.5** exclusively with a 1 eq. of [**EB**].

Interestingly, a photoredox-catalyzed synthesis of benzoniitrides **122.8** was discovered by König when attempting to extend this reaction manifold to the coupling of malonitrile ( $\text{CN})_2\text{CH}_2$  but formally constitutes the addition of cyanide ( $\text{^-\text{CN}}$ ) to an iminium (Scheme 122 and Scheme 123, method 4a).<sup>435</sup> Moderate yields were obtained (e.g., **123.4** and **123.5**), but the use malonitrile is a welcome substitute for toxic cyanide reagents. Initial optimization studies by Tan using **RB-Na<sub>2</sub>** and **TMSCN** as a source of  $\text{^-\text{CN}}$  showed that product **123.15** (Scheme 123) could be produced in 60% yield.<sup>440</sup> Curiously, when the same reaction is performed with 50 wt % graphene oxide (**GO**), the yield is improved to 97%, whereas graphite or activated carbon

lead to no such improvement (Scheme 122, method 4b). For other *N*-aryl tetrahydroisoquinolines, **GO** consistently gives at least 30% better yields than when the reactions are run in its absence. Moreover, dimethylaniline **126.1** undergoes the cyanation reaction in 87% with >99:1 selectivity for the mono-nitrile **126.2** with **GO** as an additive (Scheme 126), while a 4:1

**Scheme 126. Oxidative Cyanation of Dimethylanilines**



mixture of the mono- and bis-nitrile **126.3** is observed when **GO** is omitted. **GO** does not catalyze the reaction under irradiation in the absence of **RB-Na<sub>2</sub>**, and the role of this co-catalyst is not yet understood.

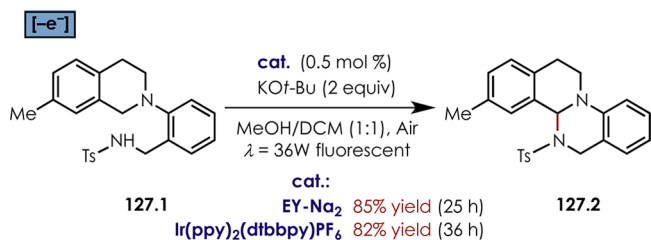
The utility of this methodology is highlighted in the synthesis of enantiomerically pure compounds **123.16** and **123.17** (Scheme 123), the latter synthesized from (*S*)-nicotine in excellent selectivity for activation of the secondary C–H bond. Using similar conditions, the authors also showed that “ $\text{^-\text{CF}}_3$ ” could be added to the photoredox-generated iminium using trifluorotrimethylsilane **TMSCF<sub>3</sub>** (Scheme 122 and Scheme 123, method 5a).<sup>440</sup> In a subsequent report, this transformation was optimized in the absence of **GO** with potassium fluoride (**KF**) as an additive, and the  $\alpha$ -trifluoromethylation of various *N*-arylisouquinolines proceeded in moderate yields (Scheme 122 and Scheme 123, method 5b).<sup>441</sup> In the same investigation, the use of catalytic copper iodide (**CuI**) was found to activate terminal alkynes toward  $\alpha$ -alkynylation of *N*-arylisouquinolines to give alkynes **123.19** (Scheme 122 and Scheme 123, method 6).<sup>441</sup>

In addition to the coupling of tetrahydroisoquinolines with carbon nucleophiles, König showed that carbon-phosphorous bonds could be forged if dialkylphosphites **122.13** were used as nucleophiles (Scheme 122 and Scheme 123, method 7).<sup>435</sup> The  $\alpha$ -amino phosphonates **123.20** were obtained in excellent yields.

Finally, a study detailing the use of  $\text{Ir}(\text{ppy})_2(\text{dtbbpy})^+$  in intramolecular cyclizations of nitrogen nucleophile-bearing tetrahydroquinolines such as **127.1** (Scheme 127) also showed that eosin Y could replace the expensive iridium photoredox catalyst with an equivalent outcome.<sup>442</sup>

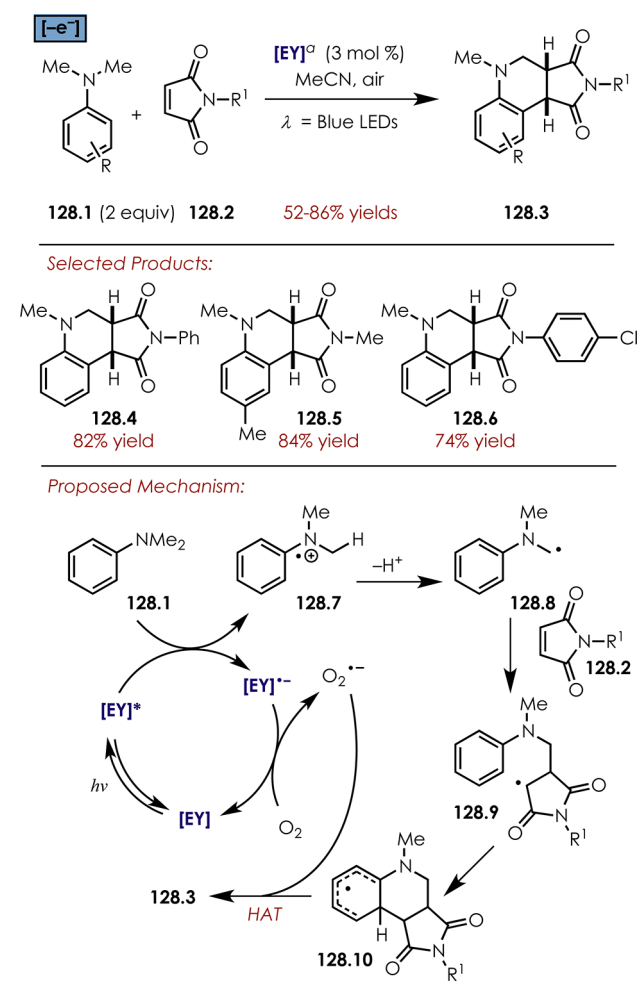
### 9.2.3. Oxidative Transformations in the Synthesis of Heterocycles. In addition to the 2 electron/1 proton oxidation

**Scheme 127. Intramolecular Dehydrogenative Coupling**



of alkylamines to iminium electrophiles, electron-rich  $\alpha$ -amino radicals can also be harnessed in radical addition reactions, as described above (Scheme 43). Although eosin Y gave inferior results compared to an iridium-based photoredox catalyst in one radical conjugate addition reaction,<sup>443</sup> a recent report demonstrated that  $\alpha$ -amino radicals can initiate a radical cascade with maleimides **128.2** which ultimately results in the cyclization to a 6-membered ring **128.3** (Scheme 128),<sup>444</sup> yielding similar

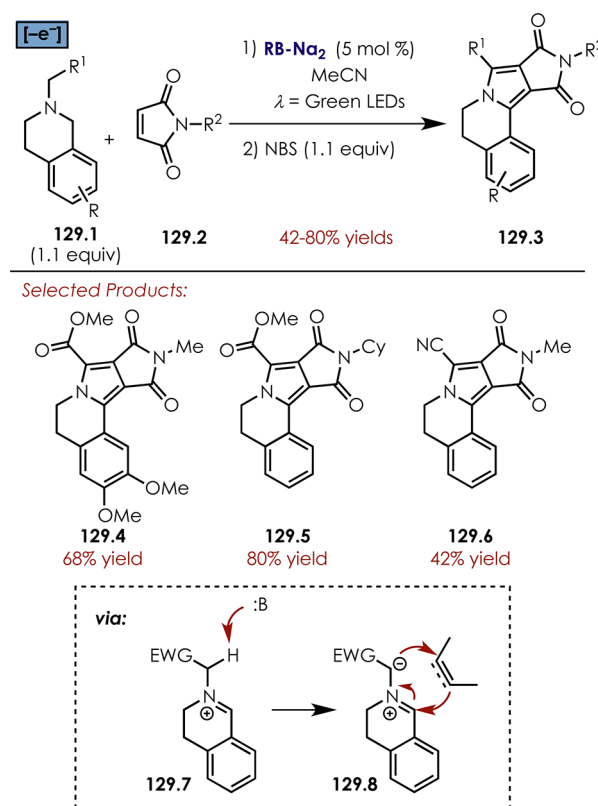
Scheme 128. Eosin Y-Catalyzed Povarov Reaction



products as in a Povarov reaction.<sup>445</sup> Under the aerobic conditions with eosin Y as the catalyst, good yields of tetrahydroquinolines **128.3** were realized when dimethylanilines **128.1** were reacted with several differently substituted *N*-aryl or *N*-methyl maleimides **128.2**. The mechanism was understood to proceed through the radical cascade shown in Scheme 128, eventually forming cyclohexadienyl radical **128.10**. The product forming step is oxidative aromatization enabled by the ability of  $O_2\bullet^-$  to abstract an H atom. As noted previously, alternative mechanisms for aromatization from cyclohexadienyl radicals are preceded.<sup>356–358</sup>

Rueping and co-workers also employed maleimides in a cyclization reaction of tertiary alkylamines: pyrroloisoquinolines **129.3** could be synthesized from tetrahydroisoquinolines in a two-stage process (Scheme 129),<sup>446</sup> where the primary step was a rose bengal enabled [3+2] cycloaddition and the second step was the addition of NBS to give the dehydrogenated heteroaromatic products such as **129.4–129.6**. Prior reports

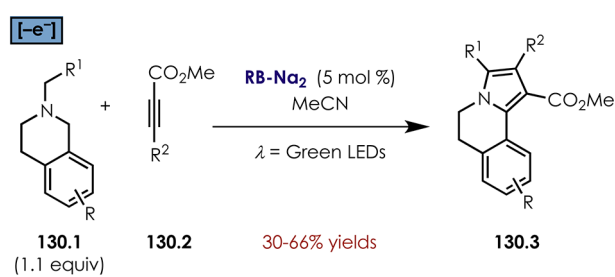
Scheme 129. Pyrroloisoquinoline Synthesis from Tetrahydroisoquinolines and Maleimides by Photoredox-Generated Azomethine Ylides



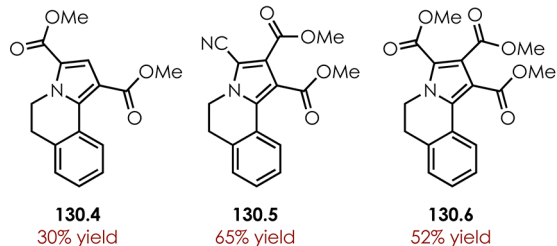
employing iridium and ruthenium photoredox catalysts to accomplish similar transformations suggest that the mechanism proceeds through an azomethine ylide **129.8** generated upon deprotonation of the iminium **129.7** formed through the aforementioned PET process.<sup>447–449</sup> When alkynes **130.2** are employed as dipolarophiles (Scheme 130), modest yields of pyrroloisoquinolines **130.3** are obtained (e.g., **130.4–130.6**), and these examples do not require an additional dehydrogenation step.

One recent report describes the use of hydrazines **131.2** as precursors of carbon-centered radicals by way of photoinduced oxidation processes (Scheme 131).<sup>450</sup> Oxidation of hydrazines has long been known to result in carbon-centered radicals,<sup>451,452</sup> and while diazonium salts are well-explored radical precursors in photoredox catalysis (see section 9.2.6), hydrazines offer an alternative to the more sensitive diazonium salts. It was demonstrated that a range of carbon-centered radicals (**131.9**) generated from hydrazines **131.2** could be captured by an biaryl isonitrile **131.1** and undergo a cascade cyclization/aromatization to form phenanthridines **131.3** under aerobic conditions using the disodium salt of eosin B ( $EB^{2-}$ ). Eosin B gave a significantly higher yield than eosin Y, rose bengal, and methylene blue for a number of irradiation sources (blue or green LED, white CFL), and the conditions were applied to the synthesis of a large number of phenanthridines **131.3**. An impressive range of carbon-centered radicals could be accessed, including aryl (**131.4**), heteroaryl (**131.5**), alkyl (**131.6**), and alkoxy carbonyl radicals (**131.7**). The proposed mechanism ultimately involved generation of radicals **131.9** from diazene cation radical **131.8** by sequential reductive quenching cycles  $EB^{2-}$ . Product formation was thought to occur by HAT from cyclohexadienyl radical

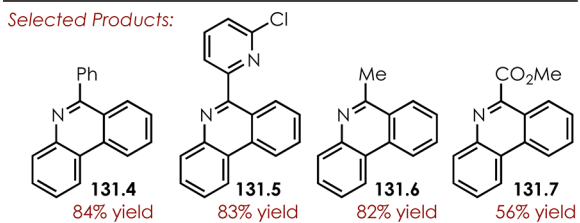
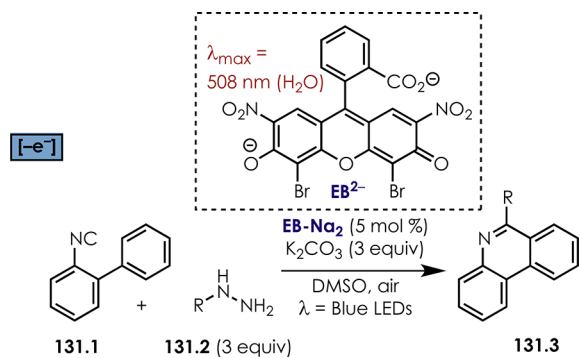
**Scheme 130.** Pyrroloisoquinoline Synthesis from Tetrahydroisoquinolines and Alkynes



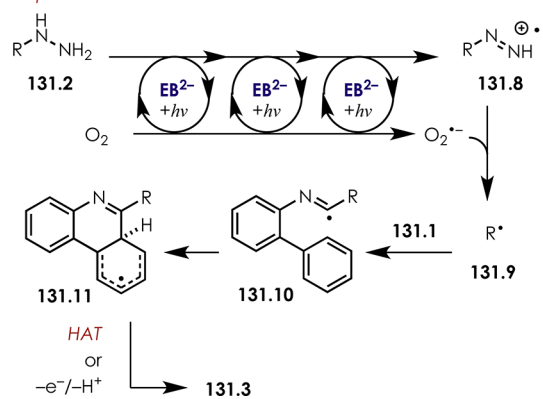
Selected Products:



**Scheme 131.** Synthesis of Phenanthridines by Photoredox Generation of Carbon-Centered Radicals from Hydrazines



Proposed Mechanism:



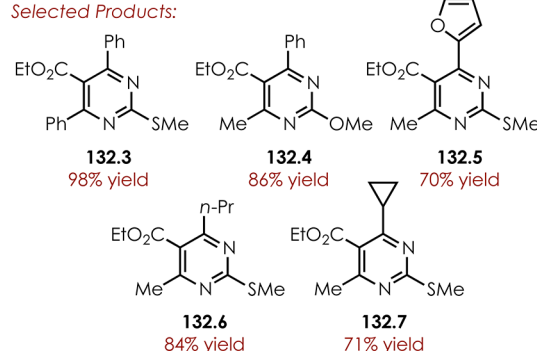
131.11 or by single electron oxidation of 131.11 followed by deprotonation.

Substituted pyrimidines could be accessed by aerobic aromatization of 1,4-dihydropyrimidines 132.1 (Scheme 132),<sup>453</sup> which are synthesized from simple starting materials

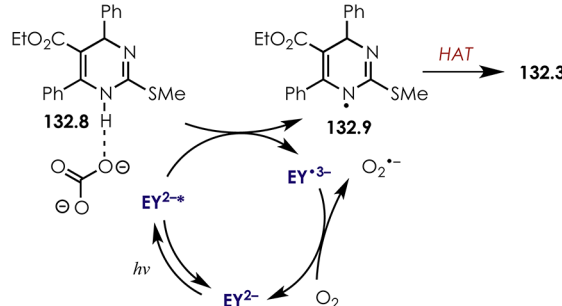
**Scheme 132.** Oxidative Dihydropyrimidine Aromatization



Selected Products:



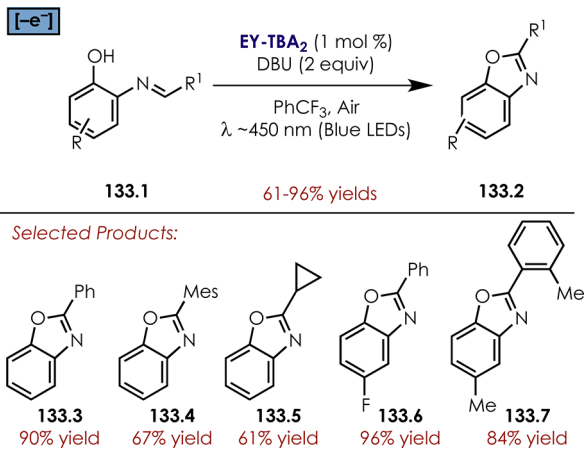
Proposed Mechanism:



through the multi-component Biginelli Reaction.<sup>454,455</sup> The protocol, which employed the bis(tetrabutylammonium salt) EY-TBA<sub>2</sub>, smoothly generates the densely substituted pyrimidines 132.2 (e.g., 132.3–132.7) in consistently high yields simply under an atmosphere of air. Several of the substrates contain functional groups that are reactive in the presence of <sup>1</sup>O<sub>2</sub>, (e.g. furan 132.5), which was considered as a possible intermediate. EPR experiments supported the conclusion that no <sup>1</sup>O<sub>2</sub> was produced when EY<sup>2-</sup> was irradiated in the presence of substrate 132.8 and K<sub>2</sub>CO<sub>3</sub>. On the other hand, transient absorption measurements showed that EY<sup>3-</sup> was generated upon photolysis in solution with 132.8 and K<sub>2</sub>CO<sub>3</sub>. Interestingly, K<sub>2</sub>CO<sub>3</sub> was found to lower the peak oxidation potential E<sub>ox</sub>(132.8•<sup>+</sup>/132.8) of 132.8 from 1.10 to 0.58 V vs NHE. From these observations, the authors inferred that the base-assisted photoinduced oxidation of 132.8 outcompetes generation of singlet oxygen by <sup>3</sup>EY<sup>2-</sup> (Scheme 132), and ground state EY<sup>2-</sup> is regenerated by reduction of O<sub>2</sub> to O<sub>2</sub>•<sup>-</sup>. Presumably, the final aromatization step involves HAT (possibly by O<sub>2</sub>•<sup>-</sup>) or sequential electron and proton transfers.

Insights obtained through development of the oxidative aromatization described in Scheme 132 prompted researchers to investigate an oxidative cyclization of 2-iminophenols 133.1 (Scheme 133).<sup>453</sup> Benzoxazoles (133.2) are often synthesized in

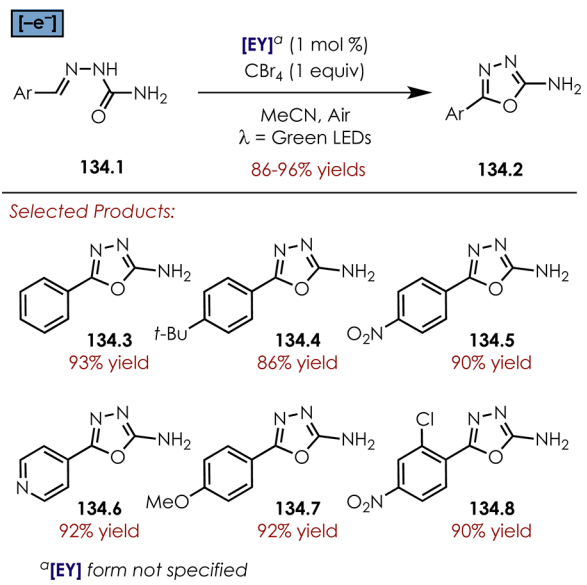
Scheme 133. Oxidative Cyclization of Iminophenols



this way, but strong oxidants or forcing conditions are usually required.<sup>456–459</sup> The aerobic conditions shown in Scheme 133 employ catalytic eosin Y ( $\text{EY-TBA}_2$ ) and offer a relatively mild preparation of an array of benzoxazoles such as 133.3–133.7. The substrate scope largely featured aryl imines; however, one example of a cyclopropyl imine (benzoxazole 133.5) demonstrated that the protocol may be more generally applicable.

Eosin Y was also shown to facilitate the oxidative cyclization of semicarbazones 134.1 to 1,3,4-oxadiazoles 134.2 (Scheme 134).<sup>460</sup>  $\text{CBr}_4$  and light were found to be essential components

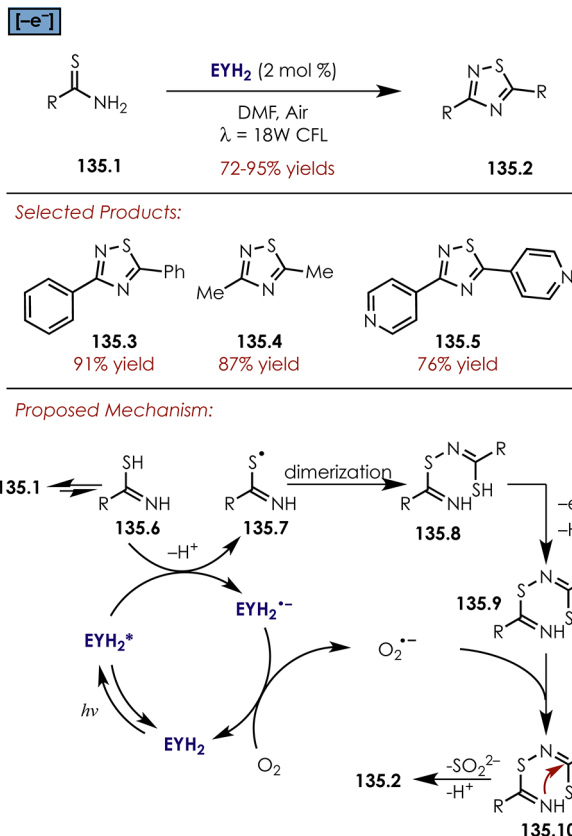
Scheme 134. Synthesis of 1,3,4-Oxadiazoles by Oxidative Cyclization of Semicarbazones



of the protocol, and although inclusion of catalytic eosin Y (1 mol %) led to the highest yields under an atmosphere of  $\text{O}_2$  or air, significant background reaction was observed (~30%) when the photoredox catalyst was omitted. The authors suggest that the catalyzed or uncatalyzed transformation proceeds through a hydrazone bromide formed by a radical bromination mechanism.

Synthesis of another class of heterocycle was enabled by the photoredox catalytic activity of eosin Y: 1,2,4-thiadiazoles 135.1 could be prepared from a single thioamide 135.1 starting material under aerobic conditions (Scheme 135).<sup>461</sup> This

Scheme 135. Cyclization of Thioamides to 1,2,4-Thiadiazoles

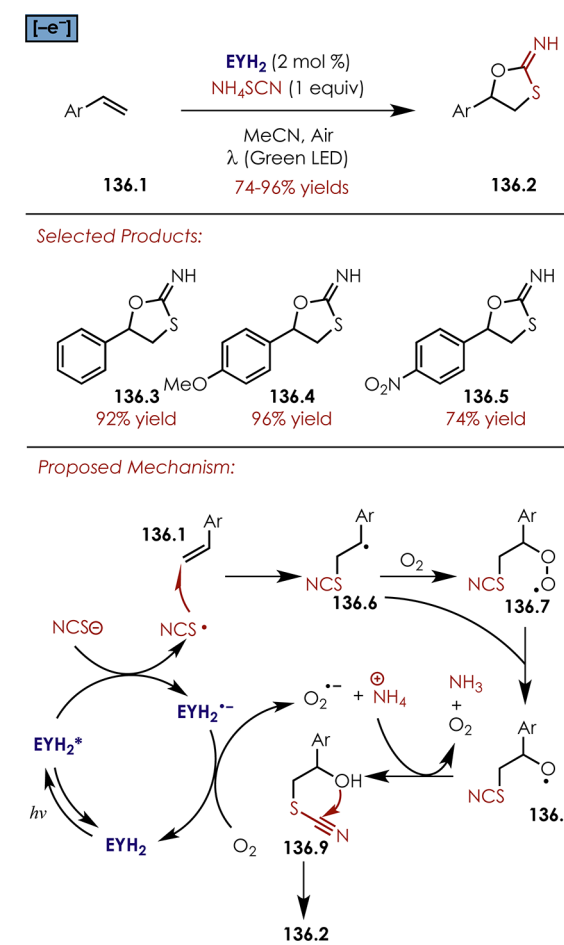


oxidative dimerization-cyclization provided the heterocyclic products such as 135.3–135.5 in excellent yields with symmetrical alkyl, aryl, or heteroaryl substitution. The authors proposed that a photoinduced oxidation of thioamide 135.1 (possibly as 135.6) by  ${}^3[\text{EY}]^*$  produces a thione-centered cation radical,<sup>274,373</sup> which is deprotonated, followed by dimerization of 135.7 to form the S–N bond. An additional round of oxidation and deprotonation affords thiyl radical 135.9, which is oxygenated under the aerobic conditions, possibly by superoxide. The ring closing step was said to involve loss of “ $\text{SO}_2^{2-}$ ” based on a previous suggestion in the literature.<sup>462</sup>

In addition to the reaction outlined in Scheme 140, the thiocyanate radical  $\text{SCN}\bullet$  generated by PET could be added to alkenes in the synthesis of 2-imino-1,3-oxathiolanes from styrenes 136.1 (Scheme 136).<sup>463</sup> rose bengal catalyzed the transformation in 72% yield, but eosin Y gave an even better performance (92% yield) under the aerobic conditions; a number of substituted styrenes were tested with this protocol. The radical addition of  $\text{SCN}\bullet$  with styrene is followed by trapping of benzylic radical 136.6 with  $\text{O}_2$ . The resulting peroxy radicals 136.7 are known to form dibenzyl peroxides which fragment to give the alkoxy radicals 136.8.<sup>337</sup> H atom abstraction from  $\text{HO}_2\bullet$  (formed by  $\text{NH}_4^+ + \text{O}_2\bullet^-$ ) furnishes benzylic alcohol 136.9, which undergoes cyclization with the tethered thiocyanate to arrive at the oxathiolane product 136.2.

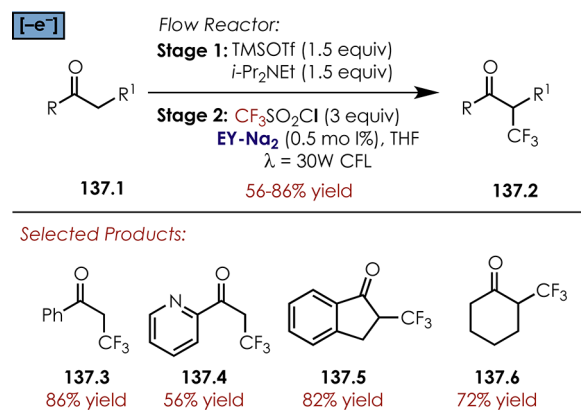
**9.2.4. Other Oxidative C–H Functionalization Reactions.** Recognizing the difficulty in synthesizing  $\alpha$ -trifluoromethyl carbonyl compounds by traditional enolate chemistry, MacMillan and co-workers presented a photoredox catalytic method for the  $\alpha$ -trifluoromethylation of aldehydes using  $\text{CF}_3\text{I}$ .<sup>464</sup> In an effort to develop a procedure that did not require the use of the gaseous reagent  $\text{CF}_3\text{I}$ , Kappe and Rincón and co-

**Scheme 136.** 2-Imino-1,3-Oxathiolanes by Difunctionalization of Styrenes



workers recognized that an in-situ generated silyl enol ether may be susceptible to addition by  $\bullet\text{CF}_3$  generated by the participation of a photoredox catalyst (Scheme 137).<sup>465</sup> Optimization

**Scheme 137.**  $\alpha$ -Trifluoromethylation of Ketones in Flow



reactions (in batch) showed that a two-step/one-pot afforded product 137.2 in ~80% yield when acetophenone was submitted to enolization conditions with TMSOTf and  $i\text{-Pr}_2\text{NEt}$ , along with EY-Na<sub>2</sub>, followed by addition of  $\text{CF}_3\text{SO}_2\text{Cl}$  then 15 min irradiation. In contrast, Ru(bpy)<sub>3</sub><sup>2+</sup> gave <5% yield under the same conditions. Having successfully identified conditions for the formation of the enol ether and for the photoredox step, flow

chemistry was successfully applied to this protocol (Figure 1), and  $\alpha$ -trifluoromethyl ketones (e.g. 137.3–137.6) were

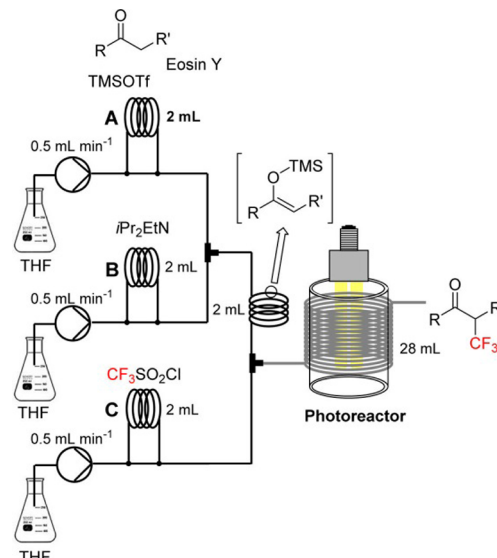
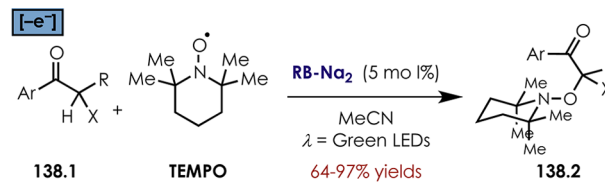


**Figure 1.** Reproduced from ref 464. Copyright 2009 American Chemical Society.

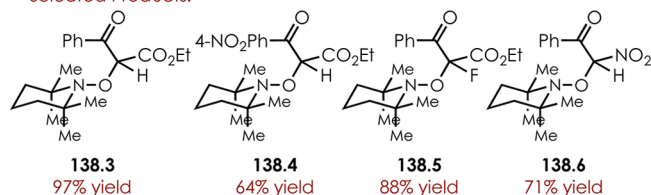
prepared in a highly efficient manner, requiring only 20 min for reaction completion. Interestingly, the authors note that, although EY-Na<sub>2</sub> is a dispersion in THF, dissolution is observed upon the addition of TMSOTf, possibly indicating silylation of the catalyst. Since EY-Na<sub>2</sub> does not negatively impact the enolization step, this change in solubility is crucial to the successful use of EY-Na<sub>2</sub> in the flow reaction. Whether silylation of [EY] is reversible or the silylated catalyst is photoredox active is unknown. Furthermore, the authors do not suggest a mechanism for the photoredox transformation, but the work of Nagib and MacMillan suggested that  $\bullet\text{CF}_3$  is generated by PET from an excited Ru(II)\* catalyst to  $\text{CF}_3\text{SO}_2\text{Cl}$  [ $E_{\text{red}}(\text{CF}_3\text{SO}_2\text{Cl}/\text{CF}_3\text{SO}_2\text{Cl}^-) = -0.18 \text{ V vs SCE}$ ].<sup>466</sup>

Rose bengal was used in the  $\alpha$ -oxyamination of arylketones, in which TEMPO was coupled with a number of arylketones 138.1 at the  $\alpha$ -position (Scheme 138).<sup>467</sup> The protocol was generally applicable to aryl  $\beta$ -ketoesters, and  $\alpha$ -substitution by nitro- and fluoro-groups were also tolerated. Aliphatic ketones were not compatible in this methodology, which prompted the researchers

**Scheme 138.**  $\alpha$ -Oxyamination of Arylketones



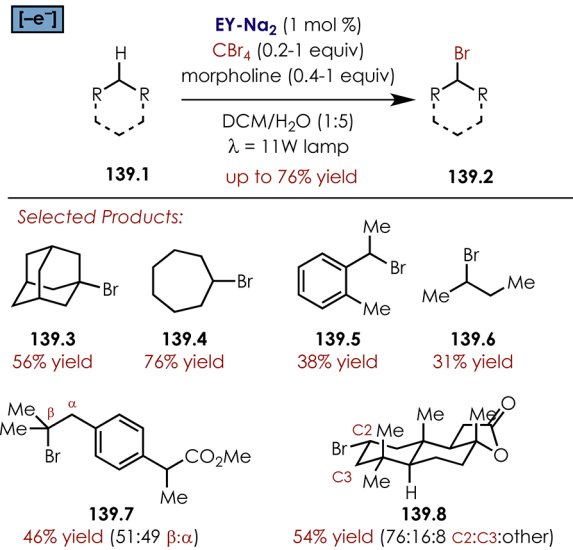
**Selected Products:**



to propose that single-electron reduction of the arylketone was a key mechanistic step; however, it is unclear how ketone reduction leads to the net oxidative outcome.

Functionalization of relatively inert  $sp^3$  C–H bonds was demonstrated in an aliphatic and benzylic bromination catalyzed by eosin Y and using  $CBr_4$  as the bromine source (Scheme 139).<sup>468</sup> Biphasic conditions (DCM/H<sub>2</sub>O, 1:5) were essential to

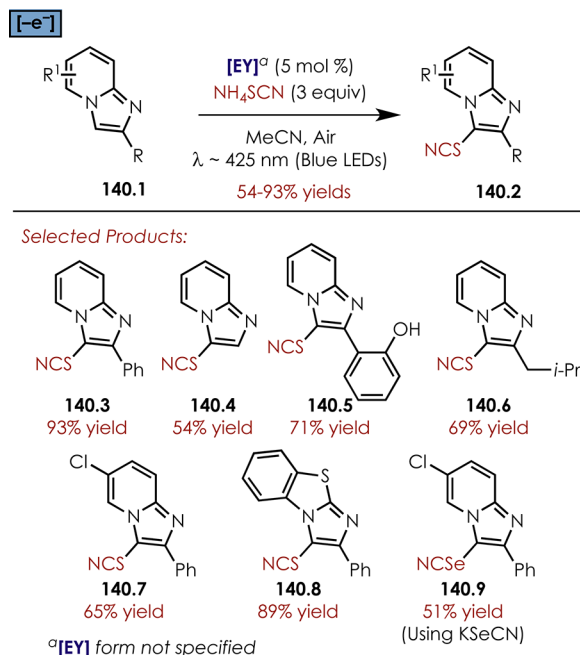
Scheme 139. Photoredox C–H Bromination of Alkanes



the success of the reaction, as was a secondary amine such as morpholine. Yields were generally moderate, although the protocol was applied to more complex substrates such as ibuprofen (bromide 139.7) and sclareolide (bromide 139.8). When directly compared to bromination by other radical bromination methods, this strategy showed some improvement in the regioselectivity of the bromination: ibuprofen underwent bromination with roughly equal selectivity (statistically corrected) for the indicated  $\alpha$  and  $\beta$  positions using the photoredox method, while bromination with  $Br_2$  gave exclusive site selectivity at the  $\alpha$  position. Sclareolide gave 76% selectivity for the “C2” bromide. A proposed mechanism was explored through computational analysis. The alkyl radicals were thought to be formed predominantly through H atom abstraction by the aminyl radical formed in a prior HAT from the amine cation radical to  $CBr_3\bullet$ .  $CBr_4$  was considered to form  $Br^-$  and  $CBr_3\bullet$  by reductive cleavage after quenching the triplet excited state  $^3EY^{2-}\bullet$ . Finally, the atom transfer from  $CBr_4$  to the alkyl radical is found to possess a low activation barrier ( $\Delta G^\ddagger = \sim 7$  kcal mol<sup>-1</sup>) as calculated by M06-2X/BS1.

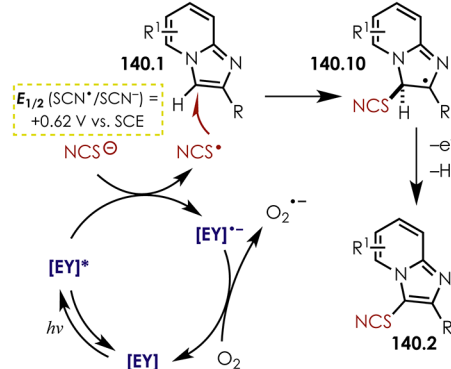
(Hetero)arene C–H bonds could also be functionalized with high regioselectivity in a photoredox-catalyzed thiocyanation of imidazoheterocycles 140.1 which uses eosin Y and ammonium thiocyanate  $NH_4SCN$  (Scheme 140).<sup>469</sup> Excellent yields could be obtained under aerobic conditions (e.g. substituent, 140.3–140.8), even in heterocycles such as imidazothiazoles (e.g., thiocyanate 140.8). An example using KSeCN as a nucleophile (140.9) demonstrated that the carbon–selenium bond could be forged using this methodology. The proposed mechanism took into account that  $E_{ox}$  ( $SCN\bullet/SCN^-$ ) was +0.62 V vs SCE and considered C–S bond formation through addition of the neutral radical  $SCN\bullet$  to the heterocycle. Subsequent oxidation and proton loss from the stabilized radical 140.10 would afford

Scheme 140. Thiocyanation of Imidazo-Heterocycles



<sup>a</sup>[EY] form not specified

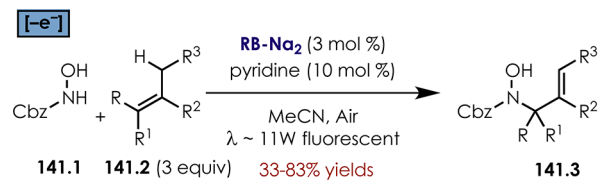
Proposed Mechanism:



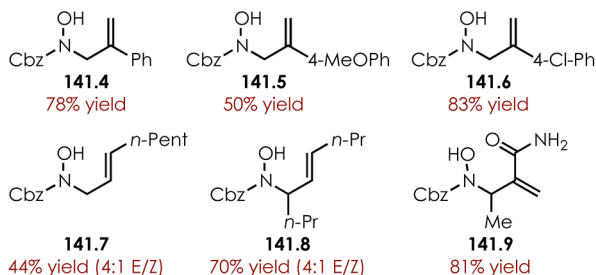
product 140.2. It is unknown whether  $O_2$  or  $O_2\bullet^-$  formed by turnover of  $[EY]\bullet^-$  is involved in this final oxidation process.

The nitroso-ene reaction is a valuable method for synthesizing allyl amines from alkene starting materials.<sup>470</sup> A photoredox catalyzed acylnitroso-ene variation was reported by Tan and co-workers (Scheme 141),<sup>471</sup> where the intermediate nitroso compound 141.12 was generated from N-protected hydroxylamine 141.1 through the photoredox activity of rose bengal ( $RB^{2-}$ ). The aerobic conditions, including pyridine as a catalytic additive, led to product formation in varying yields when aliphatic and electronically diverse styrenyl alkenes were tested (141.4–141.9). The proposed mechanism begins with oxidation of the hydroxylamine 141.1 to cation radical 141.10 by  $RB^{2-}\bullet$ .  $O_2$  turns over the catalytic cycle by oxidizing  $RB\bullet^{3-}$ , and  $O_2\bullet^-$  deprotonates 141.10, and then the peroxy radical  $HO_2\bullet$  abstracts an H atom to generate the reactive nitroso compound 141.12. Iodometry was used to qualitatively confirm the presence of  $H_2O_2$ . Quenching of fluorescence intensity was observed with hydroxylamine 141.1 as a quencher, implying that the singlet state  $^1RB^{2-}\bullet$  could be active in the PET process. Additionally, considering that rose bengal is a common sensitizer for singlet oxygen generation, the authors demonstrated that the PET process must outcompete  $^1O_2$  sensitization, since the

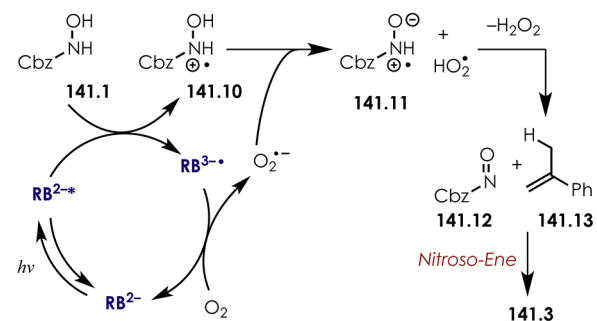
Scheme 141. Nitroso-Ene Reaction Enabled by PET



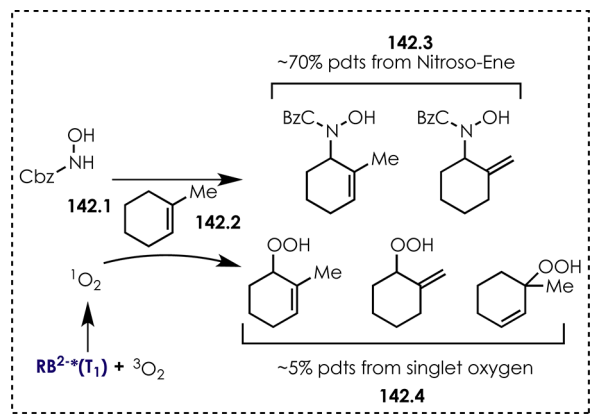
Selected Products:



Proposed Mechanism:

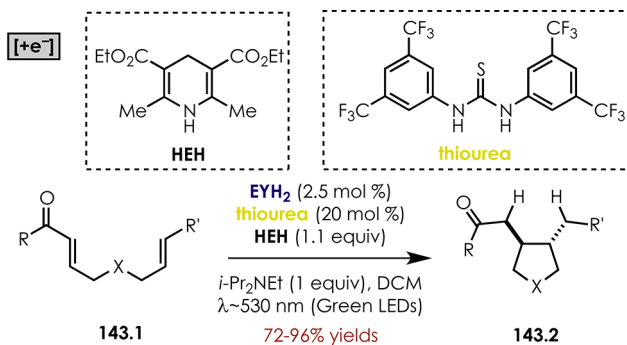


Schenck-ene products **142.4** were formed in only  $\sim$ 5% compared to  $\sim$ 70% nitroso-ene products **142.3** (Scheme 142).

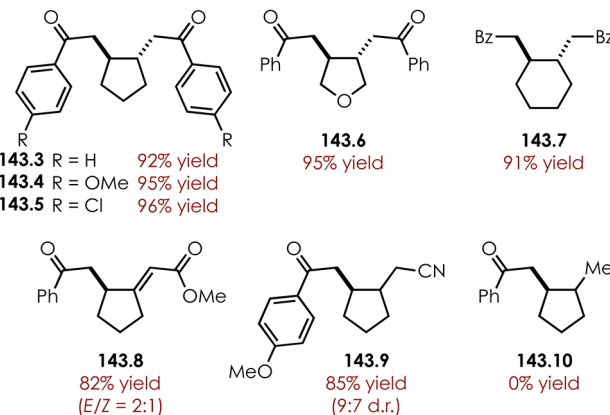
Scheme 142. Involvement of  $^1\text{O}_2$  in Photoredox Acylnitroso-Ene Reaction

**9.2.5. Reductive Transformations.** **9.2.5.1. Reductive Cyclizations.** Following the work of Yoon and co-workers on the reductive cyclization of bis-enones using  $\text{Ru}(\text{bpy})_3^{2+}$ ,<sup>233</sup> Neumann and Zeitler demonstrated this reaction could be carried out with catalytic eosin Y (Scheme 143)<sup>472</sup> shortly after Scaiano's report (Scheme 42). Eosin Y was employed as the catalyst, but this method also required a thiourea co-catalyst to give significant product formation, suggested by the authors to be important in hydrogen-bonding-mediated activation of the

Scheme 143. Reductive Intramolecular Cyclization of Bis-enones



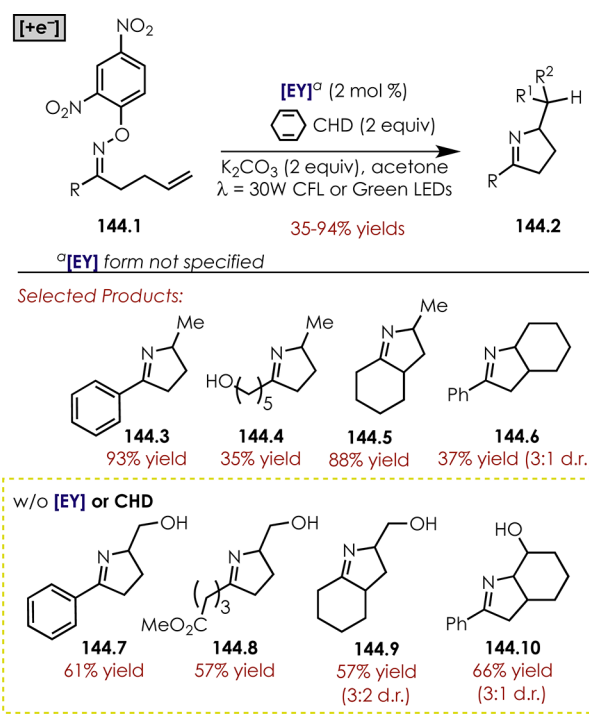
Selected Products:



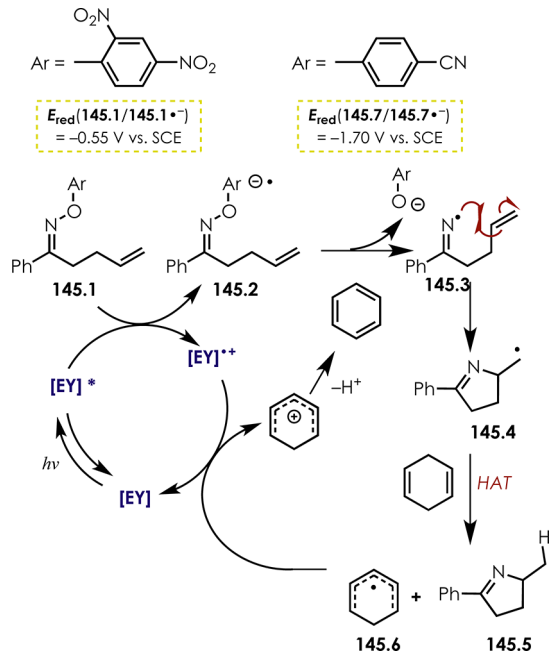
carbonyl towards single electron reduction. With a combination of the Hantzsch dihydropyridine HEH and  $i\text{-Pr}_2\text{NEt}$  as reducing equivalents, the cyclization was successfully extended to a range of substrates. The proposed mechanism was similar to that of Yoon, beginning with reduction of the excited  $[\text{EY}]^*$ , which reduces the carbonyl by one electron. It is worth reiterating that Scaiano has shown how  $\alpha$ -amino radicals, strong reductants and likely intermediates in this system, are capable of effecting the transformation by directly reducing the enone.<sup>232</sup>

Nitrogen-centered iminyl radicals are rarely encountered but useful intermediates, as demonstrated by Leonori and co-workers in their recent report of an intramolecular alkene hydroimination enabled by photoredox catalysis (Scheme 144).<sup>473</sup> The substrate **144.1** contains an  $O$ -aryloxime unit that serves as a precursor to the iminyl radical **145.3**, which engages in an intramolecular cyclization (Scheme 145), ultimately furnishing the imine product **144.2** after HAT with 1,4-cyclohexadiene (CHD). A comparison of  $\text{Ir}(\text{ppy})_3$  and eosin Y as photoredox catalysts highlights the role of photoinduced electron transfer in this system. With when the substrate contains a 4-cyano- $O$ -phenyloxime unit instead of 2,4-dinitrophenyl as in **145.1**, 91% yield of **144.3** is observed when  $\text{Ir}(\text{ppy})_3$  is the photoredox catalyst, eosin Y provides only 7% yield; in contrast, high yields of **144.3** are obtained when employing both catalysts in the hydroimination of the more electron-deficient substrate **145.1**. This divergence is consistent with the reduction potential of the 4-cyano- $O$ -phenyloxime substrate [ $E_{\text{red}}(145.7/145.7\bullet^-) = -1.70 \text{ V vs SCE}$ ], which is beyond the ability of  $^3[\text{EY}]^*$  to reduce but is less negative than the excited state oxidation potential of  $\text{Ir}(\text{ppy})_3^*$  [ $E_{\text{ox}}(\text{Ir}^{\text{IV}}/\text{Ir}^{\text{III}}*) = -1.73 \text{ V vs SCE}$ ].<sup>1</sup> On the other hand, the 2,4-dinitro  $O$ -aryloxime **145.1** [ $E_{\text{red}}(145.1/$

**Scheme 144. Intramolecular Alkene Hydroimination and Iminohydroxylation**



**Scheme 145. Proposed Mechanism of Hydroimination**



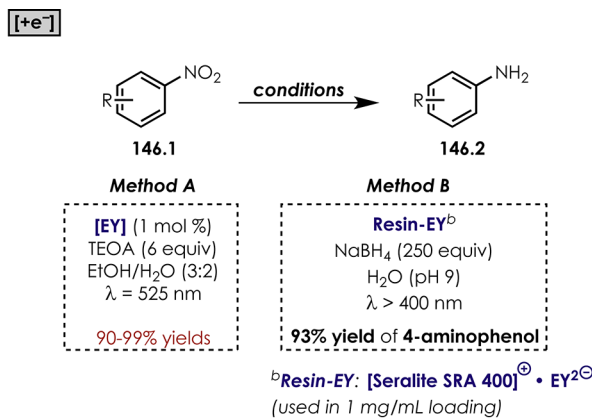
$E_{\text{red}}(145.1/145.1^{\bullet-}) = -0.55 \text{ V vs. SCE}$  can be reduced by either catalyst, and eosin Y was chosen in the evaluation of other substrates.

Observation of a color change upon addition of trimethylamine to a solution of substrate 144.1 informed the presence of an EDA complex (Scheme 144). Irradiation without a photoredox catalyst gives 47% hydrofunctionalization product 144.3 along with 41% iminohydroxylation (144.7) with 2 equiv of CHD. However, without CHD, this condition gives 85% 144.7. The divergent pathway is proposed to originate from addition of alkyl radical to dinitrophenolate. The catalyst-free trans-

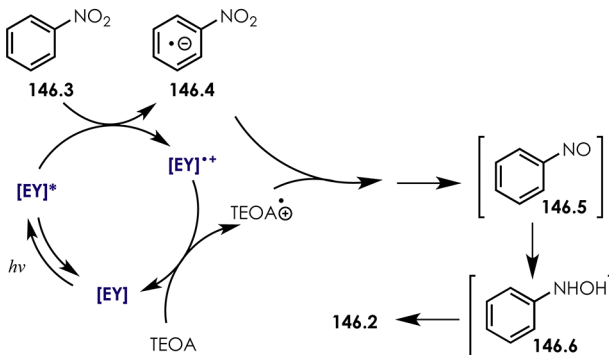
formation was found to be similarly general in scope with comparable yields to the photoredox-catalyzed hydroimination reaction.

**9.2.5.2. Reductive Deoxygenation.** In 2011, a photoredox catalytic reduction of 4-nitrophenol to 4-aminophenol was reportedly catalyzed by  $\text{EY}^{2-}$  bound to a cationic resin (Scheme 146, method B).<sup>430</sup> A large stoichiometric excess of  $\text{NaBH}_4$  (250

**Scheme 146. Hydrogenation of Nitroarenes to Anilines**



**Proposed Mechanism:**

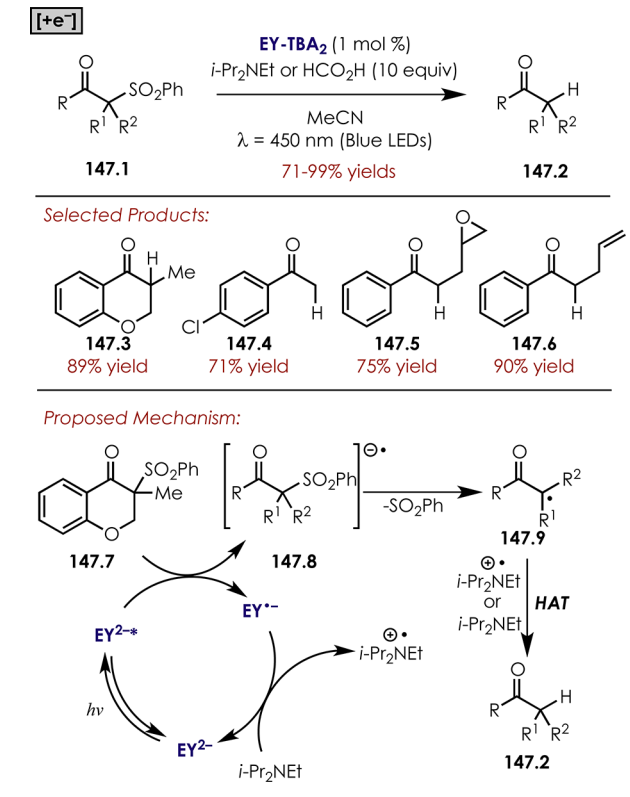


equiv) was used as the sacrificial reductant, but this process was greatly improved upon in 2014 with the conditions shown in Scheme 146, method A, which uses triethanolamine (TEOA) as the stoichiometric reductant.<sup>431</sup> The scope of the nitroarene substrates 146.1 was expanded to include para-, meta-, and ortho-substituents ranging from electron-donating to electron-withdrawing, and nearly quantitative yields were obtained in most cases. Other reducible substituents, such as aldehydes, ketones, acetylenes, and nitriles remained intact (with the exception of 2-nitrobenzonitrile, which was reduced to 2-aminobenzamide). Accompanying photophysical studies revealed that electron transfer from TEOA to  ${}^3[\text{EY}]^*$  was 2 orders of magnitude slower than electron transfer from  ${}^3[\text{EY}]^*$  to nitrobenzene. Accordingly, the mechanism is likely to involve an oxidative PET cycle, in which electrons are repeatedly donated from  ${}^3[\text{EY}]^*$  to the arene intermediates. Ultimately, the production of the aniline from a single equivalent of nitroarene is a 6-electron reduction which proceeds through nitrosobenzene 146.5 and N-phenylhydroxylamine 146.6 as intermediates, and these species were detected by  $^1\text{H}$  NMR at partial conversion.

**9.2.5.3. Reductive Desulfonylation.** Carbonyl compounds with nucleofugal substituents at the  $\alpha$ -position are known to undergo fragmentation when reduced by one electron to give an electron-deficient carbon-centered radical and an anionic leaving

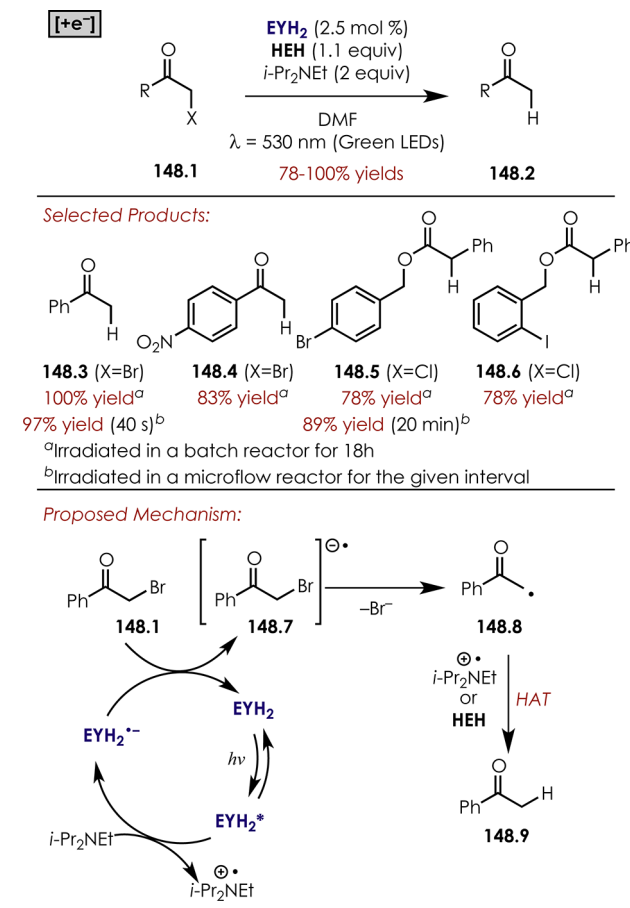
group. One example of this reactivity pattern harnessed in photoredox catalysis is in the reductive desulfonylation of ketosulfones. Preceded by the work of Ohno using  $\text{Ru}(\text{bpy})_3^{2+}$  in the 1980s, a recent report details that arylketosulfones **147.1** are desulfonylated to arylketones **147.2** with  $\text{EY-Na}_2$  as a photoredox catalyst and di-isopropylethylamine ( $i\text{-Pr}_2\text{NEt}$ ) as a sacrificial reductant (Scheme 147).<sup>474</sup> The protocol appears

Scheme 147. Reductive Desulfonylation of Ketosulfones



limited to substrates with arylsulfone and arylketone moieties, likely reflecting a requirement for substrates with sufficiently positive reduction potentials. Two possible modes of single electron reduction of **147.1** were considered in laser flash photolysis studies:  $\text{EY}\bullet^{3-}$  could be formed upon irradiation with  $i\text{-Pr}_2\text{NEt}$ ; conversely,  $\text{EY}\bullet^-$  could be generated in the presence of ketosulfone **147.1**. The authors favored the latter (oxidative) quenching mechanism (i.e., reduction of ketosulfone **147.1** by  $\text{EY}^{2-,*}$ ), which is consistent with the reduction potential of **147.7** ( $E_{\text{peak}}(147.7/147.7\bullet^-) = -1.51 \text{ V}$ , electrode not specified), indicating that a strong reductant is required to achieve this ET event. We note that the strongest reductant in this system is likely the singlet state  $^1\text{EY}^{2-,*}$  [ $E_{\text{ox}}([{\text{EY}}]\bullet^+/[{\text{EY}}]^*) = -1.58 \text{ V}$ , cf.  $E_{\text{ox}}([{\text{EY}}]\bullet^+/[{\text{EY}}]^*) = -1.18 \text{ V}$  or  $E_{\text{red}}([{\text{EY}}]/[{\text{EY}}]\bullet^-) = -1.08 \text{ V}$  vs SCE]. The proposed mechanism concludes with an HAT to radical **147.9**, possibly from  $i\text{-Pr}_2\text{NEt}$  or  $i\text{-Pr}_2\text{NEt}\bullet^+$ .

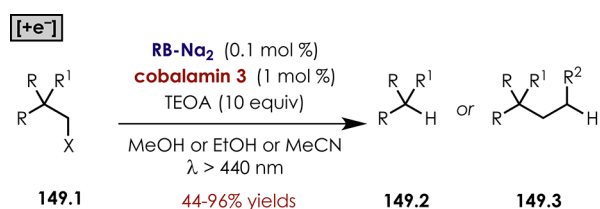
**9.2.5.4. Reductive Dehalogenation.** Transition metal photoredox catalysis has been recognized as a safe and environmentally benign alternative<sup>475,476</sup> to the typical means of reductive dehalogenation using tin-hydrides.<sup>477</sup> An entirely organic system was found to be comparable to the previously reported method employing  $\text{Ru}(\text{bpy})_3^{2+}$  for the catalytic dehalogenation of  $\alpha$ -halo carbonyl compounds **148.1** using  $\text{HEH}$  and  $i\text{-Pr}_2\text{NEt}$  as sacrificial reductants (Scheme 148).<sup>478</sup> A number of different organic dyes gave quantitative yields of acetophenone **148.2**

Scheme 148. Reductive Dehalogenation of  $\alpha$ -Halo Carbonyl Compounds

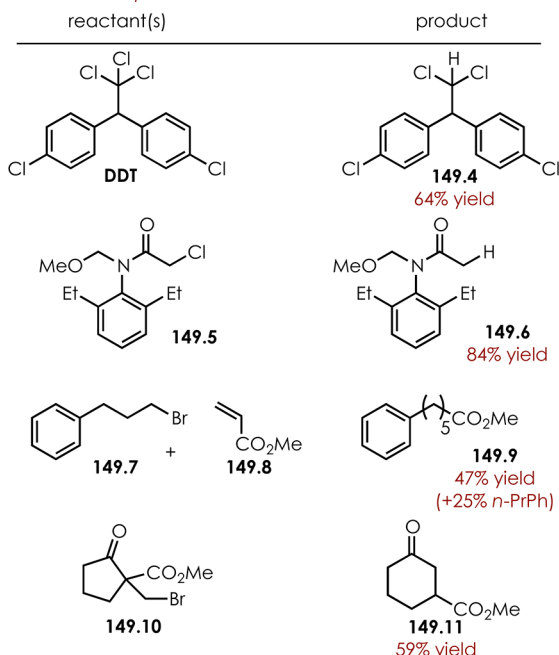
from phenacyl bromide, including a perylene diimide (see Scheme 179), fluorescein ( $\text{FLH}_2$ ), and eosin Y ( $\text{EYH}_2$ ).  $\text{EYH}_2$  was the most robust under the photolytic conditions, and a short survey of phenacyl bromides and  $\alpha$ -chlorophenylacetates gave high yields of the dehalogenated products **148.3–148.6**, leaving other reducible groups intact. With consideration of the reduction potential of phenacyl bromide [ $E_{\text{red}}(148.1/148.1\bullet^-) = -0.78 \text{ V}$  vs Ag/AgClO<sub>4</sub>]<sup>479</sup>, it was assumed that a carbon-centered radical could be generated by reduction of the  $\alpha$ -halo compound from  $\text{EYH}_2\bullet^-$  produced upon PET to  $\text{EYH}_2^*$  from  $i\text{-Pr}_2\text{NEt}$ . Both  $\text{HEH}$  and  $i\text{-Pr}_2\text{NEt}\bullet^+$  are likely to play a role in HAT to furnish the product.<sup>475,476</sup> This system was implemented in a flow reactor<sup>480</sup> to the effect of greatly reduced reaction times (40 s, compared to 18 h in batch for **148.3**) and improved yields for one substrate (**148.5**).

The highly negative reduction potentials of unactivated alkyl halide substrates preclude direct reduction-fragmentation in a photoredox system as presented above. As a solution, one group has explored a system which takes advantage of the “super-nucleophilic” behavior of a cobalt(I) complex<sup>481</sup> catalytically regenerated by the photoredox activity of rose bengal (Scheme 149).<sup>482</sup> With only 0.1 mol %  $\text{RB-Na}_2$  and 1 mol % of a Vitamin B<sub>12</sub> derivative **cobalamin 3** with TEOA as a sacrificial reductant, a range of alkyl halides could be converted to the corresponding alkanes or the putative radical intermediates intercepted by reacting with acrylate **149.8**. The ring expansion of **149.10** has been observed previously.<sup>483</sup> With a reduction potential of  $E_{\text{red}}([\text{Co}]^{II}/[\text{Co}^{I}] = -0.64 \text{ V}$  versus SCE,<sup>483</sup> it was expected that **cobalamin 3** ( $[\text{Co}^{II}]$ ) could be reduced by oxidative quenching

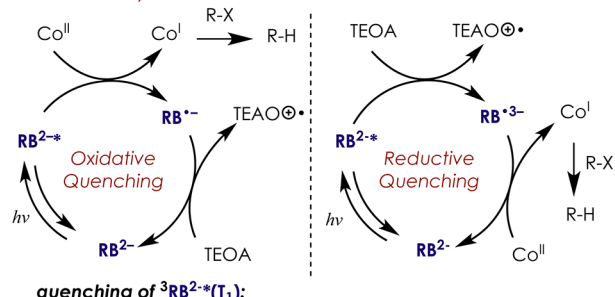
**Scheme 149. Dehalogenative Transformations of Unactivated Alkyl Halides Enabled by a Cobalamin Co-Catalyst**



**Selected Examples:**



**Possible PET cycles:**



**quenching of  ${}^3\text{RB}^{2-}\ast(\text{T}_1)$ :**

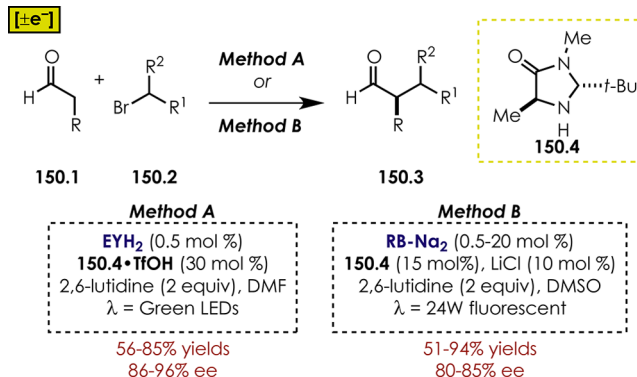
quencher	$\text{Co}^{\text{II}}$	TEOA
$k_q$	$7.2 \times 10^9 \text{ M}^{-1}\text{s}^{-1}$	$1.0 \times 10^6 \text{ M}^{-1}\text{s}^{-1}$

of  $\text{RB}^{2-}\ast$  (“Oxidative Quenching” cycle in Scheme 149) or by SET from  $\text{RB}^{\bullet 3-}$  generated through reductive quenching by TEOA (“Reductive Quenching” cycle), but a mechanistic investigation revealed that the oxidative quenching cycle was most likely. Neither TEOA nor cobalamin 3 quenched fluorescence of  ${}^1\text{RB}^{2-}\ast$ , implicating the triplet  ${}^3\text{RB}^{2-}\ast$  in the PET process. Although both TEOA and cobalamin 3 quenched  ${}^3\text{RB}^{2-}\ast$ , the  $[\text{Co}(\text{II})]$  species did so at least 3 orders of magnitude faster than TEOA. Additionally, the steady state absorption of  $\text{RB}^{2-}$  almost completely degraded under irradiation with TEOA, demonstrating that  $\text{RB}^{2-}$  is reduced to the dihydroxanthene form.<sup>484</sup> In contrast, under the optimized

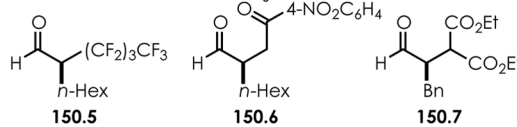
conditions  $\text{RB}^{2-}$  is mostly present after mono-dechlorination of the insecticide DDT.

**9.2.5.5. Dehalogenative Couplings.** In a conceptually similar strategy of harnessing carbon-centered radicals generated by reduction of alkyl halides, Nicewicz and MacMillan demonstrated that enantioselective  $\alpha$ -alkylation of aldehydes could be accomplished by combining the aforementioned activity of a photoredox catalyst with reactions of enamines formed by condensation of an imidazolidinone organocatalyst and an aldehyde.<sup>485</sup> Although originally reported using  $\text{Ru}(\text{bpy})_3^{2+}$ , recent reports indicate that eosin Y<sup>478</sup> and rose bengal<sup>92</sup> are competent photoredox catalysts for the transformation (Scheme 150). Moderate to good yields but high levels of enantiomeric

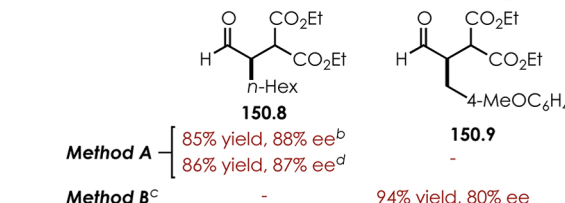
**Scheme 150. Dehalogenative  $\alpha$ -Alkylation of Aldehydes**



**Examples:**



**Method A** 56% yield, 96% ee<sup>c</sup>    82% yield, 95% ee<sup>a</sup>    76% yield, 86% ee<sup>c</sup>  
**Method B<sup>c</sup>** -    -    89% yield, 83% ee



**Method A<sup>b</sup>** 85% yield, 88% ee<sup>b</sup>  
**Method B<sup>c</sup>** 86% yield, 87% ee<sup>d</sup>

94% yield, 80% ee  
 (requires 20 mol %  $\text{RB-Na}_2$ )

<sup>a</sup>Irradiated in a batch reactor at +5 °C

<sup>b</sup>Irradiated in a batch reactor at -15 °C

<sup>c</sup>Irradiated in a batch reactor at rt

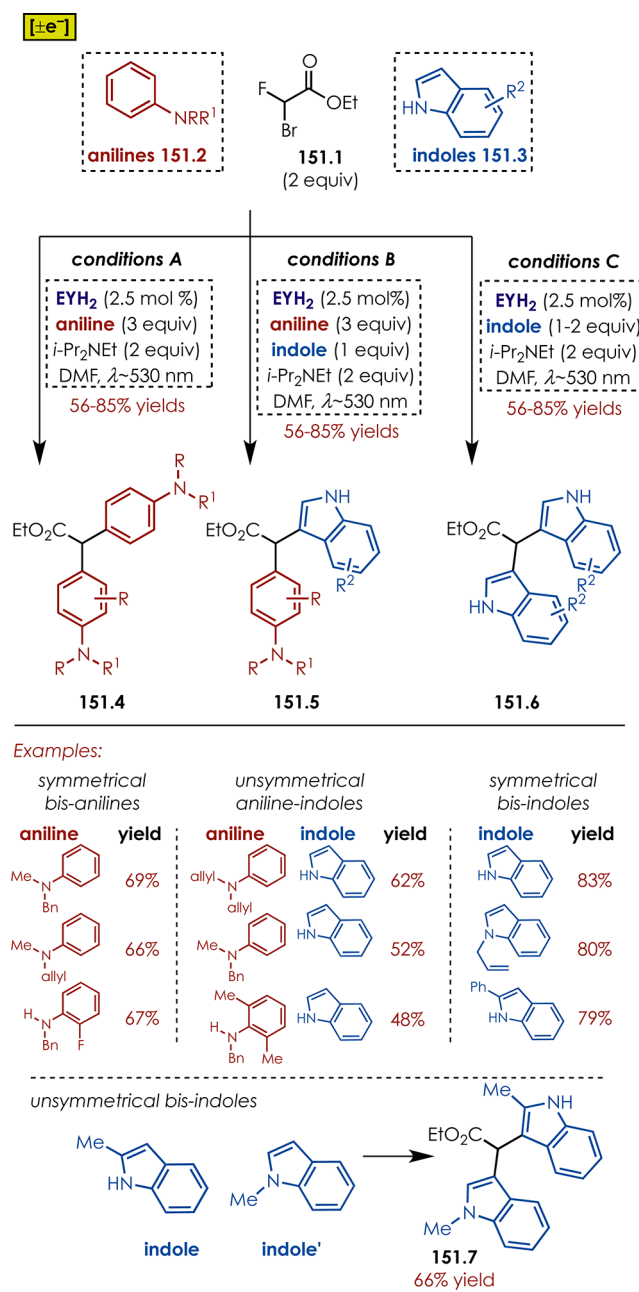
<sup>d</sup>Irradiated in a microflow reactor for 45 min at -5 °C

enrichment were observed for 150.5–150.8 in the system reported by Neumann and co-workers (Scheme 150, method A), which employs  $\text{EYH}_2$  and the imidazolidinone 150.4-TfOH. The reaction was also performed in a flow reactor, with equivalent results at shorter reaction times for aldehyde 150.8.<sup>480</sup> An alternative set of conditions was presented by Ferroud and co-workers (Scheme 150, Method B), who used  $\text{RB-Na}_2$  and lower loadings of organocatalyst 150.4. A direct comparison of product 150.7 reveals slightly better yields and comparable enantioselectivity for the rose bengal method, which was carried out at room temperature for all substrates. The anticipated mechanism is analogous to that proposed by Nicewicz and MacMillan, wherein the photoredox catalyst undergoes reductive quenching (likely by oxidation of a sacrificial

quantity of enamine to initiate the PET cycle),<sup>485</sup> and the reduced catalyst transfers an electron to the alkyl halide. The so-formed alkyl radical can add to the enamine, and the resulting  $\alpha$ -amino radical is converted to an iminium by PET. Notably, Yoon and Cismesia provided evidence that the reaction catalyzed by Ru(bpy)<sub>3</sub><sup>2+</sup> likely involves chain mechanisms,<sup>118</sup> and this possibility seems equally tenable in the organic photoredox systems.

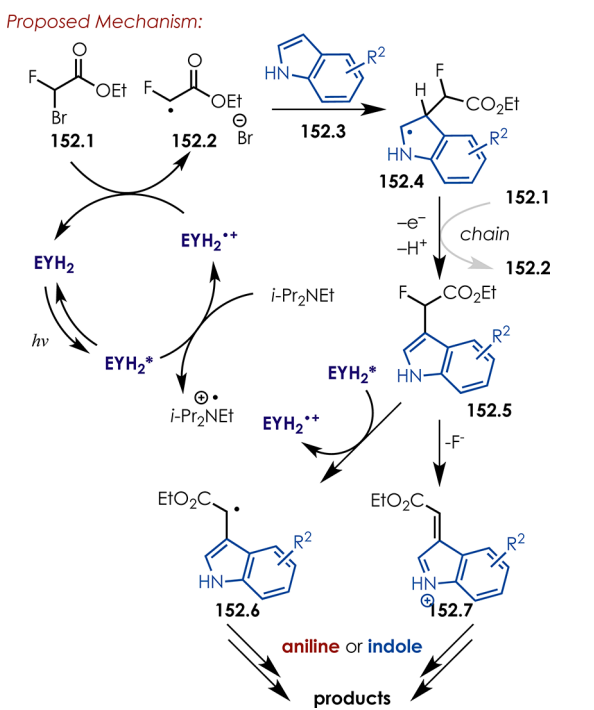
Carbonyl compounds possessing more than one nucleofuge can give rise to the formation of multiple C–C bonds by a similar pathway to the previous examples. This principle was demonstrated by Singh and co-workers, who used the photoredox catalysis of eosin Y to couple ethyl bromofluoroacetate 151.1 with anilines 151.2 and indoles 151.3 (Scheme 151).<sup>486</sup> Whereas the ethyl esters of dibromoacetate and chlorofluor-

**Scheme 151. Photoredox Activation of Ethyl Fluoro Bromoacetate**



acetate were both incompetent electrophiles, ethyl bromofluoroacetate 151.1 gave good yields of bis-anilines 151.4 and bis-indoles 151.6. Remarkably, the mixed aniline-indole products 151.5 could be obtained in reasonable yields even with anilines 151.2 employed in three-fold excess, reflecting subtle differences in reactivity between the arene and heteroarene. Moreover, even unsymmetrical bis-indoles 151.7 could be constructed using this method. A proposed mechanism (Scheme 152) begins with

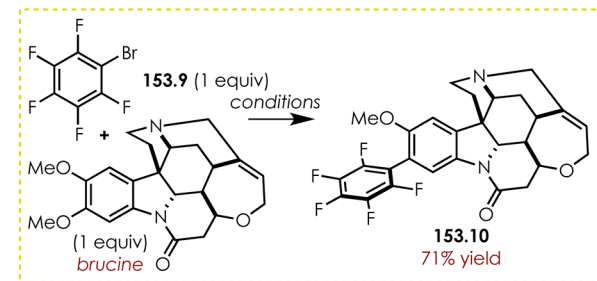
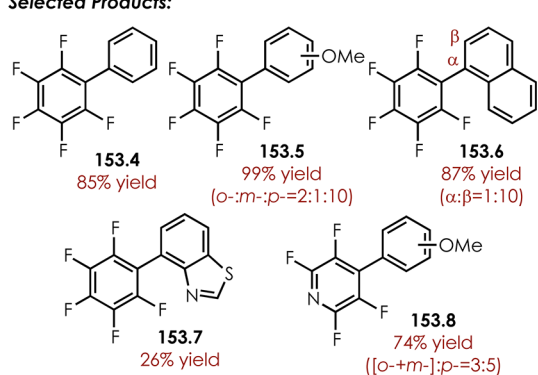
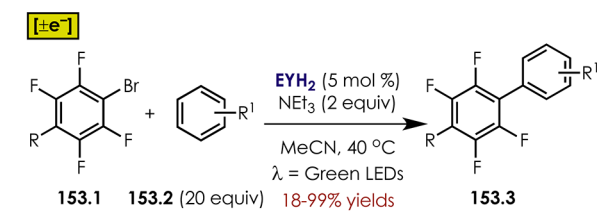
**Scheme 152. Proposed Mechanism for the Coupling of Ethyl Fluoro Bromoacetate with Indoles and Anilines**



reductive cleavage of the C–Br bond by EYH<sub>2</sub><sup>•−</sup>, and fluoroacetate radical 152.2 adds to indole 152.3 (or aniline 151.2). Oxidation of radical 152.4 may occur through the PET activity of EYH<sub>2</sub><sup>\*</sup> or by electron transfer to 152.1 to initiate a new chain. Subsequent deprotonation gives mono-coupled 152.5, which could undergo either direct elimination of fluoride to iminium 152.7 or reductive cleavage to radical 152.6. Addition of a second indole (or aniline) eventually lead to products 151.4–151.7.

Recently, a different class of dehalogenative coupling was developed by König and co-workers: perfluoroaryl bromides 153.1 were coupled with arenes 153.2 and heteroarenes using eosin Y (EYH<sub>2</sub>) as a photoredox catalyst and NEt<sub>3</sub> as a sacrificial reductant (Scheme 153).<sup>487</sup> This C–H arylation reactivity is derived from the reductive cleavage of perfluoroaryl bromide to form perfluoroaryl radicals such as 154.2, which add to arenes and heteroarenes to ultimately furnish the cross-coupled products, although the regioselectivity of the addition is variable. Mixtures of o-, m-, and p-isomers were obtained for mono-substituted arene coupling partners which were employed in 20-fold excess (e.g. 153.5 and 153.8), while heteroarenes and fused rings also gave regioisomeric mixtures (e.g. 153.6 and 153.7). However, when the *Strychnos* alkaloid brucine was submitted to the conditions, ipso-substitution of a single methoxy-substituent took place in a high yield of coupled product 153.10.

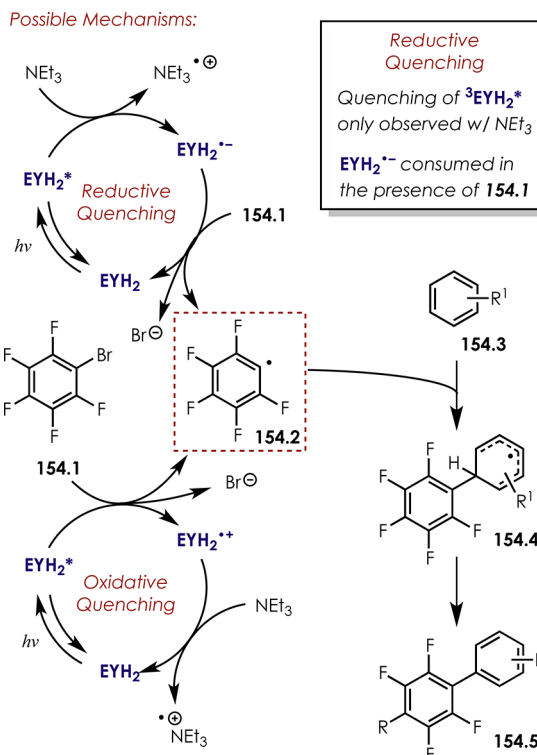
**Scheme 153. Dehalogenative Coupling of Perfluorohaloarenes with Arenes**



Two possible mechanisms of reductive cleavage of bromopentafluorobenzene **154.1** were deliberated (Scheme 154): reductive quenching of  ${}^3[\text{EY}]^*$  involving oxidation of  $\text{NEt}_3$  to form  $[\text{EY}]^{\bullet-}$  as the active species in reducing **154.1** [ $E_{\text{red}}(154.1/154.1^{\bullet-}) = -1.39$  V vs SCE, peak potential]. Alternatively, in an oxidative quenching cycle, the excited state  ${}^3[\text{EY}]^*$  is quenched by reduction of **154.1**, and the ground state  $[\text{EY}]$  is recycled by  $\text{NEt}_3$  reduction of  $[\text{EY}]^{\bullet+}$ . However, considering the redox potentials in Table 1 [ $E_{\text{red}}([\text{EY}]/[\text{EY}]^{\bullet-}) = -1.08$  V,  $E_{\text{ox}}([\text{EY}]^{\bullet+}/{}^3[\text{EY}]^*) = -1.15$  vs SCE], reduction of **154.1** is estimated to be endothermic in both scenarios. Transient absorption measurements confirm that the triplet  ${}^3[\text{EY}]^*$  is only quenched by  $\text{NEt}_3$  and also show that the resulting  $[\text{EY}]^{\bullet-}$  is consumed in the presence of **154.1**. These data support a reductive quenching cycle, and the apparently unfavorable thermodynamics of the reductive cleavage were said to be balanced by a favorable, irreversible aromatization step. The product-forming aromatization step is not studied in detail, but the authors find a low quantum yield of reaction (0.0015), which would be surprising if efficient chain transfer were occurring.

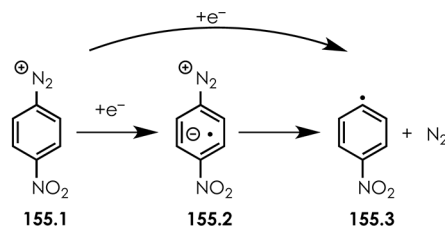
**9.2.6. Reactions of Aryldiazonium Salts.** **9.2.6.1. Carbon–Carbon Bond-Forming Reactions of Aryldiazonium Salts.** Another class of reactions that is particularly well-developed in the use of xanthenes as photoredox catalysts are reactions of aryldiazonium salts. Mechanisms involving aryl radical intermediates are generally accepted in a number of transformations of aryldiazoniums.<sup>488–490</sup> Aryldiazonium salts are highly susceptible to single-electron reduction as indicated by their reduction potentials: *p*-nitrobenzenediazonium **155.1** has a

**Scheme 154. Proposed Mechanism for Dehalogenative Couplings of Pentafluorobromobenzene**



reduction potential [ $E_{\text{red}}(155.1^+/155.2^{\bullet})$ ] of +0.20 V vs. SCE (Scheme 155),<sup>491</sup> and even diazonium species with strongly

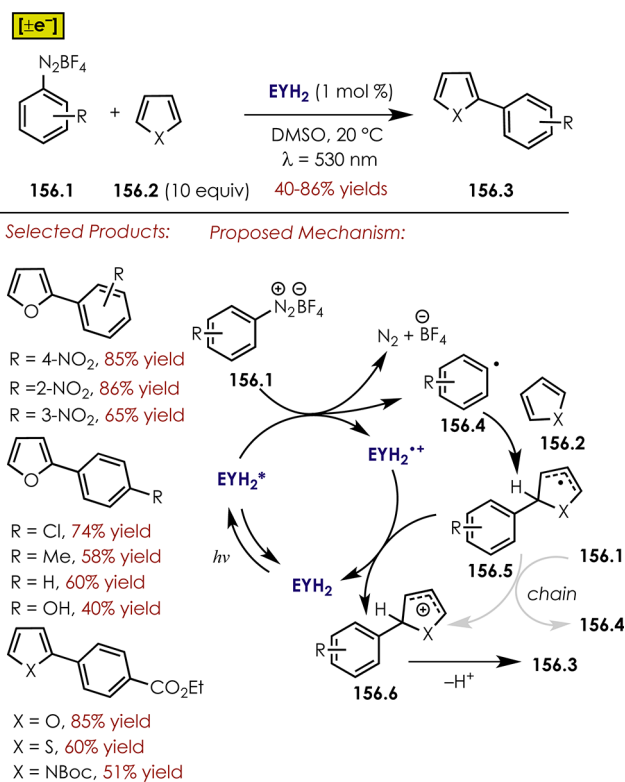
**Scheme 155. Aryldiazonium Salts as Precursors to Aryl Radicals**



electron-donating substituents are reduced near 0 V.<sup>492</sup> The aryl radical formed by expulsion of  $\text{N}_2$  after single-electron reduction has been exploited in PET-enabled synthetic processes,<sup>493–496</sup> and the following examples describe the application of xanthene dyes in this context.

König and co-workers discovered that aryldiazonium salts could be coupled with heteroarenes in a redox-neutral C–H arylation reaction using eosin Y as a photoredox catalyst (Scheme 156).<sup>497</sup> A variety of aryldiazonium tetrafluoroborate salts **156.1** were evaluated in the coupling reaction with furan, with the electron-withdrawing substituents on the aryldiazonium **156.1** generally giving higher yields. The coupling was also possible with thiophenes and *N*-Boc-pyrrole, albeit in lower yields. The proposed mechanism (Scheme 156) is consistent with redox potential data, which indicate that  $[\text{EY}]^*$  should be able to reduce diazonium **156.1**, and the aryl radical **156.4** generated by loss of  $\text{N}_2$  adds to the heteroarene at the 2-position to give the resonance-stabilized radical **156.5**. The authors recognized that

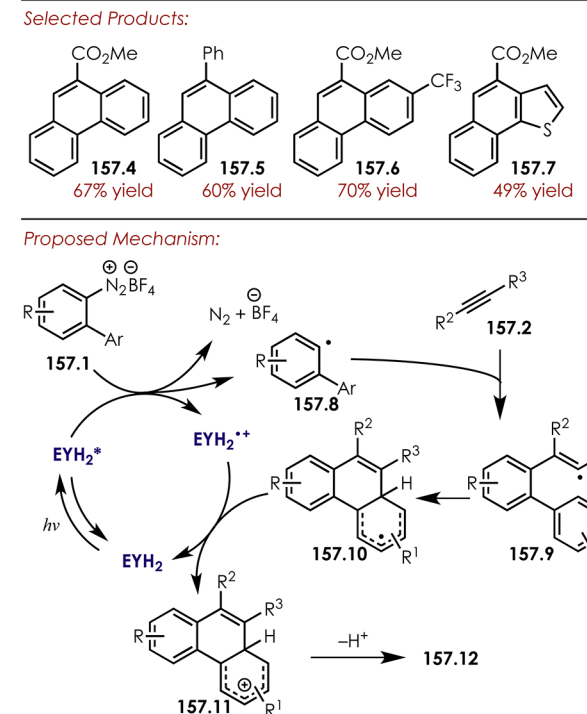
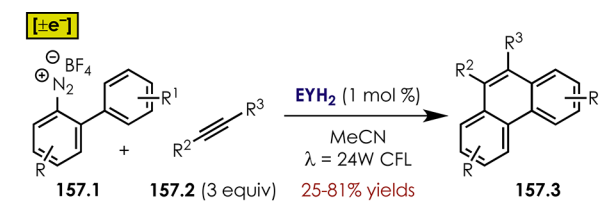
**Scheme 156.** Arylation of Heterocycles Using Aryldiazonium Salts



carbocation **156.6** is accessible through two possible pathways: oxidation by [EY]<sup>•+</sup> accomplishes turnover of the catalytic cycle, but radicals such as **156.5** may also be sufficiently reducing such that electron transfer to aryl diazonium **156.1** initiates a new chain. Later mechanistic studies by Jacobi von Wangelin and co-workers revealed the quantum yield of the reaction to be greater than unity,<sup>411</sup> supporting the initial proposal by König that a chain mechanism is tenable. Deprotonation of carbocation **156.6** furnishes the coupled product.

Eosin Y could be utilized in the synthesis of phenanthrenes **157.3** from biaryldiazoniums **157.1** and alkynes **157.2** (Scheme 157).<sup>498</sup> The aryl radical intermediate is thought to be captured by the alkyne, and cyclohexadienyl radical **157.10** is formed after a subsequent radical cyclization. Turnover of the PET cycle may occur by reduction of EYH<sub>2</sub><sup>•+</sup> by cyclohexadienyl radical; however, a chain propagating electron transfer to the diazonium starting material may be possible. The optimal reaction conditions specify addition of the diazonium salt in six successive portions, and a number of substituted phenanthrolines could be prepared in this way. Although terminal alkynes, including propiolates and arylacetylenes, gave the highest yields, several internal alkynes were included in the substrate scope, along with various substituted biaryls. The initial radical addition to the alkyne likely occurs with high selectivity to give the internal vinyl radical, as the authors do not report the other constitutional isomer being formed when unsymmetrical alkynes are employed. Jacobi von Wangelin and co-workers provided interesting mechanistic insight<sup>411</sup> which led to improved performance in this system: noting that biaryldiazonium **157.1** possessed an absorption in the visible range, the researchers discovered that photolysis of **157.1** in MeCN, in the absence of photoredox catalyst, gives an acetonilide as the Ritter product. Thus, the aryl diazonium substrate likely competes with EYH<sub>2</sub> for

**Scheme 157.** Phenanthrene Synthesis by Cyclization of Biaryldiazonium Salts with Alkynes

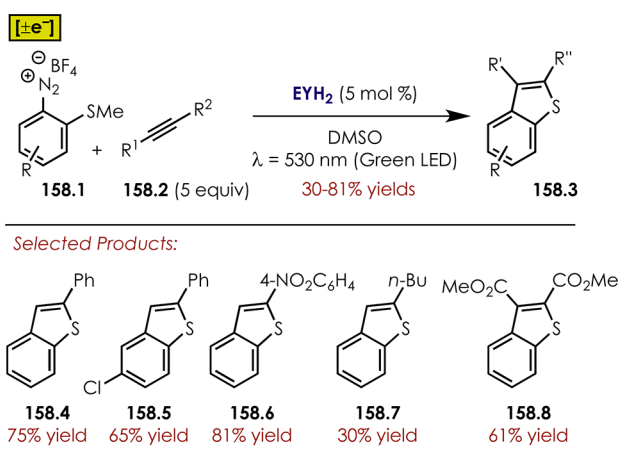


absorption of photons, which, in turn leads to consumption of the starting material in the competitive heterolytic pathway triggered by direct photolysis. Jacobi von Wangelin offered an improvement to the original protocol by performing the reaction with green LEDs to minimize direct photolysis and using DMSO as a solvent to increase the proportion of the more active EYH<sup>−</sup> or EYH<sup>2−</sup>, which resulted in an increase of ~18% yield.

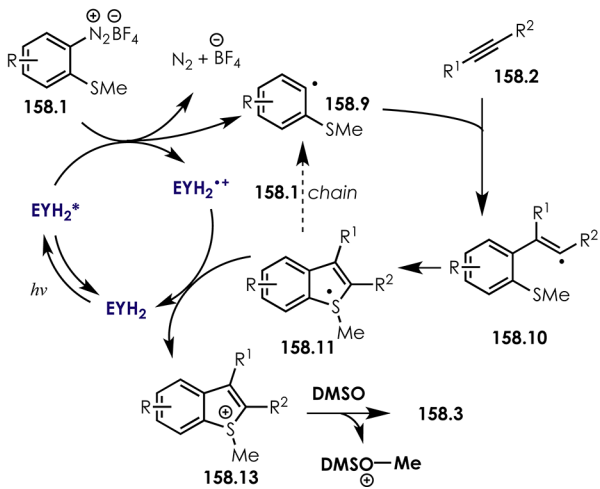
In a mechanistically related transformation, 2-methylthioaryl diazonium salts **158.1** were coupled with alkynes **158.2** to produce benzothiophenes **158.3** with eosin Y as a catalyst (Scheme 158).<sup>499</sup> Using this method, diversely substituted benzothiophenes were synthesized in useful yields from various 2-methylthioaryl diazonium salts and a range of terminal alkynes or alkyl butynedioates. A key step in the proposed mechanism is cyclization of vinyl radical **158.10** by addition at the sulfur of the thioether, forming sulfuranyl radical **158.11**. This intermediate is expected to be mildly reducing, and either chain transfer by reduction of diazonium **158.1** or regeneration of ground state EYH<sub>2</sub> by reduction of EYH<sub>2</sub><sup>•+</sup> were recognized as tenable pathways. Interestingly, Jacobi von Wangelin found that the reaction quantum yield was only 0.075;<sup>411</sup> while it does not preclude a chain mechanism,<sup>118</sup> this result would be surprising if a highly efficient chain transfer step were operative. Ultimately, sulfonium cation **158.13** must undergo demethylation to furnish the benzothiophene products **158.3**, and the solvent (DMSO) was proposed to accept the methyl group.

Concurrent reports from Jacobi von Wangelin<sup>500</sup> and Xiao<sup>501</sup> detail separate methodologies which accomplish the alkoxycar-

**Scheme 158. Synthesis of Benzothiophenes from Aryldiazonium Salts**

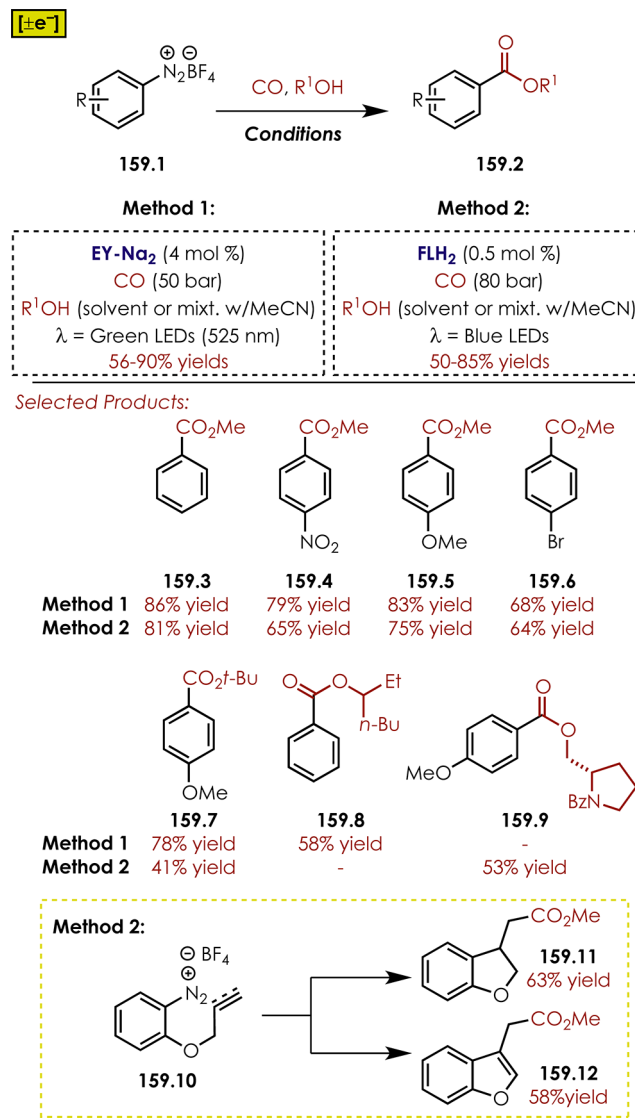


**Proposed Mechanism:**



bonylation of aryldiazonium salts in a rare example of carbon monoxide (CO) participation in photoredox catalysis (**Scheme 159**). The conditions offered by each group were similar but diverged in their choice of photoredox catalyst: while Jacobi von Wangelin and Majek found eosin Y (EY-Na<sub>2</sub>) to be optimal (**Scheme 159**, method 1), fluorescein (FLH<sub>2</sub>) was chosen by Xiao (**Scheme 159**, method 2). During optimization with irradiation from white LEDs and 80 atm CO, Xiao saw only slightly lower yields of **159.3** (~10%) when using EY-Na<sub>2</sub> instead of FLH<sub>2</sub>, whereas Jacobi von Wangelin observed greatly suppressed yields of **159.5** (~50%) when using FLH<sub>2</sub> instead of EY-Na<sub>2</sub> with irradiation from green LEDs (~525 nm). The source of irradiation in Jacobi von Wangelin's investigation is the most plausible explanation for this discrepancy, as FLH<sub>2</sub> is expected to absorb minimal light from a green LED, although Xiao also demonstrates that 80 atm CO provides ~10% improvement over 50 atm for **159.3**. Nonetheless, each method offers equally good yields of benzoate esters **159.3–159.9** in a head-to-head comparison (with the exception of **159.7** in method 2). Moreover, method 1 featured a more comprehensive evaluation of alcohol-coupling partners, while method 2 thoroughly investigated the aryldiazonium coupling partner and provided several examples where the putative aryl radical intermediate was intercepted by tethered alkenes and alkynes **159.10** (**159.11** and **159.12**). Both reports present a mechanism involving CO capture by aryl radical **160.2** to form acyl radical **160.3**.

**Scheme 159. Alkoxy carbonylation of Aryldiazonium Salts**

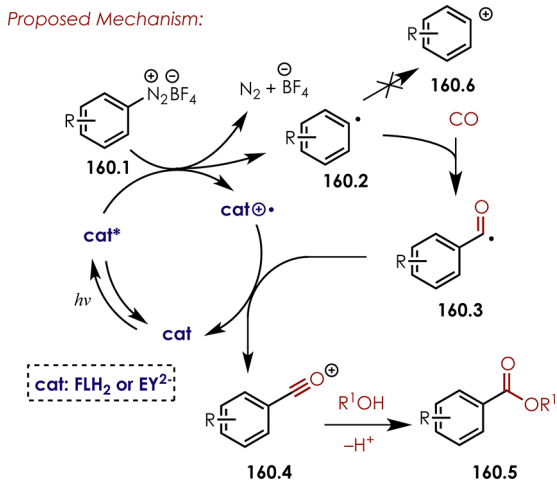


**160.3** (**Scheme 160**), citing computational evidence that the oxidation of acyl radical **160.3** by [cat]•+ is thermodynamically favorable while oxidation of aryl radical **160.2** to an aryl cation **160.6** is not. The ester products are produced upon addition of alcohol to the so-formed acylium. The possibility of chain transfer was not discussed.

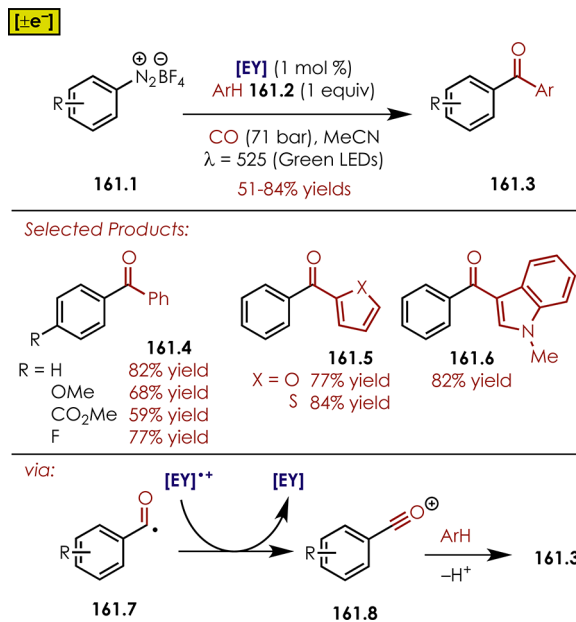
A similar carbonylation reaction of aryldiazonium salts **161.1** using CO and an arene or heteroarene nucleophile **161.2** was reported using eosin Y as a photoredox catalyst (**Scheme 161**).<sup>502</sup> The diarylketone products **161.3** could be achieved in good yields with simple arenes (**161.4**) and heteroarenes (**161.5** and **161.6**) and were proposed to form by a similar mechanism to the one shown in **Scheme 160**.

**9.2.6.2. Carbon-Heteroatom Bond-Forming Reactions of Aryldiazonium Salts.** In addition to the carbon–carbon bond-forming reactions discussed above, aryldiazonium salts were also shown to be important reagents in creating new carbon–heteroatom bonds. Arylboronic esters were produced in the photoredox catalytic process shown in **Scheme 162**, wherein bis(pinacolato)diboron **162.2** was the boron transfer reagent and eosin Y was the catalyst.<sup>503</sup> Good yields of various arylboronic esters could be obtained (**162.4–162.9**). The proposed

**Scheme 160. Proposed Mechanism for Photoredox Alkoxy carbonylation**



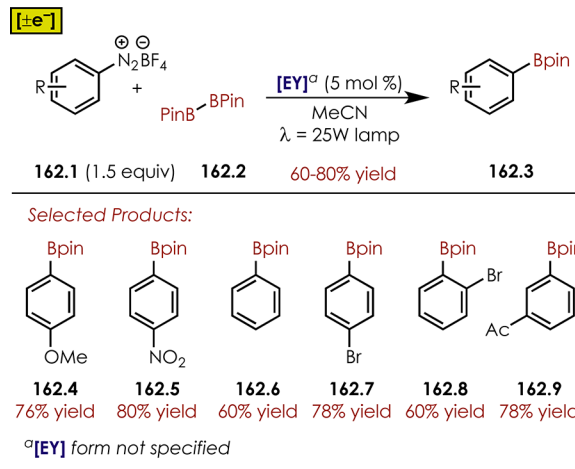
**Scheme 161. Arylcarbonylation of Aryldiazonium Salts**



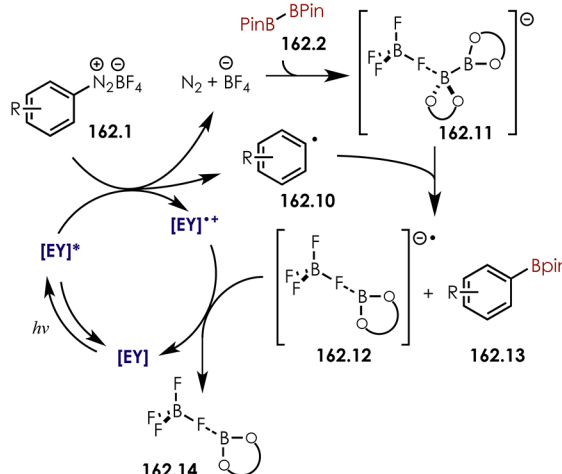
mechanism of boron transfer to aryl radical 162.10 involved activation of the diborionate ester by the  $\text{BF}_4^-$  anion, resulting in borofluoride radical anion complex 162.11. The photoredox cycle is assumed to be turned over by this species as a reductant. Jacobi von Wangelin and co-workers measured a quantum yield of reaction of 0.60 for the production of boronic ester 162.7 and also observed evidence of an EDA complex between the aryldiazonium and bis(pinacolato)diboron 162.2 in the appearance of a new absorption feature around 420 nm.<sup>411</sup> Irradiation of this absorption band (with a white LED) led to a 54% yield of 162.7 in the absence of eosin Y, an observation which might be rationalized to originate from a direct heterolysis of the aryldiazonium. Nonetheless, the originally reported catalytic reaction employed a 25 W fluorescent bulb and required eosin Y for product formation.

Aryl sulfides 163.3 were synthesized, using a similar approach, from aryldiazonium salts 163.1 and disulfides 163.2, which gave generally good yields when eosin Y was used as a catalyst under the photolytic conditions (Scheme 163).<sup>504</sup> Reaction optimiza-

**Scheme 162. Borylation of Aryldiazonium Salts**



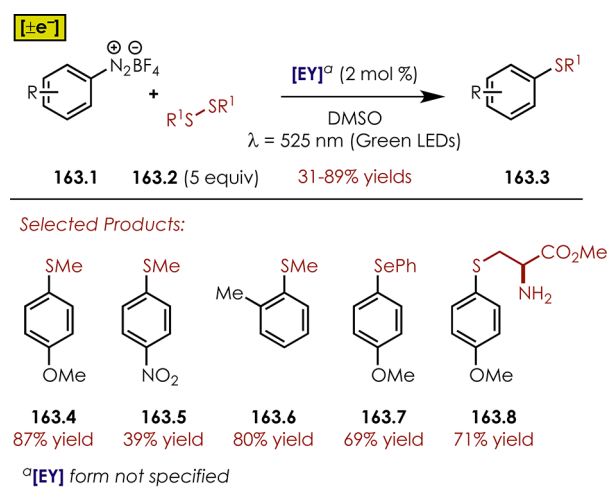
*Proposed Mechanism:*



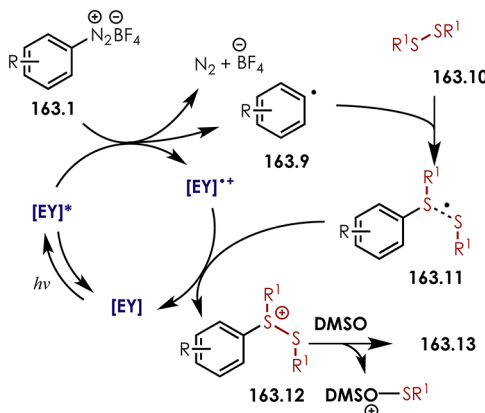
tion overcame hydrodediazotization (or reductive dediazotization), which was predominant when DMF was the solvent and identified eosin Y as the catalyst exhibiting optimal efficiency, although  $\text{Ru}(\text{bpy})_3^{2+}$  appeared to be comparable in the test reaction. Notably, the (*R*)-S-(4-methoxyphenyl)cysteine methyl ester 163.8 could be obtained when dimethyl (*R,R*)-cystinate was used as the disulfide. Additionally, diaryl selenide 163.7 was produced, demonstrating a novel way to form the Se–C bond. The mechanism considered by the authors envisaged addition of aryl radical 163.9 to disulfide 163.10, resulting in a trivalent disulfanyl radical 163.11, which is oxidized to the disulfaniun cation 163.12, an electrophilic species that likely transfers  $\text{RS}^+$  to the nucleophilic solvent DMSO. The quantum yield of reaction was 0.1, which poses no challenges to the postulated catalytic activity of eosin Y.<sup>411</sup>

**9.2.7. Other Redox-Neutral Transformations.** Recently, a polyene cyclization driven by photoredox catalysis was reported (Scheme 164).<sup>505</sup> The products (164.2) were obtained with high diastereoselectivity when phenol-containing polyene 164.1 was irradiated with eosin Y in hexafluoroisopropanol (HFIP). A number of polyene cyclizations were demonstrated, including cyclization of trien-ols (164.4) and 1,3-dicarbonyl compounds (164.5), the latter of which is notable, as there are few existing examples of enol nucleophiles in polyene cyclizations.<sup>506</sup> The products of the cyclizations contain a fully protonated “A” ring, which differs from the work of Demuth, who observed nucleophile addition to the alkene “terminus” with anti-

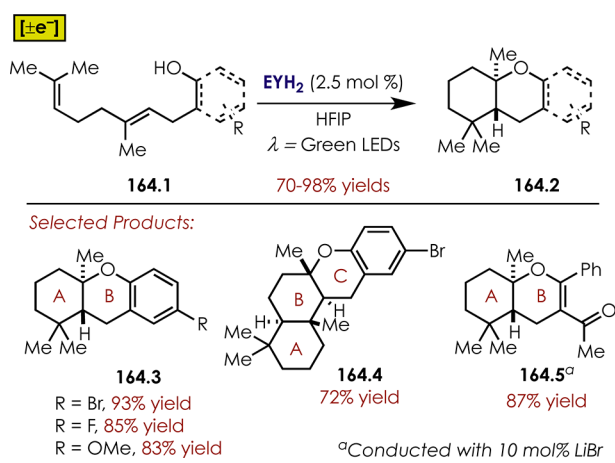
**Scheme 163.** Synthesis of Aryl Sulfides from Aryldiazonium Salts



Proposed Mechanism:



**Scheme 164.** PET-Initiated Polyene Cyclization

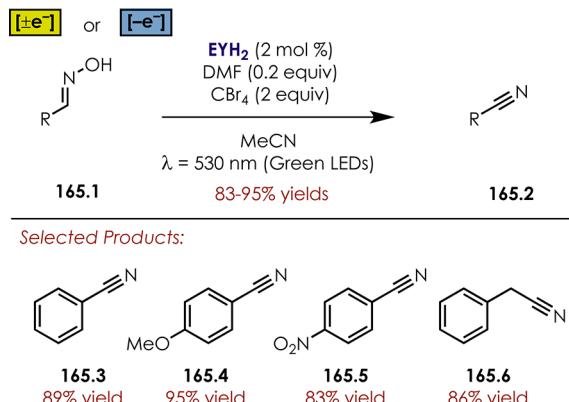


Markovnikov selectivity when an alkene cation radical was generated by PET (Scheme 16 and Scheme 69). The authors address the possibility that acid catalysis could be operating in the eosin Y conditions but found that TfOH or TsOH gives >95% conversion to a complicated mixture of adducts, including the desired product 164.3 and partially cyclized adducts. The authors suggest a mechanism that involves formation of the alkene cation radical, which is proposed to cyclize by a radical mode.<sup>507</sup> An alternative mechanism involves oxidation of the phenolic

portion, which would generate an acidic phenol cation radical [ $pK_a(\text{PhOH}\bullet^+) = -8.1$ <sup>335</sup>] capable of initiating cyclization. This is supported by quenching studies, along with the fact that the excited state reduction potential of  ${}^3\text{EYH}_2^*$  is well below what is required for oxidation of a trisubstituted aliphatic alkene [ $E_{\text{ox}}(\text{sub}\bullet^+/\text{sub}) \geq 2 \text{ V vs SCE}$ <sup>74</sup>]. Moreover, a transiently generated acid-mediated mechanism is consistent with the observation that products 164.2 are formed with the same regio- and diastereoselectivity observed in acid-catalyzed cationic polycyclizations.<sup>508-513</sup>

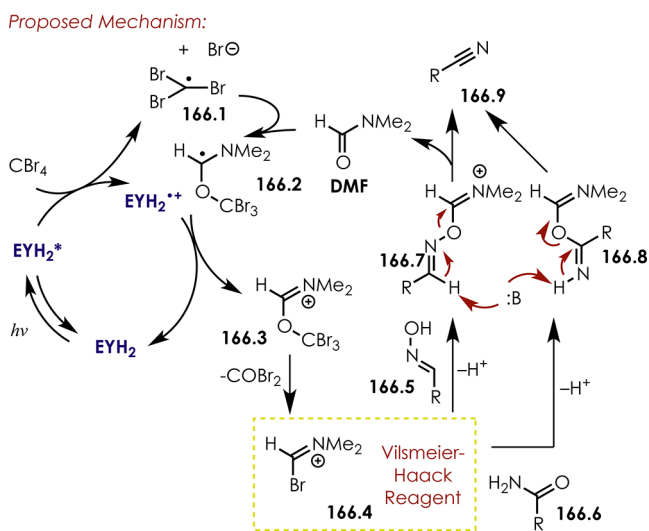
Following the lead of Stephenson and co-workers who explored the capability of transition metal photoredox catalysts in generating Vilsmeier-Haack-type salts (166.4) from DMF and  $\text{CBr}_4$ ,<sup>514,515</sup> Yadav and co-workers reported another application of the in situ generated bromoiminium 166.4 in the conversion of aldoximes and amides to nitriles (Scheme 165). With eosin

**Scheme 165.** Nitrile Synthesis from Aldoximes and Amides via Photoredox-Generated Vilsmeier-Haack Reagent



Y as the organic photoredox catalyst, both aldoximes and amides were smoothly converted to the corresponding nitriles 165.2. Remarkably, DMF could be employed in a catalytic quantity (20 mol %), which is rationalized by a proposed mechanism in which DMF can be regenerated after nitrile 166.9 is produced upon elimination from intermediate 166.7 (Scheme 166). The

**Scheme 166.** Proposed Mechanism for Photoredox-Generated Vilsmeier-Haack Reagent



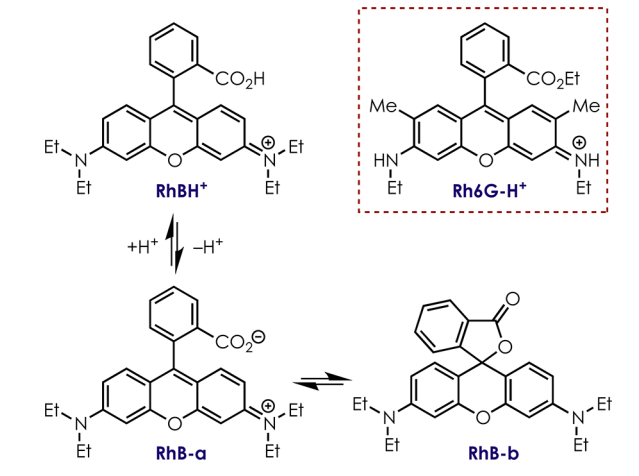
primary step in the PET cycle is a reductive cleavage of  $\text{CBr}_4$  to  $\text{CBr}_3\bullet$  and  $\text{Br}^-$ . The  $\text{CBr}_3\bullet$  radical adds to DMF to form the radical adduct **166.2**, which turns over the photoredox catalytic cycle by reduction of  $\text{EYH}_2\bullet^+$ . The authors provide a more comprehensive overview of a number other mechanistic possibilities, but the pathways shown in **Scheme 165** are sufficient to explain the apparent catalytic function of DMF.

## 10. RHODAMINES

### 10.1. Photophysical and Electrochemical Characteristics

The rhodamines share a number of structural and photophysical commonalities with their fluorescein analogues. Ease of synthesis and derivatization has allowed for design of bespoke fluorophores whose properties are tuned to applications as fluorescent probes or labels in biological studies.<sup>517</sup> Most rhodamines are highly absorptive but present similar solvent and pH sensitivities to fluoresceins. Rhodamine B (**RhB**) is an exemplar for this class and is supplied in the cationic and neutral forms, the latter existing in a solvent-dependent equilibrium between zwitterion **RhB-a** and spirolactone **RhB-b** (**Scheme 167**). While the xanthene chromophore (intact in the cationic

**Scheme 167. Forms of Two Common Rhodamine Catalysts**



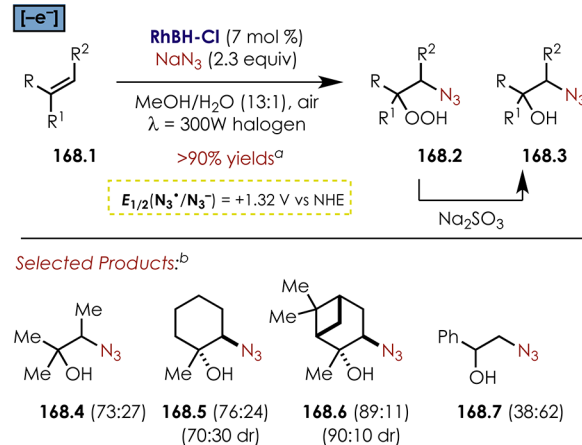
and zwitterionic forms) on Rhodamine B exhibits a strong absorption in the visible ( $\sim 550$ – $570$  nm), spirolactone **RhB-b** absorbs in the UV and is poorly fluorescent. Even though Rhodamine B possesses a moderately high fluorescence quantum yield, the properties of Rhodamine 6G (**Rh6G** or **Rh6G-H<sup>+</sup>**) are arguably better, featuring  $\phi_f > 0.9$  (di-alkyl amino-substituted rhodamines undergo deactivation of  $S_1$  by twisted intramolecular charge transfer, or TICT, whereas mono-alkyl amino-substituted do not) and enhanced apparent absorptivity (esterification of the carboxylate prevents ground state spirolactone formation). As triplet formation is typically considered to be negligible due to very low yields of ISC ( $\phi_{\text{ISC}} < 0.01$ ),<sup>97,99</sup> the singlet excited state, although short-lived ( $\sim 2$ – $4$  ns), is thought to account for most PET reactions of rhodamines.

### 10.2. Reactions

**10.2.1. Oxidation and Oxygenation Reactions.** Griesbeck and co-workers have explored a unique alkene difunctionalization reaction in a series of investigations on azidohydroperoxidation reaction facilitated by PET.<sup>518</sup>–<sup>521</sup> In an initial report,<sup>522</sup> Rhodamine B (**RhBH-Cl**) was utilized as a photoredox catalyst in the transformation along with sodium azide ( $\text{NaN}_3$ ) under

aerobic conditions, which yielded a mixture of alcohols **168.3** and hydroperoxides **168.2** as products (**Scheme 168**). The crude

**Scheme 168. Alkene Azidohydroperoxidation**



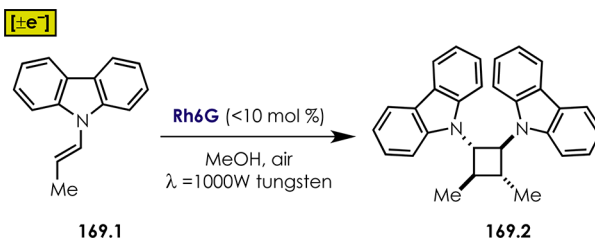
<sup>a</sup>Individual yields not specified; >90% yield of azidoalcohol is reported for all substrates after reduction with sodium sulfite ( $\text{Na}_2\text{SO}_3$ )

<sup>b</sup>(Parentheses specify the crude ratio of azidohydroperoxide to azidoalcohol)

photolysis mixtures were treated with sodium sulfite ( $\text{Na}_2\text{SO}_3$ ) to give the alcohols **168.4**–**168.7** in greater than 90% yield. The regioselectivity of the 1,2-N,O functionalization was exclusive for the products shown, demonstrating the superiority of this strategy compared to an oxirane ring opening, which gives a mixture of regioisomers.<sup>523</sup> This regioselectivity originates from an “anti-Markovnikov” addition of the azidyl radical  $\text{N}_3\bullet$  to the alkene.<sup>524</sup> The azidyl radical  $\text{N}_3\bullet$  was thought to be generated by PET from azide [ $E_{\text{ox}}(\text{N}_3\bullet/\text{N}_3^-) = 1.3$  V vs NHE]<sup>525</sup> to **RhBH<sup>++</sup>**, and this was later supported by fluorescence quenching studies.<sup>520</sup> Trapping of the alkyl radical by  $\text{O}_2$  was estimated to occur on the order of  $5 \times 10^9 \text{ M}^{-1}\text{s}^{-1}$ .<sup>520</sup>

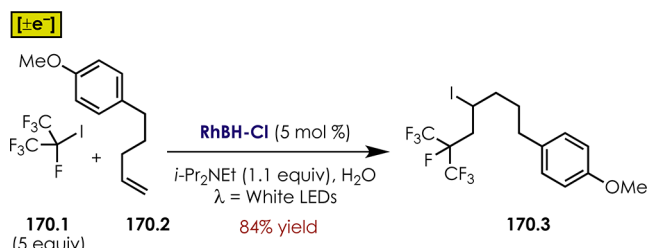
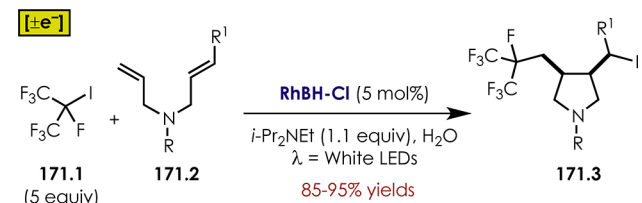
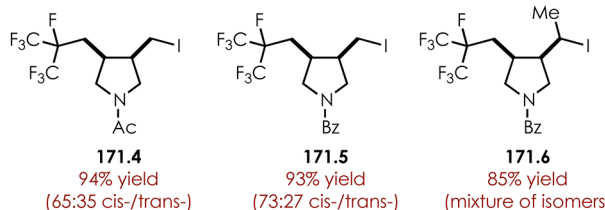
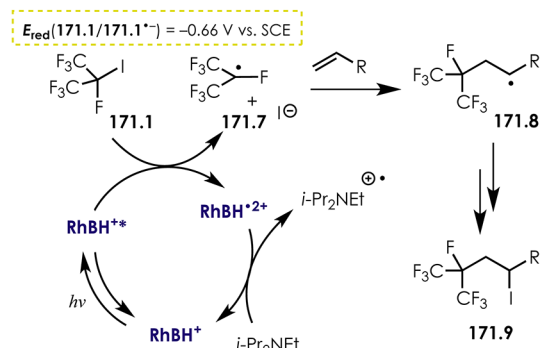
**10.2.2. Redox-Neutral Transformations.** Although Rhodamine 6G has not been extensively used as a photoredox catalyst, it was recognized by Ledwith in 1969 to mediate the cyclodimerization of enamines such as *N*-vinyl carbazole **169.1** (**Scheme 169**).<sup>526,527</sup> Other catalysts, such as **TPP<sup>+</sup>**, were also

**Scheme 169. Enamine Cyclodimerization Using Rhodamine 6G**



found to catalyze the transformation, and air evidently gave a significant improvement in reaction efficiency, prompting the authors to suggest that  $\text{O}_2$  may play a catalytic role by mediating return electron transfer to the substrate.

Harnessing the reducing activity of Rhodamine B, researchers were able to accomplish an atom transfer radical addition (ATRA) with perfluoroalkyl iodide **170.1** to alkene **170.3** (**Scheme 170**).<sup>95</sup> If the alkene substrate contained additional unsaturation (e.g., **171.2**), an intervening radical cyclization afforded cyclic products **171.4**–**171.6** (**Scheme 171**). The

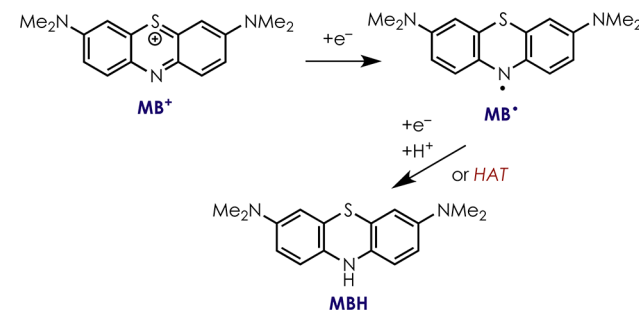
**Scheme 170. ATRA Reaction Using Rhodamine B****Scheme 171. ATRA-Intramolecular Radical Cyclization***Selected Products:**Proposed Mechanism:*

photoredox catalyst was presumed to directly reduce iodide 171.1 [ $E_{\text{red}}(171.1/171.1^\bullet) = -0.66 \text{ V vs. SCE}$ ]<sup>528</sup>, from the  $\text{RhBH}^*$  state based on the excited state oxidation potential and fluorescence quenching studies. Although a photoredox catalyst was required for the success of this reaction, triethylborane (20 mol %) was found to catalyze the transformation in comparable yields.

**11. PHENOTIAZINES****11.1. Methylene Blue: Photophysical and Electrochemical Characteristics**

Like acridine orange and protic xanthenes, methylene blue has seen diverse biological and medical applications, and its properties are likewise sensitive to solvent and protonation. Compared to the other chromophores examined in this review, methylene blue exhibits a red-shifted absorbance near 650–670 nm and is strongly absorbing ( $\epsilon = 94000$ ),<sup>85</sup> although binary and ternary aggregation results in a hypsochromic shift.<sup>529</sup> A short singlet lifetime ( $\tau_f \sim 1.0 \text{ ns}$ ) and a relatively large triplet

yield<sup>88,138</sup> render the triplet  ${}^3\text{MB}^+$  the most relevant excited state. Despite the fact that  $\text{MB}^+$  absorbs at relatively low energy,  ${}^3\text{MB}^+$  is a moderately good oxidant. Additionally, instead of behaving strictly by one-electron redox couples,  $\text{MB}^+$  can proceed from the semi-reduced form  $\text{MB}\bullet$  to *leuco*-methylene blue  $\text{MBH}$  by sequential ET or HAT mechanisms (Scheme 172).<sup>530–532</sup>

**Scheme 172. 2-Electron/1-Proton Reduction of Methylene Blue**

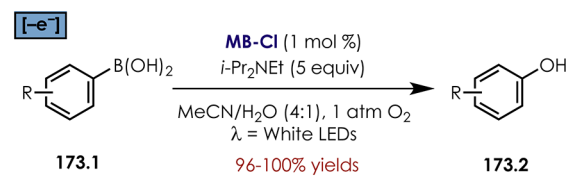
Although  $\text{MB}^+$  is an apt photosensitizer for  ${}^1\text{O}_2$  generation,<sup>88,138</sup> PET is the dominant pathway when electron donors are present in sufficient concentrations. Interestingly, the ground state reduction potential of  $\text{MB}^+$  suggests that oxidation of  $\text{MB}\bullet$  by  $\text{O}_2$  is endergonic, yet regeneration of  $\text{MB}^+$  by  $\text{O}_2$  has been observed to occur on the order of microseconds ( $k_{\text{obs}} = 5.0 \times 10^5 \text{ M}^{-1} \text{ s}^{-1}$ ).<sup>533</sup>

**11.2. Methylene Blue: Reactions**

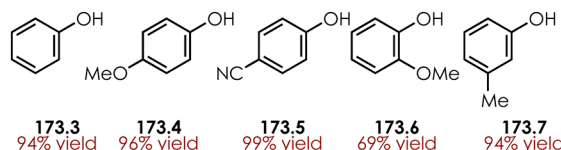
**11.2.1. Oxygenation and Oxidation Reactions.** The use of methylene blue as a photoredox catalyst was highlighted by Scaiano and co-workers in the conversion of arylboronic acids 173.1 to phenols 173.2 with  $i\text{-Pr}_2\text{NEt}$  as an additive and under an atmosphere of  $\text{O}_2$  (Scheme 173).<sup>84</sup> The reaction generally provided nearly quantitative yields for a range of arylboronic acids. A prior report disclosed that  $\text{Ru}(\text{bpy})_3^{2+}$  was capable of effecting this transformation but required at least 23 h of irradiation, and eosin Y ( $\text{EY-Na}_2$ ) afforded high yields after a 96 h reaction, whereas the methylene blue catalyzed reaction is complete after 6 h.<sup>534</sup> The previously suggested mechanism involves generation of  $\text{O}_2\bullet^-$ , which adds to the boronic acid and generates hydroperoxyborate 173.10 after H atom abstraction. Ultimately, a *B*- to *O*-1,2-aryl migration expels  $\text{OH}^-$  and creates the *O*-aryl bond. Scaiano provided an in-depth discussion of the reaction mechanism based on photophysical and kinetic studies. Laser flash photolysis studies revealed that  $i\text{-Pr}_2\text{NEt}$  quenches  ${}^3\text{MB}^{*+}$  40 times faster than the  $\text{Ru}(\text{bpy})_3^{2+}$  triplet excited state, a likely explanation for the disparity in performance of the two catalysts. Singlet oxygen was confirmed to be a negligible mechanistic intermediate, and the mechanism in Scheme 173 acknowledges that the strongly reducing  $\alpha$ -amino radical 173.8 is capable of reducing  $\text{O}_2$  along with the semi-reduced  $\text{MB}\bullet$ .

Oxidation reactions of hydrazines 174.1 were explored by Ferroud and co-workers under aerobic conditions using  $\text{MB}^+$  as a photoredox catalyst (Scheme 174).<sup>535,536</sup> Nucleophiles could add to the hydrazinium 174.6 produced by PET and subsequent loss of an H atom, giving mono-addition product 174.7. A second sequence of PET/HAT (or  $-e^-/-\text{H}^+$ ) affords the diazenium 174.8, which undergoes ring opening upon addition of a nucleophile. With  $\text{H}_2\text{O}$  and alcohols  $\text{ROH}$  as nucleophiles, aldehydes 174.2 and acetals 174.3 were produced, respectively, in moderate to excellent yields by this protocol.<sup>535</sup> With the use

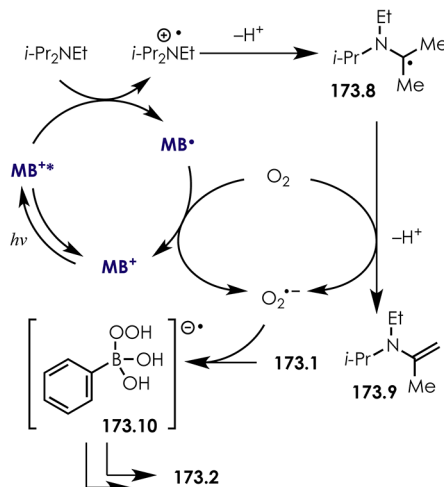
**Scheme 173.** Oxidative Hydroxylation of Arylboronic Acids



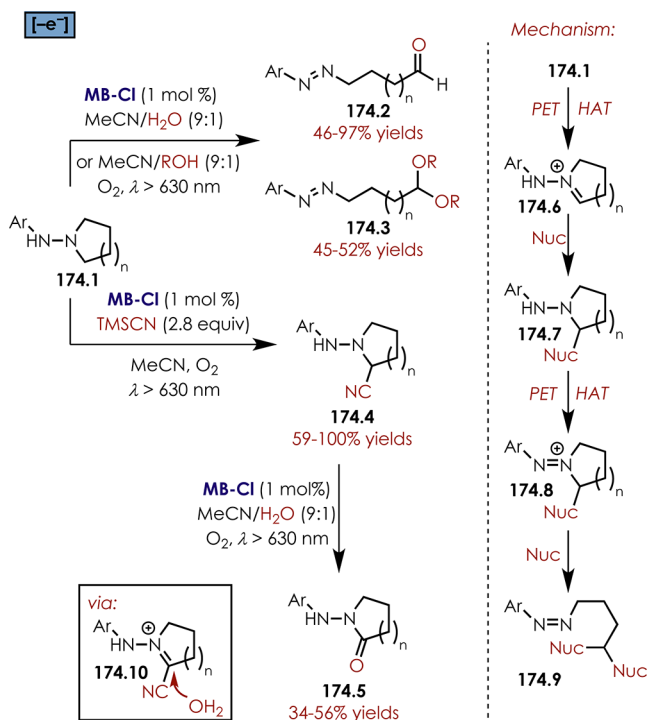
### **Selected Products:**



### *Proposed Mechanism:*



**Scheme 174. Oxidation Reactions of Pyrrolidine Hydrazines**

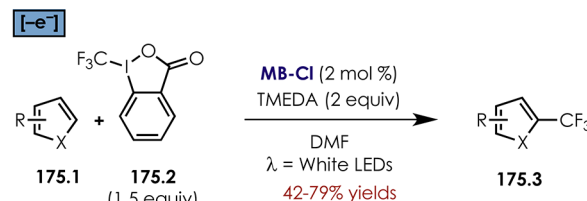


of TMSCN as a source of the  $^{13}\text{CN}$  nucleophile, only the nitriles 174–4 were observed under the conditions. However, when

nitriles **174.4** were submitted to photooxidative conditions in a mixture of MeCN/H<sub>2</sub>O, ring opening did not occur, and the lactams **174.5** were provided.<sup>536</sup> This last transformation was thought to occur by photoredox-induced formation of hydrazinium **174.10**, followed by hydrolysis and tautomerization.

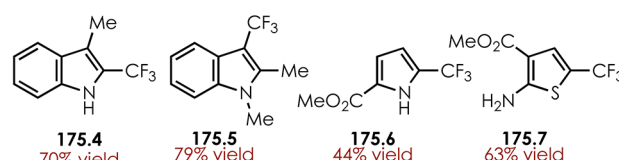
**11.2.2. Trifluoromethylation Reactions.** Scaiano and co-workers also expanded the functionality of Methylene Blue to a series of trifluoromethylation reactions with the Togni reagent 175.2 as a precursor to  $\bullet\text{CF}_3$ .<sup>537</sup> First, the C–H trifluoromethylation of heterocycles was demonstrated in a photoredox catalytic system comprised of MB-Cl and TMEDA (**Scheme 175**). A range of yields were obtained with various evaluation of

**Scheme 175. Heteroaryl C–H Trifluoromethylation**

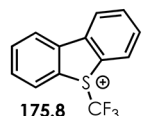


---

#### **Selected Products:**



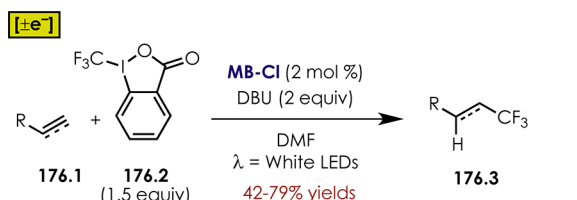
cf. 35% yield w/  
Umemoto's reagent:



indoles, pyrroles, and thiophenes under the conditions. The amine (TMEDA) was seen to play a crucial role in generating the reactive  $\bullet\text{CF}_3$  radicals: when it was omitted, only 35% yield of **175.4** was obtained. Additionally, quenching of the triplet state  $^3\text{MB}^{**}$  by TMEDA was found to be 51% efficient with the Togni reagent **175.2** present, compared to 8% quenching efficiency by TMEDA with Umemoto's reagent **175.8** used instead. These data affirm the primary function of the amine in generating the reactive  $\text{MB}\bullet$ , and the observation that Togni reagent **175.2** gives superior yields of **175.4** is consistent with the photophysical measurements. By competitively quenching  $^3\text{MB}^{**}$ , Umemoto's reagent **175.8** prevents the efficient production of  $\text{MB}\bullet$  by TMEDA.

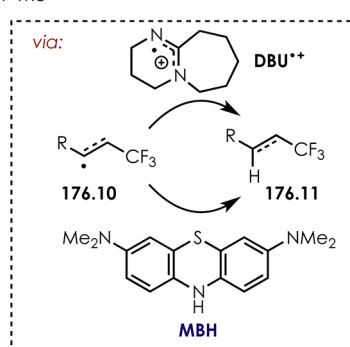
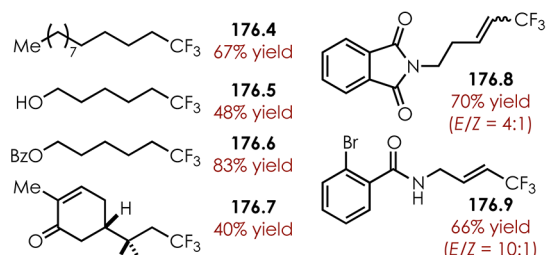
Using similar conditions, the researchers investigated trifluoromethylation of alkenes and alkynes **176.1** (**Scheme 176**).<sup>537</sup> Instead of TMEDA, 1,8-diazabicyclo[5.4.0]undec-7-ene (DBU) was used as a more efficient sacrificial reductant, and the major products were the hydrotrifluoromethylated alkenes (**176.4–176.7**) or alkynes (**176.8–176.9**) with exclusive regioselectivity. It was suggested that either the oxidized amine or the *leuco-* MBH could act as a source of hydrogen to accomplish the hydrotrifluoromethylation by HAT with the alkyl or vinyl radical **176.10**. Even though DBU was found to quench  ${}^3\text{MB}^{**}$  an order of magnitude slower than TMEDA, formation of

### Scheme 176. Olefin Hydrotrifluoromethylation



---

#### *Selected Products*



an EDA complex between DBU and  $\text{MB}^+$  in the ground state improves the efficiency of  $\text{MB}\bullet$  generation.

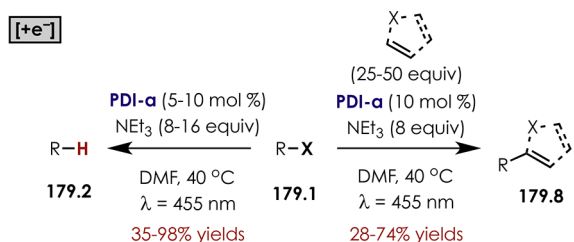
### 11.3. *N*-Phenyl Phenothiazine: Photophysical and Electrochemical Characteristics

Although employed more frequently as electron transport materials,<sup>538,539</sup> *N*-phenylphenothiazine PTh and its derivatives are electron rich and constitute good reductants in the excited state. PTh absorbs mostly in the UV with a tail in the visible and has a low ground state oxidation potential of +0.68 V vs SCE, which, in combination with a high-lying singlet and triplet excited states, contributes to the strongly reducing potentials of both excited states. Despite a short-lived singlet state, mechanistic studies have confirmed that the singlet state is operative in photoinduced oxidation of PTh. The resulting  $\text{PTh}\bullet^+$  should be sufficiently oxidizing to be turned over by an electron donor with an oxidation potential less than +0.68 V.

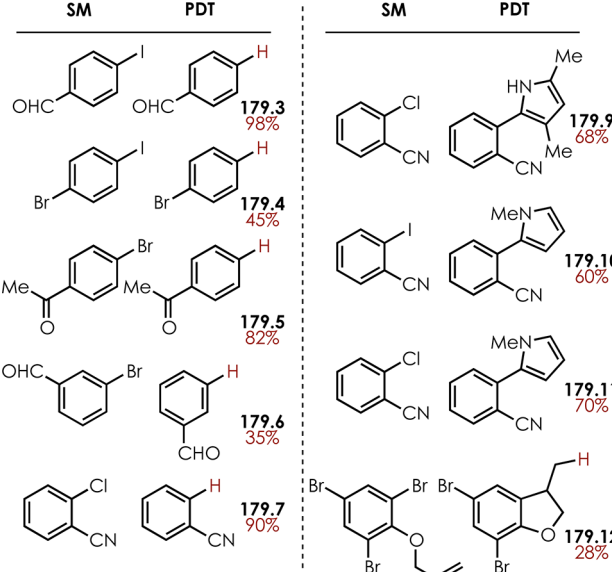
## 11.4. N-Phenyl Phenothiazine: Reactions

**11.4.1. Reductive Transformations.** In addition to its recent use as a photoredox catalyst in metal-free atom transfer radical polymerization (ATRP),<sup>83,540,541</sup> PTh was utilized by Hawker and co-workers in the hydrodehalogenation of organic halides 177.1 (Scheme 177).<sup>82</sup> With some exceptions, very good yields could be obtained from aryl iodides, bromides, and chlorides. This substrate scope is notable compared to a previous method (see Scheme 179 below), which was limited to electron deficient arenes. In contrast, the method employing PTh could hydrodehalogenate simple substrates with low reduction potentials, including bromobenzene and iodobenzene, as well as electron-rich arenes (e.g., 177.4, 177.5, and 177.8). Additionally, an alkyl bromide was successful in this protocol

**Scheme 177. Arene hydrodehalogenation**



### Examples:



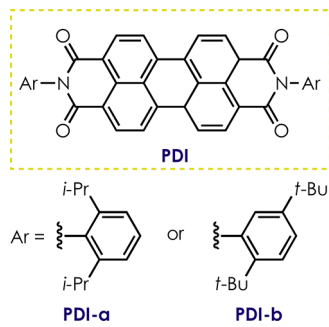
(providing 177.7), and a cyclization of an allylic ether captured the aryl radical intermediate en route to dihydrobenzofuran 177.12. The reaction can be run in the presence of O<sub>2</sub> with no penalty on yield. Moreover, fluorescence quenching was observed, implicating the singlet state <sup>1</sup>PTh\* as the active excited state, with minimal involvement of the triplet <sup>3</sup>PTh\* inferred from other mechanistic probes. The proposed mechanism accounts for <sup>1</sup>PTh\* as a strong reductant, inducing reductive cleavage of the aryl iodide to generate an aryl radical 177.13. Although formic acid HCO<sub>2</sub>H gives a slight improvement in yield when used with *n*-Bu<sub>3</sub>N, HCO<sub>2</sub>H is not essential. HAT by HCO<sub>2</sub>H is considered a minor pathway, while a majority of the hydrodehalogenated product is thought to originate from H atom abstraction from the cation radical *n*-Bu<sub>3</sub>N•<sup>+</sup> formed upon turnover of the catalytic cycle. That *n*-Bu<sub>3</sub>N is the major source of H atoms was substantiated by deuterium-labeling studies.

## 12. OTHER ORGANIC PHOTOREDOX CATALYSTS

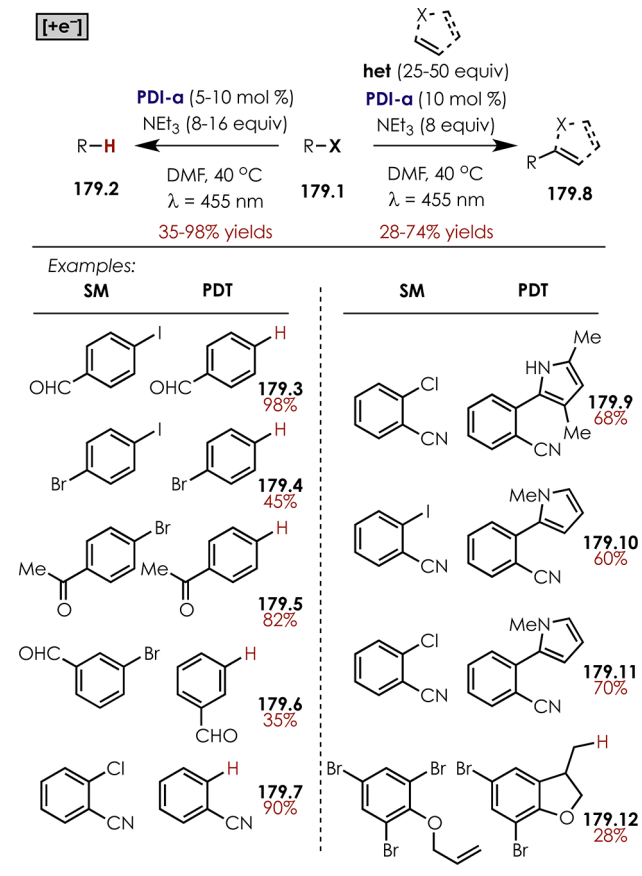
## 12.1. Perylene Diimides: Photophysical and Electrochemical Characteristics and Reactions

The hydrodehalogenation work with PTh discussed above was preceded by a report from König and co-workers which detailed the use of perylene diimide (a) (PDI-a, see Scheme 178) as a photoredox catalyst to accomplish this transformation (Scheme 179).<sup>542</sup> The yields of the dehalogenated arenes 179.2 were variable but useful, although the protocol could not be successfully applied to more electron-rich arenes or nitroarenes. However, the aryl radicals could be harnessed in the C–H

Scheme 178. Perylene Diimides



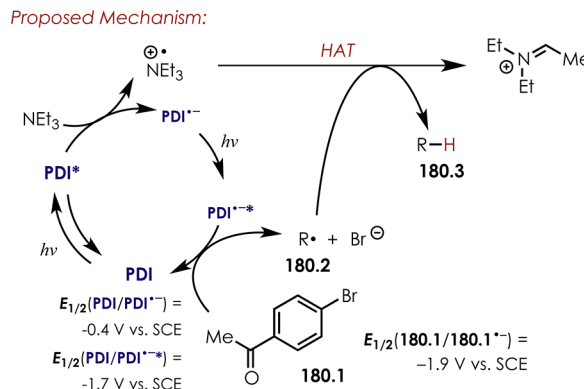
Scheme 179. Arene Hydrodehalogenation and Coupling Reactions with PDI Photoredox Catalyst



arylation of heteroarenes to give 179.9–179.11 or a cyclization to dihydrobenzofuran 179.12.

An intriguing aspect of this report is the proposed mechanism of the PET catalyst (Scheme 180), which is a two-photon process involving consecutive transfers and excitation of the radical anion  $\text{PDI}^{\bullet-}$  in order to generate the strong reductant  $\text{PDI}^{\bullet-}\text{*}$ . The researchers were prompted to consider this unusual mechanistic scenario after observing that this system was capable of hydrodehalogenation in aryl halides which possess reduction potentials that are too negative to be reduced by  $\text{PDI}^{\bullet-}$  or  $\text{PDI}^*$ : for frame of reference, 4'-bromoacetophenone 180.1 has a reduction potential of  $-1.9 \text{ V vs SCE}$ ,<sup>543</sup> while  $E_{\text{red}}(\text{PDI-b}/\text{PDI-b}^{\bullet-}) = -0.43 \text{ V vs SCE}$ <sup>106</sup> and  $E_{\text{ox}}(\text{PDI-b}^{\bullet+}/\text{PDI-b}^{\bullet-}) = -0.72 \text{ V vs SCE}$ .  $\text{PDI-a}^{\bullet-}$  was observed upon irradiation of  $\text{PDI-a}$  with  $\text{NEt}_3$ ,<sup>542</sup> and König reasoned that  $\text{PDI}^{\bullet-}\text{*}$  was the only reductant capable of achieving ET to the halides 179.1.

Scheme 180. Proposed Mechanism for Arene Hydrodehalogenation with PDI Photoredox Catalyst



$[E_{\text{ox}}(\text{PDI-b}/\text{PDI-b}^{\bullet-}\text{*}) = -1.73 \text{ V vs SCE}$ , calculated from an  $E_{0/0}$  of 1.3 eV for  $\text{PDI-b}^{\bullet-}\text{*}$ ]. Considering that  $\text{PDI-b}^{\bullet-}\text{*}$  has a lifetime of only 145 ps,<sup>106</sup> it seems possible that a preassociation between  $\text{PDI}^{\bullet-}$  and aryl halide could be at play, as the picosecond lifetime would render diffusion-controlled bimolecular chemistry unlikely.

### 12.2. Diazapyrenium: Photophysical and Electrochemical Characteristics and Reactions

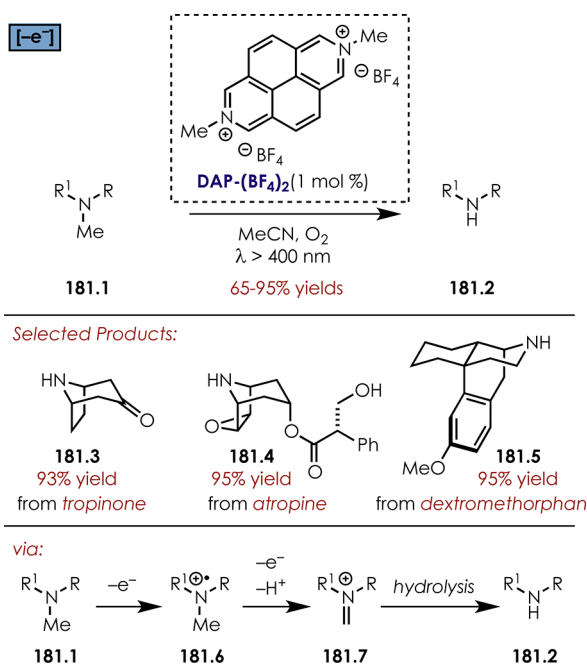
The ground state absorbance and fluorescence properties of dimethyldiazapyrenium ( $\text{DAP}^{2+}$ )<sup>544</sup> have been studied in relation to host-guest complexation<sup>103,104,545</sup> and the use of  $\text{DAP}^{2+}$  as a sensor<sup>546,547</sup> in a variety of applications. This dicationic analogue to methyl viologen absorbs in the visible (~420 nm) and is a potent oxidant in the singlet excited state. Its PET applications in the synthetic context have been little explored since Rigaudy demonstrated that  $\text{DAP}^{2+}$  was useful in  $\alpha$ -C-H functionalizations of tertiary alkyl amines.<sup>548,549</sup> First, the oxidative demethylation of tertiary alkylamines 181.1 was reported using  $\text{DAP}^{2+}$  as a photoredox catalyst and under  $\text{O}_2$  (Scheme 181).<sup>548</sup> The mechanism was assumed to follow a similar mechanism to the reactions of tertiary alkyl amines discussed throughout this review, ultimately furnishing the secondary amine products by hydrolysis of an iminium or decomposition of an  $\alpha$ -aminoperoxy species.<sup>550</sup> This method was applied to the demethylation of several pharmacologically relevant alkaloids, such as tropinone (181.3), atropine (181.4), and dextromethorphan (181.5), and the secondary amines were obtained in excellent yields.

Envisioning that an iminium intermediate generated through a similar mechanism could be trapped with a nucleophile, Rigaudy and co-workers used this system to achieve the  $\alpha$ -cyanation of tertiary amines 182.1 (Scheme 182).<sup>549</sup> With TMSCN as a source of  $^-\text{CN}$ , the aerobic conditions gave excellent yields of the  $\alpha$ -aminonitriles 182.3. Again, the substrate scope featured structurally complex alkaloids, yet the nitriles 182.4–182.8 were produced with impressive chemoselectivity and diastereoselectivity.

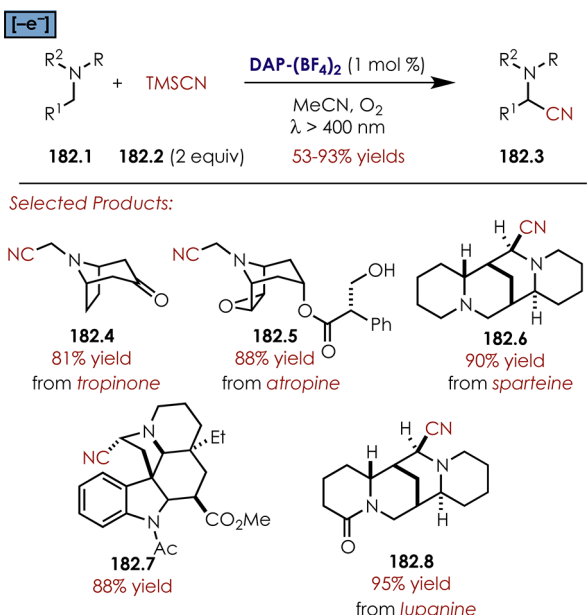
### 12.3. Phenazinium Salts: Photophysical and Electrochemical Characteristics/Reactions

N-Alkylphenazinium salts (e.g.,  $\text{PZ}^+$ , Scheme 183) are related to the phenothiazines such as methylene blue and can access the 2-electron/1-proton reduced form  $\text{PZH}$ , analogous to *leuco-MBH*. The safranin dyes, belonging to the phenazinium family, are largely used in biological applications<sup>551</sup> and despite the fact that their PET properties have been studied,<sup>88,552,553</sup> few examples

**Scheme 181.** Oxidative Demethylation of Tertiary Methylamine Alkaloids

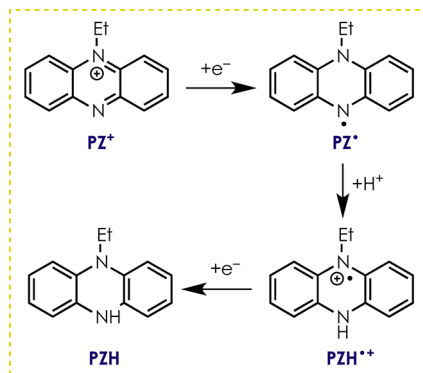


**Scheme 182.**  $\alpha$ -Cyanation of Tertiary Amine Alkaloids with TMSCN

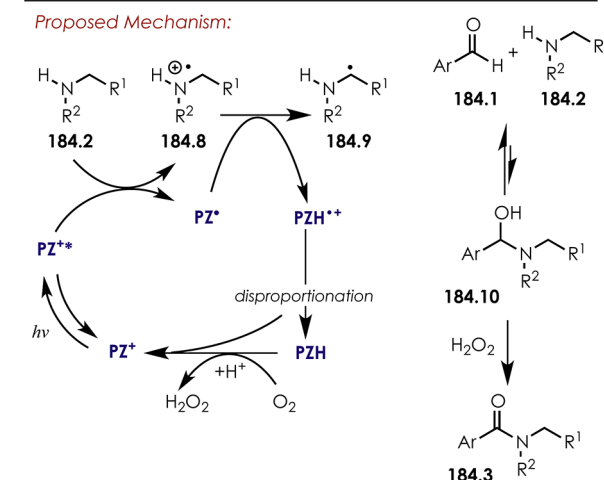
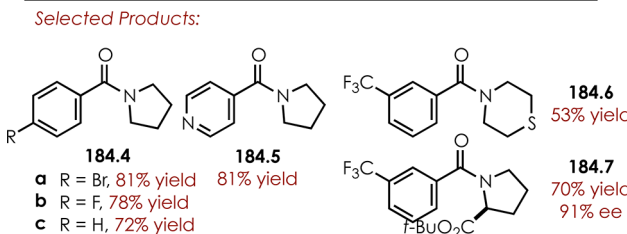
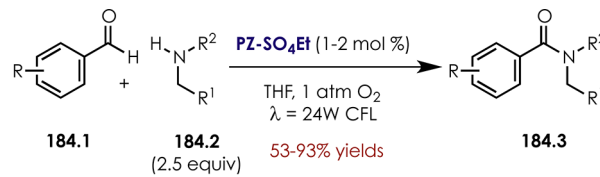


can be found where phenaziniums are used as photoredox catalysts. However, one recent example demonstrated that they can be valuable members of the photoredox catalyst toolbox: *N*-ethylphenazinium ethylsulfate **PZ-SO<sub>4</sub>Et** successfully catalyzed the light-driven oxidative coupling of secondary amines **184.2** and aryl aldehydes **184.1** (**Scheme 184**).<sup>554</sup> An extensive survey of photoredox catalysts identified the phenazinium class to give the highest yields, and ultimately, an atmosphere of O<sub>2</sub> provided the most efficient conditions with **PZ-SO<sub>4</sub>Et** as a catalyst. This methodology gave appreciable yields of amides **184.3** from a varied set of secondary amine and aryl aldehyde coupling partners. Notably, a L-proline ester was coupled with minimal

**Scheme 183.** 2-Electron/1-Proton Reduction of Phenazinium



**Scheme 184.** Amide Synthesis by Aerobic Coupling of Aldehydes with Amines



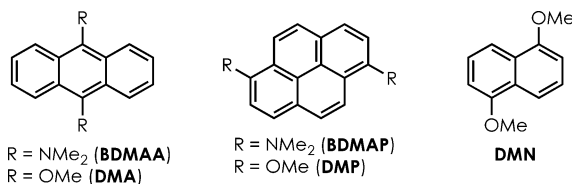
erosion of enantiomeric purity (see amide **184.7**). The oxidative amidation of aldehydes and secondary amines using H<sub>2</sub>O<sub>2</sub> is preceded,<sup>555,556</sup> and the authors' understanding of the mechanism is accordingly based on the oxidation of aminal **184.10** by H<sub>2</sub>O<sub>2</sub>. The primary role of **PZ<sup>+</sup>** in the PET cycle is to generate H<sub>2</sub>O<sub>2</sub>, and it does so by first engaging in PET with secondary amine **184.2**. After **PZ<sup>•</sup>** deprotonates the amine cation radical, the so-formed **PZH<sup>•+</sup>** undergoes disproportionation to **PZ<sup>+</sup>** and **PZH** in the presence of a base, and O<sub>2</sub> reacts with **PZH** to generate H<sub>2</sub>O<sub>2</sub>.<sup>557</sup> The secondary amine and **PZ<sup>+</sup>** were observed to reside primarily as a ground state EDA complex as indicated by a drastic change in the **PZ<sup>+</sup>** absorbance spectrum

upon addition of **184.2** and a series of fluorescence intensity measurements supported a static quenching process. Both observations are consistent with the notion that the amine, present in excess, is a sacrificial reductant for the generation of  $\text{H}_2\text{O}_2$ .

#### 12.4. Electron-Rich Anthracenes and Pyrenes: Photophysical and Electrochemical Characteristics/Reactions

Dimethylamino and dimethoxy-substituted anthracenes and pyrenes have been developed as some of the more rare examples of catalytic organic photoreductants for synthetic transformations. The vast majority of the use of these organic photoreductants has been in stoichiometric quantities and will not be covered in depth in this review, but we direct the reader to the following references for further information.<sup>558–563</sup> The four main photoredox catalysts in this category that will be discussed are 1,6-bis(dimethylamino)pyrene (**BDMAP**), 1,6-dimethoxypyrene (**DMP**), 9,10-bis(dimethylamino)anthracene (**BDMAA**), and 9,10-dimethoxyanthracene (**DMA**) (Scheme 185). In general, all of these aromatics absorb in the blue-violet

**Scheme 185.** Anthracene and Pyrene Photoreductants

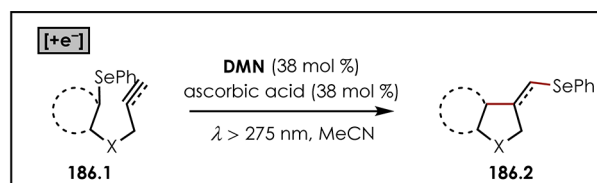


region of the electromagnetic spectrum (400–490 nm) and possess excited state oxidation potentials [ $E^*_{\text{ox}}$  between –2.0 to –2.4 V vs SCE], making them potent reductants in the excited state.<sup>564</sup> In the ground state, the two pyrenes, **BDMAP** and **DMP**, have nearly completely reversible cyclic voltammograms, whereas the two anthracene catalysts, **BDMAA** and **DMA**, do not. The irreversibility of **BDMAA** and **DMA** with respect to single-electron redox pathways certainly presents a significant challenge to their development as photoredox catalysts. The excited state donor, 1,5-dimethoxynaphthalene (**DMN**) has a reported excited state oxidation potential of  $E_{1/2}(\text{DMN}\bullet^+/\text{DMN}^*) = -2.5$  V vs SCE by virtue of absorbance further in the UV region (300 nm).<sup>559</sup>

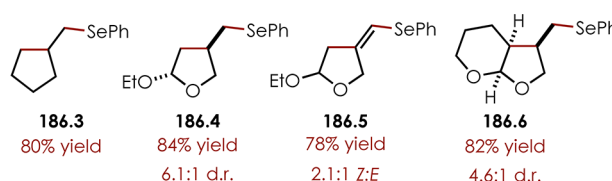
All of the aforementioned anthracene and pyrene compounds are reactive through a singlet excited state, which is a generally short-lived  $\tau$ , presenting further hurdles to the use of these compounds as effective redox catalysts. **DMN** also has a singlet excited state ( $\tau = 12.6$  ns)<sup>559</sup> that is reactive. In addition, since single-electron transfer between these compounds and a substrate produces a cation radical-anion radical pair, back electron transfer can become problematic due to electrostatic attraction. To minimize this scenario, more polar solvents are often employed.<sup>564</sup>

Some of the first use of this class of photoreductants as catalysts was for the generation of carbon radicals from alkyl selenides (**186.1**) (Scheme 186).<sup>565</sup> Pandey and coworkers employed **DMN** as the photoredox catalyst in conjunction with ascorbic acid as the stoichiometric reductant to effect atom transfer radical cyclizations. Five-membered rings cyclized in high efficiency to afford the expected atom transfer cyclization adducts (**186.2**), whereas 6-exo-type radical cyclizations at best gave 10% yields. With respect to the mechanism, it was proposed that the key step was reduction of the selenide substrates [ $E_{\text{red}}$

**Scheme 186.** Alkyl Selenide Atom Transfer Cyclizations



Selected Scope:



(**186.1/186.1•<sup>-</sup>**) = –1.0 to –0.29 V vs SCE] to effect cleavage to the alkyl radical and selenide anion. These represent mild conditions for radical generation from alkyl selenides.

Electron-rich anthracene and pyrene photoredox catalysts have been employed effectively in ketyl radical chemistry by Hasegawa and coworkers.<sup>564,566</sup> Using dimethyldihydrobenzimidazoles (e.g., **187.8**, **187.9**) as the stoichiometric electron and proton donors, the authors demonstrated  $\alpha$ -keto epoxide ring opening (**187.1**–**187.2**), radical cyclizations of alkyl bromides (**187.3**–**187.4**), ketyl radical cyclizations (**187.5**–**187.6**), and pinacol coupling of benzophenones (**187.7**–**187.8**) (Scheme 187). In the case of **187.9** as the electron donor, no additional acid additive was required as the phenol was presumed to act as the proton donor. In general, the pyrene photoreductants gave higher yields for the reactions that were investigated, potentially pointing to their higher redox stability over the anthracene photoreductants.

#### 12.5. Flavins

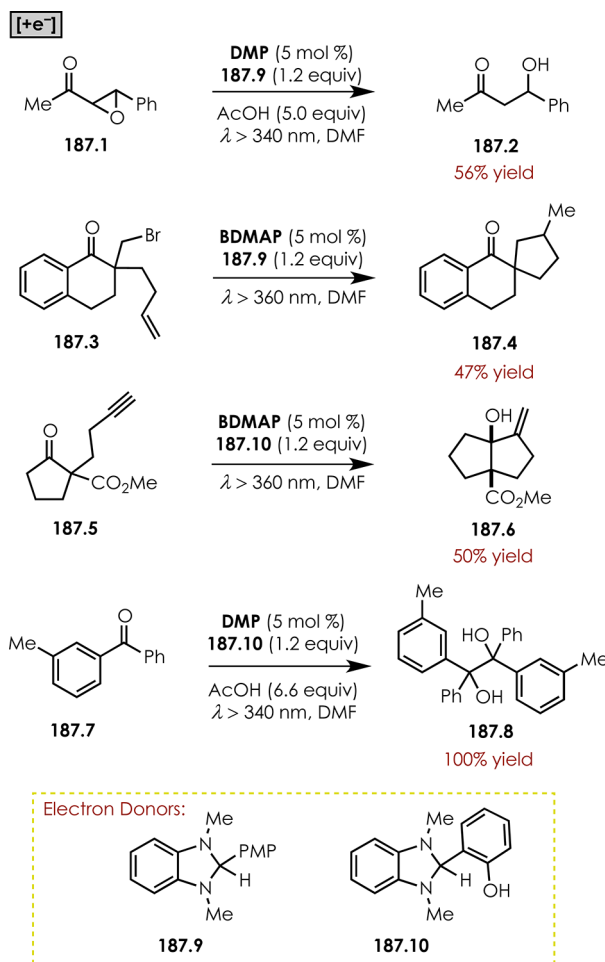
Riboflavin and riboflavin tetraacetate have also been known to mediate photoredox transformations. Photoredox catalytic benzylic oxidations, such as the one shown in Scheme 78, were demonstrated by Fukuzumi,<sup>567</sup> König,<sup>568–571</sup> and Wolf<sup>572,573</sup> using riboflavin and related derivatives. Recently, Gilmour and Metternich demonstrated that the E- to Z-isomerization of cinnamic acid derivatives **188.1** is catalyzed by (–)-riboflavin.<sup>574</sup> This likely occurs by an energy transfer process, but a subsequent report demonstrated that the isomerization can be followed by intramolecular aryl C–H functionalization with coumarins **188.2** as products when conducted under aerobic conditions.<sup>575</sup> The synthesis of the coumarins by riboflavin-mediated isomerization/C–H functionalization is shown in Scheme 188.

Several substrates tested in the decarboxylative fluorination shown in Scheme 105 also underwent reaction when riboflavin was the photoredox catalyst.<sup>394</sup>

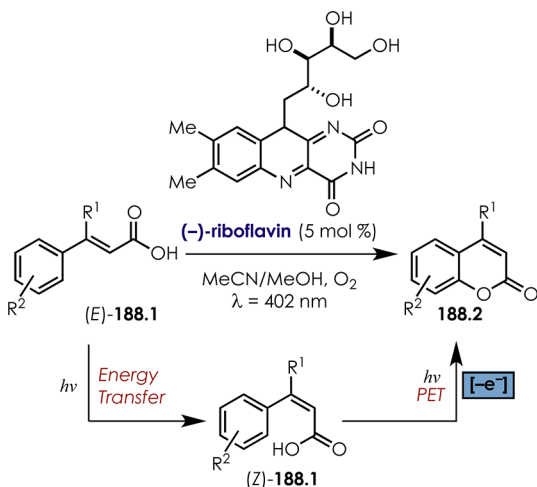
#### 12.6. BODIPY Dyes

Although boron-dipyrromethene (BODIPY) dyes comprise a vast set of light-absorbing and emitting molecules with tunable properties,<sup>576</sup> their use in organic photoredox reactions is extremely limited. Falvey demonstrated that BODIPY dyes were competent photoredox mediators for the photoinduced cleavage of *N*-alkyl-4-picolinium esters **189.1** and **189.2** as applied to the photorelease of carboxylic acids (e.g., **189.3**) and phosphates (e.g., **189.4**, Scheme 189).<sup>577</sup> Although a stoichiometric quantity of the dye was used in this method, high quantum yields suggested it might be employed as a catalyst. Additional reports

Scheme 187. Anthracene and Pyrene Photoreductants



Scheme 188. Synthesis of Coumarins from Cinnamic Acids by Riboflavin-Mediated Isomerization/C–H Functionalization

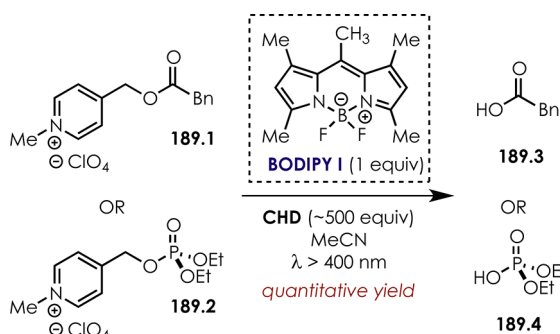


showed that several of the dehydrogenative coupling reactions of tetrahydroisoquinolines discussed in section 9.2 could also be performed with BODIPY dyes.<sup>578,579</sup>

### 13. CONCLUSIONS

It is clear from the wealth of chemical reactivity in this review that organic photoredox catalysis will offer practitioners of organic

Scheme 189. BODIPY-Mediated Photoinduced Cleavage of N-Methyl Picolinium Esters



synthesis with new tools to apply to a number of fields. The astonishing array of reactivity including cycloadditions, atom transfer cyclizations, C–H functionalizations, alkene hydrofunctionalizations, and bond cleavage reactions holds promise for utility in organic synthesis. Noteworthy is the overall mild nature of the reaction conditions that are tolerant of a variety of complex functionality.

Despite the significant advances in the last 40 years in the field of organic photoredox catalysis, there remain many opportunities for further exploration. With regard to organic photoredox catalyst development, there is a clear paucity of highly reducing catalysts that are available, and the identification of more robust chromophores is always in demand. Additionally, while there have been many reports of C–H functionalization utilizing organic photoredox catalysis, there are many challenges that remain, including site specificity and functionalization of stronger C–H bonds. Methods for controlling enantioselectivity are scarce and present exciting new challenges for researchers. Applications of organic photoredox catalysis to natural product synthesis are just starting to occur, and it will be intriguing to see how these protocols are implemented in the context of complex molecule synthesis. Lastly, it remains to be seen how or if organic photoredox will interface with other scientific disciplines such as materials science and biology. All of these areas are sure to bring a wealth of interesting and important science for decades to come.

### AUTHOR INFORMATION

#### Corresponding Author

\*E-mail: [nicewicz@unc.edu](mailto:nicewicz@unc.edu).

#### Notes

The authors declare no competing financial interest.

#### Biographies

Nathan A. Romero was born in 1990 in Grand Rapids, MI. He attended Calvin College, obtaining a B.S. in Chemistry in 2012 after carrying out undergraduate research under the supervision of Prof. Carolyn Anderson. Nathan began graduate studies at the University of North Carolina at Chapel Hill in 2012, where he joined the Nicewicz group. Nathan has a particular interest in photoredox catalytic reaction mechanisms, and his research in the Nicewicz group has focused on mechanistic analysis and the development of new transformations using acridinium photoredox catalysts.

David A. Nicewicz completed his B.S. and M.S. in Chemistry in 2000 and 2002, respectively, at the University of North Carolina at Charlotte under the direction of Professor Craig A. Ogle. David then moved to the University of North Carolina at Chapel Hill and began his graduate work with Professor Jeffrey S. Johnson in 2006. Under Professor Johnson's

direction, David's research focused on the implementation of the Brook rearrangement in synthetic methodology and its application to the total synthesis of zaragozic acid C. Upon completion of his Ph.D. studies in 2006, David returned to his native New Jersey where he was a Ruth L. Kirschstein National Institutes of Health Postdoctoral Researcher in the laboratories of Professor David MacMillan at Princeton University. While in MacMillan's lab, David developed the use of photoredox catalysis in organic synthesis. In July of 2009, Dave returned to the University of North Carolina at Chapel Hill as an Assistant Professor of Chemistry and in 2015 was promoted to Associate Professor. Research in the Nicewicz laboratory focuses on harnessing photoinduced single electron redox manifolds to discover and invent new and complex transformations in organic synthesis.

## ACKNOWLEDGMENTS

N.A.R. was supported by an NSF Predoctoral Fellowship. D.A.N. is grateful for support from Amgen Young Investigator and Camille Dreyfus Teacher-Scholar Awards.

## ABBREVIATIONS

Ad	adamantyl
ATRA	atom transfer radical addition
Bn	benzyl
Boc	<i>tert</i> -butyloxycarbonyl
Bz	benzoyl
Cbz	carboxybenzyl
CFL	compact fluorescent lamp
CHD	1,4-cyclohexadiene
Cy	cyclohexyl
DBU	1,8-diazabicyclo[5.4.0]undec-7-ene
DFT	density functional theory
DMA	<i>N,N</i> -dimethylacetamide
Fc	ferrocene
FMOC	fluorenylmethyloxycarbonyl
GO	graphene oxide
G-RuO <sub>2</sub>	graphene-supported RuO <sub>2</sub> nanocomposite
HFIP	hexafluoroisopropanol
LED	light-emitting diode
Ms	methanesulfonyl
MS	molecular sieve
MTS	methyl thiosalicylate
NHE	normal hydrogen electrode
Ns	<i>ortho</i> -nitrophenylsulfonyl
Phth	phthalimide
PMB	<i>para</i> -methoxybenzyl
PMP	<i>para</i> -methoxyphenyl
PRCC	polar radical crossover cycloaddition
RAFT	reversible addition–fragmentation chain transfer
ROMP	ring-opening metathesis polymerization
SCE	saturated calomel electrode
SDS	sodium dodecyl sulfate
TBS	<i>tert</i> -butyldimethylsilyl
TEMPO	(2,2,6,6-tetramethyl-piperidin-1-yl)oxyl
Tf	trifluoromethylsulfonyl
TFA	trifluoroacetic acid
TFE	trifluoroethanol
TMEDA	tetramethyl ethylenediamine
TMS	trimethylsilyl
Ts	<i>para</i> -toluenesulfonyl

## REFERENCES

- Prier, C. K.; Rankic, D. A.; MacMillan, D. W. C. Visible Light Photoredox Catalysis with Transition Metal Complexes: Applications in Organic Synthesis. *Chem. Rev.* **2013**, *113*, 5322–5363.
- Xi, Y.; Yi, H.; Lei, A. Synthetic Applications of Photoredox Catalysis with Visible Light. *Org. Biomol. Chem.* **2013**, *11*, 2387–2403.
- Xuan, J.; Xiao, W.-J. Visible-Light Photoredox Catalysis. *Angew. Chem., Int. Ed.* **2012**, *51*, 6828–6838.
- Tucker, J. W.; Stephenson, C. R. J. Shining Light on Photoredox Catalysis: Theory and Synthetic Applications. *J. Org. Chem.* **2012**, *77*, 1617–1622.
- Ischay, M. A.; Yoon, T. P. Accessing the Synthetic Chemistry of Radical Ions. *Eur. J. Org. Chem.* **2012**, *2012*, 3359–3372.
- Reckenthaler, M.; Griesbeck, A. G. Photoredox Catalysis for Organic Syntheses. *Adv. Synth. Catal.* **2013**, *355*, 2727–2744.
- Narayanan, J. M. R.; Stephenson, C. R. J. Visible Light Photoredox Catalysis: Applications in Organic Synthesis. *Chem. Soc. Rev.* **2011**, *40*, 102.
- Julliard, M.; Chanon, M. Photoelectron-Transfer Catalysis: Its Connections with Thermal and Electrochemical Analogs. *Chem. Rev.* **1983**, *83*, 425–506.
- Miranda, M. A.; Garcia, H. 2,4,6-Triphenylpyrylium Tetrafluoroborate as an Electron-Transfer Photosensitizer. *Chem. Rev.* **1994**, *94*, 1063–1089.
- Fagnoni, M.; Dondi, D.; Ravelli, D.; Albini, A. Photocatalysis for the Formation of the C–C Bond. *Chem. Rev.* **2007**, *107*, 2725–2756.
- Hoffmann, N. Efficient Photochemical Electron Transfer Sensitization of Homogeneous Organic Reactions. *J. Photochem. Photobiol., C* **2008**, *9*, 43–60.
- Ravelli, D.; Dondi, D.; Fagnoni, M.; Albini, A. Photocatalysis. A Multi-Faceted Concept for Green Chemistry. *Chem. Soc. Rev.* **2009**, *38*, 1999–2011.
- Ravelli, D.; Fagnoni, M.; Albini, A. Photoorganocatalysis. What For? *Chem. Soc. Rev.* **2013**, *42*, 97–113.
- Marin, M. L.; Santos-Juanes, L.; Arques, A.; Amat, A. M.; Miranda, M. A. Organic Photocatalysts for the Oxidation of Pollutants and Model Compounds. *Chem. Rev.* **2012**, *112*, 1710–1750.
- Fukuzumi, S.; Ohkubo, K. Organic Synthetic Transformations Using Organic Dyes as Photoredox Catalysts. *Org. Biomol. Chem.* **2014**, *12*, 6059–6071.
- Hari, D. P.; König, B. Synthetic Applications of Eosin Y in Photoredox Catalysis. *Chem. Commun.* **2014**, *50*, 6688–6699.
- Turro, N. J. *Principles of Molecular Photochemistry: An Introduction*; University Science Books: Sausalito, California, 2009.
- Akasaki, I. Nobel Lecture: Fascinated Journeys into Blue Light. *Rev. Mod. Phys.* **2015**, *87*, 1119–1131.
- Amano, H. Nobel Lecture: Growth of GaN on Sapphire via Low-Temperature Deposited Buffer Layer and Realization of P-Type GaN by Mg Doping Followed by Low-Energy Electron Beam Irradiation. *Rev. Mod. Phys.* **2015**, *87*, 1133–1138.
- Nakamura, S. Nobel Lecture: Background Story of the Invention of Efficient Blue InGaN Light Emitting Diodes. *Rev. Mod. Phys.* **2015**, *87*, 1139–1151.
- Mangion, D.; Kendall, J.; Arnold, D. R. Photosensitized (Electron-Transfer) Deconjugation of 1-Arylcyclohexenes. *Org. Lett.* **2001**, *3*, 45–48.
- Ohkubo, K.; Suga, K.; Morikawa, K.; Fukuzumi, S. Selective Oxygenation of Ring-Substituted Toluenes with Electron-Donating and -Withdrawing Substituents by Molecular Oxygen via Photoinduced Electron Transfer. *J. Am. Chem. Soc.* **2003**, *125*, 12850–12859.
- Arnold, D. R.; Maroulis, A. J. Radical Ions in Photochemistry. 3. Photosensitized (Electron Transfer) Cleavage Of Beta-Phenethyl Ethers. *J. Am. Chem. Soc.* **1976**, *98*, 5931–5937.
- Görner, H.; Warzecha, K.-D.; Demuth, M. Cyclization of Terpenoid Dicarbonitrile Polyalkenes upon Photoinduced Electron Transfer to 1,4-Dicyano-2,3,5,6-Tetramethylbenzene and Other Cyanoarenes. *J. Phys. Chem. A* **1997**, *101*, 9964–9973.

- (25) Wang, Y.; Haze, O.; Dinnocenzo, J. P.; Farid, S.; Farid, R. S.; Gould, I. R. Bonded Exciplexes. A New Concept in Photochemical Reactions. *J. Org. Chem.* **2007**, *72*, 6970–6981.
- (26) Gould, I. R.; Ege, D.; Moser, J. E.; Farid, S. Efficiencies of Photoinduced Electron-Transfer Reactions: Role of the Marcus Inverted Region in Return Electron Transfer within Geminate Radical-Ion Pairs. *J. Am. Chem. Soc.* **1990**, *112*, 4290–4301.
- (27) Darmanyan, A. P. Experimental Study of Singlet-Triplet Energy Transfer in Liquid Solutions. *Chem. Phys. Lett.* **1984**, *110*, 89–94.
- (28) Kanner, R. C.; Foote, C. S. Singlet Oxygen Production from Singlet and Triplet States of 9,10-Dicyanoanthracene. *J. Am. Chem. Soc.* **1992**, *114*, 678–681.
- (29) Heller, H. C. Utilization of ( $N,\pi^*$ ) Excitation Bands in the Formation of Radicals. II. Thiobenzophenone Anion Radical. *J. Am. Chem. Soc.* **1967**, *89*, 4288–4294.
- (30) Timpe, H.-J.; Kronfeld, K.-P.; Lammel, U.; Fouassier, J.-P.; Lougnot, D.-J. Excited States of Ketones as Electron Donors—ketone—iodonium Salt Systems as Photoinitiators for Radical Polymerization. *J. Photochem. Photobiol., A* **1990**, *52*, 111–122.
- (31) Timpe, H.-J.; Kronfeld, K.-P. Light-Induced Polymer and Polymerization Reactions XXXII: Direct Photoinitiation of Methyl Methacrylate Polymerization by Excited States of Ketones. *J. Photochem. Photobiol., A* **1989**, *46*, 253–267.
- (32) Suppan, P. Photoreactivity of Michler's Ketone in Solution. *J. Chem. Soc., Faraday Trans. 1* **1975**, *71*, 539–547.
- (33) Pavlishchuk, V. V.; Addison, A. W. Conversion Constants for Redox Potentials Measured versus Different Reference Electrodes in Acetonitrile Solutions at 25°C. *Inorg. Chim. Acta* **2000**, *298*, 97–102.
- (34) Loutfy, R. O.; Loutfy, R. O. Correlations between the Electrochemical and Spectroscopic Behavior of Some Benzophenones and Thiobenzophenones. *J. Phys. Chem.* **1972**, *76*, 1650–1655.
- (35) Schweitzer, C.; Mehrdad, Z.; Noll, A.; Grabner, E.-W.; Schmidt, R. Oxygen Quenching of  $N\pi^*$  Triplet Phenyl Ketones: Local Excitation and Local Deactivation. *Helv. Chim. Acta* **2001**, *84*, 2493–2507.
- (36) Ghosh, I.; Mukhopadhyay, A.; Koner, A. L.; Samanta, S.; Nau, W. M.; Moorthy, J. N. Excited-State Properties of Fluorenones: Influence of Substituents, Solvent and Macrocyclic Encapsulation. *Phys. Chem. Chem. Phys.* **2014**, *16*, 16436–16445.
- (37) Xia, J.-B.; Zhu, C.; Chen, C. Visible Light-Promoted Metal-Free C–H Activation: Diarylketone-Catalyzed Selective Benzylic Mono- and Difluorination. *J. Am. Chem. Soc.* **2013**, *135*, 17494–17500.
- (38) Malval, J.-P.; Jin, M.; Morlet-Savary, F.; Chaumeil, H.; Defoin, A.; Soppera, O.; Scheul, T.; Bouriau, M.; Baldeck, P. L. Enhancement of the Two-Photon Initiating Efficiency of a Thioxanthone Derivative through a Chevron-Shaped Architecture. *Chem. Mater.* **2011**, *23*, 3411–3420.
- (39) Del Giacco, T.; Baciocchi, E.; Lanzalunga, O.; Elisei, F. Competitive Decay Pathways of the Radical Ions Formed by Photoinduced Electron Transfer between Quinones and 4,4'-Dimethoxydiphenylmethane in Acetonitrile. *Chem. - Eur. J.* **2001**, *7*, 3005–3013.
- (40) Rathore, R.; Hubig, S. M.; Kochi, J. K. Direct Observation and Structural Characterization of the Encounter Complex in Bimolecular Electron Transfers with Photoactivated Acceptors. *J. Am. Chem. Soc.* **1997**, *119*, 11468–11480.
- (41) Görner, H. Photoreactions of P-Quinones with Dimethyl Sulfide and Dimethyl Sulfoxide in Aqueous Acetonitrile. *Photochem. Photobiol.* **2006**, *82*, 71–77.
- (42) Yamago, S.; Miyazoe, H.; Iida, K.; Yoshida, J. Highly Efficient and Chemoselective Reductive Bis-Silylation of Quinones by Silyltellurides. *Org. Lett.* **2000**, *2*, 3671–3673.
- (43) Ohkubo, K.; Fujimoto, A.; Fukuzumi, S. Visible-Light-Induced Oxygenation of Benzene by the Triplet Excited State of 2,3-Dichloro-5,6-Dicyano-P-Benzoquinone. *J. Am. Chem. Soc.* **2013**, *135*, 5368–5371.
- (44) Hubig, S. M.; Kochi, J. K. Electron-Transfer Mechanisms with Photoactivated Quinones. The Encounter Complex versus the Rehm–Weller Paradigm. *J. Am. Chem. Soc.* **1999**, *121*, 1688–1694.
- (45) Reta, M. R.; Cartana, R.; Anunziata, J. D.; Silber, J. J. Solvatochromism of Anthraquinone and Symmetrical Dihydroxy Derivatives. Local Interactions. *Spectrochim. Acta Part Mol. Spectrosc.* **1993**, *49*, 903–912.
- (46) Serpa, C.; Arnaut, L. G. Does Molecular Size Matter in Photoinduced Electron Transfer Reactions? *J. Phys. Chem. A* **2000**, *104*, 11075–11086.
- (47) Kasha, M. Paths of Molecular Excitation. *Radiat. Res., Suppl.* **1960**, *2*, 243.
- (48) Akaba, R.; Sakuragi, H.; Tokumaru, K. Triphenylpyrylium-Salt-Sensitized Electron Transfer Oxygenation of Adamantylideneadamantane Product, Fluorescence Quenching, and Laser Flash Photolysis Studies. *J. Chem. Soc., Perkin Trans. 2* **1991**, No. 3, 291–297.
- (49) Searle, R.; Williams, J. L. R.; DeMeyer, D. E.; Doty, J. C. The Sensitization of Stilbene Isomerization. *Chem. Commun.* **1967**, No. 22, 1165–1165.
- (50) Martiny, M.; Steckhan, E.; Esch, T. Cycloaddition Reactions Initiated by Photochemically Excited Pyrylium Salts. *Chem. Ber.* **1993**, *126*, 1671–1682.
- (51) Parret, S.; Morlet-Savary, F.; Fouassier, J.-P.; Inomata, K.; Matsumoto, T.; Heisel, F. Fluorescence Properties of Pyrylium and Thiopyrylium Salts. *Bull. Chem. Soc. Jpn.* **1995**, *68*, 2791–2795.
- (52) Miranda, M. A.; Izquierdo, M. A.; Pérez-Ruiz, R. Direct Photophysical Evidence for Quenching of the Triplet Excited State of 2,4,6-Triphenyl(thia)pyrylium Salts by 2,3-Diaryloxetanes. *J. Phys. Chem. A* **2003**, *107*, 2478–2482.
- (53) Isse, A. A.; Gennaro, A. Absolute Potential of the Standard Hydrogen Electrode and the Problem of Interconversion of Potentials in Different Solvents. *J. Phys. Chem. B* **2010**, *114*, 7894–7899.
- (54) Akaba, R.; Kamata, M.; Koike, A.; Mogi, K.-I.; Kuriyama, Y.; Sakuragi, H. Thiopyrylium Salt-Sensitized Electron Transfer Reactions of Trans-Stilbene. Dimerization and Oxygenation. *J. Phys. Org. Chem.* **1997**, *10*, 861–869.
- (55) Jayanthi, S. S.; Ramamurthy, P. Excited Singlet State Reactions of Thiopyrylium with Electron Donors: Electron Transfer, Induction of Triplet by Internal and External Heavy Atom Effect, and Comparison of Pyrylium and Thiopyrylium Reactions. *J. Phys. Chem. A* **1998**, *102*, 511–518.
- (56) Baciocchi, E.; Giacco, T. D.; Elisei, F.; Gerini, M. F.; Guerra, M.; Lapi, A.; Liberati, P. Electron Transfer and Singlet Oxygen Mechanisms in the Photooxygenation of Dibutyl Sulfide and Thioanisole in MeCN Sensitized by N-Methylquinolinium Tetrafluoroborate and 9,10-Dicyanoanthracene. The Probable Involvement of a Thiadioxirane Intermediate in Electron Transfer Photooxygenations. *J. Am. Chem. Soc.* **2003**, *125*, 16444–16454.
- (57) Fukuzumi, S.; Fujita, M.; Noura, S.; Ohkubo, K.; Suenobu, T.; Araki, Y.; Ito, O. Regioreversed Thermal and Photochemical Reduction of 10-Methylacridinium and 1-Methylquinolinium Ions by Organosilanes and Organostannanes. *J. Phys. Chem. A* **2001**, *105*, 1857–1868.
- (58) Chao, S. C.; Tretzel, J.; Schneider, F. W. Excited State Adduct Formation between Excited Substituted Quinolinium Cations and Specific Inorganic Anions. *J. Am. Chem. Soc.* **1979**, *101*, 134–139.
- (59) Yoon, U. C.; Quillen, S. L.; Mariano, P. S.; Swanson, R.; Stavinoha, J. L.; Bay, E. Exploratory and Mechanistic Aspects of the Electron-Transfer Photochemistry of Olefin-N-Heteroaromatic Cation Systems. *J. Am. Chem. Soc.* **1983**, *105*, 1204–1218.
- (60) Baciocchi, E.; Del Giacco, T.; Lanzalunga, O.; Mencarelli, P.; Procacci, B. Photosensitized Oxidation of Alkyl Phenyl Sulfoxides. C–S Bond Cleavage in Alkyl Phenyl Sulfoxide Radical Cations. *J. Org. Chem.* **2008**, *73*, 5675–5682.
- (61) Kitaguchi, H.; Ohkubo, K.; Ogo, S.; Fukuzumi, S. Electron-Transfer Oxidation Properties of Unsaturated Fatty Acids and Mechanistic Insight into Lipoxygenases. *J. Phys. Chem. A* **2006**, *110*, 1718–1725.
- (62) Fukuzumi, S.; Kitano, T. Mechanisms of Reductive Methylation of NAD<sup>+</sup> Analogues by a *Trans*-dimethylcobalt(III) Complex. *J. Chem. Soc., Perkin Trans. 2* **1991**, No. 1, 41–45.
- (63) Fukuzumi, S.; Nishimine, M.; Ohkubo, K.; Tkachenko, N. V.; Lemmettyinen, H. Driving Force Dependence of Photoinduced Electron Transfer Dynamics of Intercalated Molecules in DNA. *J. Phys. Chem. B* **2003**, *107*, 12511–12518.

- (64) Weber, G.; Teale, F. W. J. Determination of the Absolute Quantum Yield of Fluorescent Solutions. *Trans. Faraday Soc.* **1957**, *53*, 646–655.
- (65) Fukuzumi, S.; Ohkubo, K.; Suenobu, T.; Kato, K.; Fujitsuka, M.; Ito, O. Photoalkylation of 10-Alkylacridinium Ion via a Charge-Shift Type of Photoinduced Electron Transfer Controlled by Solvent Polarity. *J. Am. Chem. Soc.* **2001**, *123*, 8459–8467.
- (66) van Willigen, H.; Jones, G.; Farahat, M. S. Time-Resolved EPR Study of Photoexcited Triplet-State Formation in Electron-Donor-Substituted Acridinium Ions. *J. Phys. Chem.* **1996**, *100*, 3312–3316.
- (67) Fox, M. A. Photoinduced Electron Transfer. *Photochem. Photobiol.* **1990**, *52*, 617–627.
- (68) Benniston, A. C.; Harriman, A.; Li, P.; Rostron, J. P.; Verhoeven, J. W. Illumination of the 9-Mesityl-10-Methylacridinium Ion Does Not Give a Long-Lived Photoredox State. *Chem. Commun.* **2005**, No. 21, 2701.
- (69) Benniston, A. C.; Harriman, A.; Li, P.; Rostron, J. P.; van Ramesdonk, H. J.; Groeneveld, M. M.; Zhang, H.; Verhoeven, J. W. Charge Shift and Triplet State Formation in the 9-Mesityl-10-Methylacridinium Cation. *J. Am. Chem. Soc.* **2005**, *127*, 16054–16064.
- (70) Romero, N. A.; Nicewicz, D. A. Mechanistic Insight into the Photoredox Catalysis of Anti-Markovnikov Alkene Hydrofunctionalization Reactions. *J. Am. Chem. Soc.* **2014**, *136*, 17024–17035.
- (71) Ohkubo, K.; Fukuzumi, S. 100 Selective Oxygenation of *P*-Xylene to *P*-Tolualdehyde via Photoinduced Electron Transfer. *Org. Lett.* **2000**, *2*, 3647–3650.
- (72) Fukuzumi, S.; Ohkubo, K.; Suenobu, T. Long-Lived Charge Separation and Applications in Artificial Photosynthesis. *Acc. Chem. Res.* **2014**, *47*, 1455–1464.
- (73) Eisenhart, T. T.; Dempsey, J. L. Photo-Induced Proton-Coupled Electron Transfer Reactions of Acridine Orange: Comprehensive Spectral and Kinetics Analysis. *J. Am. Chem. Soc.* **2014**, *136*, 12221–12224.
- (74) Roth, H.; Romero, N.; Nicewicz, D. Experimental and Calculated Electrochemical Potentials of Common Organic Molecules for Applications to Single-Electron Redox Chemistry. *Synlett* **2016**, *27*, 714–723.
- (75) Chan, M. S.; Bolton, J. R. Mechanism of the Photosensitized Redox Reactions of Acridine Orange in Aqueous Solutions—a System of Interest in the Photochemical Storage of Solar Energy. *Photochem. Photobiol.* **1981**, *34*, 537–547.
- (76) Parker, C. A.; Joyce, T. A. Prompt and Delayed Fluorescence of Some DNA Adsorbates. *Photochem. Photobiol.* **1973**, *18*, 467–474.
- (77) Shen, T.; Zhao, Z.-G.; Yu, Q.; Xu, H.-J. Photosensitized Reduction of Benzil by Heteroatom-Containing Anthracene Dyes. *J. Photochem. Photobiol., A* **1989**, *47*, 203–212.
- (78) Chambers, R. W.; Kearns, D. R. Triplet States of Some Common Photosensitizing Dyes. *Photochem. Photobiol.* **1969**, *10*, 215–219.
- (79) Ghosh, T.; Slanina, T.; König, B. Visible Light Photocatalytic Reduction of Aldehydes by Rh(III)–H: A Detailed Mechanistic Study. *Chem. Sci.* **2015**, *6*, 2027–2034.
- (80) Pilani, M. P.; Graetzel, M. Light-Induced Redox Reactions of Proflavine in Aqueous and Micellar Solution. *J. Phys. Chem.* **1980**, *84*, 2402–2406.
- (81) Lee, W. E.; Galley, W. C. Perturbations to the Intersystem Crossing of Proflavine upon Binding to DNA and Poly d(A-IU) from Triplet-Delayed Emission Spectroscopy. *Biophys. J.* **1988**, *54*, 627–635.
- (82) Discekici, E. H.; Treat, N. J.; Poelma, S. O.; Mattson, K. M.; Hudson, Z. M.; Luo, Y.; Hawker, C. J.; de Alaniz, J. R. A Highly Reducing Metal-Free Photoredox Catalyst: Design and Application in Radical Dehalogenations. *Chem. Commun.* **2015**, *51*, 11705–11708.
- (83) Treat, N. J.; Sprafke, H.; Kramer, J. W.; Clark, P. G.; Barton, B. E.; Read de Alaniz, J.; Fors, B. P.; Hawker, C. J. Metal-Free Atom Transfer Radical Polymerization. *J. Am. Chem. Soc.* **2014**, *136*, 16096–16101.
- (84) Pitre, S. P.; McTiernan, C. D.; Ismaili, H.; Scaiano, J. C. Mechanistic Insights and Kinetic Analysis for the Oxidative Hydroxylation of Arylboronic Acids by Visible Light Photoredox Catalysis: A Metal-Free Alternative. *J. Am. Chem. Soc.* **2013**, *135*, 13286–13289.
- (85) Bergmann, K.; O'Konski, C. T. A Spectroscopic Study of Methylen Blue Monomer, Dimer, and Complexes with Montmorillonite. *J. Phys. Chem.* **1963**, *67*, 2169–2177.
- (86) Merkelo, H.; Hartman, S. R.; Mar, T.; Govindjee, G. S. S. Mode-Locked Lasers: Measurements of Very Fast Radiative Decay in Fluorescent Systems. *Science* **1969**, *164*, 301–302.
- (87) Wetzler, D. E.; García-Fresnadillo, D.; Orellana, G. A Clean, Well-Defined Solid System for Photosensitized  $^1\text{O}_2$  Production Measurements. *Phys. Chem. Chem. Phys.* **2006**, *8*, 2249–2256.
- (88) Timpe, H.-J.; Neuenfeld, S. Photoreduction of Some Dyes by Styrene. *J. Chem. Soc., Faraday Trans.* **1992**, *88*, 2329–2336.
- (89) Nemoto, M.; Kokubun, H.; Koizumi, M. Determination of the  $\text{S}^*-\text{T}$  Transition Probabilities of Some Xanthene and Thiazine Dyes on the Basis of the T-Energy Transfer. I. Experiment in Ethanol Solutions. *Bull. Chem. Soc. Jpn.* **1969**, *42*, 1223–1230.
- (90) Zhang, X.-F.; Zhang, L.; Liu, L. Photophysics of Halogenated Fluoresceins: Involvement of Both Intramolecular Electron Transfer and Heavy Atom Effect in the Deactivation of Excited States. *Photochem. Photobiol.* **2010**, *86*, 492–498.
- (91) Talla, A.; Driessens, B.; Straathof, N. J. W.; Milroy, L.-G.; Brunsved, L.; Hessel, V.; Noël, T. Metal-Free Photocatalytic Aerobic Oxidation of Thiols to Disulfides in Batch and Continuous-Flow. *Adv. Synth. Catal.* **2015**, *357*, 2180–2186.
- (92) Fidal, K.; Ceballos, C.; Falguières, A.; Veitia, M. S.-I.; Guy, A.; Ferroud, C. Visible Light Photoredox Organocatalysis: A Fully Transition Metal-Free Direct Asymmetric  $\alpha$ -Alkylation of Aldehydes. *Green Chem.* **2012**, *14*, 1293–1297.
- (93) Martin, M. M.; Lindqvist, L. The pH Dependence of Fluorescein Fluorescence. *J. Lumin.* **1975**, *10*, 381–390.
- (94) Lambert, C. R.; Kochavar, I. E. Electron Transfer Quenching of the Rose Bengal Triplet State. *Photochem. Photobiol.* **1997**, *66*, 15–25.
- (95) Yoshioka, E.; Kohtani, S.; Jichu, T.; Fukazawa, T.; Nagai, T.; Takemoto, Y.; Miyabe, H. Direct Photoinduced Electron Transfer from Excited State of Rhodamine B for Carbon-Radical Generation. *Synlett* **2015**, *26*, 265–270.
- (96) Yuan, L.; Lin, W.; Yang, Y.; Chen, H. A Unique Class of Near-Infrared Functional Fluorescent Dyes with Carboxylic-Acid-Modulated Fluorescence ON/OFF Switching: Rational Design, Synthesis, Optical Properties, Theoretical Calculations, and Applications for Fluorescence Imaging in Living Animals. *J. Am. Chem. Soc.* **2012**, *134*, 1200–1211.
- (97) Magde, D.; Rojas, G. E.; Seybold, P. G. Solvent Dependence of the Fluorescence Lifetimes of Xanthene Dyes. *Photochem. Photobiol.* **1999**, *70*, 737–744.
- (98) Magde, D.; Wong, R.; Seybold, P. G. Fluorescence Quantum Yields and Their Relation to Lifetimes of Rhodamine 6G and Fluorescein in Nine Solvents: Improved Absolute Standards for Quantum Yields. *Photochem. Photobiol.* **2002**, *75*, 327–334.
- (99) Korobov, V. E.; Shubin, V. V.; Chibisov, A. K. Triplet State of Rhodamine Dyes and Its Role in Production of Intermediates. *Chem. Phys. Lett.* **1977**, *45*, 498–501.
- (100) Yasui, S.; Tsujimoto, M.; Itoh, K.; Ohno, A. Quenching of a Photosensitized Dye through Single-Electron Transfer from Trivalent Phosphorus Compounds. *J. Org. Chem.* **2000**, *65*, 4715–4720.
- (101) Jones, G., II; Wang, X.; Hu, J. Photochemistry of Rhodamine Dye Salts Involving Intra-Ion-Pair Electron Transfer. *Can. J. Chem.* **2003**, *81*, 789–798.
- (102) Park, S. M.; Bard, A. J. Electrogenerated Chemiluminescence. *J. Electroanal. Chem. Interfacial Electrochem.* **1977**, *77*, 137–152.
- (103) Bergamini, G.; Molloy, J. K.; Fermi, A.; Ceroni, P.; Klärner, F.-G.; Hahn, U. Diazapyrenium Cored Dendrimers: Electron Poor Guests for a Molecular Clip Host. *New J. Chem.* **2012**, *36*, 354–359.
- (104) Becker, H.-C.; Broo, A.; Nordén, B. Ground- and Excited-State Properties of Molecular Complexes between Adenine and 2,7-Diazapyrene and Its N-Methylated Cations. *J. Phys. Chem. A* **1997**, *101*, 8853–8860.
- (105) Ford, W. E.; Kamat, P. V. Photochemistry of 3,4,9,10-Perylenetetracarboxylic Dianhydride Dyes. 3. Singlet and Triplet Excited-State Properties of the bis(2,5-Di-Tert-Butylphenyl)imide Derivative. *J. Phys. Chem.* **1987**, *91*, 6373–6380.

- (106) Gosztola, D.; Niemczyk, M. P.; Svec, W.; Lukas, A. S.; Wasielewski, M. R. Excited Doublet States of Electrochemically Generated Aromatic Imide and Diimide Radical Anions. *J. Phys. Chem. A* **2000**, *104*, 6545–6551.
- (107) Lee, S. K.; Zu, Y.; Herrmann, A.; Geerts, Y.; Müllen, K.; Bard, A. J. Electrochemistry, Spectroscopy and Electrogenerated Chemiluminescence of Perylene, Terrylene, and Quaterrylene Diimides in Aprotic Solution. *J. Am. Chem. Soc.* **1999**, *121*, 3513–3520.
- (108) McNaught, A.; Wilkinson, A. Gibbs Energy of Photoinduced Electron Transfer. In *IUPAC Compendium of Chemical Terminology*, 2nd ed. (the “Gold Book”); Nič, M., Jirát, J., Košata, B., Jenkins, A., Eds.; Blackwell Scientific Publications: Oxford, 1997.
- (109) McNaught, A.; Wilkinson, A. Rehm–Weller Equation. In *IUPAC Compendium of Chemical Terminology*, 2nd ed. (the “Gold Book”); Nič, M., Jirát, J., Košata, B., Jenkins, A., Eds.; Blackwell Scientific Publications: Oxford, 1997.
- (110) Rehm, D.; Weller, A. Kinetik Und Mechanismus Der Elektronübertragung Bei Der Fluoreszenzlösung in Acetonitril. *Bunsen-Ges. Phys. Chem. Ber.* **1969**, *73*, 834–839.
- (111) Rehm, D.; Weller, A. Kinetics of Fluorescence Quenching by Electron and H-Atom Transfer. *Isr. J. Chem.* **1970**, *8*, 259–271.
- (112) Lakowicz, J. R. *Principles of Fluorescence Spectroscopy*, 3rd ed.; Springer: New York, 2006.
- (113) Farid, S.; Dinnocenzo, J. P.; Merkel, P. B.; Young, R. H.; Shukla, D.; Guirado, G. Reexamination of the Rehm–Weller Data Set Reveals Electron Transfer Quenching That Follows a Sandros–Boltzmann Dependence on Free Energy. *J. Am. Chem. Soc.* **2011**, *133*, 11580–11587.
- (114) Farid, S.; Dinnocenzo, J. P.; Merkel, P. B.; Young, R. H.; Shukla, D. Bimolecular Electron Transfers That Follow a Sandros–Boltzmann Dependence on Free Energy. *J. Am. Chem. Soc.* **2011**, *133*, 4791–4801.
- (115) Richert, S.; Rosspeintner, A.; Landgraf, S.; Grampf, G.; Vauthay, E.; Kattnig, D. R. Time-Resolved Magnetic Field Effects Distinguish Loose Ion Pairs from Exciplexes. *J. Am. Chem. Soc.* **2013**, *135*, 15144–15152.
- (116) Rosspeintner, A.; Angulo, G.; Vauthay, E. Bimolecular Photoinduced Electron Transfer Beyond the Diffusion Limit: The Rehm–Weller Experiment Revisited with Femtosecond Time Resolution. *J. Am. Chem. Soc.* **2014**, *136*, 2026–2032.
- (117) Jacques, P.; Burget, D. On the Necessity of Distinguishing “n” from “π” Quenchers in Electron Transfer Studies. *J. Photochem. Photobiol. A* **1992**, *68*, 165–168.
- (118) Cismesia, M. A.; Yoon, T. P. Characterizing Chain Processes in Visible Light Photoredox Catalysis. *Chem. Sci.* **2015**, *6*, 5426–5434.
- (119) Rao, P. S.; Hayon, E. Redox Potentials of Free Radicals. I. Simple Organic Radicals. *J. Am. Chem. Soc.* **1974**, *96*, 1287–1294.
- (120) Wayner, D. D. M.; McPhee, D. J.; Griller, D. Oxidation and Reduction Potentials of Transient Free Radicals. *J. Am. Chem. Soc.* **1988**, *110*, 132–137.
- (121) Fu, Y.; Liu, L.; Yu, H.-Z.; Wang, Y.-M.; Guo, Q.-X. Quantum-Chemical Predictions of Absolute Standard Redox Potentials of Diverse Organic Molecules and Free Radicals in Acetonitrile. *J. Am. Chem. Soc.* **2005**, *127*, 7227–7234.
- (122) Megerle, U.; Lechner, R.; König, B.; Riedle, E. Laboratory Apparatus for the Accurate, Facile and Rapid Determination of Visible Light Photoreaction Quantum Yields. *Photochem. Photobiol. Sci.* **2010**, *9*, 1400–1406.
- (123) Kochi, J. K. Charge-Transfer Excitation of Molecular Complexes in Organic and Organometallic Chemistry. *Pure Appl. Chem.* **1991**, *63*, 255–264.
- (124) Rosokha, S. V.; Kochi, J. K. Fresh Look at Electron-Transfer Mechanisms via the Donor/Acceptor Bindings in the Critical Encounter Complex. *Acc. Chem. Res.* **2008**, *41*, 641–653.
- (125) Rosokha, S. V.; Kochi, J. K. Continuum of Outer- and Inner-Sphere Mechanisms for Organic Electron Transfer. Steric Modulation of the Precursor Complex in Paramagnetic (Ion-Radical) Self-Exchanges. *J. Am. Chem. Soc.* **2007**, *129*, 3683–3697.
- (126) Rosokha, S. V.; Kochi, J. K. Strong Electronic Coupling in Intermolecular (Charge-Transfer) Complexes. Mechanistic Relevance to Thermal and Optical Electron Transfer from Aromatic Donors. *New J. Chem.* **2002**, *26*, 851–860.
- (127) Arceo, E.; Bahamonde, A.; Bergonzini, G.; Melchiorre, P. Enantioselective Direct  $\alpha$ -Alkylation of Cyclic Ketones by Means of Photo-Organocatalysis. *Chem. Sci.* **2014**, *5*, 2438–2442.
- (128) Nappi, M.; Bergonzini, G.; Melchiorre, P. Metal-Free Photochemical Aromatic Perfluoroalkylation of  $\alpha$ -Cyano Arylacetates. *Angew. Chem., Int. Ed.* **2014**, *53*, 4921–4925.
- (129) Silvi, M.; Arceo, E.; Jurberg, I. D.; Cassani, C.; Melchiorre, P. Enantioselective Organocatalytic Alkylation of Aldehydes and Enals Driven by the Direct Photoexcitation of Enamines. *J. Am. Chem. Soc.* **2015**, *137*, 6120–6123.
- (130) Woźniak, Ł.; Murphy, J. J.; Melchiorre, P. Photo-Organocatalytic Enantioselective Perfluoroalkylation of  $\beta$ -Ketoesters. *J. Am. Chem. Soc.* **2015**, *137*, 5678–5681.
- (131) da Silva, G. P.; Ali, A.; da Silva, R. C.; Jiang, H.; Paixão, M. W. Tris(trimethylsilyl)silane and Visible-Light Irradiation: A New Metal- and Additive-Free Photochemical Process for the Synthesis of Indoles and Oxindoles. *Chem. Commun.* **2015**, *51*, 15110–15113.
- (132) Gould, I. R.; Farid, S. Dynamics of Bimolecular Photoinduced Electron-Transfer Reactions. *Acc. Chem. Res.* **1996**, *29*, 522–528.
- (133) Wilkinson, F. Transfer of Triplet State Energy and The Chemistry of Excited States. *J. Phys. Chem.* **1962**, *66*, 2569–2574.
- (134) Zhao, J.; Wu, W.; Sun, J.; Guo, S. Triplet Photosensitizers: From Molecular Design to Applications. *Chem. Soc. Rev.* **2013**, *42*, 5323–5351.
- (135) Clennan, E. L.; Pace, A. Advances in Singlet Oxygen Chemistry. *Tetrahedron* **2005**, *61*, 6665–6691.
- (136) Gorman, A. A.; Rodgers, M. A. J. Singlet Molecular Oxygen. *Chem. Soc. Rev.* **1981**, *10*, 205–231.
- (137) Ohloff, G. Singlet Oxygen: A Reagent in Organic Synthesis. *Pure Appl. Chem.* **1975**, *43*, 481–502.
- (138) Tanielian, C.; Wolff, C. Determination of the Parameters Controlling Singlet Oxygen Production via Oxygen and Heavy-Atom Enhancement of Triplet Yields. *J. Phys. Chem.* **1995**, *99*, 9831–9837.
- (139) Prein, M.; Adam, W. The Schenck Ene Reaction: Diastereoselective Oxyfunctionalization with Singlet Oxygen in Synthetic Applications. *Angew. Chem., Int. Ed. Engl.* **1996**, *35*, 477–494.
- (140) Ni, T.; Caldwell, R. A.; Melton, L. A. The Relaxed and Spectroscopic Energies of Olefin Triplets. *J. Am. Chem. Soc.* **1989**, *111*, 457–464.
- (141) Kuriyama, Y.; Arai, T.; Sakuragi, H.; Tokumaru, K. Effects of Sensitizer Spin Multiplicity on Electron-Transfer Initiated Isomerization of Cis-Stillbene. *Chem. Lett.* **1988**, *17*, 1193–1196.
- (142) Akaba, R.; Ohshima, K.; Kawai, Y.; Obuchi, Y.; Negishi, A.; Sakuragi, H.; Tokumaru, K. Triplet-Mediated Electron Transfer Oxygenation of Stillbene Derivatives with 2,4,6-Triphenylpyrylium Tetrafluoroborate. *Tetrahedron Lett.* **1991**, *32*, 109–112.
- (143) Sawyer, D. T.; Chiericato, G.; Angelis, C. T.; Nanni, E. J.; Tsuchiya, T. Effects of Media and Electrode Materials on the Electrochemical Reduction of Dioxygen. *Anal. Chem.* **1982**, *54*, 1720–1724.
- (144) Roth, H. D.; Herbertz, T.; Sauers, R. R.; Weng, H. Intramolecular Nucleophilic Capture of Radical Cations by Tethered Hydroxy Functions. *Tetrahedron* **2006**, *62*, 6471–6489.
- (145) Gassman, P. G.; Bottorff, K. J. Photoinduced Lactonization. a Useful but Mechanistically Complex Single Electron Transfer Process. *J. Am. Chem. Soc.* **1987**, *109*, 7547–7548.
- (146) Lewis, F. D.; Dykstra, R. E.; Gould, I. R.; Farid, S. Cage Escape Yields and Direct Observation of Intermediates in Photoinduced Electron-Transfer Reactions of Cis- and Trans-Stillbene. *J. Phys. Chem.* **1988**, *92*, 7042–7043.
- (147) Pandey, G.; Karthikeyan, M.; Murugan, A. New Intramolecular  $\alpha$ -Arylation Strategy of Ketones by the Reaction of Silyl Enol Ethers to Photosensitized Electron Transfer Generated Arene Radical Cations: Construction of Benzannulated and Benzospiroannulated Compounds. *J. Org. Chem.* **1998**, *63*, 2867–2872.
- (148) Pandey, G. Photoinduced Electron Transfer (PET) in Organic Synthesis. In *Photoinduced Electron Transfer*; Mattay, P. D. J., Eds.;

- Topics in Current Chemistry; Springer: Berlin Heidelberg, 1993; pp 175–221.
- (149) Pandey, G.; Murugan, A.; Balakrishnan, M. A New Strategy towards the Total Synthesis of Phenanthridone Alkaloids: Synthesis of (+)-2,7-Dideoxypancratistatin as a Model Study. *Chem. Commun.* **2002**, No. 6, 624–625.
- (150) Pandey, G.; Sochanchingwung, R. Photoinduced Electron Transfer (PET) Promoted Cross-Coupling of Organoselenium and Organosilicon Compounds: A New Carbon–Carbon Bond Formation Strategy. *J. Chem. Soc., Chem. Commun.* **1994**, No. 17, 1945–1946.
- (151) Pandey, G.; Sekhar, B. B. V. S.; Bhalerao, U. T. Photoinduced Single Electron Transfer Initiated Heterolytic Carbon–Selenium Bond Dissociation. Sequential One-Pot Selenenylation and Deselenenylation Reaction. *J. Am. Chem. Soc.* **1990**, *112*, 5650–5651.
- (152) Nakamura, M.; Dohno, R.; Majima, T. Photoinduced Electron-Transfer Reactions of Tri-1-Naphthylphosphate and Di-1-Naphthyl Methylphosphonate Sensitized by 9,10-Dicyanoanthracene. *Chem. Commun.* **1997**, No. 14, 1291–1292.
- (153) Nakamura, M.; Dohno, R.; Majima, T. Intramolecular Binaphthyl Formation from Radical Cations of Tri-1-Naphthyl Phosphate and Related Compounds in Photoinduced Electron-Transfer Reactions Sensitized by 9,10-Dicyanoanthracene. *J. Org. Chem.* **1998**, *63*, 6258–6265.
- (154) Pandey, G.; Laha, R. Visible-Light-Catalyzed Direct Benzylic C(sp<sup>3</sup>)–H Amination Reaction by Cross-Dehydrogenative Coupling. *Angew. Chem., Int. Ed.* **2015**, *54*, 14875–14879.
- (155) Pandey, G.; Lakshmaiah, G.; Kumaraswamy, G. A New and Efficient Strategy for Non-Stabilized Azomethine Ylide via Photoinduced Electron Transfer (PET) Initiated Sequential Double Desilylation. *J. Chem. Soc., Chem. Commun.* **1992**, No. 18, 1313–1314.
- (156) Cho, D. W.; Parthasarathi, R.; Pimentel, A. S.; Maestas, G. D.; Park, H. J.; Yoon, U. C.; Dunaway-Mariano, D.; Gnanakaran, S.; Langan, P.; Mariano, P. S. Nature and Kinetic Analysis of Carbon–Carbon Bond Fragmentation Reactions of Cation Radicals Derived from SET-Oxidation of Lignin Model Compounds. *J. Org. Chem.* **2010**, *75*, 6549–6562.
- (157) Hintz, S.; Mattay, J.; van Eldik, R.; Fu, W.-F. Regio- and Stereoselective Cyclization Reactions of Unsaturated Silyl Enol Ethers by Photoinduced Electron Transfer – Mechanistic Aspects and Synthetic Approach. *Eur. J. Org. Chem.* **1998**, *1998*, 1583–1596.
- (158) Beckwith, A. L. J.; Schiesser, C. H. Selectivity and Synthetic Applications of Radical reactionsRegio- and Stereo-Selectivity of Alkenyl Radical Ring Closure: A Theoretical Study. *Tetrahedron* **1985**, *41*, 3925–3941.
- (159) Hoffmann, U.; Gao, Y.; Pandey, B.; Klinge, S.; Warzecha, K. D.; Krueger, C.; Roth, H. D.; Demuth, M. Light-Induced Polyene Cyclizations via Radical Cations in Micellar Medium. *J. Am. Chem. Soc.* **1993**, *115*, 10358–10359.
- (160) Johnson, W. S.; Cherala, B.; Tham, F. S.; Kullnig, R. K. Cation-Stabilizing Auxiliaries in Polyene Cyclizations. 4. The Fluorine Atom as a Cation-Stabilizing Auxiliary in Biomimetic Polyene Cyclizations. 1. Background and Exploratory Experiments. *J. Am. Chem. Soc.* **1993**, *115*, 493–497.
- (161) Warzecha, K.-D.; Xing, X.; Demuth, M.; Goddard, R.; Kessler, M.; Krüger, C. Cascade Cyclizations of Terpenoid Polyalkenes Triggered by Photoelectron Transfer – Biomimetics with Photons. *Helv. Chim. Acta* **1995**, *78*, 2065–2076.
- (162) Heinemann, C.; Demuth, M. Short Biomimetic Synthesis of a Steroid by Photoinduced Electron Transfer and Remote Asymmetric Induction. *J. Am. Chem. Soc.* **1999**, *121*, 4894–4895.
- (163) Jonas, M.; Blechert, S.; Steckhan, E. Photochemically Induced Electron Transfer (PET) Catalyzed Radical Cyclization: A Practical Method for Inducing Structural Changes in Peptides by Formation of Cyclic Amino Acid Derivatives. *J. Org. Chem.* **2001**, *66*, 6896–6904.
- (164) Rinderhagen, H.; Mattay, J. Synthetic Applications in Radical/Radical Cationic Cascade Reactions. *Chem. - Eur. J.* **2004**, *10*, 851–874.
- (165) Waske, P. A.; Mattay, J. Synthesis of Cyclopropyl Silyl Ethers and Their Facile Ring Opening by Photoinduced Electron Transfer as Key Step in Radical/radical Cationic Cascade Reactions. *Tetrahedron* **2005**, *61*, 10321–10330.
- (166) Rinderhagen, H.; Waske, P. A.; Mattay, J. Facile Ring Opening of Siloxy Cyclopropanes by Photoinduced Electron Transfer. A New Way to β-Keto Radicals. *Tetrahedron* **2006**, *62*, 6589–6593.
- (167) Guttenberger, G.; Steckhan, E.; Blechert, S. α-Silyl Ethers as Hydroxymethyl Anion Equivalents in Photoinduced Radical Electron Transfer Additions. *Angew. Chem., Int. Ed.* **1998**, *37* (5), 660–662.
- (168) Fagnoni, M.; Mella, M.; Albini, A. Electron-Transfer-Photo-sensitized Conjugate Alkylation. *J. Org. Chem.* **1998**, *63*, 4026–4033.
- (169) Yoshimi, Y.; Masuda, M.; Mizunashi, T.; Nishikawa, K.; Maeda, K.; Koshida, N.; Itou, T.; Morita, T.; Hatanaka, M. Inter- and Intramolecular Addition Reactions of Electron-Deficient Alkenes with Alkyl Radicals, Generated by SET-Photochemical Decarboxylation of Carboxylic Acids, Serve as a Mild and Efficient Method for the Preparation of γ-Amino Acids and Macrocyclic Lactones. *Org. Lett.* **2009**, *11*, 4652–4655.
- (170) Yoshimi, Y.; Washida, S.; Okita, Y.; Nishikawa, K.; Maeda, K.; Hayashi, S.; Morita, T. Radical Addition to Acrylonitrile via Catalytic Photochemical Decarboxylation of Aliphatic Carboxylic Acids. *Tetrahedron Lett.* **2013**, *54*, 4324–4326.
- (171) Chu, L.; Ohta, C.; Zuo, Z.; MacMillan, D. W. C. Carboxylic Acids as A Traceless Activation Group for Conjugate Additions: A Three-Step Synthesis of (±)-Pregabalin. *J. Am. Chem. Soc.* **2014**, *136*, 10886–10889.
- (172) Albini, A.; Arnold, D. R. Radical Ions in Photochemistry. 6. The Photosensitized (Electron Transfer) Ring Opening of Aryloxiranes. *Can. J. Chem.* **1978**, *56*, 2985–2993.
- (173) Müller, F.; Mattay, J. [3 + 2] Cycloadditions with Azirine Radical Cations: A New Synthesis of N-Substituted Imidazoles. *Angew. Chem., Int. Ed. Engl.* **1991**, *30*, 1336–1337.
- (174) Müller, F.; Mattay, J. A New Synthesis for Imidazolo- and Pyrrolophanes by [3+2]Cycloaddition with Azaallenyl Radical Cations. *Angew. Chem., Int. Ed. Engl.* **1992**, *31*, 209–210.
- (175) Mueller, F.; Mattay, J.; Steenken, S. Radical Ions and Photochemical Charge-Transfer Phenomena. 39. Cycloadditions. 42. Radical Cation [3 + 2] Cycloadditions of 2H-Azirines. Mechanistic Studies Concerning the Intermediate Radical Cation. *J. Org. Chem.* **1993**, *58*, 4462–4464.
- (176) Albrecht, E.; Averdung, J.; Bischof, E. W.; Heidbreder, A.; Kirschberg, T.; Müller, F.; Mattay, J. Photoinduced Electron Transfer (PET) in Organic Synthesis. [3 + 2]-Type Cycloaddition, Cyclization and C–C Bond Cleavage Reactions. *J. Photochem. Photobiol. A* **1994**, *82*, 219–232.
- (177) Jones, C. R.; Allman, B. J.; Mooring, A.; Spahic, B. Photosensitized [4 + 2] Cyclodimerization of 1,3-Cyclohexadiene. *J. Am. Chem. Soc.* **1983**, *105*, 652–654.
- (178) Arai, N.; Tanaka, K.; Ohkuma, T. Photosensitized Intramolecular Cyclization of Furan and Non-Activated Alkene: Pathway Switching by the Substituent on the Furan Ring. *Tetrahedron Lett.* **2010**, *S1*, 1273–1275.
- (179) Nakabayashi, K.; Kojima, J.; Tanabe, K.; Yasuda, M.; Shima, K. Organic Photochemical Reactions. XXXI. Photosensitized Ring-Cleavage Reactions of 2,2-Diaryloxetanes by Aromatic Nitriles. *Bull. Chem. Soc. Jpn.* **1989**, *62*, 96–101.
- (180) Shigemitsu, Y.; Arnold, D. R. Radical Ions in Photochemistry. Sensitised (Electron-Transfer) Photochemical Reactions of Some 1-Phenylcycloalkenes in Polar, Nucleophilic Solvents. *J. Chem. Soc., Chem. Commun.* **1975**, No. 11, 407–408.
- (181) Maroulis, A. J.; Shigemitsu, Y.; Arnold, D. R. Radical Ions in Photochemistry. 5. Photosensitized (Electron Transfer) Cyanation of Olefins. *J. Am. Chem. Soc.* **1978**, *100*, 535–541.
- (182) Maroulis, A. J.; Arnold, D. R. Radical Ions in Photochemistry; 11. The Photosensitized (Electron Transfer) Preparation of Some 2,2,2-Trifluoroethyl Ethers. *Synthesis* **1979**, *1979*, 819–820.
- (183) Mizuno, K.; Nakanishi, I.; Ichinose, N.; Otsuji, Y. Structural Dependence on Photoaddition of Methanol to Arylalkenes. Solvent and Additive Effects on Photoinduced Electron Transfer Reaction. *Chem. Lett.* **1989**, *18*, 1095–1098.

- (184) Yasuda, M.; Pac, C.; Sakurai, H. Photochemical Reactions of Aromatic Compounds. XXXIII. Photoreactions of 1-Cyano-naphthalene with Indene in Various Solvents. *Bull. Chem. Soc. Jpn.* **1980**, *53*, 502–507.
- (185) Yasuda, M.; Yamashita, T.; Shima, K.; Pac, C. Photochemical Reactions of Aromatic Compounds. 43. Direct Photoamination of Arenes with Ammonia and Primary Amines in the Presence of Electron Acceptors. *J. Org. Chem.* **1987**, *52*, 753–759.
- (186) Yasuda, M.; Kojima, R.; Ohira, R.; Shiragami, T.; Shima, K. Photoamination of Alkenyl-naphthalenes with Ammonia via Electron Transfer. *Bull. Chem. Soc. Jpn.* **1998**, *71*, 1655–1660.
- (187) Yamashita, T.; Shiomori, K.; Yasuda, M.; Shima, K. Photo-induced Nucleophilic Addition of Ammonia and Alkylamines to Aryl-Substituted Alkenes in the Presence of *P*-Dicyanobenzene. *Bull. Chem. Soc. Jpn.* **1991**, *64*, 366–374.
- (188) Yamashita, T.; Yasuda, M.; Isami, T.; Tanabe, K.; Shima, K. Photoinduced Nucleophilic Addition of Ammonia and Alkylamines to Methoxy-Substituted Styrene Derivatives. *Tetrahedron* **1994**, *50*, 9275–9286.
- (189) Gassman, P. G.; Bottorff, K. J. Anti-Markovnikov Addition of Nucleophiles to a Non-Conjugated Olefin via Single Electron Transfer Photochemistry. *Tetrahedron Lett.* **1987**, *28*, 5449–5452.
- (190) Gassman, P. G.; De Silva, S. A. Use of Sterically Hindered Sensitizers for Improved Photoinduced Electron-Transfer Reactions. *J. Am. Chem. Soc.* **1991**, *113*, 9870–9872.
- (191) Jiang, Z. Q.; Foote, C. S. Electron-Transfer Photooxygenation, 8. Trapping of Internal Nucleophiles. *Tetrahedron Lett.* **1983**, *24*, 461–464.
- (192) Arnold, D. R.; Chan, M. S.; McManus, K. A. Photochemical Nucleophile-Olefin Combination, Aromatic Substitution (Photo-NOCAS) Reaction, Part 12. Factors Controlling the Regiochemistry of the Reaction with Alcohol as the Nucleophile. *Can. J. Chem.* **1996**, *74*, 2143–2166.
- (193) Arnold, D. R.; Du, X. The Photochemical Nucleophile–olefin Combination, Aromatic Substitution (Photo-NOCAS) Reaction. Part 5: Methanol–monoterpenes ( $\alpha$ - and  $\beta$ -Pinene, Tricyclene, and Nopol), 1,4-Dicyanobenzene. *Can. J. Chem.* **1994**, *72*, 403–414.
- (194) Adam, W.; Denninger, U.; Finzel, R.; Kita, F.; Platsch, H.; Walter, H.; Zang, G. Comparative Study of the Pyrolysis, Photoinduced Electron Transfer (PET), and Laser-Jet and 185-Nm Photochemistry of Alkyl-Substituted Bicyclic Azoalkanes. *J. Am. Chem. Soc.* **1992**, *114*, 5027–5035.
- (195) Adam, W.; Sendelbach, J. Denitrogenation of Bicyclic Azoalkanes through Photosensitized Electron Transfer: Generation and Intramolecular Trapping of Radical Cations. *J. Org. Chem.* **1993**, *58*, 5316–5322.
- (196) Kavarnos, G. J.; Turro, N. J. Photosensitization by Reversible Electron Transfer: Theories, Experimental Evidence, and Examples. *Chem. Rev.* **1986**, *86*, 401–449.
- (197) Gould, I. R.; Young, R. H.; Moody, R. E.; Farid, S. Contact and Solvent-Separated Geminate Radical Ion Pairs in Electron-Transfer Photochemistry. *J. Phys. Chem.* **1991**, *95*, 2068–2080.
- (198) Mattay, J. Photoinduced Electron Transfer in Organic Synthesis. *Synthesis* **1989**, *1989*, 233–252.
- (199) DiNocenzo, J. P.; Farid, S.; Goodman, J. L.; Gould, I. R.; Mattes, S. L.; Todd, W. P. Nucleophile-Assisted Cleavage of Silane Cation Radicals. *J. Am. Chem. Soc.* **1989**, *111*, 8973–8975.
- (200) Mangion, D.; Arnold, D. R. Photochemical Nucleophile–Olefin Combination, Aromatic Substitution Reaction. Its Synthetic Development and Mechanistic Exploration. *Acc. Chem. Res.* **2002**, *35*, 297–304.
- (201) McNally, A.; Prier, C. K.; MacMillan, D. W. C. Discovery of an  $\alpha$ -Amino C-H Arylation Reaction Using the Strategy of Accelerated Serendipity. *Science* **2011**, *334*, 1114–1117.
- (202) Zhao, Y.; Zhang, C.; Chin, K. F.; Pytela, O.; Wei, G.; Liu, H.; Bureš, F.; Jiang, Z. Dicyanopyrazine-Derived Push–pull Chromophores for Highly Efficient Photoredox Catalysis. *RSC Adv.* **2014**, *4*, 30062–30067.
- (203) Liu, X.; Ye, X.; Bureš, F.; Liu, H.; Jiang, Z. Controllable Chemoselectivity in Visible-Light Photoredox Catalysis: Four Diverse Aerobic Radical Cascade Reactions. *Angew. Chem., Int. Ed.* **2015**, *54*, 11443–11447.
- (204) Luo, J.; Zhang, J. Donor–Acceptor Fluorophores for Visible-Light-Promoted Organic Synthesis: Photoredox/Ni Dual Catalytic  $C(sp^3)$ – $C(sp^2)$  Cross-Coupling. *ACS Catal.* **2016**, *6*, 873–877.
- (205) Bensasson, R.; Land, E. J. Triplet-Triplet Extinction Coefficients via Energy Transfer. *Trans. Faraday Soc.* **1971**, *67*, 1904–1915.
- (206) Hayon, E.; Ibata, T.; Lichtin, N. N.; Simic, M. Electron and Hydrogen Atom Attachment to Aromatic Carbonyl Compounds in Aqueous Solution. Absorption Spectra and Dissociation Constants of Ketetyl Radicals. *J. Phys. Chem.* **1972**, *76*, 2072–2078.
- (207) Cohen, S. G.; Parola, A.; Parsons, G. H. Photoreduction by Amines. *Chem. Rev.* **1973**, *73*, 141–161.
- (208) Cohen, S. G.; Litt, A. D. Rate Constants of Interaction of Benzophenone Triplet with Amines. *Tetrahedron Lett.* **1970**, *11*, 837–840.
- (209) Inbar, S.; Linschitz, H.; Cohen, S. G. Primary Quantum Yields of Ketetyl Radicals in Photoreduction by Amines. Abstraction of Hydrogen from Nitrogen. *J. Am. Chem. Soc.* **1980**, *102*, 1419–1421.
- (210) Inbar, S.; Linschitz, H.; Cohen, S. G. Nanosecond Flash Studies of Reduction of Benzophenone by Aliphatic Amines. Quantum Yields and Kinetic Isotope Effects. *J. Am. Chem. Soc.* **1981**, *103*, 1048–1054.
- (211) Dondi, D.; Cardarelli, A. M.; Fagnoni, M.; Albini, A. Photomediated Synthesis of  $\beta$ -Alkylketones from Cycloalkanes. *Tetrahedron* **2006**, *62*, 5527–5535.
- (212) Manfrotto, C.; Mella, M.; Freccero, M.; Fagnoni, M.; Albini, A. Photochemical Synthesis of 4-Oxobutanal Acetals and of 2-Hydroxycyclobutanone Ketals. *J. Org. Chem.* **1999**, *64*, 5024–5028.
- (213) Yang, N. C.; Yang, D.-D. H. Photochemical Reactions of Ketones in Solution. *J. Am. Chem. Soc.* **1958**, *80*, 2913–2914.
- (214) Dondi, D.; Protti, S.; Albini, A.; Carpio, S. M.; Fagnoni, M. Synthesis of  $\gamma$ -Lactols,  $\gamma$ -Lactones and 1,4-Monoprotected Succinaldehydes under Moderately Concentrated Sunlight. *Green Chem.* **2009**, *11*, 1653–1659.
- (215) Cantillo, D.; de Frutos, O.; Rincón, J. A.; Mateos, C.; Kappe, C. O. A Continuous-Flow Protocol for Light-Induced Benzylic Fluorinations. *J. Org. Chem.* **2014**, *79*, 8486–8490.
- (216) Wayner, D. D. M.; Dannenberg, J. J.; Griller, D. Oxidation Potentials of  $\alpha$ -Aminoalkyl Radicals: Bond Dissociation Energies for Related Radical Cations. *Chem. Phys. Lett.* **1986**, *131*, 189–191.
- (217) Lewis, F. D. Proton-Transfer Reactions of Photogenerated Radical Ion Pairs. *Acc. Chem. Res.* **1986**, *19*, 401–405.
- (218) Lewis, F. D.; Ho, T.-I.; Simpson, J. T. Photochemical Addition of Tertiary Amines to Stilbene. Stereoelectronic Control of Tertiary Amine Oxidation. *J. Org. Chem.* **1981**, *46*, 1077–1082.
- (219) Lewis, F. D.; Ho, T. I.; Simpson, J. T. Photochemical Addition of Tertiary Amines to Stilbene. Free-Radical and Electron-Transfer Mechanisms for Amine Oxidation. *J. Am. Chem. Soc.* **1982**, *104*, 1924–1929.
- (220) Xu, W.; Mariano, P. S. Substituent Effects on Amine Cation Radical Acidity. Regiocontrol of  $\beta$ -(Aminoethyl)cyclohexenone Photocyclizations. *J. Am. Chem. Soc.* **1991**, *113*, 1431–1432.
- (221) Nelsen, S. F.; Ippoliti, J. T. The Deprotonation of Trialkylamine Cation Radicals by Amines. *J. Am. Chem. Soc.* **1986**, *108*, 4879–4881.
- (222) Parker, V. D.; Tilset, M. Facile Proton-Transfer Reactions of N,N-Dimethylaniline Cation Radicals. *J. Am. Chem. Soc.* **1991**, *113*, 8778–8781.
- (223) Das, S.; von Sonntag, C. The Oxidation of Trimethylamine by OH Radicals in Aqueous Solution, as Studied by Pulse Radiolysis, ESR, and Product Analysis. The Reactions of the Alkylamine Radical Cation, the Aminoalkyl Radical, and the Protonated Aminoalkyl Radical. *Z. Naturforsch., B: J. Chem. Sci.* **1986**, *41*, 4, 505–513 [10.1515/znb-1986-0418](https://doi.org/10.1515/znb-1986-0418).
- (224) Zhang, X.; Yeh, S.-R.; Hong, S.; Freccero, M.; Albini, A.; Falvey, D. E.; Mariano, P. S. Dynamics of  $\alpha$ -CH Deprotonation and  $\alpha$ -Desilylation Reactions of Tertiary Amine Cation Radicals. *J. Am. Chem. Soc.* **1994**, *116*, 4211–4220.

- (225) Dinnocenzo, J. P.; Banach, T. E. Deprotonation of Tertiary Amine Cation Radicals. A Direct Experimental Approach. *J. Am. Chem. Soc.* **1989**, *111*, 8646–8653.
- (226) Lewis, F. D.; Reddy, G. D.; Bassani, D. M. Styrene-Amine and Stilbene-Amine Intramolecular Addition Reactions. *Pure Appl. Chem.* **1992**, *64* (9), 1271–1277.
- (227) Griller, D.; Lossing, F. P. Thermochemistry of  $\alpha$ -Aminoalkyl Radicals. *J. Am. Chem. Soc.* **1981**, *103*, 1586–1587.
- (228) Nicholas, A. M. de P.; Arnold, D. R. Thermochemical Parameters for Organic Radicals and Radical Ions. Part 1. The Estimation of the  $pK_a$  of Radical Cations Based on Thermochemical Calculations. *Can. J. Chem.* **1982**, *60*, 2165–2179.
- (229) Nicholas, A. M. de P.; Boyd, R. J.; Arnold, D. R. Thermochemical Parameters for Organic Radicals and Radical Ions. Part 2. The Protonation of Hydrocarbon Radicals in the Gas Phase. *Can. J. Chem.* **1982**, *60*, 3011–3018.
- (230) Chow, Y. L.; Danen, W. C.; Nelsen, S. F.; Rosenblatt, D. H. Nonaromatic Aminium Radicals. *Chem. Rev.* **1978**, *78*, 243–274.
- (231) Malatesta, V.; Ingold, K. U. Kinetic Applications of Electron Paramagnetic Resonance Spectroscopy. XI. Aminium Radicals. *J. Am. Chem. Soc.* **1973**, *95*, 6400–6404.
- (232) Ismaili, H.; Pitre, S. P.; Scaiano, J. C. Active Participation of Amine-Derived Radicals in Photoredox Catalysis as Exemplified by a Reductive Cyclization. *Catal. Sci. Technol.* **2013**, *3*, 935–937.
- (233) Du, J.; Espelt, L. R.; Guzei, I. A.; Yoon, T. P. Photocatalytic Reductive Cyclizations of Enones: Divergent Reactivity of Photo-generated Radical and Radical Anion Intermediates. *Chem. Sci.* **2011**, *2*, 2115–2119.
- (234) Bauer, A.; Westkämper, F.; Grimme, S.; Bach, T. Catalytic Enantioselective Reactions Driven by Photoinduced Electron Transfer. *Nature* **2005**, *436*, 1139–1140.
- (235) Cooper, H. R. Photoreduction of Anthraquinone Sulphonates in Aqueous Organic Media. *Trans. Faraday Soc.* **1966**, *62*, 2865–2875.
- (236) Phillips, G. O.; Worthington, N. W.; McKellar, J. F.; Sharpe, R. R. Role of Sodium 9,10-Anthraquinone-2-Sulphonate in Photo-Oxidation Reactions. *J. Chem. Soc. A* **1969**, No. 0, 767–773.
- (237) Moore, J. N.; Phillips, D.; Nakashima, N.; Yoshihara, K. Photophysics and Photochemistry of Sulphonated Derivatives of 9,10-Anthraquinone. “Strong” versus “weak” Sensitisers. *J. Chem. Soc., Faraday Trans. 2* **1987**, *83*, 1487–1508.
- (238) Goor, G.; Glenneberg, J.; Jacobi, S. Hydrogen Peroxide. In *Ullmann's Encyclopedia of Industrial Chemistry*; Wiley-VCH Verlag GmbH & Co. KGaA, 2000.
- (239) Kuzmin, V. A.; Chibisov, A. K. One-Electron Photo-Oxidation of Inorganic Anions by 9,10-Anthraquinone-2,6-Disulphonic Acid in the Triplet State. *J. Chem. Soc. D* **1971**, No. 23, 1559–1560.
- (240) Buckle, D. R.; Collier, S. J.; McLaw, M. D. 2,3-Dichloro-5,6-Dicyano-1,4-Benzo-Quinone. In *Encyclopedia of Reagents for Organic Synthesis*; John Wiley & Sons, Ltd, Ed.; John Wiley & Sons, Ltd, Chichester, UK, 2005.
- (241) Allen, N. S.; McKellar, J. F. The Photochemistry of Commercial Polyamides. *Macromol. Revs.* **1978**, *13*, 241–281.
- (242) Allen, N. S.; Hurley, J. P.; Bannister, D.; Follows, G. W. Photochemical Crosslinking of Nylon-6,6 Induced by 2-Substituted Anthraquinones. *Eur. Polym. J.* **1992**, *28*, 1309–1314.
- (243) Allen, N. S.; Hurley, J. P.; Bannister, D.; Follows, G. W.; Navaratnam, S.; Parsons, B. J. Laser and Microsecond Flash Photolysis of 2-Substituted Anthraquinones and Photochemical Cross-Linking of Nylon 6,6 Polymer. *J. Photochem. Photobiol., A* **1992**, *68*, 213–226.
- (244) Walker, D.; Hiebert, J. D. 2,3-Dichloro-5,6-Dicyanobenzoquinone and Its Reactions. *Chem. Rev.* **1967**, *67*, 153–195.
- (245) Bharate, S. B. 2,3-Dichloro-5,6-Dicyano-1,4-Benzoquinone (DDQ). *Synlett* **2006**, No. 3, 0496–0497.
- (246) Shen, Z.; Dai, J.; Xiong, J.; He, X.; Mo, W.; Hu, B.; Sun, N.; Hu, X. 2,3-Dichloro-5,6-Dicyano-1,4-Benzoquinone (DDQ)/*tert*-Butyl Nitrite/Oxygen: A Versatile Catalytic Oxidation System. *Adv. Synth. Catal.* **2011**, *353*, 3031–3038.
- (247) Gould, I. R.; Moser, J. E.; Armitage, B.; Farid, S.; Goodman, J. L.; Herman, M. S. Electron-Transfer Reactions in the Marcus Inverted Region. Charge Recombination versus Charge Shift Reactions. *J. Am. Chem. Soc.* **1989**, *111*, 1917–1919.
- (248) Vogel, K.; Reichardt, C.; Dimroth, K. 2,4,6-Triphenylpyrylium Tetrafluoroborate. *Org. Synth.* **1969**, *49*, 121.
- (249) Todd, W. P.; Dinnocenzo, J. P.; Farid, S.; Goodman, J. L.; Gould, I. R. Efficient Photoinduced Generation of Radical Cations in Solvents of Medium and Low Polarity. *J. Am. Chem. Soc.* **1991**, *113*, 3601–3602.
- (250) Miranda, M. A.; Garcia, H. 2,4,6-Triphenylpyrylium Tetrafluoroborate as an Electron-Transfer Photosensitizer. *Chem. Rev.* **1994**, *94*, 1063–1089.
- (251) Che, Y.; Ma, W.; Ji, H.; Zhao, J.; Zang, L. Visible Photooxidation of Dibenzothiophenes Sensitized by 2-(4-Methoxyphenyl)-4, 6-Diphenylpyrylium: An Electron Transfer Mechanism without Involvement of Superoxide. *J. Phys. Chem. B* **2006**, *110*, 2942–2948.
- (252) Conrow, K.; Radlick, P. C. 2,2',4,4',6,6'-Hexamethyl-4,4'-bi-4H-Pyran. *J. Org. Chem.* **1961**, *26*, 2260–2263.
- (253) Balaban, A. T.; Bratu, C.; Rentea, C. N. One-Electron Reduction of Pyrylium Salts. *Tetrahedron* **1964**, *20*, 265–269.
- (254) Pragst, F.; Seydewitz, U. Zur Elektrochemie von Pyryliumverbindungen. I. Kathodische Dimerisierung von 2,6-Diphenylpyrylium-perchlorat. *J. Prakt. Chem.* **1977**, *319*, 952–958.
- (255) Pragst, F.; Ziebig, R.; Seydewitz, U.; Diesel, G. Electrochemistry of Pyrylium compounds—II. Structural Effects on the Voltammetric Behavior in Acetonitrile. *Electrochim. Acta* **1980**, *25*, 341–352.
- (256) Kawata, H.; Niizuma, S. Pyranyl Radicals and Their Dimers. *Bull. Chem. Soc. Jpn.* **1989**, *62*, 2279–2283.
- (257) Zimmermann, T.; Fischer, G. W.; Reinhardt, M. Einelektronenübertragung von Alkoholationen Auf 2,4,6-Triphenyl-Pyrylium- Und -Thiopyryliumkationen. *Z. Chem.* **1986**, *26*, 400–401.
- (258) Miyashi, T.; Konno, A.; Takahashi, Y. Evidence for a Chair Cyclohexane-1,4-Radical Cation Intermediate in the Single Electron-Transfer-Induced Cope Rearrangement of 2,5-Diaryl-1,5-Hexadienes. *J. Am. Chem. Soc.* **1988**, *110*, 3676–3677.
- (259) Parrish, J. D.; Ischay, M. A.; Lu, Z.; Guo, S.; Peters, N. R.; Yoon, T. P. Endoperoxide Synthesis by Photocatalytic Aerobic [2 + 2 + 2] Cycloadditions. *Org. Lett.* **2012**, *14*, 1640–1643.
- (260) Gesmundo, N. J.; Nicewicz, D. A. Cyclization–endoperoxidation Cascade Reactions of Dienes Mediated by a Pyrylium Photoredox Catalyst. *Beilstein J. Org. Chem.* **2014**, *10*, 1272–1281.
- (261) Ledwith, A. Cation Radicals in Electron Transfer Reactions. *Acc. Chem. Res.* **1972**, *5*, 133–139.
- (262) Crellin, R. A.; Lambert, M. C.; Ledwith, A. Photochemical 2 + 2 Cycloaddition via a Cation-Radical Chain Reaction. *J. Chem. Soc. D* **1970**, No. 11, 682–683.
- (263) Bauld, N. L.; Bellville, D. J.; Harirchian, B.; Lorenz, K. T.; Pabon, R. A.; Reynolds, D. W.; Wirth, D. D.; Chiou, H. S.; Marsh, B. K. Cation Radical Pericyclic Reactions. *Acc. Chem. Res.* **1987**, *20*, 371–378.
- (264) Ischay, M. A.; Ament, M. S.; Yoon, T. P. Crossed Intermolecular [2 + 2] Cycloaddition of Styrenes by Visible Light Photocatalysis. *Chem. Sci.* **2012**, *3*, 2807–2811.
- (265) Riener, M.; Nicewicz, D. A. Synthesis of Cyclobutane Lignans via an Organic Single Electron Oxidant–electron Relay System. *Chem. Sci.* **2013**, *4*, 2625–2629.
- (266) Gieseler, A.; Steckhan, E.; Wiest, O.; Knoch, F. Photochemically Induced Radical-Cation Diels-Alder Reaction of Indole and Electron-Rich Dienes. *J. Org. Chem.* **1991**, *56*, 1405–1411.
- (267) McIoch, J.; Steckhan, E. Photochemically Initiated, Electron-Transfer-Catalyzed Diels-Alder Reactions of Electron-Rich Dienophiles. *Angew. Chem., Int. Ed. Engl.* **1985**, *24*, 412–414.
- (268) Peglow, T.; Blechert, S.; Steckhan, E. Radical Cation Diels-Alder Reaction between Indoles and Exocyclic 1,3-Dienes with Incorporated Intentional Cleaving Points. *Chem. Commun.* **1999**, No. 5, 433–434.
- (269) Zhang, W.; Jia, X.; Yang, L.; Liu, Z.-L. Photosensitized Diels-Alder Reactions of N-Arylimines: Synthesis of Tetrahydroquinoline Derivatives. *Tetrahedron Lett.* **2002**, *43*, 9433–9436.
- (270) Zhang, W.; Guo, Y.; Liu, Z.; Jin, X.; Yang, L.; Liu, Z.-L. Photochemically Catalyzed Diels–Alder Reaction of Arylimines with N-Vinylpyrrolidinone and N-Vinylcarbazole by 2,4,6-Triphenylpyrylium

- Salt: Synthesis of 4-Heterocycle-Substituted Tetrahydroquinoline Derivatives. *Tetrahedron* **2005**, *61*, 1325–1333.
- (271) Pérez-Ruiz, R.; Domingo, L. R.; Jiménez, M. C.; Miranda, M. A. Experimental and Theoretical Studies on the Radical-Cation-Mediated Imino-Diels–Alder Reaction. *Org. Lett.* **2011**, *13*, 5116–5119.
- (272) Argüello, J. E.; Pérez-Ruiz, R.; Miranda, M. A. Novel [4 + 2] Cycloaddition between Thiobenzophenone and Aryl-Substituted Alkenes via Photoinduced Electron Transfer. *Org. Lett.* **2007**, *9*, 3587–3590.
- (273) Domingo, L. R.; Pérez-Ruiz, R.; Argüello, J. E.; Miranda, M. A. DFT Study on the Molecular Mechanism of the [4 + 2] Cycloaddition between Thiobenzophenone and Arylalkenes via Radical Cations. *J. Phys. Chem. A* **2009**, *113*, 5718–5722.
- (274) Perkowski, A. J.; Cruz, C. L.; Nicewicz, D. A. Ambient-Temperature Newman–Kwart Rearrangement Mediated by Organic Photoredox Catalysis. *J. Am. Chem. Soc.* **2015**, *137*, 15684–15687.
- (275) Ogawa, K. A.; Goetz, A. E.; Boydston, A. J. Metal-Free Ring-Opening Metathesis Polymerization. *J. Am. Chem. Soc.* **2015**, *137*, 1400–1403.
- (276) Goetz, A. E.; Boydston, A. J. Metal-Free Preparation of Linear and Cross-Linked Polydicyclopentadiene. *J. Am. Chem. Soc.* **2015**, *137*, 7572–7575.
- (277) Ogawa, K.; Goetz, A.; Boydston, A. Developments in Externally Regulated Ring-Opening Metathesis Polymerization. *Synlett* **2016**, *27*, 203–214.
- (278) Chiba, K.; Miura, T.; Kim, S.; Kitano, Y.; Tada, M. Electrocatalytic Intermolecular Olefin Cross-Coupling by Anodically Induced Formal [2+2] Cycloaddition between Enol Ethers and Alkenes. *J. Am. Chem. Soc.* **2001**, *123*, 11314–11315.
- (279) Miura, T.; Kim, S.; Kitano, Y.; Tada, M.; Chiba, K. Electrochemical Enol Ether/Olefin Cross-Metathesis in a Lithium Perchlorate/Nitromethane Electrolyte Solution. *Angew. Chem., Int. Ed.* **2006**, *45*, 1461–1463.
- (280) Perkowski, A. J.; You, W.; Nicewicz, D. A. Visible Light Photoinitiated Metal-Free Living Cationic Polymerization of 4-Methoxystyrene. *J. Am. Chem. Soc.* **2015**, *137*, 7580–7583.
- (281) Pérez-Ruiz, R.; Jiménez, M. C.; Miranda, M. A. Hetero-Cycloreversions Mediated by Photoinduced Electron Transfer. *Acc. Chem. Res.* **2014**, *47*, 1359–1368.
- (282) Miranda, M. A.; Izquierdo, M. A.; Galindo, F. Steady-State and Time-Resolved Studies on Oxetane Cycloreversion Using (Thia)-pyrylium Salts as Electron-Transfer Photosensitizers. *Org. Lett.* **2001**, *3*, 1965–1967.
- (283) Miranda, M. A.; Izquierdo, M. A.; Galindo, F. Involvement of Triplet Excited States and Olefin Radical Cations in Electron-Transfer Cycloreversion of Four-Membered Ring Compounds Photosensitized by (Thia)-pyrylium Salts. *J. Org. Chem.* **2002**, *67*, 4138–4142.
- (284) Miranda, M. A.; Izquierdo, M. A. Stepwise Cycloreversion of Oxetane Radical Cations with Initial C–O Bond Cleavage. *J. Am. Chem. Soc.* **2002**, *124*, 6532–6533.
- (285) Elias Argüello, J.; Pérez-Ruiz, R.; Miranda, M. A. Photoinduced Electron-Transfer Cycloreversion of Thietanes: The Role of Ion–Molecule Complexes. *Org. Lett.* **2010**, *12*, 1884–1887.
- (286) Pérez-Ruiz, R.; Sáez, J. A.; Domingo, L. R.; Jiménez, M. C.; Miranda, M. A. Oxetane Ring Enlargement through Nucleophilic Trapping of Radical Cations by Acetonitrile. *Org. Lett.* **2012**, *14*, 5700–5703.
- (287) Bramley, R.; Johnson, M. D. 239. N-Substituted Heterocyclic Cations. Part V. The Use of Proton Magnetic Resonance Spectroscopy in the Solution of Some Classical Structural Problems. *J. Chem. Soc.* **1965**, No. 0, 1372–1376.
- (288) Bunting, J. W.; Fitzgerald, N. P. Kinetic and Thermodynamic Control of Pseudobase Formation from C-3 Substituted 1-Methyl-quinolinium Cations. *Can. J. Chem.* **1984**, *62*, 1301–1307.
- (289) Michael Bockman, T.; Kochi, J. K. Nucleophilic Addition versus Electron Transfer in Carbonylmethallate Salts. Donor–acceptor Interactions in the Precursor Ion Pairs. *J. Phys. Org. Chem.* **1997**, *10*, 542–562.
- (290) Šturala, J.; Boháčová, S.; Chudoba, J.; Metelková, R.; Cibulka, R. Electron-Deficient Heteroarenium Salts: An Organocatalytic Tool for Activation of Hydrogen Peroxide in Oxidations. *J. Org. Chem.* **2015**, *80*, 2676–2699.
- (291) Fukuzumi, S.; Noura, S. Regioselective Reduction of 1-Methylquinolinium Ions by Tributyltin Hydride and Tris(trimethylsilyl)silane via Photoinduced Electron Transfer. *J. Chem. Soc., Chem. Commun.* **1994**, No. 3, 287–288.
- (292) Kotani, H.; Ohkubo, K.; Fukuzumi, S. Formation of a Long-Lived Electron-Transfer State of a Naphthalene–quinolinium Ion Dyad and the π-Dimer Radical Cation. *Faraday Discuss.* **2012**, *155*, 89–102.
- (293) Clennan, E. L.; Liao, C. Role of Sulfide Radical Cations in Electron Transfer Promoted Molecular Oxygenations at Sulfur. *J. Am. Chem. Soc.* **2008**, *130*, 4057–4068.
- (294) Baciocchi, E.; Del Giacco, T.; Giombolini, P.; Lanzalunga, O. C–S Bond Cleavage in the Sensitized Photooxygenation of *Tert*-Alkyl Phenyl Sulfides. The Role of Superoxide Anion. *Tetrahedron* **2006**, *62*, 6566–6573.
- (295) Ohkubo, K.; Kobayashi, T.; Fukuzumi, S. Direct Oxygenation of Benzene to Phenol Using Quinolinium Ions as Homogeneous Photocatalysts. *Angew. Chem., Int. Ed.* **2011**, *50*, 8652–8655.
- (296) Ohkubo, K.; Kobayashi, T.; Fukuzumi, S. Photocatalytic Alkoxylation of Benzene with 3-Cyano-1-Methylquinolinium Ion. *Opt. Express* **2012**, *20*, A360.
- (297) Ohkubo, K.; Fujimoto, A.; Fukuzumi, S. Photocatalytic Monofluorination of Benzene by Fluoride via Photoinduced Electron Transfer with 3-Cyano-1-Methylquinolinium. *J. Phys. Chem. A* **2013**, *117*, 10719–10725.
- (298) Kumar, V. S.; Floreancig, P. E. Electron Transfer Initiated Cyclizations: Cyclic Acetal Synthesis through Carbon–Carbon σ-Bond Activation. *J. Am. Chem. Soc.* **2001**, *123*, 3842–3843.
- (299) Wan, S.; Gunaydin, H.; Houk, K. N.; Floreancig, P. E. An Experimental and Computational Approach to Defining Structure/Reactivity Relationships for Intramolecular Addition Reactions to Bicyclic Epoxonium Ions. *J. Am. Chem. Soc.* **2007**, *129*, 7915–7923.
- (300) Dockery, K. P.; Dinnocenzo, J. P.; Farid, S.; Goodman, J. L.; Gould, I. R.; Todd, W. P. Nucleophile-Assisted Cleavage of Benzyltrialkylsilane Cation Radicals. *J. Am. Chem. Soc.* **1997**, *119*, 1876–1883.
- (301) Kumar, V. S.; Aubele, D. L.; Floreancig, P. E. Aerobic Organocatalytic Photoinitiated Arene Oxidations: Application to Electron Transfer Initiated Cyclization Reactions. *Org. Lett.* **2001**, *3*, 4123–4125.
- (302) Aubele, D. L.; Floreancig, P. E. Oxidative Synthesis of Cyclic Acyl Aminals through Carbon–Carbon σ-Bond Activation. *Org. Lett.* **2002**, *4*, 3443–3446.
- (303) Kumar, V. S.; Aubele, D. L.; Floreancig, P. E. Electron Transfer Initiated Heterogenerative Cascade Cyclizations: Polyether Synthesis under Nonacidic Conditions. *Org. Lett.* **2002**, *4*, 2489–2492.
- (304) Green, M. E.; Rech, J. C.; Floreancig, P. E. Total Synthesis of Theopederin D. *Angew. Chem., Int. Ed.* **2008**, *47*, 7317–7320.
- (305) Ozser, M. E.; Icil, H.; Makhnyia, Y.; Demuth, M. Electron-Transfer-Initiated Cascade Cyclizations of Terpenoid Polyalkenes in a Low-Polarity Solvent: One-Step Synthesis of Mono- and Polycyclic Terpenoids with Various Functionalities. *Eur. J. Org. Chem.* **2004**, *2004*, 3686–3692.
- (306) Suga, K.; Ohkubo, K.; Fukuzumi, S. Photocatalytic Oxygenation of Pivalic Acid with Molecular Oxygen via Photoinduced Electron Transfer Using 10-Methylacridinium Ions. *J. Phys. Chem. A* **2006**, *110*, 3860–3867.
- (307) Zhou, D.; Khatmullin, R.; Walpita, J.; Miller, N. A.; Luk, H. L.; Vyas, S.; Hadad, C. M.; Glusac, K. D. Mechanistic Study of the Photochemical Hydroxide Ion Release from 9-Hydroxy-10-Methyl-9-Phenyl-9,10-Dihydroacridine. *J. Am. Chem. Soc.* **2012**, *134*, 11301–11303.
- (308) Jonker, S. A.; Ariese, F.; Verhoeven, J. W. Cation Complexation with Functionalized 9-Acridinium Ions: Possible Applications in the Development of Cation-Selective Optical Probes. *Recl. Trav. Chim. Pays-Bas* **1989**, *108*, 109–115.

- (309) Jones, G., II; Farahat, M. S.; Greenfield, S. R.; Gosztola, D. J.; Wasielewski, M. R. Ultrafast Photoinduced Charge-Shift Reactions in Electron Donor-Acceptor 9-Arylacridinium Ions. *Chem. Phys. Lett.* **1994**, *229*, 40–46.
- (310) Fukuzumi, S.; Kotani, H.; Ohkubo, K.; Ogo, S.; Tkachenko, N. V.; Lemmetyinen, H. Electron-Transfer State of 9-Mesityl-10-Methylacridinium Ion with a Much Longer Lifetime and Higher Energy Than That of the Natural Photosynthetic Reaction Center. *J. Am. Chem. Soc.* **2004**, *126*, 1600–1601.
- (311) Kotani, H.; Ohkubo, K.; Fukuzumi, S. Photocatalytic Oxygenation of Anthracenes and Olefins with Dioxygen via Selective Radical Coupling Using 9-Mesityl-10-Methylacridinium Ion as an Effective Electron-Transfer Photocatalyst. *J. Am. Chem. Soc.* **2004**, *126*, 15999–16006.
- (312) Hering, T.; Slanina, T.; Hancock, A.; Wille, U.; König, B. Visible Light Photooxidation of Nitrate: The Dawn of a Nocturnal Radical. *Chem. Commun.* **2015**, *51*, 6568–6571.
- (313) Fukuzumi, S.; Kotani, H.; Ohkubo, K. Response: Why Had Long-Lived Electron-Transfer States of Donor-Substituted 10-Methylacridinium Ions Been Overlooked? Formation of the Dimer Radical Cations Detected in the near-IR Region. *Phys. Chem. Chem. Phys.* **2008**, *10*, 5159.
- (314) Verhoeven, J. W.; Ramesdonk, H. J.; Zhang, H.; Groeneveld, M. M.; Benniston, A. C.; Harriman, A. Long-Lived Charge-Transfer States in 9-Aryl-Acridinium Ions; a Critical Reinvestigation. *Int. J. Photoenergy* **2005**, *7*, 103–108.
- (315) Benniston, A. C.; Harriman, A.; Verhoeven, J. W. Comment: Electron-Transfer Reactions in the 9-Mesityl-10-Methylacridinium Ion: Impurities, Triplet States and Infinitely Long-Lived Charge-Shift States? *Phys. Chem. Chem. Phys.* **2008**, *10*, 5156.
- (316) Hoshino, M.; Uekusa, H.; Tomita, A.; Koshihara, S.; Sato, T.; Nozawa, S.; Adachi, S.; Ohkubo, K.; Kotani, H.; Fukuzumi, S. Determination of the Structural Features of a Long-Lived Electron-Transfer State of 9-Mesityl-10-Methylacridinium Ion. *J. Am. Chem. Soc.* **2012**, *134*, 4569–4572.
- (317) Fukuzumi, S.; Ohkubo, K.; Suenobu, T. Long-Lived Charge Separation and Applications in Artificial Photosynthesis. *Acc. Chem. Res.* **2014**, *47*, 1455–1464.
- (318) Lin, Y.-C.; Chen, C.-T. Acridinium Salt-Based Fluoride and Acetate Chromofluorescent Probes: Molecular Insights into Anion Selectivity Switching. *Org. Lett.* **2009**, *11*, 4858–4861.
- (319) Wilger, D. J.; Grandjean, J.-M. M.; Lammert, T. R.; Nicewicz, D. A. The Direct Anti-Markovnikov Addition of Mineral Acids to Styrenes. *Nat. Chem.* **2014**, *6*, 720–726.
- (320) Romero, N. A.; Margrey, K. A.; Tay, N. E.; Nicewicz, D. A. Site-Selective Arene C–H Amination via Photoredox Catalysis. *Science* **2015**, *349*, 1326–1330.
- (321) Ohkubo, K.; Mizushima, K.; Iwata, R.; Souma, K.; Suzuki, N.; Fukuzumi, S. Simultaneous Production of *P*-Tolualdehyde and Hydrogen Peroxide in Photocatalytic Oxygenation of *P*-Xylene and Reduction of Oxygen with 9-Mesityl-10-Methylacridinium Ion Derivatives. *Chem. Commun.* **2010**, *46*, 601–603.
- (322) Ohkubo, K.; Fujimoto, A.; Fukuzumi, S. Metal-Free Oxygenation of Cyclohexane with Oxygen Catalyzed by 9-Mesityl-10-Methylacridinium and Hydrogen Chloride under Visible Light Irradiation. *Chem. Commun.* **2011**, *47*, 8515.
- (323) Kadija, I. V. Measurements of the Steady-State Activation Overpotential of Chlorine Evolving Electrodes. *J. Electrochem. Soc.* **1984**, *131*, 601–608.
- (324) Eriksen, J.; Foote, C. S.; Parker, T. L. Photosensitized Oxygenation of Alkenes and Sulfides via a Non-Singlet-Oxygen Mechanism. *J. Am. Chem. Soc.* **1977**, *99*, 6455–6456.
- (325) Eriksen, J.; Foote, C. S. Electron-Transfer Photooxygenation. 5. Oxidation of Phenyl-Substituted Alkenes Sensitized by Cyanoanthracenes. *J. Am. Chem. Soc.* **1980**, *102*, 6083–6088.
- (326) Kabe, Y.; Takata, T.; Ueno, K.; Ando, W. Stereochemical Studies of Dioxetane Formation with Hindered Olefins. *J. Am. Chem. Soc.* **1984**, *106*, 8174–8180.
- (327) Suga, K.; Ohkubo, K.; Fukuzumi, S. Oxygenation of  $\alpha$ -Methylstyrene with Molecular Oxygen, Catalyzed by 10-Methylacridinium Ion via Photoinduced Electron Transfer. *J. Phys. Chem. A* **2003**, *107*, 4339–4346.
- (328) Griesbeck, A. G.; Cho, M. 9-Mesityl-10-Methylacridinium: An Efficient Type II and Electron-Transfer Photooxygenation Catalyst. *Org. Lett.* **2007**, *9*, 611–613.
- (329) Baciocchi, E.; Giacco, T. D.; Murgia, S. M.; Sebastiani, G. V. Rate and Mechanism for the Reaction of the Nitrate Radical with Aromatic and Alkylnaromatic Compounds in Acetonitrile. *J. Chem. Soc., Chem. Commun.* **1987**, No. 16, 1246–1248.
- (330) Wille, U.; Lietzau, L. Diastereoselective Formation of Anellated Tetrahydrofurans Using a Nitrate Radical Induced Oxidative, Self-Terminating Radical Cyclization Cascade. *Tetrahedron* **1999**, *55*, 10119–10134.
- (331) Wille, U.; Lietzau, L. Stereoselection in 5-Exo Radical Cyclizations of Polysubstituted 2-Oxahex-5-Enyl Radicals: A Systematic Study of the Combination Substituent Effect. *Tetrahedron* **1999**, *55*, 11465–11474.
- (332) Benniston, A. C.; Elliott, K. J.; Harrington, R. W.; Clegg, W. On the Photochemical Stability of the 9-Mesityl-10-Methylacridinium Cation. *Eur. J. Org. Chem.* **2009**, *2009*, 253–258.
- (333) Xu, H. J.; Xu, X. L.; Fu, Y.; Feng, Y. S. Photocatalytic Oxidation of Primary and Secondary Benzyl Alcohol Catalyzed by Two Coenzyme NAD<sup>+</sup> Models. *Chin. Chem. Lett.* **2007**, *18*, 1471–1475.
- (334) Baciocchi, E.; Bietti, M.; Lanzalunga, O. Mechanistic Aspects of  $\beta$ -Bond-Cleavage Reactions of Aromatic Radical Cations. *Acc. Chem. Res.* **2000**, *33*, 243–251.
- (335) Bordwell, F. G.; Cheng, J. P. Radical-Cation Acidities in Solution and in the Gas Phase. *J. Am. Chem. Soc.* **1989**, *111*, 1792–1795.
- (336) Schmittel, M.; Burghart, A. Understanding Reactivity Patterns of Radical Cations. *Angew. Chem., Int. Ed. Engl.* **1997**, *36*, 2550–2589.
- (337) da Silva, G.; Hamdan, M. R.; Bozzelli, J. W. Oxidation of the Benzyl Radical: Mechanism, Thermochemistry, and Kinetics for the Reactions of Benzyl Hydroperoxide. *J. Chem. Theory Comput.* **2009**, *5*, 3185–3194.
- (338) Ohkubo, K.; Suga, K.; Fukuzumi, S. Solvent-Free Selective Photocatalytic Oxidation of Benzyl Alcohol to Benzaldehyde by Molecular Oxygen Using 9-Phenyl-10-Methylacridinium. *Chem. Commun.* **2006**, No. 19, 2018–2020.
- (339) Ohkubo, K.; Mizushima, K.; Fukuzumi, S. Oxygenation and Chlorination of Aromatic Hydrocarbons with Hydrochloric Acid Photosensitized by 9-Mesityl-10-Methylacridinium under Visible Light Irradiation. *Res. Chem. Intermed.* **2013**, *39*, 205–220.
- (340) Chew, A. A.; Atkinson, R.; Aschmann, S. M. Kinetics of the Gas-Phase Reactions of NO<sub>3</sub> Radicals with a Series of Alcohols, Glycol Ethers, Ethers and Chloroalkenes. *J. Chem. Soc., Faraday Trans.* **1998**, *94*, 1083–1089.
- (341) Xu, H.-J.; Zhu, F.-F.; Shen, Y.-Y.; Wan, X.; Feng, Y.-S. Baeyer–Villiger Oxidation of Cyclobutanones with 10-Methylacridinium as an Efficient Organocatalyst. *Tetrahedron* **2012**, *68*, 4145–4151.
- (342) Bruice, T. C.; Noar, J. B.; Ball, S. S.; Venkataram, U. V. Monooxygen Donation Potential of 4a-Hydroperoxyflavins as Compared with Those of a Percarboxylic Acid and Other Hydroperoxides. Monooxygen Donation to Olefin, Tertiary Amine, Alkyl Sulfide, and Iodide Ion. *J. Am. Chem. Soc.* **1983**, *105*, 2452–2463.
- (343) Murahashi, S.-I.; Ono, S.; Imada, Y. Asymmetric Baeyer–Villiger Reaction with Hydrogen Peroxide Catalyzed by a Novel Planar-Chiral Bisflavin. *Angew. Chem., Int. Ed.* **2002**, *41*, 2366–2368.
- (344) Jung, H. H.; Floreancig, P. E. Mechanistic Analysis of Oxidative C–H Cleavages Using Inter- and Intramolecular Kinetic Isotope Effects. *Tetrahedron* **2009**, *65*, 10830–10836.
- (345) Xiang, M.; Meng, Q.-Y.; Li, J.-X.; Zheng, Y.-W.; Ye, C.; Li, Z.-J.; Chen, B.; Tung, C.-H.; Wu, L.-Z. Activation of C–H Bonds through Oxidant-Free Photoredox Catalysis: Cross-Coupling Hydrogen-Evolution Transformation of Isochromans and  $\beta$ -Keto Esters. *Chem. - Eur. J.* **2015**, *21*, 18080–18084.

- (346) Dempsey, J. L.; Brunschwig, B. S.; Winkler, J. R.; Gray, H. B. Hydrogen Evolution Catalyzed by Cobaloximes. *Acc. Chem. Res.* **2009**, *42*, 1995–2004.
- (347) Hu, X.; Cossairt, B. M.; Brunschwig, B. S.; Lewis, N. S.; Peters, J. C. Electrocatalytic Hydrogen Evolution by Cobalt Difluoroboryl-Diglyoximate Complexes. *Chem. Commun.* **2005**, No. 37, 4723–4725.
- (348) Chateauneuf, J.; Luszyk, J.; Ingold, K. U. Spectroscopic and Kinetic Characteristics of Aroyloxy Radicals. 2. Benzyloxy and Ring-Substituted Aroyloxy Radicals. *J. Am. Chem. Soc.* **1988**, *110*, 2886–2893.
- (349) Ramirez, N. P.; Bosque, I.; Gonzalez-Gomez, J. C. Photocatalytic Dehydrogenative Lactonization of 2-Arylbenzoic Acids. *Org. Lett.* **2015**, *17*, 4550–4553.
- (350) Pandey, G.; Krishna, A.; Rao, J. M. Single Electron Transfer Initiated Photocyclization of Substituted Cinnamic Acids to Corresponding Coumarins. *Tetrahedron Lett.* **1986**, *27*, 4075–4076.
- (351) Togo, H.; Muraki, T.; Yokoyama, M. Remote Functionalization (1): Synthesis of  $\gamma$ - and  $\delta$ -Lactones from Aromatic Carboxylic Acids. *Tetrahedron Lett.* **1995**, *36*, 7089–7092.
- (352) Ohkubo, K.; Mizushima, K.; Iwata, R.; Fukuzumi, S. Selective Photocatalytic Aerobic Bromination with Hydrogen Bromide via an Electron-Transfer State of 9-Mesityl-10-Methylacridinium Ion. *Chem. Sci.* **2011**, *2*, 715–722.
- (353) Podgoršek, A.; Stavber, S.; Zupan, M.; Iskra, J. Environmentally Benign Electrophilic and Radical Bromination “on Water”:  $H_2O_2$ –HBr System versus N-Bromosuccinimide. *Tetrahedron* **2009**, *65*, 4429–4439.
- (354) Hagel, M.; Liu, J.; Muth, O.; Estevez Rivera, H. J.; Schwake, E.; Sripanom, L.; Henkel, G.; Dyker, G. P-Quinoid Compounds by Nucleophilic Aromatic Substitution with Hydride as Leaving Group. *Eur. J. Org. Chem.* **2007**, *2007*, 3573–3582.
- (355) Morofuji, T.; Shimizu, A.; Yoshida, J. Direct C–N Coupling of Imidazoles with Aromatic and Benzylidene Compounds via Electrooxidative C–H Functionalization. *J. Am. Chem. Soc.* **2014**, *136*, 4496–4499.
- (356) Pan, X.-M.; Schuchmann, M. N.; von Sonntag, C. Oxidation of Benzene by the OH Radical. A Product and Pulse Radiolysis Study in Oxygenated Aqueous Solution. *J. Chem. Soc., Perkin Trans. 2* **1993**, No. 3, 289–297.
- (357) Pan, X.-M.; Schuchmann, M. N.; von Sonntag, C. Hydroxyl-Radical-Induced Oxidation of Cyclohexa-1, 4-Diene by  $O_2$  in Aqueous Solution. A Pulse Radiolysis and Product Study. *J. Chem. Soc., Perkin Trans. 2* **1993**, No. 6, 1021–1028.
- (358) Fang, X.; Pan, X.-M.; Rahmann, A.; Schuchmann, H.-P.; von Sonntag, C. Reversibility in the Reaction of Cyclohexadienyl Radicals with Oxygen in Aqueous Solution. *Chem. - Eur. J.* **1995**, *1*, 423–429.
- (359) Lyons, T. W.; Sanford, M. S. Palladium-Catalyzed Ligand-Directed C–H Functionalization Reactions. *Chem. Rev.* **2010**, *110*, 1147–1169.
- (360) Louillat, M.-L.; Patureau, F. W. Oxidative C–H Amination Reactions. *Chem. Soc. Rev.* **2014**, *43*, 901–910.
- (361) Arnold, D. R.; Chan, M. S.; McManus, K. A. Photochemical Nucleophile-Olefin Combination, Aromatic Substitution (Photo-NOCAS) Reaction, Part 12. Factors Controlling the Regiochemistry of the Reaction with Alcohol as the Nucleophile. *Can. J. Chem.* **1996**, *74*, 2143–2166.
- (362) Larsen, A. G.; Holm, A. H.; Roberson, M.; Daasbjerg, K. Substituent Effects on the Oxidation and Reduction Potentials of Phenylthiyl Radicals in Acetonitrile. *J. Am. Chem. Soc.* **2001**, *123*, 1723–1729.
- (363) Hamilton, D. S.; Nicewicz, D. A. Direct Catalytic Anti-Markovnikov Hydroetherification of Alkenols. *J. Am. Chem. Soc.* **2012**, *134*, 18577–18580.
- (364) Perkowski, A. J.; Nicewicz, D. A. Direct Catalytic Anti-Markovnikov Addition of Carboxylic Acids to Alkenes. *J. Am. Chem. Soc.* **2013**, *135*, 10334–10337.
- (365) Nguyen, T. M.; Nicewicz, D. A. Anti-Markovnikov Hydroamination of Alkenes Catalyzed by an Organic Photoredox System. *J. Am. Chem. Soc.* **2013**, *135*, 9588–9591.
- (366) Nguyen, T. M.; Manohar, N.; Nicewicz, D. A. Anti-Markovnikov Hydroamination of Alkenes Catalyzed by a Two-Component Organic Photoredox System: Direct Access to Phenethylamine Derivatives. *Angew. Chem., Int. Ed.* **2014**, *53*, 6198–6201.
- (367) Markownikoff, W. I. Über Die Abhängigkeit Der Verschiedenen Vertretbarkeit Des Radicalwasserstoffs in Den Isomeren Buttersäuren. *Justus Liebigs Ann. Chem.* **1870**, *153*, 228–259.
- (368) Carey, F. A.; Sundberg, R. J. *Advanced Organic Chemistry*, 5th ed.; Springer: New York, 2007.
- (369) Grandjean, J.-M. M.; Nicewicz, D. A. Synthesis of Highly Substituted Tetrahydrofurans by Catalytic Polar-Radical-Crossover Cycloadditions of Alkenes and Alkenols. *Angew. Chem., Int. Ed.* **2013**, *52*, 3967–3971.
- (370) Zeller, M. A.; Riener, M.; Nicewicz, D. A. Butyrolactone Synthesis via Polar Radical Crossover Cycloaddition Reactions: Diastereoselective Syntheses of Methylenolactocin and Protolichesterinic Acid. *Org. Lett.* **2014**, *16*, 4810–4813.
- (371) Gesmundo, N. J.; Grandjean, J.-M. M.; Nicewicz, D. A. Amide and Amine Nucleophiles in Polar Radical Crossover Cycloadditions: Synthesis of  $\gamma$ -Lactams and Pyrrolidines. *Org. Lett.* **2015**, *17*, 1316–1319.
- (372) Cavanaugh, C. L.; Nicewicz, D. A. Synthesis of  $\alpha$ -Benzylxyamino- $\gamma$ -Butyrolactones via a Polar Radical Crossover Cycloaddition Reaction. *Org. Lett.* **2015**, *17*, 6082–6085.
- (373) Morse, P. D.; Nicewicz, D. A. Divergent Regioselectivity in Photoredox-Catalyzed Hydrofunctionalization Reactions of Unsaturated Amides and Thioamides. *Chem. Sci.* **2015**, *6* (1), 270–274.
- (374) Schwerkendiek, K.; Glorius, F. Efficient Oxidative Synthesis of 2-Oxazolines. *Synthesis* **2006**, *2006* (18), 2996–3002.
- (375) Wilger, D. J.; Gesmundo, N. J.; Nicewicz, D. A. Catalytic Hydrotrifluoromethylation of Styrenes and Unactivated Aliphatic Alkenes via an Organic Photoredox System. *Chem. Sci.* **2013**, *4*, 3160–3165.
- (376) Langlois, B. R.; Laurent, E.; Roidot, N. Trifluoromethylation of Aromatic Compounds with Sodium Trifluoromethanesulfinate under Oxidative Conditions. *Tetrahedron Lett.* **1991**, *32*, 7525–7528.
- (377) Langlois, B. R.; Laurent, E.; Roidot, N. Pseudo-Cationic” Trifluoromethylation of Enol Esters with Sodium Trifluoromethane-sulfinate. *Tetrahedron Lett.* **1992**, *33*, 1291–1294.
- (378) Tommasino, J.-B.; Brondex, A.; Médebielle, M.; Thomalla, M.; Langlois, B. R.; Billard, T. Trifluoromethylation Reactions with Potassium Trifluoromethanesulfinate under Electrochemical Oxidation. *Synlett* **2002**, No. 10, 1697–1699.
- (379) Mizuta, S.; Verhoog, S.; Engle, K. M.; Khotavivattana, T.; O’Duill, M.; Wheelhouse, K.; Rassias, G.; Médebielle, M.; Gouverneur, V. Catalytic Hydrotrifluoromethylation of Unactivated Alkenes. *J. Am. Chem. Soc.* **2013**, *135*, 2505–2508.
- (380) Eberson, L.; Hartshorn, M. P.; Persson, O.; Radner, F. Making Radical Cations Live Longer. *Chem. Commun.* **1996**, No. 18, 2105–2112.
- (381) Seiple, I. B.; Su, S.; Rodriguez, R. A.; Gianatassio, R.; Fujiwara, Y.; Sobel, A. L.; Baran, P. S. Direct C–H Arylation of Electron-Deficient Heterocycles with Arylboronic Acids. *J. Am. Chem. Soc.* **2010**, *132*, 13194–13196.
- (382) Uchiyama, N.; Shirakawa, E.; Nishikawa, R.; Hayashi, T. Iron-Catalyzed Oxidative Coupling of Arylboronic Acids with Benzene Derivatives through Homolytic Aromatic Substitution. *Chem. Commun.* **2011**, *47*, 11671–11673.
- (383) Yasu, Y.; Koike, T.; Akita, M. Visible Light-Induced Selective Generation of Radicals from Organoborates by Photoredox Catalysis. *Adv. Synth. Catal.* **2012**, *354*, 3414–3420.
- (384) Miyazawa, K.; Yasu, Y.; Koike, T.; Akita, M. Visible-Light-Induced Hydroalkoxymethylation of Electron-Deficient Alkenes by Photoredox Catalysis. *Chem. Commun.* **2013**, *49*, 7249–7251.
- (385) Miyazawa, K.; Koike, T.; Akita, M. Hydroaminomethylation of Olefins with Aminomethyltrifluoroborate by Photoredox Catalysis. *Adv. Synth. Catal.* **2014**, *356*, 2749–2755.

- (386) Tellis, J. C.; Primer, D. N.; Molander, G. A. Single-Electron Transmetalation in Organoboron Cross-Coupling by Photoredox/nickel Dual Catalysis. *Science* **2014**, *345*, 433–436.
- (387) Chinzei, T.; Miyazawa, K.; Yasu, Y.; Koike, T.; Akita, M. Redox-Economical Radical Generation from Organoborates and Carboxylic Acids by Organic Photoredox Catalysis. *RSC Adv.* **2015**, *5*, 21297–21300.
- (388) Cassani, C.; Bergonzini, G.; Wallentin, C.-J. Photocatalytic Decarboxylative Reduction of Carboxylic Acids and Its Application in Asymmetric Synthesis. *Org. Lett.* **2014**, *16*, 4228–4231.
- (389) Griffin, J. D.; Zeller, M. A.; Nicewicz, D. A. Hydro-decarboxylation of Carboxylic and Malonic Acid Derivatives via Organic Photoredox Catalysis: Substrate Scope and Mechanistic Insight. *J. Am. Chem. Soc.* **2015**, *137* (35), 11340–11348.
- (390) Hilborn, J. W.; Pincock, J. A. Rates of Decarboxylation of Acyloxy Radicals Formed in the Photocleavage of Substituted 1-Naphthylmethyl Alkanoates. *J. Am. Chem. Soc.* **1991**, *113*, 2683–2686.
- (391) Fraind, A.; Turncliff, R.; Fox, T.; Sodano, J.; Ryzhkov, L. R. Exceptionally High Decarboxylation Rate of a Primary Aliphatic Acyloxy Radical Determined by Radical Product Yield Analysis and Quantitative  $^1\text{H}$ -CIDNP Spectroscopy. *J. Phys. Org. Chem.* **2011**, *24*, 809–820.
- (392) Rueda-Becerril, M.; Mahé, O.; Drouin, M.; Majewski, M. B.; West, J. G.; Wolf, M. O.; Sammis, G. M.; Paquin, J.-F. Direct C–F Bond Formation Using Photoredox Catalysis. *J. Am. Chem. Soc.* **2014**, *136*, 2637–2641.
- (393) Ventre, S.; Petronijevic, F. R.; MacMillan, D. W. C. Decarboxylative Fluorination of Aliphatic Carboxylic Acids via Photoredox Catalysis. *J. Am. Chem. Soc.* **2015**, *137*, 5654–5657.
- (394) Wu, X.; Meng, C.; Yuan, X.; Jia, X.; Qian, X.; Ye, J. Transition-Metal-Free Visible-Light Photoredox Catalysis at Room-Temperature for Decarboxylative Fluorination of Aliphatic Carboxylic Acids by Organic Dyes. *Chem. Commun.* **2015**, *51*, 11864–11867.
- (395) Ohkubo, K.; Iwata, R.; Miyazaki, S.; Kojima, T.; Fukuzumi, S. Photocatalytic Formation of Dimethyllepidopterene from 9,10-Dimethylanthracene via Electron-Transfer Oxidation. *Org. Lett.* **2006**, *8*, 6079–6082.
- (396) Xuan, J.; Xia, X.-D.; Zeng, T.-T.; Feng, Z.-J.; Chen, J.-R.; Lu, L.-Q.; Xiao, W.-J. Visible-Light-Induced Formal [3+2] Cycloaddition for Pyrrole Synthesis under Metal-Free Conditions. *Angew. Chem., Int. Ed.* **2014**, *53*, 5653–5656.
- (397) Farney, E. P.; Yoon, T. P. Visible-Light Sensitization of Vinyl Azides by Transition-Metal Photocatalysis. *Angew. Chem., Int. Ed.* **2014**, *53*, 793–797.
- (398) Zeng, T.-T.; Xuan, J.; Ding, W.; Wang, K.; Lu, L.-Q.; Xiao, W.-J. [3 + 2] Cycloaddition/Oxidative Aromatization Sequence via Photoredox Catalysis: One-Pot Synthesis of Oxazoles from 2H-Azirines and Aldehydes. *Org. Lett.* **2015**, *17*, 4070–4073.
- (399) Kellmann, A. Primary Photochemical Processes of Cationic Acridine Orange in Aqueous Solution Studied by Flash Photolysis. *Photochem. Photobiol.* **1974**, *20*, 103–108.
- (400) Kellmann, A. A Flash Photolysis Study of the Triplet State of Acridine Orange in Basic Solvents. *Photochem. Photobiol.* **1971**, *14*, 85–93.
- (401) Vogelmann, E.; Rauscher, W.; Krämer, H. E. A. Reactivity of Acridine Dye Triplet States in Electron Transfer Reactions. *Photochem. Photobiol.* **1979**, *29*, 771–776.
- (402) Krasna, A. I. Proflavin Catalyzed Photoproduction of Hydrogen from Organic Compounds. *Photochem. Photobiol.* **1979**, *29*, 267–276.
- (403) Younou, M.-T.; Ziessel, R. Synthesis and Molecular Structure of a New Family of Iridium-(III) and rhodium(III) Complexes:  $[(\eta^5\text{-Me}_5\text{C}_5)\text{Ir}(\text{LL})\text{X}]^+$  and  $[(\eta^5\text{-Me}_5\text{C}_5)\text{Rh}(\text{LL})\text{Cl}]^+$ ; LL = 2,2'-Bipyridine or 1,10-Phenanthroline; X = Cl or H. Single Crystal Structures of  $[(\eta^5\text{-Me}_5\text{C}_5)\text{Ir}(\text{bpy})\text{Cl}]^+$  and  $[(\eta^5\text{-Me}_5\text{C}_5)\text{Rh}(\text{phen})\text{Cl}]^+$ . *J. Organomet. Chem.* **1989**, *363*, 197–208.
- (404) Hollmann, F.; Schmid, A.; Steckhan, E. The First Synthetic Application of a Monooxygenase Employing Indirect Electrochemical NADH Regeneration. *Angew. Chem., Int. Ed.* **2001**, *40*, 169–171.
- (405) Lo, H. C.; Buriez, O.; Kerr, J. B.; Fish, R. H. Regioselective Reduction of NAD $^+$  Models with  $[\text{Cp}^*\text{Rh}(\text{bpy})\text{H}]^+$ : Structure–Activity Relationships and Mechanistic Aspects in the Formation of the 1,4-NADH Derivatives. *Angew. Chem., Int. Ed.* **1999**, *38*, 1429–1432.
- (406) Leiva, C.; Lo, H. C.; Fish, R. H. Aqueous Organometallic Chemistry. 3. Catalytic Hydride Transfer Reactions with Ketones and Aldehydes Using  $[\text{Cp}^*\text{Rh}(\text{bpy})(\text{H}_2\text{O})](\text{OTf})_2$  as the Precatalyst and Sodium Formate as the Hydride Source: Kinetic and Activation Parameters, and the Significance of Steric and Electronic Effects. *J. Organomet. Chem.* **2010**, *695*, 145–150.
- (407) Himeda, Y.; Onozawa-Komatsuzaki, N.; Sugihara, H.; Arakawa, H.; Kasuga, K. Transfer Hydrogenation of a Variety of Ketones Catalyzed by Rhodium Complexes in Aqueous Solution and Their Application to Asymmetric Reduction Using Chiral Schiff Base Ligands. *J. Mol. Catal. A: Chem.* **2003**, *195*, 95–100.
- (408) Nam, D. H.; Park, C. B. Visible Light-Driven NADH Regeneration Sensitized by Proflavine for Biocatalysis. *ChemBioChem* **2012**, *13*, 1278–1282.
- (409) Neckers, D. C. The Indian Happiness Wart in the Development of Photodynamic Action. *J. Chem. Educ.* **1987**, *64*, 649.
- (410) Neckers, D. C.; Valdes-Aguilera, O. M. Photochemistry of the Xanthene Dyes. In *Advances in Photochemistry*; Volman, D. H., Hammond, G. S., Neckers, D. C., Eds.; John Wiley & Sons, Inc., 1993; pp 315–394.
- (411) Majek, M.; Filace, F.; von Wangelin, A. J. On the Mechanism of Photocatalytic Reactions with Eosin Y. *Beilstein J. Org. Chem.* **2014**, *10*, 981–989.
- (412) Penzkofer, A.; Beidoun, A.; Daiber, M. Intersystem-Crossing and Excited-State Absorption in Eosin Y Solutions Determined by Picosecond Double Pulse Transient Absorption Measurements. *J. Lumin.* **1992**, *51*, 297–314.
- (413) Fleming, G. R.; Knight, A. W. E.; Morris, J. M.; Morrison, R. J. S.; Robinson, G. W. Picosecond Fluorescence Studies of Xanthene Dyes. *J. Am. Chem. Soc.* **1977**, *99*, 4306–4311.
- (414) Kasche, V.; Lindqvist, L. Transient Species in the Photochemistry of Eosin\*. *Photochem. Photobiol.* **1965**, *4*, 923–933.
- (415) Wintgens, V.; Scaiano, J. C.; Linden, S. M.; Neckers, D. C. Transient Phenomena in the Laser Flash Photolysis of Rose Bengal C-2' Ethyl Ester C-6 Sodium Salt. *J. Org. Chem.* **1989**, *54*, 5242–5246.
- (416) Redmond, R. W.; Gamlin, J. N. A Compilation of Singlet Oxygen Yields from Biologically Relevant Molecules. *Photochem. Photobiol.* **1999**, *70*, 391–475.
- (417) Murasecco-Suardi, P.; Gassmann, E.; Braun, A. M.; Oliveros, E. Determination of the Quantum Yield of Intersystem Crossing of Rose Bengal. *Helv. Chim. Acta* **1987**, *70*, 1760–1773.
- (418) Meyers, A. I.; Nolen, R. L.; Collington, E. W.; Narwid, T. A.; Strickland, R. C. Total Synthesis of Camptothecin and Desethyldesoxycamptothecin. *J. Org. Chem.* **1973**, *38*, 1974–1982.
- (419) Oelgemöller, M.; Jung, C.; Ortner, J.; Mattay, J.; Zimmermann, E. Green Photochemistry: Solar Photooxygenations with Medium Concentrated Sunlight. *Green Chem.* **2005**, *7*, 35–38.
- (420) Liu, Q.; Li, Y.-N.; Zhang, H.-H.; Chen, B.; Tung, C.-H.; Wu, L.-Z. Reactivity and Mechanistic Insight into Visible-Light-Induced Aerobic Cross-Dehydrogenative Coupling Reaction by Organophotocatalysts. *Chem. - Eur. J.* **2012**, *18*, 620–627.
- (421) Lee, P. C. C.; Rodgers, M. A. J. Laser Flash Photokinetic Studies of Rose Bengal Sensitized Photodynamic Interactions of Nucleotides and DNA. *Photochem. Photobiol.* **1987**, *45*, 79–86.
- (422) Kornblum, N.; Powers, J. W.; Anderson, G. J.; Jones, W. J.; Larson, H. O.; Levand, O.; Weaver, W. M. A New and Selective Method of Oxidation. *J. Am. Chem. Soc.* **1957**, *79*, 6562–6562.
- (423) Kornblum, N.; Jones, W. J.; Anderson, G. J. A New and Selective Method of Oxidation. The Conversion of Alkyl Halides and Alkyl Tosylates to Aldehydes. *J. Am. Chem. Soc.* **1959**, *81*, 4113–4114.
- (424) Li, J.; Wang, H.; Liu, L.; Sun, J. Metal-Free, Visible-Light Photoredox Catalysis: Transformation of Arylmethyl Bromides to Alcohols and Aldehydes. *RSC Adv.* **2014**, *4*, 49974–49978.
- (425) Su, Y.; Zhang, L.; Jiao, N. Utilization of Natural Sunlight and Air in the Aerobic Oxidation of Benzyl Halides. *Org. Lett.* **2011**, *13*, 2168–2171.

- (426) Liu, Z.; Zhang, Y.; Cai, Z.; Sun, H.; Cheng, X. Photoredox Removal of P-Methoxybenzyl Ether Protecting Group with Hydrogen Peroxide as Terminal Oxidant. *Adv. Synth. Catal.* **2015**, *357*, 589–593.
- (427) Keshari, T.; Yadav, V. K.; Srivastava, V. P.; Yadav, L. D. S. Visible Light Organophotoredox Catalysis: A General Approach to  $\beta$ -Keto Sulfoxidation of Alkenes. *Green Chem.* **2014**, *16*, 3986–3992.
- (428) Yadav, A. K.; Srivastava, V. P.; Yadav, L. D. S. Visible-Light-Mediated Eosin Y Catalyzed Aerobic Desulfurization of Thioamides into Amides. *New J. Chem.* **2013**, *37*, 4119–4124.
- (429) Meyer, A. U.; Jäger, S.; Prasad Hari, D.; König, B. Visible Light-Mediated Metal-Free Synthesis of Vinyl Sulfones from Aryl Sulfinate. *Adv. Synth. Catal.* **2015**, *357*, 2050–2054.
- (430) Gazi, S.; Ananthakrishnan, R. Metal-Free-Photocatalytic Reduction of 4-Nitrophenol by Resin-Supported Dye under the Visible Irradiation. *Appl. Catal., B* **2011**, *105*, 317–325.
- (431) Yang, X.-J.; Chen, B.; Zheng, L.-Q.; Wu, L.-Z.; Tung, C.-H. Highly Efficient and Selective Photocatalytic Hydrogenation of Functionalized Nitrobenzenes. *Green Chem.* **2014**, *16*, 1082–1086.
- (432) Yang, W.; Yang, S.; Li, P.; Wang, L. Visible-Light Initiated Oxidative Cyclization of Phenyl Propiolates with Sulfonic Acids to Coumarin Derivatives under Metal-Free Conditions. *Chem. Commun.* **2015**, *51*, 7520–7523.
- (433) Witt, D. Recent Developments in Disulfide Bond Formation. *Synthesis* **2008**, *2008*, 2491–2509.
- (434) Noble, A.; Anderson, J. C. Nitro-Mannich Reaction. *Chem. Rev.* **2013**, *113*, 2887–2939.
- (435) Hari, D. P.; König, B. Eosin Y Catalyzed Visible Light Oxidative C–C and C–P Bond Formation. *Org. Lett.* **2011**, *13*, 3852–3855.
- (436) Pan, Y.; Kee, C. W.; Chen, L.; Tan, C.-H. Dehydrogenative Coupling Reactions Catalysed by Rose Bengal Using Visible Light Irradiation. *Green Chem.* **2011**, *13*, 2682–2685.
- (437) Meng, Q.-Y.; Zhong, J.-J.; Liu, Q.; Gao, X.-W.; Zhang, H.-H.; Lei, T.; Li, Z.-J.; Feng, K.; Chen, B.; Tung, C.-H.; et al. A Cascade Cross-Coupling Hydrogen Evolution Reaction by Visible Light Catalysis. *J. Am. Chem. Soc.* **2013**, *135*, 19052–19055.
- (438) Zhong, J.-J.; Meng, Q.-Y.; Liu, B.; Li, X.-B.; Gao, X.-W.; Lei, T.; Wu, C.-J.; Li, Z.-J.; Tung, C.-H.; Wu, L.-Z. Cross-Coupling Hydrogen Evolution Reaction in Homogeneous Solution without Noble Metals. *Org. Lett.* **2014**, *16*, 1988–1991.
- (439) Sundberg, R. J.; Desos, P.; Gadamasetti, K. G.; Sabat, M. Photoactive C16-C21 Fragmentation of Catharanthine. *Tetrahedron Lett.* **1991**, *32*, 3035–3038.
- (440) Pan, Y.; Wang, S.; Kee, C. W.; Dubuisson, E.; Yang, Y.; Loh, K. P.; Tan, C.-H. Graphene Oxide and Rose Bengal: Oxidative C–H Functionalisation of Tertiary Amines Using Visible Light. *Green Chem.* **2011**, *13*, 3341–3344.
- (441) Fu, W.; Guo, W.; Zou, G.; Xu, C. Selective Trifluoromethylation and Alkylation of Tetrahydroisoquinolines Using Visible Light Irradiation by Rose Bengal. *J. Fluorine Chem.* **2012**, *140*, 88–94.
- (442) Xuan, J.; Feng, Z.-J.; Duan, S.-W.; Xiao, W.-J. Room Temperature Synthesis of isoquin[2,1-a][3,1]oxazine and isoquinino-[2,1-A]pyrimidine Derivatives via Visible Light Photoredox Catalysis. *RSC Adv.* **2012**, *2*, 4065–4068.
- (443) Miyake, Y.; Nakajima, K.; Nishibayashi, Y. Visible-Light-Mediated Utilization of  $\alpha$ -Aminoalkyl Radicals: Addition to Electron-Deficient Alkenes Using Photoredox Catalysts. *J. Am. Chem. Soc.* **2012**, *134*, 3338–3341.
- (444) Liang, Z.; Xu, S.; Tian, W.; Zhang, R. Eosin Y-Catalyzed Visible-Light-Mediated Aerobic Oxidative Cyclization of *N,N*-Dimethylanilines with Maleimides. *Beilstein J. Org. Chem.* **2015**, *11*, 425–430.
- (445) Kouznetsov, V. V. Recent Synthetic Developments in a Powerful Imino Diels–Alder Reaction (Povarov Reaction): Application to the Synthesis of *N*-Polyheterocycles and Related Alkaloids. *Tetrahedron* **2009**, *65*, 2721–2750.
- (446) Vila, C.; Lau, J.; Rueping, M. Visible-Light Photoredox Catalyzed Synthesis of Pyrroloisoquinolines via Organocatalytic oxidation/[3 + 2] Cycloaddition/oxidative Aromatization Reaction Cascade with Rose Bengal. *Beilstein J. Org. Chem.* **2014**, *10*, 1233–1238.
- (447) Rueping, M.; Leonori, D.; Poisson, T. Visible Light Mediated Azomethine Ylide Formation—photoredox Catalyzed [3+2] Cycloadditions. *Chem. Commun.* **2011**, *47*, 9615–9617.
- (448) Zou, Y.-Q.; Lu, L.-Q.; Fu, L.; Chang, N.-J.; Rong, J.; Chen, J.-R.; Xiao, W.-J. Visible-Light-Induced Oxidation/[3+2] Cycloaddition/Oxidative Aromatization Sequence: A Photocatalytic Strategy To Construct Pyrrolo[2,1-A]isoquinolines. *Angew. Chem., Int. Ed.* **2011**, *50*, 7171–7175.
- (449) Chandrasekhar, D.; Borra, S.; Kapure, J. S.; Shivaji, G. S.; Srinivasulu, G.; Maurya, R. A. Visible-Light Photoredox Catalysis: Direct Synthesis of Fused  $\beta$ -Carbolines through an oxidation/[3 + 2] Cycloaddition/oxidative Aromatization Reaction Cascade in Batch and Flow Microreactors. *Org. Chem. Front.* **2015**, *2*, 1308–1312.
- (450) Xiao, T.; Li, L.; Lin, G.; Wang, Q.; Zhang, P.; Mao, Z.; Zhou, L. Synthesis of 6-Substituted Phenanthridines by Metal-Free, Visible-Light Induced Aerobic Oxidative Cyclization of 2-Isocyanobiphenyls with Hydrazines. *Green Chem.* **2014**, *16*, 2418–2421.
- (451) Chattaway, F. D. CXXII.—The Oxidation of Hydrazines by Free Oxygen. *J. Chem. Soc., Trans.* **1907**, *91*, 1323–1330.
- (452) Hardie, R. L.; Thomson, R. H. 488. The Oxidation of Phenylhydrazine. *J. Chem. Soc.* **1957**, No. 0, 2512–2518.
- (453) Wang, L.; Ma, Z.-G.; Wei, X.-J.; Meng, Q.-Y.; Yang, D.-T.; Du, S.-F.; Chen, Z.-F.; Wu, L.-Z.; Liu, Q. Synthesis of 2-Substituted Pyrimidines and Benzoxazoles via a Visible-Light-Driven Organocatalytic Aerobic Oxidation: Enhancement of the Reaction Rate and Selectivity by a Base. *Green Chem.* **2014**, *16*, 3752–3757.
- (454) Oliver Kappe, C. 100 Years of the Biginelli Dihydropyrimidine Synthesis. *Tetrahedron* **1993**, *49*, 6937–6963.
- (455) Kappe, C. O. Recent Advances in the Biginelli Dihydropyrimidine Synthesis. New Tricks from an Old Dog. *Acc. Chem. Res.* **2000**, *33*, 879–888.
- (456) Chang, J.; Zhao, K.; Pan, S. Synthesis of 2-Arylbenzoxazoles via DDQ Promoted Oxidative Cyclization of Phenolic Schiff Bases—a Solution-Phase Strategy for Library Synthesis. *Tetrahedron Lett.* **2002**, *43*, 951–954.
- (457) Praveen, C.; Kumar, K. H.; Muralidharan, D.; Perumal, P. T. Oxidative Cyclization of Thiophenolic and Phenolic Schiff's Bases Promoted by PCC: A New Oxidant for 2-Substituted Benzothiazoles and Benzoxazoles. *Tetrahedron* **2008**, *64*, 2369–2374.
- (458) Varma, R. S.; Saini, R. K.; Prakash, O. Hypervalent Iodine Oxidation of Phenolic Schiff's Bases: Synthesis of 2-Arylbenzoxazoles. *Tetrahedron Lett.* **1997**, *38*, 2621–2622.
- (459) Chen, Y.-X.; Qian, L.-F.; Zhang, W.; Han, B. Efficient Aerobic Oxidative Synthesis of 2-Substituted Benzoxazoles, Benzothiazoles, and Benzimidazoles Catalyzed by 4-Methoxy-TEMPO. *Angew. Chem., Int. Ed.* **2008**, *47*, 9330–9333.
- (460) Kapoor, R.; Singh, S.; Tripathi, S.; Yadav, L. Photocatalytic Oxidative Heterocyclization of Semicarbazones: An Efficient Approach for the Synthesis of 1,3,4-Oxadiazoles. *Synlett* **2015**, *26*, 1201–1206.
- (461) Srivastava, V.; Yadav, A.; Yadav, L. Eosin Y Catalyzed Visible-Light-Driven Aerobic Oxidative Cyclization of Thioamides to 1,2,4-Thiadiazoles. *Synlett* **2013**, *24*, 465–470.
- (462) Chang, H. S.; Yon, G. H.; Kim, Y. H. Facile Synthesis of 2-Substituted Aminobenzoxazole. One Pot Cyclodesulfurization of *N*-(2-Hydroxyphenyl)-*N'*-Phenylthioureas with Superoxide Radical Anion. *Chem. Lett.* **1986**, *15*, 1291–1294.
- (463) Yadav, A. K.; Yadav, L. D. S. Visible-Light-Mediated Difunctionalization of Styrenes: An Unprecedented Approach to 5-Aryl-2-Imino-1,3-Oxathiolanes. *Green Chem.* **2015**, *17*, 3515–3520.
- (464) Nagib, D. A.; Scott, M. E.; MacMillan, D. W. C. Enantioselective  $\alpha$ -Trifluoromethylation of Aldehydes via Photoredox Organocatalysis. *J. Am. Chem. Soc.* **2009**, *131*, 10875–10877.
- (465) Cantillo, D.; de Frutos, O.; Rincón, J. A.; Mateos, C.; Kappe, C. O. Continuous Flow  $\alpha$ -Trifluoromethylation of Ketones by Metal-Free Visible Light Photoredox Catalysis. *Org. Lett.* **2014**, *16*, 896–899.
- (466) Nagib, D. A.; MacMillan, D. W. C. Trifluoromethylation of Arenes and Heteroarenes by Means of Photoredox Catalysis. *Nature* **2011**, *480*, 224–228.

- (467) Liu, H.; Feng, W.; Kee, C. W.; Zhao, Y.; Leow, D.; Pan, Y.; Tan, C.-H. Organic Dye Photocatalyzed  $\alpha$ -Oxyamination through Irradiation with Visible Light. *Green Chem.* **2010**, *12*, 953–956.
- (468) Kee, C. W.; Chan, K. M.; Wong, M. W.; Tan, C.-H. Selective Bromination of sp<sup>3</sup> C–H Bonds by Organophotoredox Catalysis. *Asian J. Org. Chem.* **2014**, *3*, 536–544.
- (469) Mitra, S.; Ghosh, M.; Mishra, S.; Hajra, A. Metal-Free Thiocyanation of Imidazoheterocycles through Visible Light Photoredox Catalysis. *J. Org. Chem.* **2015**, *80*, 8275–8281.
- (470) Adam, W.; Krebs, O. The Nitroso Ene Reaction: A Regioselective and Stereoselective Allylic Nitrogen Functionalization of Mechanistic Delight and Synthetic Potential. *Chem. Rev.* **2003**, *103*, 4131–4146.
- (471) Teo, Y. C.; Pan, Y.; Tan, C. H. Organic Dye-Photocatalyzed Acylnitroso Ene Reaction. *ChemCatChem* **2013**, *5*, 235–240.
- (472) Neumann, M.; Zeitler, K. A Cooperative Hydrogen-Bond-Promoted Organophotoredox Catalysis Strategy for Highly Diastereoselective, Reductive Enone Cyclization. *Chem. - Eur. J.* **2013**, *19*, 6950–6955.
- (473) Davies, J.; Booth, S. G.; Essafi, S.; Dryfe, R. A. W.; Leonori, D. Visible-Light-Mediated Generation of Nitrogen-Centered Radicals: Metal-Free Hydroimination and Iminohydroxylation Cyclization Reactions. *Angew. Chem.* **2015**, *127*, 14223–14227.
- (474) Yang, D.-T.; Meng, Q.-Y.; Zhong, J.-J.; Xiang, M.; Liu, Q.; Wu, L.-Z. Metal-Free Desulfonylation Reaction Through Visible-Light Photoredox Catalysis. *Eur. J. Org. Chem.* **2013**, *2013*, 7528–7532.
- (475) Fukuzumi, S.; Mochizuki, S.; Tanaka, T. Photocatalytic Reduction of Phenacyl Halides by 9,10-Dihydro-10-Methylacridine: Control between the Reductive and Oxidative Quenching Pathways of Tris(bipyridine)ruthenium Complex Utilizing an Acid Catalysis. *J. Phys. Chem.* **1990**, *94*, 722–726.
- (476) Narayanan, J. M. R.; Tucker, J. W.; Stephenson, C. R. J. Electron-Transfer Photoredox Catalysis: Development of a Tin-Free Reductive Dehalogenation Reaction. *J. Am. Chem. Soc.* **2009**, *131*, 8756–8757.
- (477) Alonso, F.; Beletskaya, I. P.; Yus, M. Metal-Mediated Reductive Hydrodehalogenation of Organic Halides. *Chem. Rev.* **2002**, *102*, 4009–4092.
- (478) Neumann, M.; Füldner, S.; König, B.; Zeitler, K. Metal-Free, Cooperative Asymmetric Organophotoredox Catalysis with Visible Light. *Angew. Chem., Int. Ed.* **2011**, *50*, 951–954.
- (479) Tanner, D. D.; Singh, H. K. Reduction of  $\alpha$ -Halo Ketones by Organotin Hydrides. An Electron-Transfer-Hydrogen Atom Abstraction Mechanism. *J. Org. Chem.* **1986**, *51*, 5182–5186.
- (480) Neumann, M.; Zeitler, K. Application of Microflow Conditions to Visible Light Photoredox Catalysis. *Org. Lett.* **2012**, *14*, 2658–2661.
- (481) Schrauzer, G. N.; Deutsch, E.; Windgassen, R. J. The Nucleophilicity of Vitamin B<sub>12S</sub>. *J. Am. Chem. Soc.* **1968**, *90*, 2441–2442.
- (482) Tahara, K.; Hisaeda, Y. Eco-Friendly Molecular Transformations Catalyzed by a Vitamin B12 Derivative with a Visible-Light-Driven System. *Green Chem.* **2011**, *13*, 558–561.
- (483) Hisaeda, Y.; Nishioka, T.; Inoue, Y.; Asada, K.; Hayashi, T. Electrochemical Reactions Mediated by Vitamin B12 Derivatives in Organic Solvents. *Coord. Chem. Rev.* **2000**, *198*, 21–37.
- (484) Zakrzewski, A.; Neckers, D. C. Bleaching Products of Rose Bengal under Reducing Conditions. *Tetrahedron* **1987**, *43*, 4507–4512.
- (485) Nicewicz, D. A.; MacMillan, D. W. C. Merging Photoredox Catalysis with Organocatalysis: The Direct Asymmetric Alkylation of Aldehydes. *Science* **2008**, *322*, 77–80.
- (486) Jadhav, S. D.; Bakshi, D.; Singh, A. Visible Light Mediated Organocatalytic Activation of Ethyl Bromofluoroacetate: Coupling with Indoles and Anilines. *J. Org. Chem.* **2015**, *80*, 10187–10196.
- (487) Meyer, A. U.; Slanina, T.; Yao, C.-J.; König, B. Metal-Free Perfluorarylation by Visible Light Photoredox Catalysis. *ACS Catal.* **2016**, *6*, 369–375.
- (488) Kochi, J. K. The Mechanism of the Sandmeyer and Meerwein Reactions. *J. Am. Chem. Soc.* **1957**, *79*, 2942–2948.
- (489) Galli, C. Radical Reactions of Arenediazonium Ions: An Easy Entry into the Chemistry of the Aryl Radical. *Chem. Rev.* **1988**, *88*, 765–792.
- (490) Mo, F.; Dong, G.; Zhang, Y.; Wang, J. Recent Applications of Arene Diazonium Salts in Organic Synthesis. *Org. Biomol. Chem.* **2013**, *11*, 1582.
- (491) Allongue, P.; Delamar, M.; Desbat, B.; Fagebaume, O.; Hitmi, R.; Pinson, J.; Savéant, J.-M. Covalent Modification of Carbon Surfaces by Aryl Radicals Generated from the Electrochemical Reduction of Diazonium Salts. *J. Am. Chem. Soc.* **1997**, *119*, 201–207.
- (492) Elofson, R. M.; Gadallah, F. F. Substituent Effects in the Polarography of Aromatic Diazonium Salts. *J. Org. Chem.* **1969**, *34*, 854–857.
- (493) Cano-Yelo, H.; Deronzier, A. Photocatalysis of the Pschorr Reaction by Tris-(2,2'-bipyridyl)ruthenium(II) in the Phenanthrene Series. *J. Chem. Soc., Perkin Trans. 2* **1984**, No. 6, 1093–1098.
- (494) Cano-Yelo, H.; Deronzier, A. Photo-Oxidation of Some Carbinols by the Ru(II) Polypyridyl Complex-Aryl Diazonium Salt System. *Tetrahedron Lett.* **1984**, *25*, 5517–5520.
- (495) Schroll, P.; Hari, D. P.; König, B. Photocatalytic Arylation of Alkenes, Alkynes and Enones with Diazonium Salts. *ChemistryOpen* **2012**, *1*, 130–133.
- (496) Hering, T.; Hari, D. P.; König, B. Visible-Light-Mediated  $\alpha$ -Arylation of Enol Acetates Using Aryl Diazonium Salts. *J. Org. Chem.* **2012**, *77*, 10347–10352.
- (497) Hari, D. P.; Schroll, P.; König, B. Metal-Free, Visible-Light-Mediated Direct C–H Arylation of Heteroarenes with Aryl Diazonium Salts. *J. Am. Chem. Soc.* **2012**, *134*, 2958–2961.
- (498) Xiao, T.; Dong, X.; Tang, Y.; Zhou, L. Phenanthrene Synthesis by Eosin Y-Catalyzed, Visible Light-Induced [4+2] Benzannulation of Biaryl diazonium Salts with Alkynes. *Adv. Synth. Catal.* **2012**, *354*, 3195–3199.
- (499) Hari, D. P.; Hering, T.; König, B. Visible Light Photocatalytic Synthesis of Benzothiophenes. *Org. Lett.* **2012**, *14*, 5334–5337.
- (500) Majek, M.; Jacobi von Wangenheim, A. Metal-Free Carbonylations by Photoredox Catalysis. *Angew. Chem., Int. Ed.* **2015**, *54*, 2270–2274.
- (501) Guo, W.; Lu, L.-Q.; Wang, Y.; Wang, Y.-N.; Chen, J.-R.; Xiao, W.-J. Metal-Free, Room-Temperature, Radical Alkoxy carbonylation of Aryldiazonium Salts through Visible-Light Photoredox Catalysis. *Angew. Chem., Int. Ed.* **2015**, *54*, 2265–2269.
- (502) Gu, L.; Jin, C.; Liu, J. Metal-Free, Visible-Light-Mediated Transformation of Aryl Diazonium Salts and (Hetero)arenes: An Efficient Route to Aryl Ketones. *Green Chem.* **2015**, *17*, 3733–3736.
- (503) Yu, J.; Zhang, L.; Yan, G. Metal-Free, Visible Light-Induced Borylation of Aryldiazonium Salts: A Simple and Green Synthetic Route to Arylboronates. *Adv. Synth. Catal.* **2012**, *354*, 2625–2628.
- (504) Majek, M.; von Wangenheim, A. J. Organocatalytic Visible Light Mediated Synthesis of Aryl Sulfides. *Chem. Commun.* **2013**, *49*, 5507–5509.
- (505) Yang, Z.; Li, H.; Zhang, L.; Zhang, M.-T.; Cheng, J.-P.; Luo, S. Organic Photocatalytic Cyclization of Polyenes: A Visible-Light-Mediated Radical Cascade Approach. *Chem. - Eur. J.* **2015**, *21*, 14723–14727.
- (506) Gopalan, A. S.; Prieto, R.; Mueller, B.; Peters, D. Polyene Cyclizations Using Mercury (II) Triflate-N,N-Dimethylaniline Complex - Participation by Internal Nucleophiles. *Tetrahedron Lett.* **1992**, *33*, 1679–1682.
- (507) Justicia, J.; de Cienfuegos, L. Á.; Campaña, A. G.; Miguel, D.; Jakoby, V.; Gansäuer, A.; Cuerva, J. M. Bioinspired Terpene Synthesis: A Radical Approach. *Chem. Soc. Rev.* **2011**, *40*, 3525–3537.
- (508) Ishihara, K.; Nakamura, S.; Yamamoto, H. The First Enantioselective Biomimetic Cyclization of Polyprenoids. *J. Am. Chem. Soc.* **1999**, *121*, 4906–4907.
- (509) Ishihara, K.; Ishibashi, H.; Yamamoto, H. Enantioselective Biomimetic Cyclization of Homo(polypropenyl)arenes. A New Entry to (+)-Podocarpa-8,11,13-Triene Diterpenoids and (−)-Tetracyclic Polyprenoid of Sedimentary Origin. *J. Am. Chem. Soc.* **2001**, *123*, 1505–1506.

- (510) Ishibashi, H.; Ishihara, K.; Yamamoto, H. A New Artificial Cyclase for Polyprenoids: Enantioselective Total Synthesis of (−)-Chromazonarol, (+)-8-Epi-Puupehedione, and (−)-11'-Deoxytaondiol Methyl Ether. *J. Am. Chem. Soc.* **2004**, *126*, 11122–11123.
- (511) Johnson, W. S. Biomimetic Polyene Cyclizations. *Bioorg. Chem.* **1976**, *5*, 51–98.
- (512) Yoder, R. A.; Johnston, J. N. A Case Study in Biomimetic Total Synthesis: Polyolefin Carbocyclizations to Terpenes and Steroids. *Chem. Rev.* **2005**, *105*, 4730–4756.
- (513) Tantillo, D. J. Biosynthesis via Carbocations: Theoretical Studies on Terpene Formation. *Nat. Prod. Rep.* **2011**, *28*, 1035.
- (514) Dai, C.; Narayanan, J. M. R.; Stephenson, C. R. J. Visible-Light-Mediated Conversion of Alcohols to Halides. *Nat. Chem.* **2011**, *3*, 140–145.
- (515) Konieczynska, M. D.; Dai, C.; Stephenson, C. R. J. Synthesis of Symmetric Anhydrides Using Visible Light-Mediated Photoredox Catalysis. *Org. Biomol. Chem.* **2012**, *10*, 4509–4511.
- (516) Yadav, A. K.; Srivastava, V. P.; Yadav, L. D. S. Visible-Light-Mediated Efficient Conversion of Aldoximes and Primary Amides into Nitriles. *RSC Adv.* **2014**, *4*, 4181–4186.
- (517) Beija, M.; Afonso, C. A. M.; Martinho, J. M. G. Synthesis and Applications of Rhodamine Derivatives as Fluorescent Probes. *Chem. Soc. Rev.* **2009**, *38*, 2410–2433.
- (518) Griesbeck, A. G.; Hundertmark, T.; Steinwascher, J. Regio- and Diastereoselective Formation of 1,2-Azidohydroperoxides by Photo-oxygenation of Alkenes in the Presence of Azide Anions. *Tetrahedron Lett.* **1996**, *37*, 8367–8370.
- (519) Griesbeck, A. G.; Reckenthaler, M.; Uhlig, J. Photoinduced Azidohydroperoxidation of Myrtenyl Hydroperoxide with Semiconductor Particles and Lucigenin as PET-Catalysts. *Photochem. Photobiol. Sci.* **2010**, *9*, 775–778.
- (520) Griesbeck, A. G.; Lex, J.; Saygin, K. M.; Steinwascher, J. Azidohydroperoxidation of Pinenes: Stereoselectivity Pattern and the First X-Ray Structure of a 2-Azidohydroperoxide. *Chem. Commun.* **2000**, No. 22, 2205–2206.
- (521) Griesbeck, A. G.; Steinwascher, J.; Reckenthaler, M.; Uhlig, J. Azide/oxygen Photocatalysis with Homogeneous and Heterogeneous Photocatalysts for 1,2-Aminohydroxylation of Acyclic/cyclic Alkenes and Michael Acceptors. *Res. Chem. Intermed.* **2013**, *39*, 33–42.
- (522) Griesbeck, A. G.; Hundertmark, T.; Steinwascher, J. Regio- and Diastereoselective Formation of 1,2-Azidohydroperoxides by Photo-oxygenation of Alkenes in the Presence of Azide Anions. *Tetrahedron Lett.* **1996**, *37*, 8367–8370.
- (523) Meguro, M.; Asao, N.; Yamamoto, Y. Ytterbium Triisopropoxide Catalysed Ring Opening of Epoxides with Trimethylsilyl Azide. *J. Chem. Soc., Chem. Commun.* **1995**, No. 10, 1021–1022.
- (524) Workentin, M. S.; Wagner, B. D.; Lusztyk, J.; Wayner, D. D. M. Azidyl Radical Reactivity.  $\text{N}_6^{\bullet-}$  as a Kinetic Probe for the Addition Reactions of Azidyl Radicals with Olefins. *J. Am. Chem. Soc.* **1995**, *117*, 119–126.
- (525) DeFelippis, M. R.; Faraggi, M.; Klapper, M. H. Redox Potentials of the Azide and Dithiocyanate Radicals. *J. Phys. Chem.* **1990**, *94*, 2420–2424.
- (526) Carruthers, R. A.; Crellin, R. A.; Ledwith, A. Cation-Radicals: Oxygen Catalysis in the Photosensitised Cyclodimerisation of Aromatic Enamines. *J. Chem. Soc. D* **1969**, No. 6, 252–253.
- (527) Bell, F. A.; Crellin, R. A.; Fujii, H.; Ledwith, A. Cation-Radicals: Metal-Catalysed Cyclodimerisation of Aromatic Enamines. *J. Chem. Soc. D* **1969**, No. 6, 251–252.
- (528) Rozhkov, I. N.; Igumnov, S. M.; Bekker, G. Y.; Pletnev, S. I.; Rempel', G. D.; Deev, L. E. Oxidative Properties of Perfluoroalkyl Halides. *Bull. Acad. Sci. USSR, Div. Chem. Sci.* **1989**, *38*, 2041–2043.
- (529) Cenens, J. Visible Spectroscopy of Methylene Blue on Hectorite, Laponite B, and Barasym in Aqueous Suspension. *Clays Clay Miner.* **1988**, *36*, 214–224.
- (530) Matsumoto, S. Flash Photolysis of Methylene Blue. I. Reversible Photolysis in the Absence of a Reducing Agent and in the Presence of Certain Kinds of Reducing Agents. *Bull. Chem. Soc. Jpn.* **1964**, *37*, 491–498.
- (531) Matsumoto, S. Flash Photolysis of Methylene Blue. II. Photolysis in an Aqueous Solvent in the Presence of N-Phenylglycines and Photolysis in Organic Solvents. *Bull. Chem. Soc. Jpn.* **1964**, *37*, 499–503.
- (532) Kato, S.; Morita, M.; Koizumi, M. Studies of the Transient Intermediates in the Photoreduction of Methylene Blue. *Bull. Chem. Soc. Jpn.* **1964**, *37*, 117–124.
- (533) Klimov, A. D.; Lebedkin, S. F.; Emokhonor, V. N. Dye-Sensitized Chemiluminescence of Luminol and Related Cyclic Hydrazides. *J. Photochem. Photobiol. A* **1992**, *68*, 191–203.
- (534) Zou, Y.-Q.; Chen, J.-R.; Liu, X.-P.; Lu, L.-Q.; Davis, R. L.; Jørgensen, K. A.; Xiao, W.-J. Highly Efficient Aerobic Oxidative Hydroxylation of Arylboronic Acids: Photoredox Catalysis Using Visible Light. *Angew. Chem., Int. Ed.* **2012**, *51*, 784–788.
- (535) Cocquet, G.; Ferroud, C.; Guy, A. A Mild and Efficient Procedure for Ring-Opening Reactions of Piperidine and Pyrrolidine Derivatives by Single Electron Transfer Photooxidation. *Tetrahedron* **2000**, *56*, 2975–2984.
- (536) Cocquet, G.; Ferroud, C.; Simon, P.; Taberna, P.-L. Single Electron Transfer Photoinduced Oxidation of Piperidine and Pyrrolidine Derivatives to the Corresponding Lactams. *J. Chem. Soc. Perkin Trans. 2* **2000**, No. 6, 1147–1153.
- (537) Pitre, S. P.; McTiernan, C. D.; Ismaili, H.; Scaiano, J. C. Metal-Free Photocatalytic Radical Trifluoromethylation Utilizing Methylene Blue and Visible Light Irradiation. *ACS Catal.* **2014**, *4*, 2530–2535.
- (538) Casselman, M. D.; Kaur, A. P.; Narayana, K. A.; Elliott, C. F.; Risko, C.; Odom, S. A. The Fate of Phenothiazine-Based Redox Shuttles in Lithium-Ion Batteries. *Phys. Chem. Chem. Phys.* **2015**, *17*, 6905–6912.
- (539) Yang, C.-J.; Chang, Y. J.; Watanabe, M.; Hon, Y.-S.; Chow, T. J. Phenothiazine Derivatives as Organic Sensitzers for Highly Efficient Dye-Sensitized Solar Cells. *J. Mater. Chem.* **2012**, *22*, 4040–4049.
- (540) Pan, X.; Lamson, M.; Yan, J.; Matyjaszewski, K. Photoinduced Metal-Free Atom Transfer Radical Polymerization of Acrylonitrile. *ACS Macro Lett.* **2015**, *4*, 192–196.
- (541) Chen, M.; MacLeod, M. J.; Johnson, J. A. Visible-Light-Controlled Living Radical Polymerization from a Trithiocarbonate Initiator Mediated by an Organic Photoredox Catalyst. *ACS Macro Lett.* **2015**, *4*, 566–569.
- (542) Ghosh, I.; Ghosh, T.; Bardagi, J. I.; König, B. Reduction of Aryl Halides by Consecutive Visible Light-Induced Electron Transfer Processes. *Science* **2014**, *346*, 725–728.
- (543) Wipf, D. O.; Wightman, R. M. Rapid Cleavage Reactions of Haloaromatic Radical Anions Measured with Fast-Scan Cyclic Voltammetry. *J. Phys. Chem.* **1989**, *93*, 4286–4291.
- (544) Hünig, S.; Groß, J.; Lier, E. F.; Quast, H. Synthese Und Polarographie von Quartärsalzen Der Phenanthroline, Des 2,7-Diazapyrens Sowie Der Diazoniapentaphene. *Justus Liebigs Ann. Chem.* **1973**, *1973*, 339–358.
- (545) Jagadesan, P.; Mondal, B.; Parthasarathy, A.; Rao, V. J.; Ramamurthy, V. Photochemical Reaction Containers as Energy and Electron-Transfer Agents. *Org. Lett.* **2013**, *15*, 1326–1329.
- (546) Lilenthal, N. D.; Alsafar, H.; Conerty, J.; Fernandez, R.; Kong, C.; Smith, D. K. Development of Chemical Sensors Based on Redox-Dependent Receptors:  $\text{N},\text{N}'$ -Dimethylazopyrenium-Modified Electrodes. *Anal. Chem.* **2003**, *75*, 3322–3328.
- (547) Lin, C.-F.; Liu, Y.-H.; Lai, C.-C.; Peng, S.-M.; Chiu, S.-H. An Extremely Stable Host–Guest Complex That Functions as a Fluorescence Probe for Calcium Ions. *Chem. - Eur. J.* **2006**, *12*, 4594–4599.
- (548) Santamaría, J.; Ouchabane, R.; Rigaudy, J. Electron-Transfer Activation. Photochemical  $\text{N}$ -Demethylation of Tertiary Amines. *Tetrahedron Lett.* **1989**, *30*, 2927–2928.
- (549) Santamaría, J.; Kaddachi, M. T.; Rigaudy, J. Electron-Transfer Activation. Photocyanation of Tertiary Amines. *Tetrahedron Lett.* **1990**, *31*, 4735–4738.
- (550) Santamaría, J.; Ouchabane, R.; Rigaudy, J. Electron-Transfer Activation. Salt Effects on the Photooxidation of Tertiary Amines: A Useful  $\text{N}$ -Demethylation Method. *Tetrahedron Lett.* **1989**, *30*, 3977–3980.

- (551) Rosenberg, L. Chemical Basis for the Histological Use of Safranin O in the Study of Articular Cartilage. *J. Bone Joint Surg. Am.* **1971**, *53*, 69–82.
- (552) Gómez, M. L.; Previtali, C. M.; Montejano, H. A. Photophysical Properties of Saframine O in Protic Solvents. *Spectrochim. Acta, Part A* **2004**, *60*, 2433–2439.
- (553) Neumann, M. G.; Pastre, I. A.; Previtali, C. M. Comparison of Photoinduced Electron Transfer to Singlet and Triplet States of Safranine T. *J. Photochem. Photobiol., A* **1991**, *61*, 91–98.
- (554) Leow, D. Phenazinium Salt-Catalyzed Aerobic Oxidative Amidation of Aromatic Aldehydes. *Org. Lett.* **2014**, *16*, 5812–5815.
- (555) Tank, R.; Pathak, U.; Vimal, M.; Bhattacharyya, S.; Pandey, L. K. Hydrogen Peroxide Mediated Efficient Amidation and Esterification of Aldehydes: Scope and Selectivity. *Green Chem.* **2011**, *13*, 3350–3354.
- (556) Liu, X.; Jensen, K. F. Direct Oxidative Amidation of Aromatic Aldehydes Using Aqueous Hydrogen Peroxide in Continuous Flow Microreactor Systems. *Green Chem.* **2012**, *14*, 1471–1474.
- (557) Halaka, F. G.; Babcock, G. T.; Dye, J. L. Properties of 5-Methylphenazinium Methyl Sulfate. Reaction of the Oxidized Form with NADH and of the Reduced Form with Oxygen. *J. Biol. Chem.* **1982**, *257*, 1458–1461.
- (558) Lee, G. A.; Israel, S. H. Photosensitized (Electron-Transfer) Rearrangements of Cinnamyl Alcohol Derivatives. *J. Org. Chem.* **1983**, *48*, 4557–4563.
- (559) Hamada, T.; Nishida, A.; Yonemitsu, O. Selective Removal of Electron-Accepting *P*-Toluene- and Naphthalenesulfonyl Protecting Groups for Amino Function via Photoinduced Donor Acceptor Ion Pairs with Electron-Donating Aromatics. *J. Am. Chem. Soc.* **1986**, *108*, 140–145.
- (560) Nishida, A.; Hamada, T.; Yonemitsu, O. Hydrolysis of Tosyl Esters Initiated by an Electron Transfer from Photoexcited Electron-Rich Aromatic Compounds. *J. Org. Chem.* **1988**, *53*, 3386–3387.
- (561) Okada, K.; Okamoto, K.; Oda, M. A New and Practical Method of Decarboxylation: Photosensitized Decarboxylation of *N*-Acyloxyphthalimides via Electron-Transfer Mechanism. *J. Am. Chem. Soc.* **1988**, *110*, 8736–8738.
- (562) Banerjee, A.; Falvey, D. E. Protecting Groups That Can Be Removed through Photochemical Electron Transfer: Mechanistic and Product Studies on Photosensitized Release of Carboxylates from Phenacyl Esters. *J. Org. Chem.* **1997**, *62*, 6245–6251.
- (563) Pandey, G.; Rao, K. S. S. P.; Rao, K. V. N. PhSeSiR<sub>3</sub>-Catalyzed Group Transfer Radical Reactions. *J. Org. Chem.* **2000**, *65*, 4309–4314.
- (564) Hasegawa, E.; Takizawa, S.; Seida, T.; Yamaguchi, A.; Yamaguchi, N.; Chiba, N.; Takahashi, T.; Ikeda, H.; Akiyama, K. Photoinduced Electron-Transfer Systems Consisting of Electron-Donating Pyrenes or Anthracenes and Benzimidazolines for Reductive Transformation of Carbonyl Compounds. *Tetrahedron* **2006**, *62*, 6581–6588.
- (565) Pandey, G.; Sesha Poleswara Rao, K. S.; Rao, K. V. N. Photosensitized Electron Transfer Promoted Reductive Activation of Carbon–Selenium Bonds To Generate Carbon-Centered Radicals: Application for Unimolecular Group Transfer Radical Reactions. *J. Org. Chem.* **1996**, *61*, 6799–6804.
- (566) Hasegawa, E.; Seida, T.; Chiba, N.; Takahashi, T.; Ikeda, H. Contrastive Photoreduction Pathways of Benzophenones Governed by Regiospecific Deprotonation of Imidazoline Radical Cations and Additive Effects. *J. Org. Chem.* **2005**, *70*, 9632–9635.
- (567) Fukuzumi, S.; Tanii, K.; Tanaka, T. Protonated Pteridine and Flavin Analogues Acting as Efficient and Substrate-Selective Photocatalysts in the Oxidation of Benzyl Alcohol Derivatives by Oxygen. *J. Chem. Soc., Chem. Commun.* **1989**, No. 13, 816–818.
- (568) Svoboda, J.; Schmaderer, H.; König, B. Thiourea-Enhanced Flavin Photooxidation of Benzyl Alcohol. *Chem. - Eur. J.* **2008**, *14*, 1854–1865.
- (569) Schmaderer, H.; Hilgers, P.; Lechner, R.; König, B. Photooxidation of Benzyl Alcohols with Immobilized Flavins. *Adv. Synth. Catal.* **2009**, *351*, 163–174.
- (570) Lechner, R.; König, B. Oxidation and Deprotection of Primary Benzylamines by Visible Light Flavin Photocatalysis. *Synthesis* **2010**, *2010*, 1712–1718.
- (571) Lechner, R.; Kümmel, S.; König, B. Visible Light Flavin Photo-Oxidation of Methylbenzenes, Styrenes and Phenylacetic Acids. *Photochem. Photobiol. Sci.* **2010**, *9*, 1367–1377.
- (572) Mühlendorf, B.; Wolf, R. Photocatalytic Benzylic C–H Bond Oxidation with a Flavin Scandium Complex. *Chem. Commun.* **2015**, *51*, 8425–8428.
- (573) Mühlendorf, B.; Wolf, R. C–H Photooxygenation of Alkyl Benzenes Catalyzed by Riboflavin Tetraacetate and a Non-Heme Iron Catalyst. *Angew. Chem., Int. Ed.* **2016**, *55*, 427–430.
- (574) Metternich, J. B.; Gilmour, R. A Bio-Inspired, Catalytic E → Z Isomerization of Activated Olefins. *J. Am. Chem. Soc.* **2015**, *137*, 11254–11257.
- (575) Metternich, J. B.; Gilmour, R. One Photocatalyst, n Activation Modes Strategy for Cascade Catalysis: Emulating Coumarin Biosynthesis with (–)-Riboflavin. *J. Am. Chem. Soc.* **2016**, *138*, 1040–1045.
- (576) Loudet, A.; Burgess, K. BODIPY Dyes and Their Derivatives: Syntheses and Spectroscopic Properties. *Chem. Rev.* **2007**, *107*, 4891–4932.
- (577) Sundararajan, C.; Falvey, D. E. Photorelease of Carboxylic Acids, Amino Acids, and Phosphates from *N*-Alkylpicolinium Esters Using Photosensitization by High Wavelength Laser Dyes. *J. Am. Chem. Soc.* **2005**, *127*, 8000–8001.
- (578) Huang, L.; Zhao, J. Iodo-Bodipys as Visible-Light-Absorbing Dual-Functional Photoredox Catalysts for Preparation of Highly Functionalized Organic Compounds by Formation of C–C Bonds via Reductive and Oxidative Quenching Catalytic Mechanisms. *RSC Adv.* **2013**, *3*, 23377–23388.
- (579) Guo, S.; Tao, R.; Zhao, J. Photoredox Catalytic Organic Reactions Promoted with Broadband Visible Light-Absorbing Bodipy-Iodo-Aza-Bodipy Triad Photocatalyst. *RSC Adv.* **2014**, *4*, 36131–36139.